Coastal Erosion at Spratt Bight Beach, San Andrés

A study on its cause and the applicability of the Building with Nature approach

J. van Overeem

13 July 2022

TU Delft

ARCADIS

Coastal Erosion at Spratt Bight Beach, San Andrés

A study on its cause and the applicability of the Building with Nature approach

by

J. van Overeem

in partial fulfillment of the requirements to obtain the degree of

Master of Science
in Civil Engineering

at the Delft University of Technology (TU Delft)

to be defended publicly on July 13th, 2022
in Lecture Hall G of the faculty of Civil Engineering & Geosciences of the TU Delft

Chairman committee:	Prof. dr. ir. S. G. J. Aarninkhof,	Delft University of Technology
Committee members:	ir. M.C. Onderwater,	Arcadis / Delft University of Technology
	Drs. J. P. G. N. Klooster,	Arcadis
	Dr. M. F. S. Tissier,	Delft University of Technology

Cover: Google Earth Pro 7.3.4.8248. (2019, March). SAI, San Andrés, Providencia y Santa Catalina, Colombia: Maxar Technologies. Retrieved July 2021, from http://www.google.com/earth/index.html

Preface

Going through the process of a thesis research is not an easy task. Many obstacles and set-backs were encountered along the way. Of course, besides the less pleasant parts, there were also always good aspects about doing a master thesis. There are many people I have to thank for making the process bearable, pleasant, and sometimes even great!

First of all, the committee, for always making me feel comfortable and positive about my work. Every progress, kick-off, Green Light meeting we had were always experienced as very pleasant. I want to thank Martijn for our weekly meetings and always being so positive, even during uncertain moments. Marion for bringing technical depth into my research, for helping with my abstract model and conceptual questions, always taking more than enough time for me. Stefan for his always on point feedback, overall overview of my research and advise on the 'and what next?' questions. Jeroen for providing this incredible experience of being part of the San Andrés project team and making me feel what it is to be a real coastal engineer.

I also want to thank the San Andrés Project team as a whole, especially Jorge Enrique Saenz and Cristal Ange for believing in my Spanish skills and helping me present our work during workshops and webinars. I want to thank the RKZ team of Arcadis for everyone's advice, for the coffee moments and always creating a 'gezellig' environment at the office and during the 'borrels'. I specially want to thank Jos van der Baan for always helping me out with my model challenges and for providing me expert judgement for the (sometimes challenging) model results. Robbin van Santen for the advice on XBeach and the overall research picture. Rufus Velhorst for helping me out with Python and Delf3D. Sanne van der Heijden for helping me with XBeach and MATLAB. And of course, all the interns (of which some are now working at Arcadis) for the valuable conversations, coffee moments and borrels.

Finally, I want to thank my father, my mother, and my brother for being a source of inspiration and my personal mentors during this trajectory and my whole life. My (room)mates for their support and always being there when I needed to take a time off of my thesis. At last, but far from least, I want to thank Michelle for the incredible amount of love, support, and understanding during these, sometimes hard, times.

I could fill an entire document of the length of this thesis with grateful words for everyone that were there and made my experience at the university an unforgettable one. Unfortunately, there is just this amount of space to do so, therefore I also want to thank everyone I didn't mention! With these words I finalize this 9 years chapter of my life and I'm ready to start the next!

Jan van Overeem
Delft, July 2022

Abstract

San Andrés is a Colombian-Caribbean Island located 800 km from the Colombian coast. On its Eastern side there is a barrier reef formation protecting the island from offshore incident waves. Due to the protected environment created by the coral reef, sandy beaches can be formed on the East side of the island.

During normal conditions, waves come predominantly form the East (90% of the wave climate), have significant wave height of 2 m and period of 8 s. Besides, San Andrés is situated on the Caribbean hurricane route, which can cause an enormous damage to the island. The storm season at San Andrés is between October and December, which is also when major erosion events take place.

The economy of San Andrés is mostly built upon tourism, specially related to its biodiverse ecosystems and Caribbean beaches. The island's ecological environment is composed by mangroves, seagrasses, and coral reefs, attracting a wide spectrum of fauna and flora to its ecosystems.

During the Masterplan for Coastal Erosion (PMEC), San Andrés was pointed out as a location in which coastal erosion is problematic. In a follow-up of this Masterplan, the island was elected to be part of a program in which solutions against coastal erosion would be presented. This research is part of this project, as a parallel trajectory to get a more profound understanding of the system and the possible mitigation measures that could be applied on the island.

With increasing urbanization and frequency of extreme weather events, erosion is becoming a problem with which San Andrés and its residents are repeatedly having to deal. Erosion is specially problematic for the Northern part of the island, called Spratt Bight. This region is not only the most densely populated area of the island, but also economically and touristically very important. Its beach presents periodically eroding patterns during storm seasons, when wave action drives the sediment towards the East, decreasing its beach width almost to none. A decreasing beach width has a direct negative impact on tourism, making coastal erosion in Spratt Bight not only a coastal safety problem, but also an economic issue.

This study aims to look into the main hydro- and morphological processes driving coastal erosion in Spratt Bight and, using the Building with Nature philosophy, propose a set of solutions to mitigate this problem. To reach this objective data analysis and literature research has been carried out, after which different environmental conditions were modelled using the numerical model Delft3D.

During these activities it was found that independently of its direction, waves approaching San Andrés break upon the coral reef and induce a water level set up inside the coral lagoon. The difference in water level in- and outside the lagoon generates a current and sediment transport, which is directed towards the western opening in the coral reef.

When the Northern waves approach the island (1.5% of the wave climate), the same water level set-up phenomenon is observed. However, as waves are approaching form the North, they not only break upon the reef, but are also able to enter the sheltered lagoon through the western opening in the coral reef. These waves are able to bend around the reef reaching the shore and the headland on the Northern part of the island, inducing a longshore current and a sediment transport that is southeastward directed. The result is that Northern waves are mostly responsible for a strong westward

and erosive sediment transport pattern. These waves are mostly observed between October and March, which coincides with the storm season in San Andrés.

Besides, it was found that the Eastern waves are responsible for restoring the (dynamic) equilibrium profile of Spratt Bight Beach. However, this restoring force has a less strong intensity, taking more time to restore the beach than to disrupt its equilibrium.

The solutions proposed include seagrass restoration to enhance ecology, restrain sediment transport and attenuate wave heights; the beneficial reuse of dredged material, to nourish Spratt Bight Beach; and finally, the implementation of artificial coral reefs as breakwaters to prevent the newly nourished sediment to be lost from the system. Besides, artificial coral reefs enhance the ecosystem by attracting fauna and flora increasing biodiversity. All proposed solutions have a positive impact on the beaches and therefore on tourism and the economy of the island. This makes them multifunctional solutions, serving the main goal of protecting the beach while at the same time creating benefits for other functions and values in the area. Following in this way the prescriptions of the Building with Nature design approach by van Eekelen and Bouw (2020).

Contents

List of Acronyms

BwN	Building with Nature
GDP	Gross Domestic Product
MCA	Multi Criteria Analysis
NbS	Nature-based Solution
RVO	Rijksdienst voor Ondernemend Nederland (Dutch Enterprise Agency)
SAI	San Andrés Island
WW3	Wave model WaveWatch III
MSL	Mean Sea Level
SFBR	Sea Flower Biosphere Reserve
XB-NH	Non-Hydrostatic module of XBeach model
XB-SB	Surfbeat module of XBeach model
D3D-W	Wave module of Delft3D model
D3D-F	Flow module of Delft3D model
PoT	Peak over Threshold
PMEC	Plan Maestro Erosion Costera
SDG	Sustainable Development Goals

List of Symbols

N, NE, E, SE, S, SW, W, NW	North, Northeast, East, Southeast, South, West, Northwest (respectively)
H_s	Significant wave height (equal to $H_{1/3}$)
$H_{1/3}$	Weighted average wave height of the highest 1/3 waves (equal to H_s)
$H_{1\%}$	Weighted average wave height of the highest 1% waves
H_{rms}	Root mean square wave height
T_p	Peak wave period
$T_{1\%}$	Weighted average wave period of the longest 1% waves
ρ	Water density
g	Gravity acceleration
h	still-water depth
η	Wave-induced water level set-up
$S_{xx,\ yx,\ xy,\ yy}$	Radiation stress
F_x	Wave force
P_x	Pressure force
k	Wave number
λ	Wavelength
c_g	Group velocity
c	Celerity (phase speed)
n	ratio between the wave group velocity and the phase velocity
S_t	Total sediment transport
S_s	Suspended load
S_b	Bed load
μ	Ripple coefficient for bed load formulation
U, $\tilde{u}$	Time average and oscillatory flow components (respectively)
C_h	Chezy coefficient
τ	Bed shear stress
τ_C	Current component of the bed shear stress
τ_{SW}	Short wave component of the bed shear stress
τ_{IG}	Infragravity wave component of the bed shear stress
C, $\tilde{c}$	Time average and oscillatory concentration components (respectively)
D_{50}	Sediment median particle diameter
φ_w	Wave angle

1 Introduction

The introduction gives the context in which this research is situated and the reason the subject is relevant. In this Chapter the coastal erosion background of Colombia will be explained, after which the focus will be set on the San Andrés Island (SAI), which is the case study of this research. Furthermore, in the next sections the research objective, research questions and methodology are described.

This thesis is meant as a final research assignment in order to obtain the Master of Science degree of Hydraulic Engineering at the Delft University of Technology. The research was done in co-operation with Arcadis Nederland in the context of the 'Partners voor Water' program of the Dutch Enterprise Agency (RVO). The project "Cooperación Técnica Prevención de la Erosión Costera en San Andrés, Colombia" is part of this program on which Arcadis NL is working, leading a consortium with JESyCa, Funcación Herencia Ambiantal Caribe, Deltares and Wetlands International. This research is part of this project, as a parallel trajectory to get a more profound understanding of the system and the possible mitigation measures that could be applied on the island.

1.1 Background and Problem Description

With more than 50 million inhabitants, Colombia is the second most populated country of South America, and it is one of the most diverse countries in the world with respect to geography, biodiversity, and culture (The World Bank, 2019).

Figure 1.1: On the left a satellite image of San Andrés retrieved from the Google Earth tool (2019). On the right the location of SAI in the Caribbean Sea, indicated with the red circle (Milenioscuro, 2021).

The Colombian coastal zone has a length of 3,513 km and can be categorized in four different types: the Pacific coast, the Caribbean coast, the insular zone of the Pacific and the insular zone of the Caribbean (INVEMAR, 2015). This research will focus on the latter, more specifically on the Island of San Andrés, shown in Figure 1.1.

San Andrés is a small Caribbean coral island located 700 km North of Colombia and 200 km East of Nicaragua, at 12° 34' North and 81° 44' West. It has a total estimated population of 80.000 inhabitants, spread over an area of 27 km^2 (12.6 km in N-S and 3.7 km in W-E direction), making it one of the most densely populated islands of the America's (Baine, Howard, Kerr, Graham, & Toral, 2007).

The main source of income of the island of San Andrés is provided by tourism, therefore a big part of the island's revenue is tourism related. In a study by Castaño-Isaza et al. (2015) it has been estimated that 39.3% of SAI's GDP is derived from the touristic sector. The same study indicates that tourists visiting SAI considered its beaches as the main reason for choosing the destination. Therefore, besides its ecological and its coastal safety related value, the beaches of San Andrés are an important source of income to its inhabitants. It is estimated that in case erosion would decrease the beach width by half, San Andrés could potentially lose up to 66,6% of its revenue coming from tourism (Castaño-Isaza, Newball, Roach, & Lau, 2015).

The coast of San Andrés is facing an increased erosion problem that is affecting tourism, coastal infrastructure, ecosystems, and protected areas. An example of this can be seen in Figure 1.2. The main causes of coastal erosion on the island are relative sea level rise, damage to the barrier reef, mangrove forest degradation, sea grass degradation, extreme weather events, placement of coastal structures, illegal sand mining, coastal squeeze, and other anthropogenic factors. In San Andrés numerous breakwaters, seawalls and even sandbags are placed along the coast in an attempt to protect the beaches from erosion. Such measures often result in bigger problems downstream of these structures (Klooster, 2020).

Figure 1.2: Placement of sandbags in order to protect the road along the southeast coast of San Andrés against coastal erosion (Klooster, 2020).

1.1.1 PMEC - Coastal Erosion Master Plan

Colombia is facing a country wide erosion problem. To mitigate this problem the Colombian government, in collaboration with 'Rijksdienst voor Ondernemend Nederland' (RVO) (in English, Dutch Enterprise Agency), came up with a master plan called 'Plan Maestro Erosion Costera' (PMEC) (in English, Coastal Erosion Master Plan). Along with other Dutch and Colombian companies, Arcadis formed a consortium which worked on the initial phase of this Master Plan. As described in the final report produced during the project (2017), the objective of PMEC is to develop a long-term strategy to prevent, mitigate and control erosion on the coasts of Colombia. To achieve this objective, the Building with Nature philosophy will play an important role.

During the project several critical locations were identified along the Colombian coast. Figure 1.3 shows the different locations on the map. The Master Plan presented 36 critical erosion sites, from which 16 were approved for the implementation of urgent mitigation measures by the Colombian Government. Two of these locations are situated in the archipelago of San Andrés and Providencia.

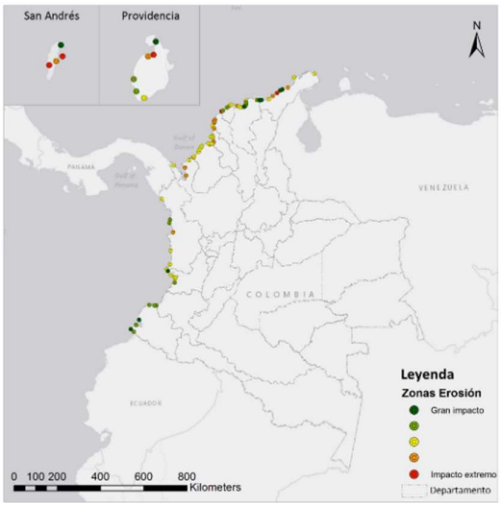

Figure 1.3: Result of the study made by the Dutch-Colombian consortium to identify the locations where coastal erosion can be observed in Colombia. The green dots represent high erosion, and as the dots become red erosion reaches extreme levels (Klooster, 2017)

After this diagnosis, a follow up of the master plan was carried out in which the focus was put on San Andrés. In the resulting report a further diagnosis is made specifically for SAI, where different types of solutions were presented (Klooster, 2020). The figure below shows an overview of the locations on the island diagnosed with coastal erosion problems.

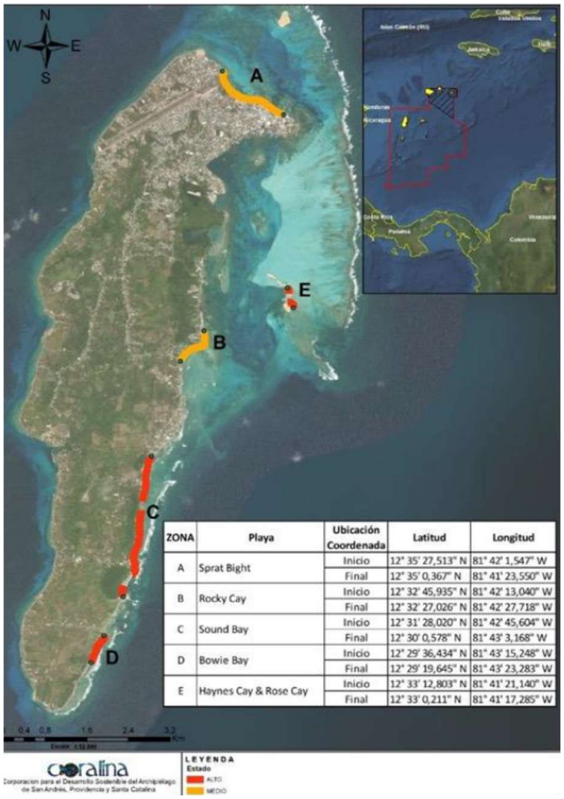

ZONA	Playa	Ubicación Coordenada	Latitud	Longitud
A	Sprat Bight	Inicio	12° 35' 27,513" N	81° 42' 1,547" W
		Final	12° 35' 0,367" N	81° 41' 23,550" W
B	Rocky Cay	Inicio	12° 32' 45,935" N	81° 42' 13,040" W
		Final	12° 32' 27,026" N	81° 42' 27,718" W
C	Sound Bay	Inicio	12° 31' 28,020" N	81° 42' 45,604" W
		Final	12° 30' 0,578" N	81° 43' 3,168" W
D	Bowie Bay	Inicio	12° 29' 36,434" N	81° 43' 15,248" W
		Final	12° 29' 19,645" N	81° 43' 23,283" W
E	Haynes Cay & Rose Cay	Inicio	12° 33' 12,803" N	81° 41' 21,140" W
		Final	12° 33' 0,211" N	81° 41' 17,285" W

Figure 1.4: Overview of locations where coastal erosion problems are more sever. The red lines indicate a qualitatively high erosive state and yellow a medium erosive state (Klooster, 2020)

1.2 Study Area: Spratt Bight

The main beaches showing signs of erosion in San Andrés are Spratt Bight, Rocky Cay, Sound Bay, Bowie Bay, Haynes Cay, and Rose Cay. In this research the focus lies on the Northern beach of **Spratt Bight**.

Spratt Bight is located at the Northern side of San Andrés and is the most densely populated and touristic area of the island. Spratt Bight Beach is the longest uninterrupted beach on the island and due to its touristic value, it is considered to be the most important beach of San Andrés.

Figure 1.5: Location of Spratt Bight.

The beach can be divided in 3 sections from East to West:

- Between the southeaster headland and Espolón Tiuna
- Between Espolón Tiuna and Espolón Jeno's Pizza
- Between Espolón Jeno's Pizza and Espolón de los Pescadores

Figure 1.6: Position of the different breakwaters in Spratt Bight.

Along Spratt Bight Beach mostly hotels, restaurants and resorts can be found. On the Northwestern part of the island, at 'Espolón de los Pescadores', the fisheries are situated. From that point fishermen living in Spratt Bight go to open sea for their fishing activities.

1.3 Research Objective & Research Questions

The focus of this research is set on Spratt Bight Beach mainly because of its economic, political, and cultural values. It is the main beach of the island and where the majority of the tourists are situated. As the touristic sector is part of the main economic activity of SAI, Spratt Bight is, economically speaking, the most important beach of San Andrés. Besides, it is located on the most densely populated area of the island, in the North, where also the political center of the San Andrés is situated. Finally, due to its popularity and importance, there is also more data available, and more research have been done about this area.

1.3.1 Main Research Question

The aim of this research is to provide insights into the morphodynamic behavior of the beach of Spratt Bight and, through the Building with Nature (BwN) philosophy, propose solutions to mitigate its erosion problem. To fulfill this objective, a research question and a set of sub-questions have been formulated.

- ***What are the main causes of coastal erosion at the Spratt Bight Beach and, using the Building with Nature approach, what possible mitigation measures could be applied?***

The research question is divided in two parts: 1) causes of erosion and 2) possible solutions. To come up with effective and relevant mitigation measures against coastal erosion that are in line with the BwN philosophy, the design steps proposed by van Eekelen & Bouw (2020) should be followed. These design steps are shown in Figure 1.7.

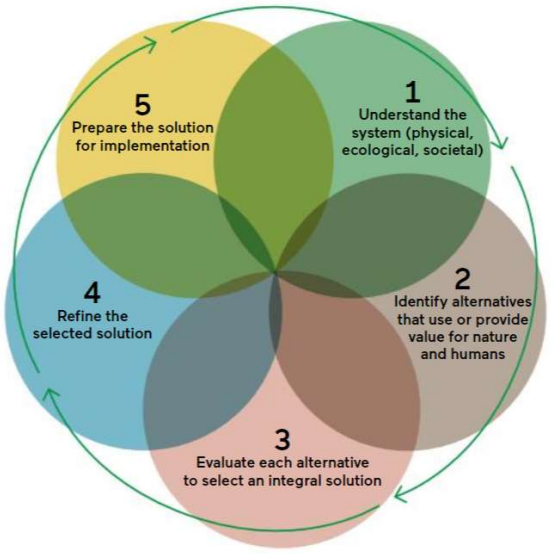

Figure 1.7: Building with Nature design approach from van Eekelen and Bouw (2020)

For this research the first two steps of the Building with Nature design approach will be applied:

1. Understand the system (physical, ecological, and societal)
2. Identify alternatives that use or provide value for nature and humans

This is done due to the time constrain imposed by this research. In Chapter 8 (Recommendations) it is further explained what should be done if the entire design approach is followed.

1.3.2 Sub-questions

Sub-questions were developed to help answer the main research question. These sub-questions are divided in two parts: cause of erosion and possible solutions, which is further explained below.

Cause of erosion

The morphological behavior of the coast of San Andrés is triggered by different loads to which the island is subject to. These are wave action, wind, currents, relative sea level rise and extreme weather events. To understand more specifically how these factors affect Spratt Bight, an integral understanding of the morphological behavior of the coastal system of San Andrés is required. The following sub-questions have been formulated in order to understand the causes of the erosion in San Andrés.

1. ***What are the loads acting on the coastal system?***
2. ***How are the hydrodynamic processes causing erosion on Spratt Bight?***

To answer these research questions sediment transport processes of the coastal area of San Andrés must be investigated. It will be necessary to analyze, review and model the coastal area of the island. With that being done, the main causes of erosion can be identified, and more sustainable and long-term solutions proposed.

Mitigation Measures: Building with Nature

The possible mitigation measures for Spratt Bight Beach should be proposed following the Building with Nature approach and philosophy. Therefore, the following sub-question has been developed:

3. ***What mitigation measures can at the same time protect Spratt Bight, enhance the ecosystem, and benefit society?***

1.4 Methodology

To carry out this research in a structured way, the approach should clearly be described. This is done in this section. For each research objective the taken approach is explained.

1.4.1 Cause of Erosion

Literature study

To have a better understanding of the environmental conditions and erosion problem in San Andrés, a literature study is carried out. This is done through scientific papers and technical reports from Colombian studies on the area. The literature provides a basis to carry out a qualitative analysis to identify sediment's sinks and sources and understand hydrodynamic and morphodynamic characteristics of the area.

Data Gathering

During the literature study the available physical data is gathered and analyzed. In this way, the physical system and the morphodynamic behavior of the coast of San Andrés can be modelled and described. This data consists of wave conditions, sediment characteristics and bathymetry.

San Andrés is a data poor environment, which means that there is not much data available. There no wave measurement buoys, periodic beach profile measurements, water level data, between many other relevant data to understand the system. This limitation will be further discussed in Chapters 2.

Numerical Modelling

To understand what factors are the most important in terms of beach erosion on SAI, the hydrodynamic conditions of and around the island were analyzed. As there is only offshore wave data available, **Delft3D-WAVE (D3D-W)** is used to transform the offshore to nearshore wave conditions. To simulate the sediment transport patterns and the hydrodynamic response to these wave conditions in the study area, **Deldft3D-FLOW (D3D-F)** is used.

Delft3D is a process-based model developed by Deltares (2022), which makes an effort to approach reality by explicitly representing all the essential physical processes acting on sediment and morphology in the coastal environment. The model has different modules that can be used for different purposes, of which D3D-W and D3D-F are applied in this research. These modules are ideal to estimate the sediment transport response of the coast of San Andrés during different wave conditions. The further explanation on the model choice and methodology is described in Chapter 3.

There is not enough available morphological data to have the models calibrated correctly. Calibration and validation of the model is therefore done through expert judgement and satellite images. The objective of the modelling study is to use the model as an **engineering tool**. This means that instead of completely relying on their results, the model is used to test the sensitivities of the different coastal elements to erosion and give an indication of what processes induce sediment transport and erosion.

1.4.2 Mitigation Measures

The mitigation measures will be proposed according to the Building with Nature philosophy and to do so the design steps presented in Figure 1.7 will be followed.

Literature Study

The societal system of San Andrés is analyzed to better understand what the necessities of the local communities are and to understand what parties and entities are involved in decision making (and what their power and their interest is). Besides, the ecological system must be investigated and analyzed to have a clear overview and come up with effective solutions using the Building with Nature approach. This is also done through literature review.

Identifying Alternatives

The Building with Nature philosophy will be applied to propose solutions against coastal erosion. Through literature study and analysis of the different Building with Nature concepts explained by EcoShape (Van Eekelen & Bouw, 2020), different mitigation measures are identified and analyzed as possible alternatives to prevent coastal erosion. Besides that, the ecological and societal analysis will be used as input, respecting the Building with Nature design approach steps presented in Figure 1.7.

2 System Analysis

In this chapter the different aspects of San Andrés and more specifically Spratt Bight are described. In the Physical Analysis (Section 2.2) the environmental conditions on the island are described. In the Ecological System (Section 2.3) is analyzed and the different fauna and flora living on and near Spratt Bight are brought to light. In the Socio-economic System (Section 2.4) the social, economic, and historical context are discussed.

2.1 Data Poor Environment

In Colombia, coastal data is not widely available. Although a lot of research has been done about coastal erosion and environmental conditions, not much of its data is widely and publicly available. INVEMAR, CIOH and DIMAR are the largest oceanographic research institutes that are active in Colombian Caribbean, and for many years they have been carrying out studies and research about the coast of San Andrés. Although their reports and results should be available to the public, difficulties are found when retrieving the data used to produce these reports.

Due to a consortium agreement between INVEMAR and Arcadis, a few datasets were made available for this research. A list of the local available data is shown below:

- One bathymetry measurement campaign from 2016
- A Nautical chart from 2008
- Sediment Characteristics from measurement campaign carried out in November 2021

As the hydrodynamic and morphodynamic processes are mainly influenced by the wave forces acting on the island of San Andrés, wave data is of the essence for this study. For this reason, this data had to be retrieved from other sources. Wave data was made available using the global wave model WaveWatch III (WW3DG, 2019), which uses measurement buoy stations around the world to hindcast and validate worldwide wave data.

Other data that were not available and were not able to be retrieved by other means are wind and water level data. The influence of the absence of this data is discussed in the Discussion (Chapter 6).

Validation

Another consequence of being in a data poor environment for a modelling study is the impossibility of validating the model results (shown in Chapter 4) using real data. For this reason, expert judgement is used to assess 1) whether the results are realistic given the environmental conditions and, 2) if the results can be used to draw conclusions about the hydro- and morphological conditions on the island.

2.2 Physical Analysis

2.2.1 Geography

San Andrés has a volcanic origin during the early Cenozoic, after which slow subsidence of the volcanoes and colonization of their tops by coral species followed. These allowed the formation of carbonate platforms bordered by shallow reefs, which became atolls once the subsidence stopped (INVEMAR, 2015).

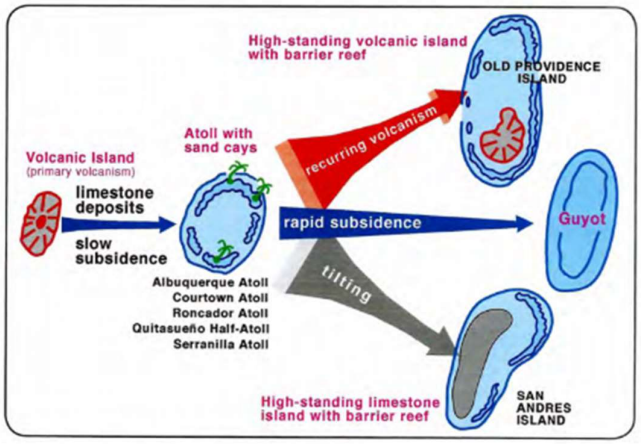

Figure 2.1: Origin of San Andrés, Providencia and other atolls of the Archipelago (Geister & Dias, 2007)

Due to a tilting movement of the atoll, the West side of the island started to sink while the East side rose until a height of approximately 90 m above sea level (which remains until now). With the subsidence of the East side of the atoll, a shallow platform was created on which the barrier reef and the coral lagoon of San Andrés could be formed. The origin of island explains lack of high elevated areas (mean elevation of 1.5 m and max peak elevation of 90 m) and the steep slopes on the West coast (INVEMAR, 2015).

The archipelago of San Andrés is located on the SE edge of the Nicaraguan continental shelf. For this reason, the edges of the island present relatively steep slopes. Figure 2.2 shows part of the bathymetry of the Caribbean Sea and how the island is located just outside the continental shelf.

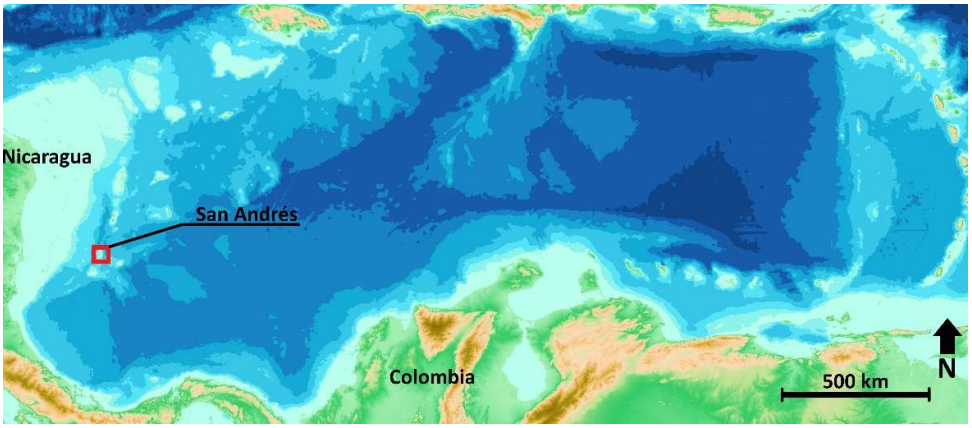

Figure 2.2: Part of the bathymetry of the Caribbean Sea (GEBCO, 2020). The Nicaraguan Continental Shelf can be identified by the light blue colored area around the coast of Nicaragua.

2.2.1.1 Climate

San Andrés Island is located at the Northern side of the Intertropical Convergence Zone (ITCZ). The climate is warm, humid, the Trade Winds blow from the NE and the yearly mean temperatures is 27.5 °C with little variation in between months (INVEMAR, 2009). The archipelago has a bi-modal regime with a dry season, between January and April, and a rainy season, between May and December (Rodrigues Romero, et al., 2020).

As San Andrés is located near the tropics, tropical storms are often developed over sea under the influence of high surface temperatures, approaching the island and potentially causing great damage (Bosboom & Stive, 2021).

2.2.1.2 Extreme weather conditions

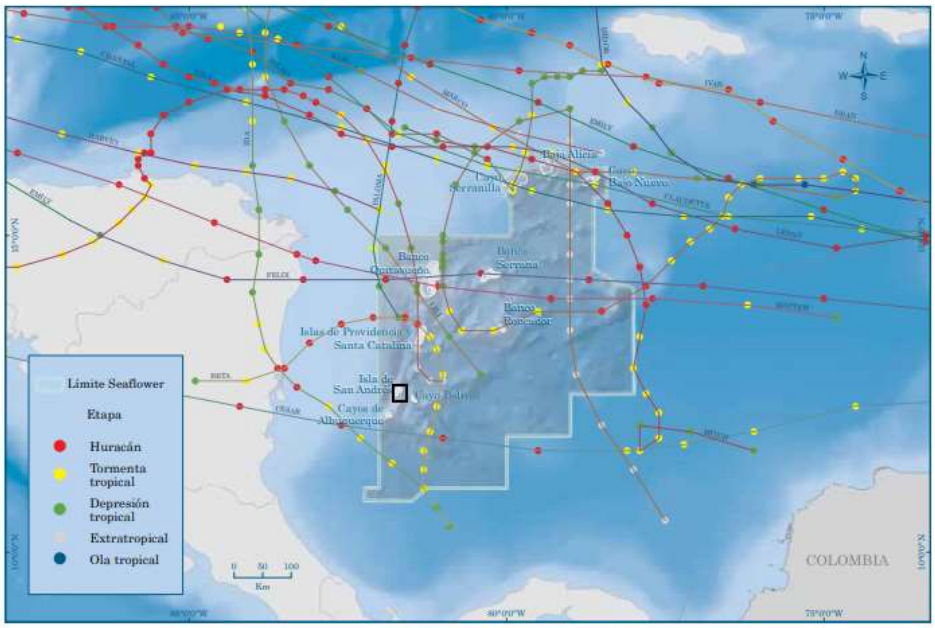

Figure 2.3: Tracks of different storms that influenced San Andrés in the past 25 years. The trajectories of the storms are mostly from E and SE. The black square indicates the location of San Andrés, and the colors correspond to the different type of storm (D. I. López, C. Segura-Quintero, P. C. Sierra-Correa, & J. Garay-Tinoco, 2012).

As described before, the prevailing winds on San Andrés are the Trade Winds from the NE. However, between the months of September to November extreme weather events can be observed on the island (and in the rest of the Caribbean). Figures 2.3 and 2.4 show the hurricanes and storms by which San Andrés has been influenced in the past 60 years.

Hurricanes and tropical storms registered around San Andrés between 1952 and 2011

Name	Date	type	Name	Date	type
Fox	Oct-52	Hurricane	Chantal	Aug-01	Hurricane
Carla	Sep-61	Tropical Storm	Isidor	Sep-02	Hurricane
Hattie	Oct-61	Hurricane	Claudette	Jul-03	Tropical Storm
Alma	Jun-66	Hurricane	Ivan	Sep-05	Hurricane
Beulah	Sep-67	Hurricane	Emily	Jul-05	Hurricane
Alma	May-70	Hurricane	Wilma	May-05	Hurricane
Edith	Sep-71	Hurricane	Beta	Oct-05	Hurricane
Gilbert	Sep-88	Hurricane	Dean	Aug-07	Hurricane
Joan	Oct-88	Hurricane	Felix	Aug-07	Hurricane
Bret	Sep-93	Hurricane	Paloma	Nov-08	Hurricane
Cesar	Aug-96	Hurricane	Ida	Nov-09	Hurricane
Lili	Oct-96	Hurricane	Karl	Sep-10	Hurricane
Marco	Nov-96	Hurricane	Matthew	Sep-10	Hurricane
Mitch	Nov-98	Hurricane	Harvey	Aug-11	Tropical Storm
Lenny	Nov-99	Hurricane	Rina	Oct-11	Hurricane

Figure 2.4: On the left: tracks of different storms that influenced San Andrés in the past 25 years. The trajectories of the storms are mostly from E and SE. The black square indicates the location of San Andrés, and the colors correspond to the different type of storm. On the right a table with tropical storms and hurricanes registered around San Andrés in the past 60 years Data retrieved from NOAA (D. I. López, C. Segura-Quintero, P. C. Sierra-Correa, & J. Garay-Tinoco, 2012).

When reaching the coast of San Andrés, these events produce storm waves of up to 6 m, heavy rains, and wind velocities of over 120 km/h. Studies show that on average the island of San Andrés is heavily affected by hurricanes at least once every 10 years (Royero et al., 2015; Rangel-Buitrago et al., 2015).

Figure 2.5: Top view of Spratt Bight. The coral barrier reef can be identified by the offshore breaking waves on the NE side of the island.

As shown in Figure 2.5, Spratt Bight is protected by a coral barrier reef. During extreme weather events, waves reaching the beaches behind the coral reef have less than 1 m of significant height, as will be shown in Chapter 4. Figure 2.6 shows the significant wave heights and periods around San Andrés during extreme weather conditions caused by hurricane Joan in October 1988 (the biggest of the last 40 years).

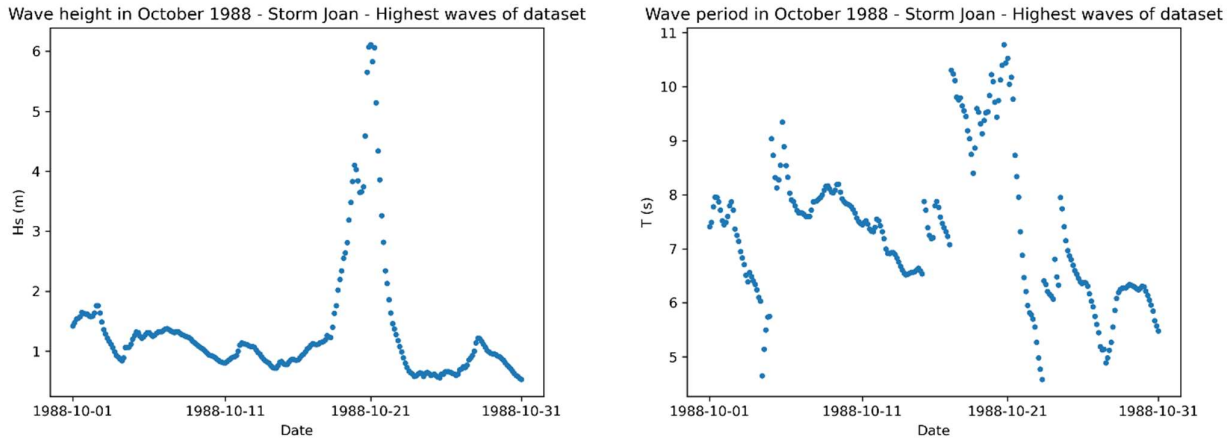

Figure 2.6: Wave height and wave period during storm Joan in October 1988, the biggest storm of the past 40 years. Wave heights reached over 6 m with wave periods above 10 s. Dataset retrieved from WW3.

2.2.2 Bathymetry

The bathymetry data is retrieved from different sources:

- Data received from a field study performed by INVEMAR in 2018.
- NAVIONICS nautical chart (2021)
- CIOH (Center of Ocean and Hydrological Investigation of Colombia) Nautical chart (2008)
- Information from a study made by FINDETER (Territorial Development Financer in Colombia) (2020)
- GEBCO (2020)

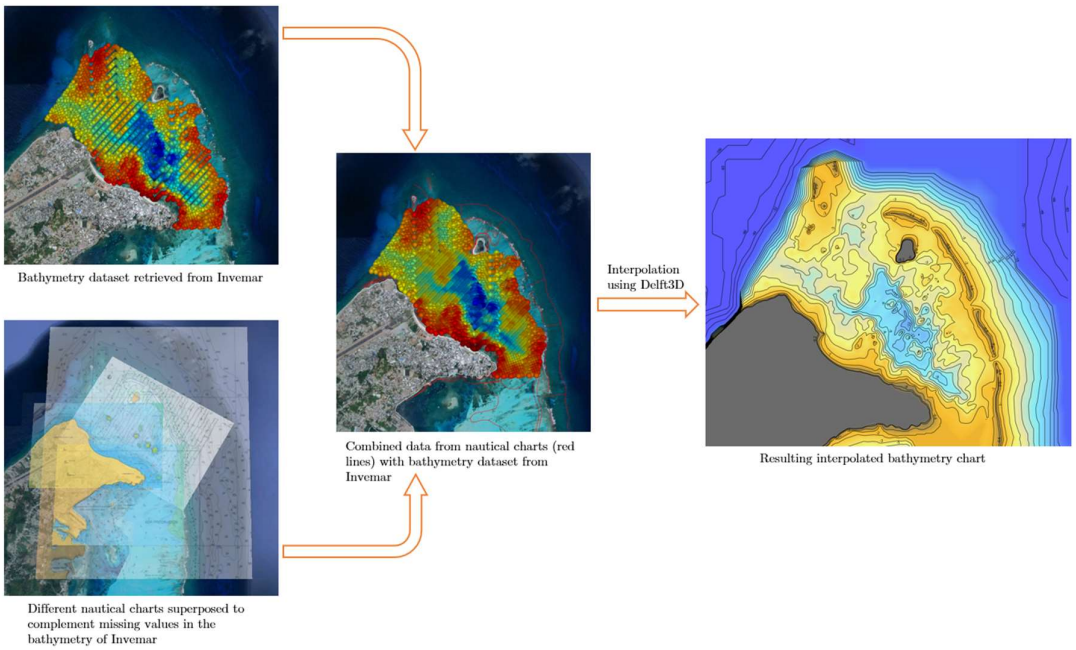

Figure 2.7: Method used to obtain an integral and complete bathymetry dataset based on the retrieved data from INVEMAR and other sources.

The data received from INVEMAR was used as the main and most reliable data source, and therefore the basis for the dataset. However, as there were a few missing gaps in the retrieved data, complementary information needed to be consulted. In Appendix A the composition of the bathymetry data is in depth described and in Section 6 the consequence of having multiple data sources for the bathymetry is discussed. Figure 2.7 shows a schematization of how the bathymetry was composed.

2.2.2.1 Analysis of the bathymetry

The bathymetry of the coastal and nearshore area of San Andrés consists of a few features that greatly influence the wave environment and sediment transport in the area. Figure 2.8 shows a schematization of the bathymetry based on a survey made in 2018 by INVEMAR (Institute for Marine and Coastal Investigation).

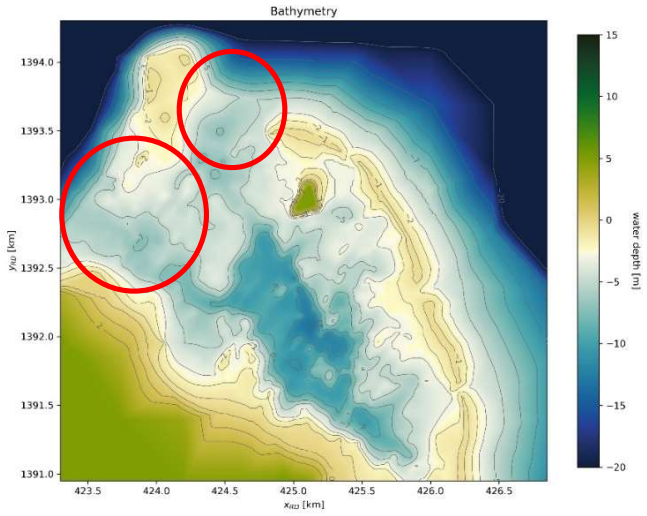

Figure 2.8: Bathymetry of the focus area of this study, in Spratt Bight, San Andrés. The red circles indicate the openings in the coral reef through which wave energy can penetrate.

SAI it is surrounded by a coral reef with an approximate depth of 0.5 m below MSL. This reef is an important wave breaking feature that dampens and reduces the waves. This less energetic environment in the lagoon behind the reef allows sand to accumulate in the behind laying beaches. Spratt Bight Beach can therefore exist in (dynamic) equilibrium. The lagoon is approximately 2.5 km wide (between coast and coral) and has an important wave attenuation effect, decreasing the wave height due to wave-seabed interaction before reaching the shore.

In the barrier coral chain, a few gaps have been observed through which waves propagate inside the lagoon. As a result of these gaps, the environment within the lagoon can get more energetic depending on the waves approaching the island. As can be seen in Figure 2.8, on the NW side of the island 2 major openings can be observed through which wave energy can penetrate the inner lagoon. The Northern and Western openings are respectively 700 m and 1 km wide. They have both a maximum depth of 6 m.

Breakwaters

The breakwaters of Spratt Bight also take part of its morphological system. Figure 2.9 shows the location of the 3 breakwaters in Spratt Bight Beach: Espolón Pescadores, Espolón Tiúna and Espolón Jenos Pizza. There is not much data about their condition, exact depth, and effectivity. From satellite data it can be seen that sand might be retained by Espolón Pescadores and Espolón Tiuna.

Figure 2.9: Location of the breakwaters at Spratt Bight Beach.

Espolón Jenos Pizza and Espolón Tiúna were not properly included in the retrieved bathymetry dataset. This might have some consequences for the modelling study presented in Chapter 4. This limitation will be further explained in Chapter 6.

2.2.3 Hydrodynamic Conditions

2.2.3.1 Data source

Wave data was retrieved from a dataset of 30 years (between 1979 and 2009) at measuring station 42058 located at 14.394° N 74.816° W, approximately 775 km E from San Andrés. To be converted into usable data for the location of San Andrés, a wave transformation was made using hindcast model WaveWatchIII (WW3) (2019). WW3 is a third-generation wave model developed at NOAA/NCEP and is an already validated global hindcast wave model, where data can be extracted at specific geographical locations.

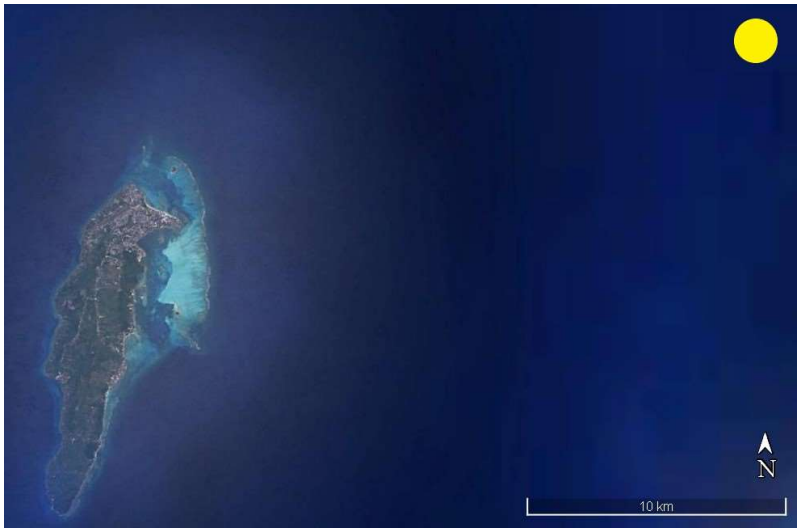

Figure 2.10: The yellow dot indicates the location from which the WW3 wave data was retrieved.

WW3 has a grid width of 0.1° in both North-South and East-West directions. Figure 2.10 shows the location at which the data used was extracted from the model. Further information about the offshore wave data is described in Appendix B. Figure 2.11 shows the timeseries of the wave height retrieved from WW3.

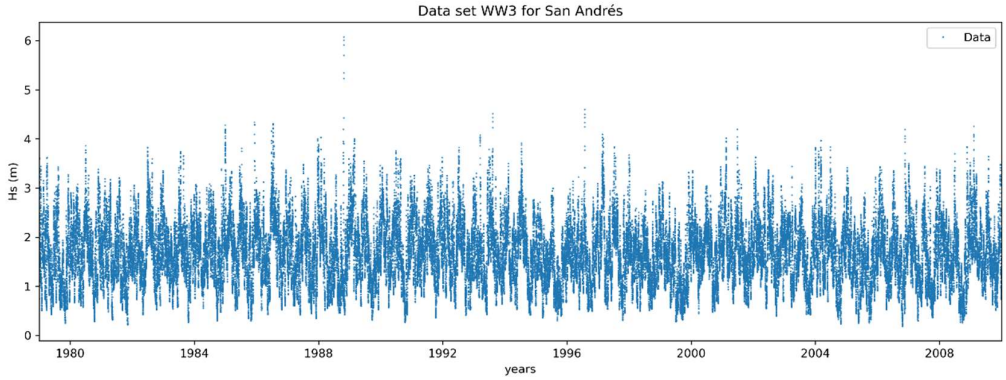

Figure 2.11: Timeseries of 30 years retrieved from WW3 model at the location indicated in Figure 2.10.

2.2.3.2 Wave climate

As described before, the hydrodynamic conditions in San Andrés are characterized as a wave dominated environment. The wave climate at the island is mainly composed by wind and swell waves, generated by the Trade Winds and storms in the Caribbean Sea. There, the fetch length can reach up to 2000 km, which means that there is no fetch restriction. As described in Section 2.2.1.2 , during storms, the maximum wave height can reach up over 6 m with a corresponding wave period of over 11 s.

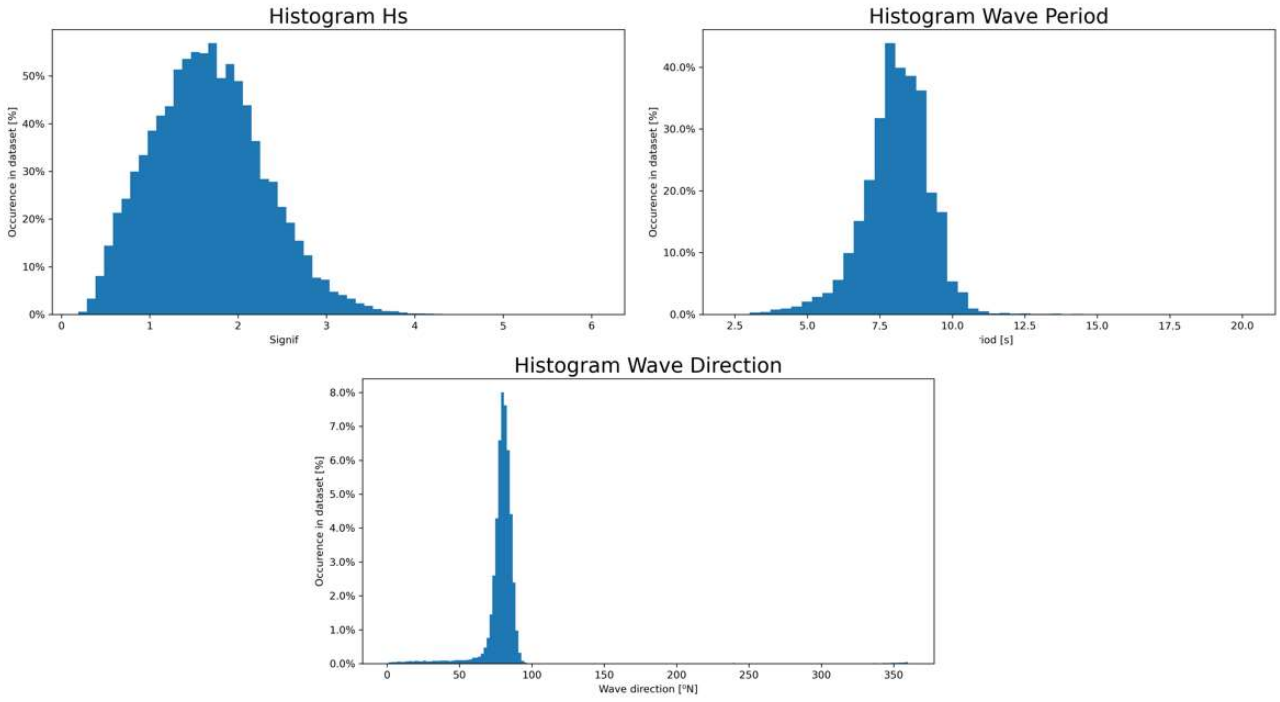

Figure 2.12: Histograms of the wave climate in San Andrés. On the left the wave height, on the right the wave period and the lower figure represents the wave direction. The histograms were produced using the 30 years dataset shown in Figure 2.11.

Deep water waves approaching the island are predominantly from the East ($\varphi_{w,mean} = 80^oN$) and exhibit typically a wave period between 6 s and 10 s (T_p= 8 s) and wave heights between 0.5 m and 3 m (H_s = 2.1 m). A wave height of 3.5 m

is exceeded 1% per year ($H_{1\%} = 3.5$ m, $T_{1\%} = 10$ s). The histograms above show the statistics of the offshore wave climate of San Andrés.

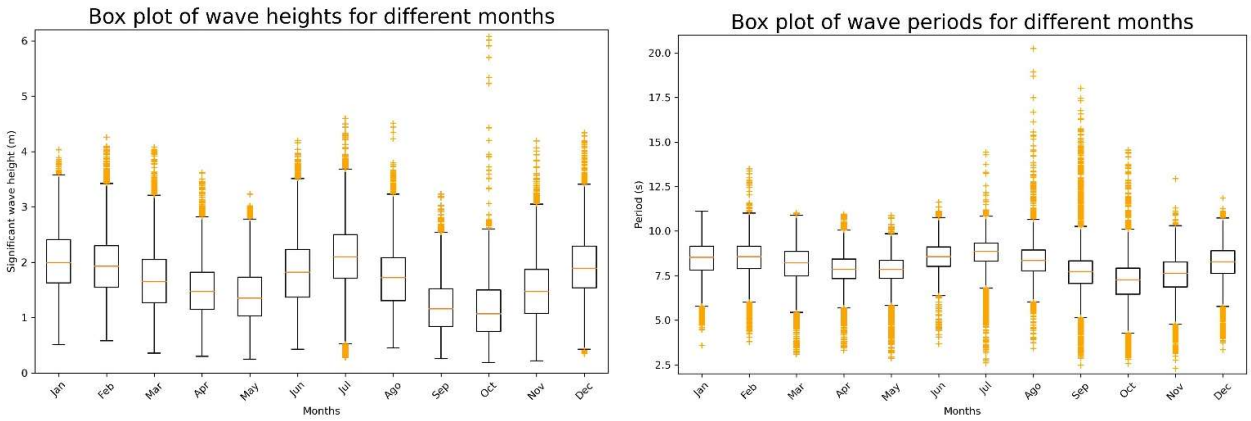

Figure 2.13: Boxplots representing seasonal wave height and wave period on San Andrés. The boxplots are produced using the 30 years dataset.

The boxplots of Figure 2.13 show the wave heights and period over the different months. It can be seen that the highest during the storm months (northern hemisphere winter) and in July, which coincides with the most rainy month on the island (Rodrigues Romero, et al., 2020). It can also be seen that the high period events (swell) can mostly be observed between July and October.

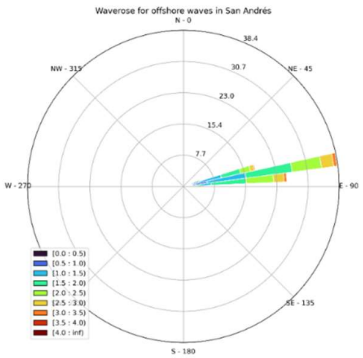

Figure 2.14: Wave rose for offshore waves approaching San Andrés

Figure 2.14 shows the wave rose for the offshore waves approaching San Andrés. It can be seen that the wave direction is very concentrated and from the East, such that 90% of the waves are coming between 70°N and 90°N. This is further reinforced by the histogram of Figure 2.12. The consequence of that is that beaches (including Spratt Bight), and mostly the barrier reef on the east side of the island are under constant wave attack.

A less frequently observed wave angle of incidence are that of the Northern waves. 1.5% of the incident waves are coming between -20°N and 20°N. However, these waves might have a great impact on the morphology of Spratt Bight (as will be seen in the next sections). The figure below shows a boxplot of the whole wave climate over the different months. It can be seen that most of the outliers towards the north happen between October and March, which coincides with the storm season which is between October and December.

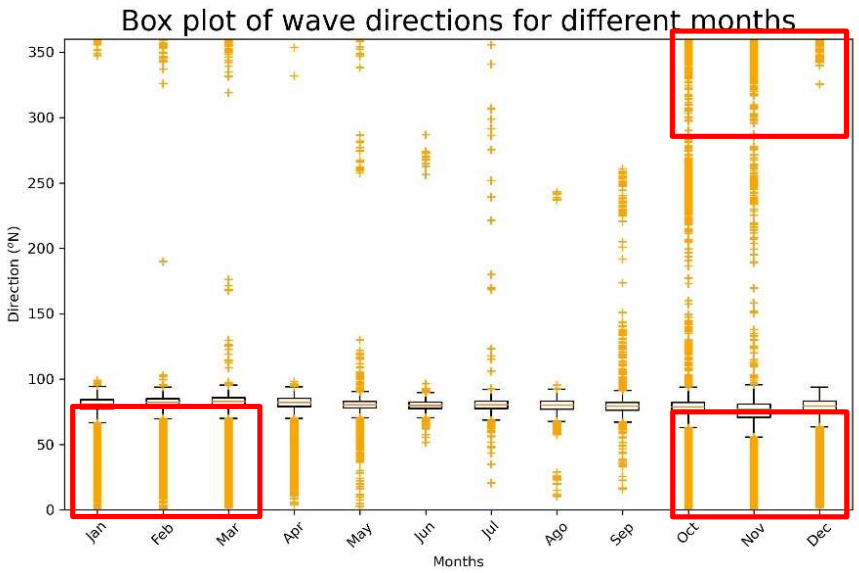

Figure 2.15: Boxplot representing seasonal wave direction on San Andrés. The red rectangles indicate the periods in which the northern waves are mostly observed as outliers. The boxplot is produced using the 30 years dataset.

This seasonality of the Northern waves is confirmed by the figure below. Figure 2.16 shows a histogram indicating at which months the Northern waves were observed in the past 30 years. It can be seen that, as also shown in the boxplot above, most of these waves are observed between October and March.

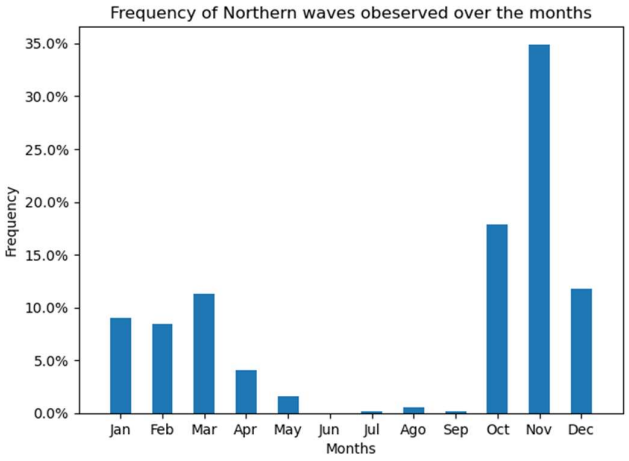

Figure 2.16: Histogram showing the months in which Northern waves are reaching San Andrés.

These waves have similar characteristics to the mean wave environment presented in the boxplots and histograms of Figure 2.12 and Figure 2.13. From waves coming from the North significant wave heights of $H_{s,North} = 2.3$ m and peak period of $T_{p,North} = 9$ s can be observed.

Figure 2.17 shows the boxplots of the significant wave height and wave period for waves coming from the north. It can be seen that the wave heights over the months are relatively similar to those for the total wave climate, except for the fact that between April and September there are almost no Northern waves.

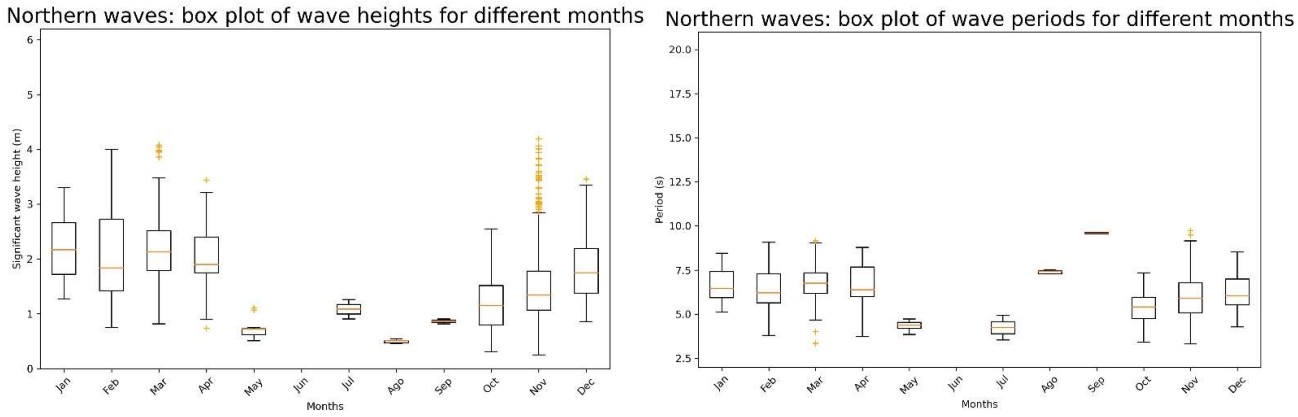

Figure 2.17: Boxplot representing seasonal wave height (on the left) and period (on the right) for Northern waves approaching San Andrés. The boxplots are produced using waves coming from the North (between -20°N and 20°N) within the 30 years dataset.

A larger difference can be observed between the wave periods of the Northern waves and the year around conditions. This can be explained by the fact that no swell kind of events can be observed coming from the North. This is most likely due to the shorter fetch length observed in northern direction and the Trade winds and storms that are mostly from the East. When decomposing the wave height and period into different bins of 20° as shown in the figure below, this effect can be better observed.

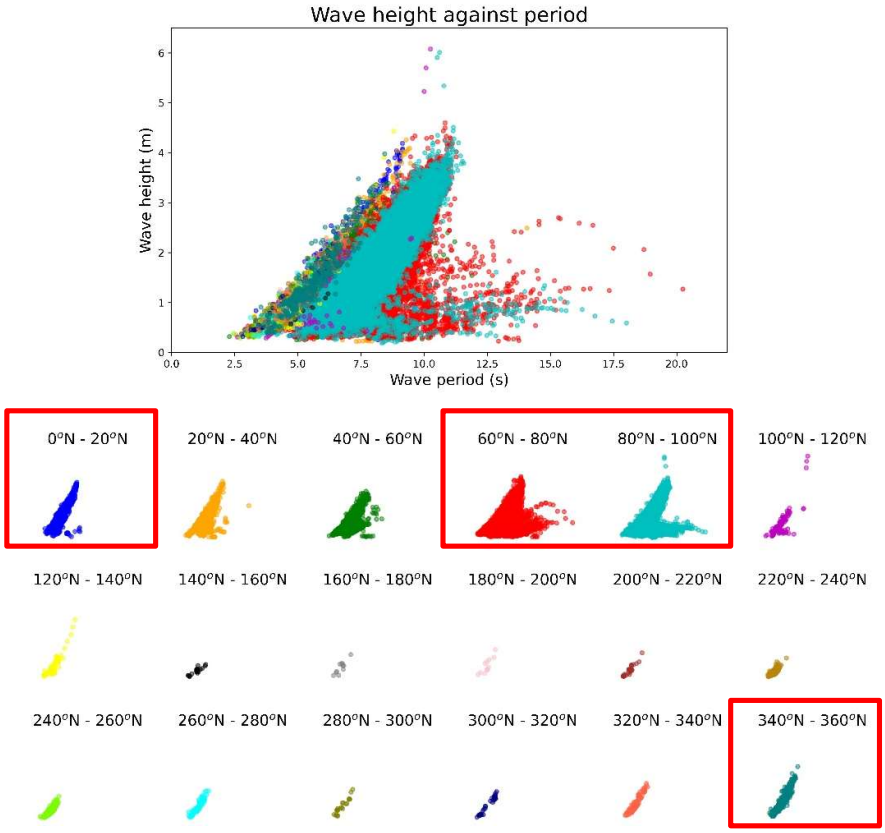

Figure 2.18: Wave height plotted against wave period. The different colors represent bins of 20° from 0°N to 360°N. The red squares indicated the waves coming from the North (340°N - 360°N & 0°N - 20°N) and waves coming from the East (60°N – 100°N), which is the most dominant direction.

Figure 2.18 shows the wave height plotted against the wave period for different directions (represented by the different colors. It can be seen that waves coming from the East (between 60°N and 100°N) contain sea waves as well as swell waves (long period and small height). On the other hand, the Northern waves are predominantly composed by sea waves. These wave characteristics are further reinforced with Figure 2.19, in which the mean wave height, period and steepness are shown for each 2° bin (as done in the direction histogram in Figure 2.12).

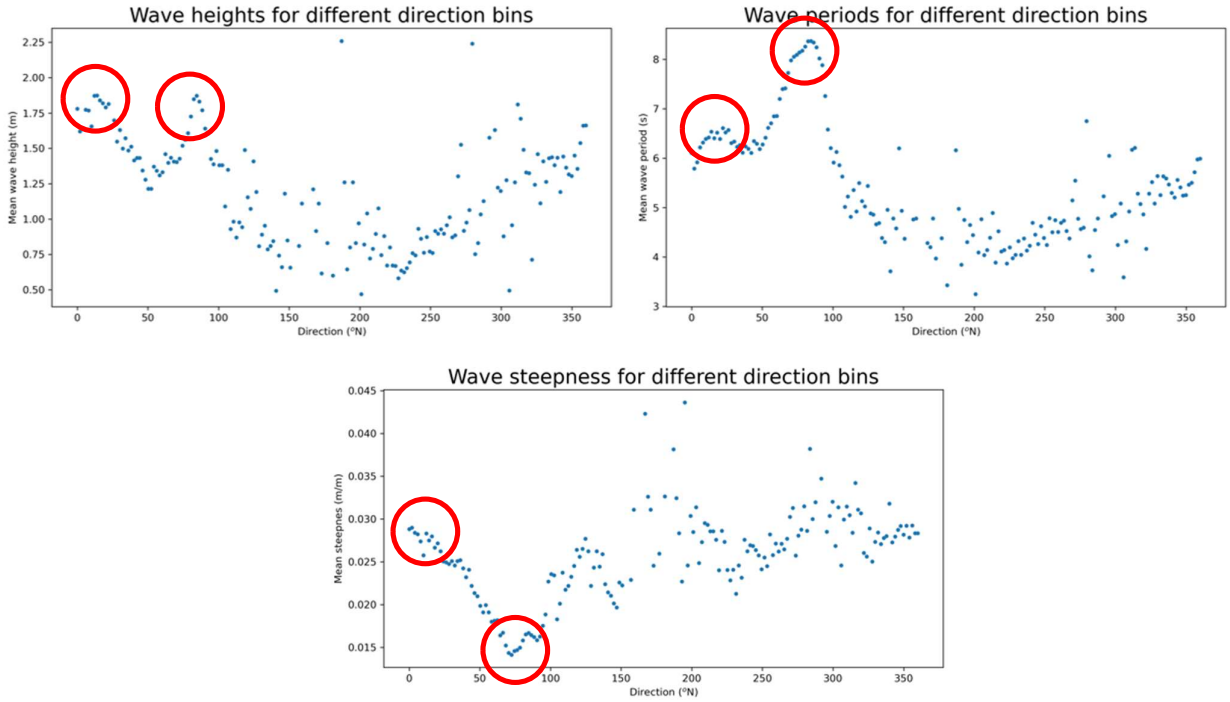

Figure 2.19: Mean wave height, period, and steepness for waves within direction bins of 2° (as shown in the direction histogram of Figure 2.12). For every bin the wave height, period and steepness were calculated. The used is from the 30 years dataset.

It can be seen that waves coming from the North (indicated with the red circles close to 0°N) have similar mean wave heights to those coming from the East, however the mean wavelength and steepness differ.

2.2.3.3 Tidal conditions

Although water level data was not made available, it is known that the tidal environment of the Colombian Caribbean Sea is quite regular throughout the year. Figure 2.20 the tidal characteristics of the Caribbean Sea. As shown in the figure the tidal environment of San Andrés is characterized by being a micro-tidal environment, mixed (mainly semi-diurnal), with a maximum range not higher than 0.5 m.

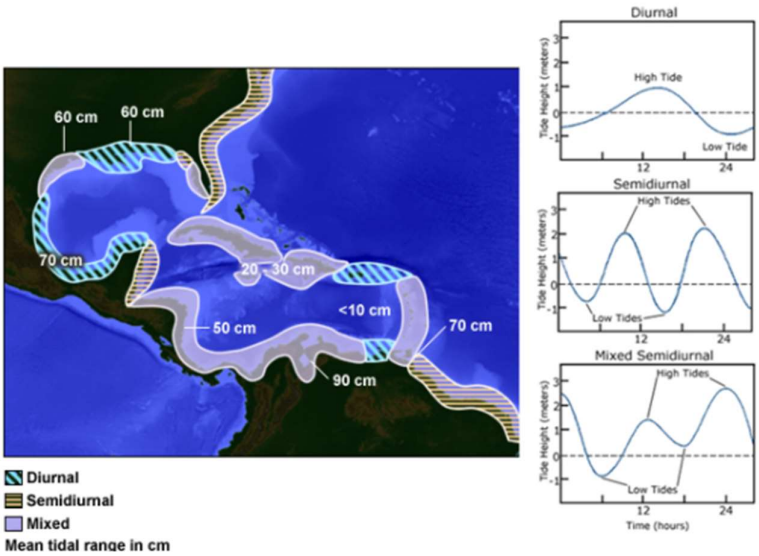

Figure 2.20: Tidal regime of the Greater Caribbean (Smithsonian Tropical Reaserch Institute, 2015)

As the tidal maximum tidal range in San Andrés is between 0.3 and 0.4 m (Rodrigues Romero, et al., 2020) and the significant wave height of the approaching waves is higher than 2 m, the environment on SAI can be defined as being wave dominated. Figure 2.21, shows the relationship between mean tidal range and wave height, confirming the wave dominance in the area.

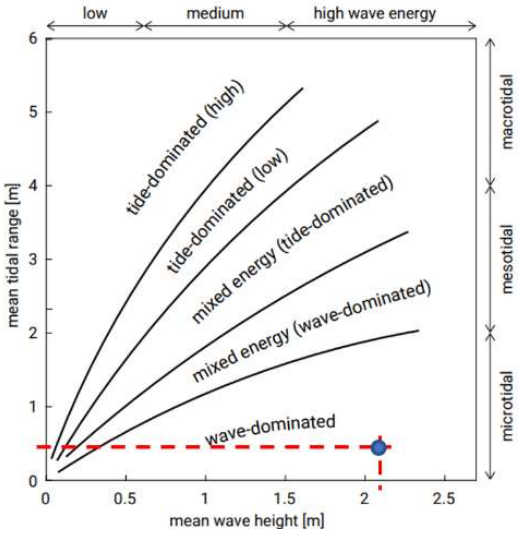

Figure 2.21: Relationship between mean tidal range and wave height, defining wave and tide dominance (Bosboom & Stive, 2021)

The influence of the tide on the system is limited due to its small tidal range. The horizontal tide can be assumed to be very small, even negligible. However, the vertical tidal component might be of some importance regarding the amount of the wave energy that can be passed through the coral reef and reach the beach at Spratt Bight. During high tide more wave energy is able to reach the beach than during low tide, when the coral reef can better block the waves. More explanation about the assumptions made in this research is made in Section 3.2.

2.2.3.4 Relative Sea Level Rise

Considering that San Andrés is not highly elevated above sea level (on average 1.5 m above sea level), SLR (Sea Level Rise) presents a threat to the island. Besides, small subsidence rates has been observed on the island due to tectonic activity (Geister & Dias, 2007). This, in combination with eustatic SLR, can lead to an increased relative sea level rise, consequently resulting in higher erosion rates.

However (as shown in the figure below), studies show that the sea level in the Colombian Caribbean have (relatively) risen approximately 22 cm in the last fifty years, which is under the world average (Posada, Henao Pineda, & Morales-Giraldo, 2011).

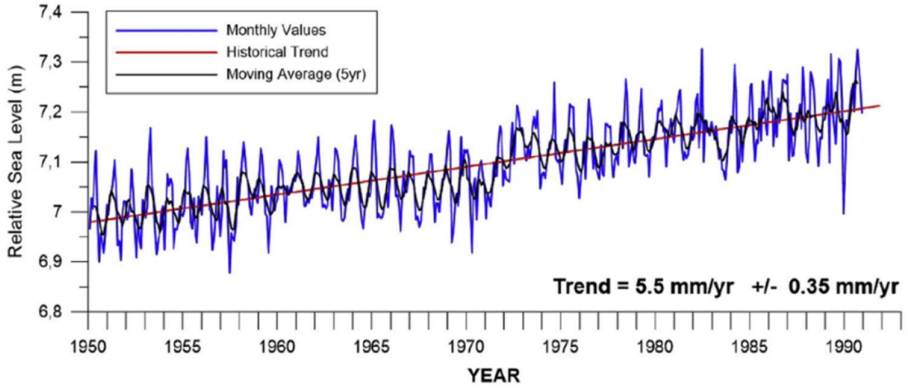

Figure 2.22: Sea level time series of the past 50 years for the Cartagena de Indias station (Rangel-Buitrago, Anfuso, & Williams, 2015)

2.2.4 Morphology

2.2.4.1 Sediment characteristics

The sandy beaches of San Andrés are formed by fine white sand with pink tones due to its biogenic origin. The sand is composed of small particles of calcium carbonate originated from corals, algae, and microscopic shells. In the vicinity of mangroves (southern part of the Island), the sediment tends to be finer and have particles of decomposed organic matter. A field study carried out by INVEMAR in 2021 in the same context as this research, presented an indication of the grainsizes and material type that can be found near Spratt Bight. The figure below indicates the sites in which the samples were collected.

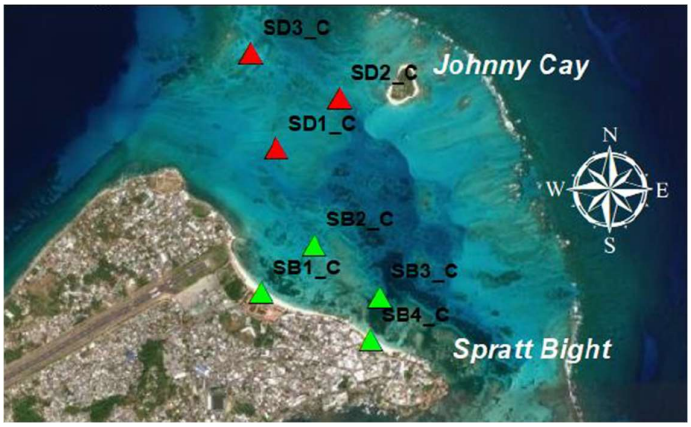

Figure 2.23: Locations in Spratt Bight from which samples were collected for a granulometric analysis.

Figure 2.24 shows the results from the granulometric study. It can be seen that the sediment types are very similar all around the Spratt Bight coastal area. At the beach (indicated by SB1 and SB4), fine medium and coarse sand are dominated, while further away from the beach coarser sand starts dominating. This is probably due to the coral particles that are still in the process of decay and becoming finer sand.

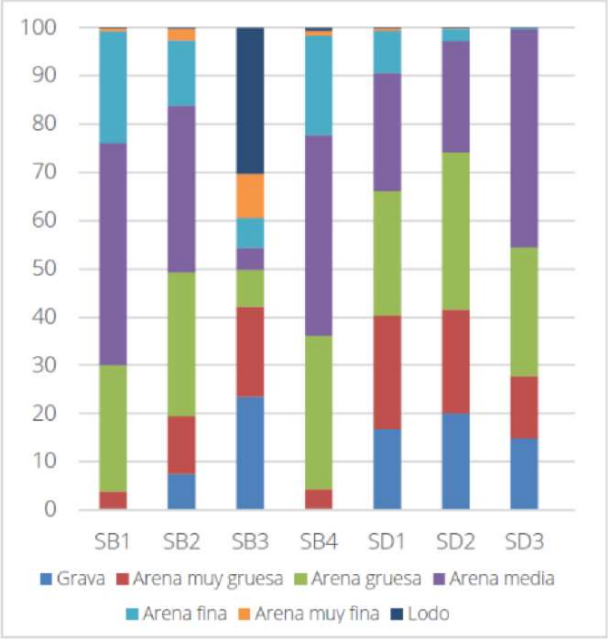

Figure 2.24: Results of the granulometric study done by INVEMAR. The sediment is described for the different locations at which samples were collected. The blue bar represents gravel ($d_{50} > 2$ mm), the red bar represents very coarse sand (2 mm $> d_{50} > 1$ mm), the green bar represents coarse sand (1 mm $> d_{50} > 500$ µm), the purple bar represents medium sand (500 µm $> d_{50} > 250$ µm), the light blue bar represents fine sand (250 µm $> d_{50} > 125$ µm), the orange bar represents very find sand (125 µm $> d_{50} > 63$ µm) and the dark blue bar represents clay ($d_{50} < 63$ µm).

As there are no sediment providing rivers or other sources, decomposed and grinded coral and seagrasses are the main sources of sediment to the island's beaches (Coca-Domínguez, et al., 2019; Rodrigues Romero, et al., 2020). It has been found that a seagrass specie called Halimeda (also known as watercress alga or 'alga calcárea' in Spanish) can be responsible up to 50% of the sediment sources in the Caribbean, which could also count for also in San Andrés. When these seagrasses die out, a calcareous skeleton is left, which when crushed form organic sediment particles. It would be of importance estimate the portion of which Halimeda is responsible for the sediment source in San Andrés in order to be able to understand the main sediment sources on the island (Universidad del Norte - IDEHA, 2009).

2.2.4.2 Sediment Transport

In Spratt Bight, high morphological variability is observed during the months of December and January, where the beach presents big differences of accretion and erosion areas. This is related to the season's strong winds and waves associated with the storm season, which is approximately in the same period (Coca-Domínguez, Ricaurte Villota, D.F. Morales-Giraldo, & Luna, 2019).

During the calmer months (between March and August), accretion can be observed towards the West side of the beach, while during more energetic storm events erosion is observed on the west and accretion on the east of Spratt Bight Beach (Coca-Domínguez, Ricaurte Villota, D.F. Morales-Giraldo, & Luna, 2019; FINEDETER, 2020). Figure 2.25 shows an overall impression of the sediment transport patterns at the Spratt Bight Beach during episodic events and under normal conditions, retrieved from a report made by FINDETER (2020) about the erosion problem in SAI.

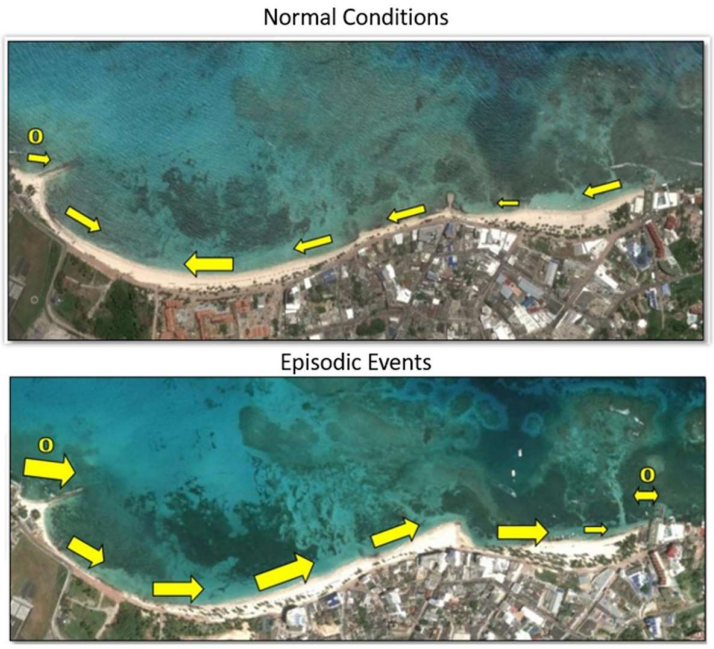

Figure 2.25: Sediment transport patterns on the Spratt Bight Beach. The yellow arrows indicate the direction of the sediment transport rates (FINEDETER, 2020).

The same study showed that beach profiles in Spratt Bight (between 2004 to 2016) have varied up to 30 m (seawards and landwards) between the different years. Nevertheless, when comparing similar months over different years, there is no clear evidence of structural erosion. What can be observed is a shift of sediment volume from NW to SE and vice-versa. There is no clear evidence of net sediment loss in any case. The figure below shows the results from the study made by FINDETER with the different beach profiles over the years.

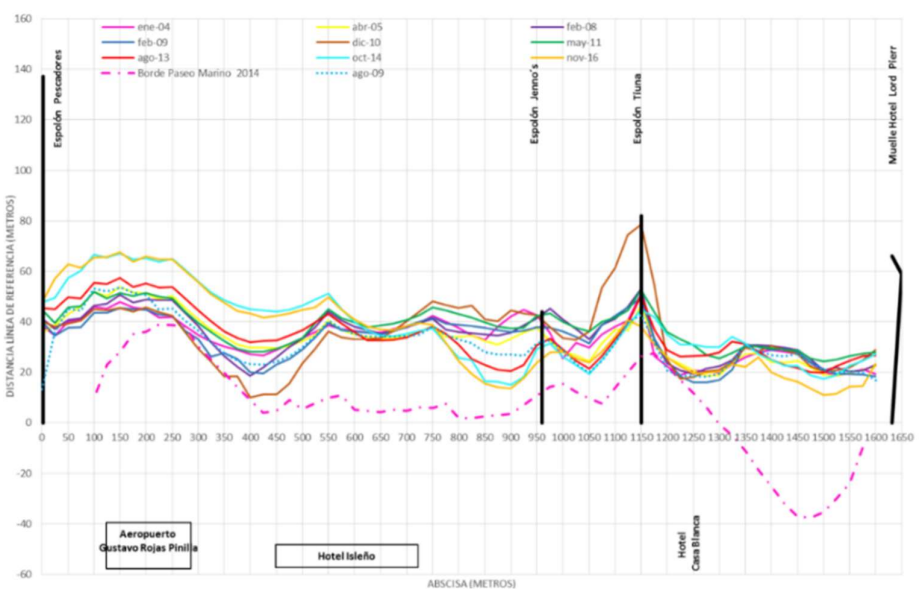

Figure 2.26: Beach profiles over the years within different months (seen from above). In the figure the different break waters are schematized with the thick black lines and the boulevard is represented with the pink dashed lined. The remaining colored lines represent the beach profiles over the years (FINEDETER, 2020).

As can be seen in the figure above, depending on the months, seasons and years, erosion and accretion rates can vary a lot. Longshore transport patterns move sand not only in NW/SE direction, but also in the cross-shore direction having net erosion in some periods and accretion in others depending on seasonality. This is compared by the analysis made in Figure 2.27, which shows a comparison of the beach profiles between the more variable seasons (between November and February) and the milder periods (between April and August).

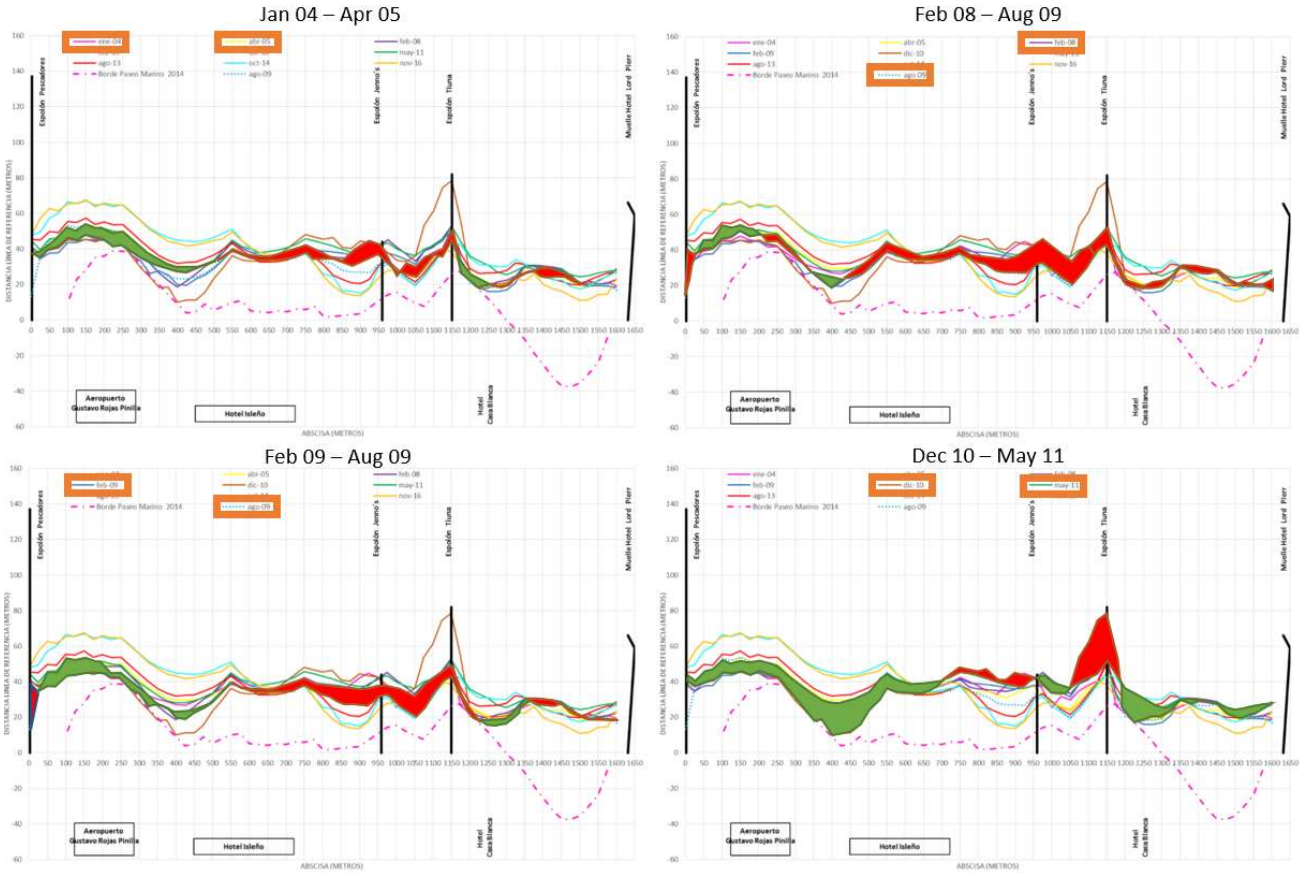

Figure 2.27 Schematization of erosion (green shaded) and accretion (red shaded) over the years at Spratt Bight Beach. The upper left figure compares the beach profile of January 2004 with April 2005. The upper right figure compares the beach profile of February 2008 with August 2009. The lower left figure compares the beach profile of February 2009 with August 2009. Finally, the lower right figure compares the beach profile of December 2010 with May 2011. The thick black lines represent the breakwaters of Spratt Bight Beach. Modified from (FINEDETER, 2020).

Figure 2.27 compares beach profiles during the mild seasons with the profiles during energetic and variable seasons. When comparing these two periods, it can be seen that during mild seasons, erosion is observed near the west side of the Espolón Tiúna (breakwater on the East). At the same time, accretion is observed on the east side of the Espolón Pescadores (breakwater on the West). This means that during the more energetic periods the opposite happens: erosion on the West side of the beach and accretion on the East.

In Figure 2.28 a clear example of this effect is shown. Here the beach profile of August 2009 is compared to the beach profile of December 2010. It can be seen that in December 2010 there was an erosion event at Espolón Pescadores, where the waterline reached the boulevard of Spratt Bight (pink dashed line). At the same time, a great accretion pattern can be observed the west side of Espolón Tiúna. This accretion/erosion behavior suggests a sediment transport pattern direct to the east during these months, while a westward directed sediment transport pattern is observed during the milder months

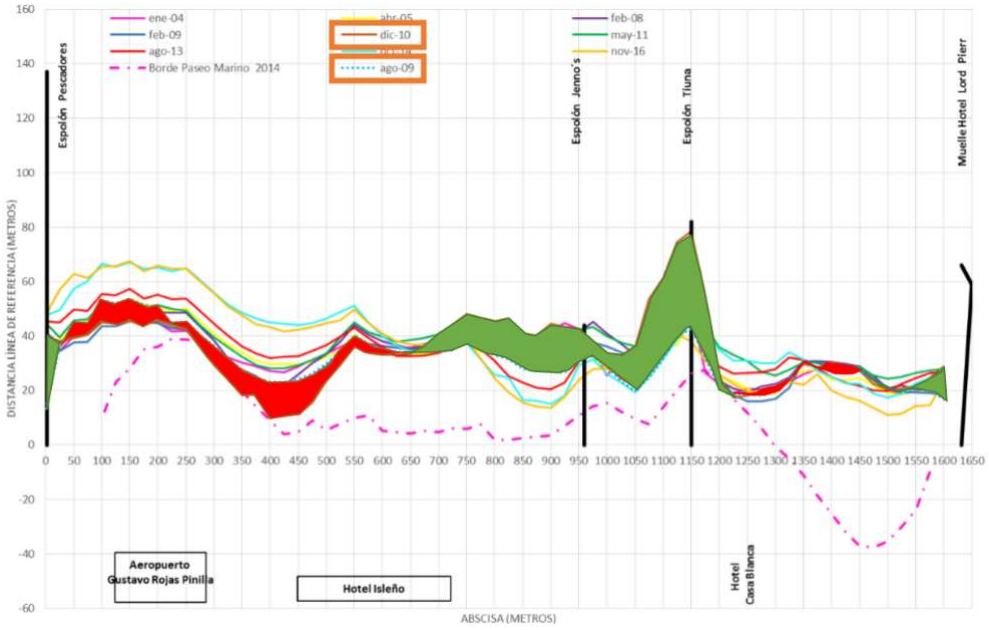

Figure 2.28 Schematization of erosion and accretion over the years at Spratt Bight Beach. Red represents erosion and green accretion. The image compares the beach profile of August 2009 and December 2010. The thick black lines represent the breakwaters of Spratt Bight Beach. Modified from (FINEDETER, 2020).

These periods in which these patterns are perceived coincide with the periods in which the Northern incoming waves are most frequent (as shown in the histograms and boxplots of Section 2.1.2.3). While the regeneration period coincides with the milder seasons.

Wind driven transport

As mentioned in Section 2.2.1.2, San Andrés can highly be impacted by extreme weather conditions. These phenomena facilitate loss of sediment from the upper beach to landward direction (as can be seen on the left part of Figure 2.29). Part of the sediment is then lost and disconnected as isolated dunes on the boulevard, generating a continuous output of sediment of the system (Martín-Prieto, et al., 2013).

Figure 2.29: (from left to right) Sand losses from the upper beach by wind action and remains of isolated dunes (Martín-Prieto, et al., 2013)

Dunes are a natural buffer of sediment for the beaches. When dunes are formed outside of the beach and get isolated inland (as shown on the left in Figure 2.29), they become unable to nourish the beach during erosion periods. In this the beaches cannot use this buffer and net erosion rates can increase even more.

2.3 Ecological Analysis

Ecologically speaking, the island of San Andrés and its surrounding marine environment include sandy beaches, mangrove forests, extensive coral reefs (atolls, barriers, and fringing reefs), sea grass beds and deep-water areas (Baine, Howard, Kerr, Graham, & Toral, 2007). All these different environments contribute to the benefits that ecosystems services provide to the inhabitants of the island.

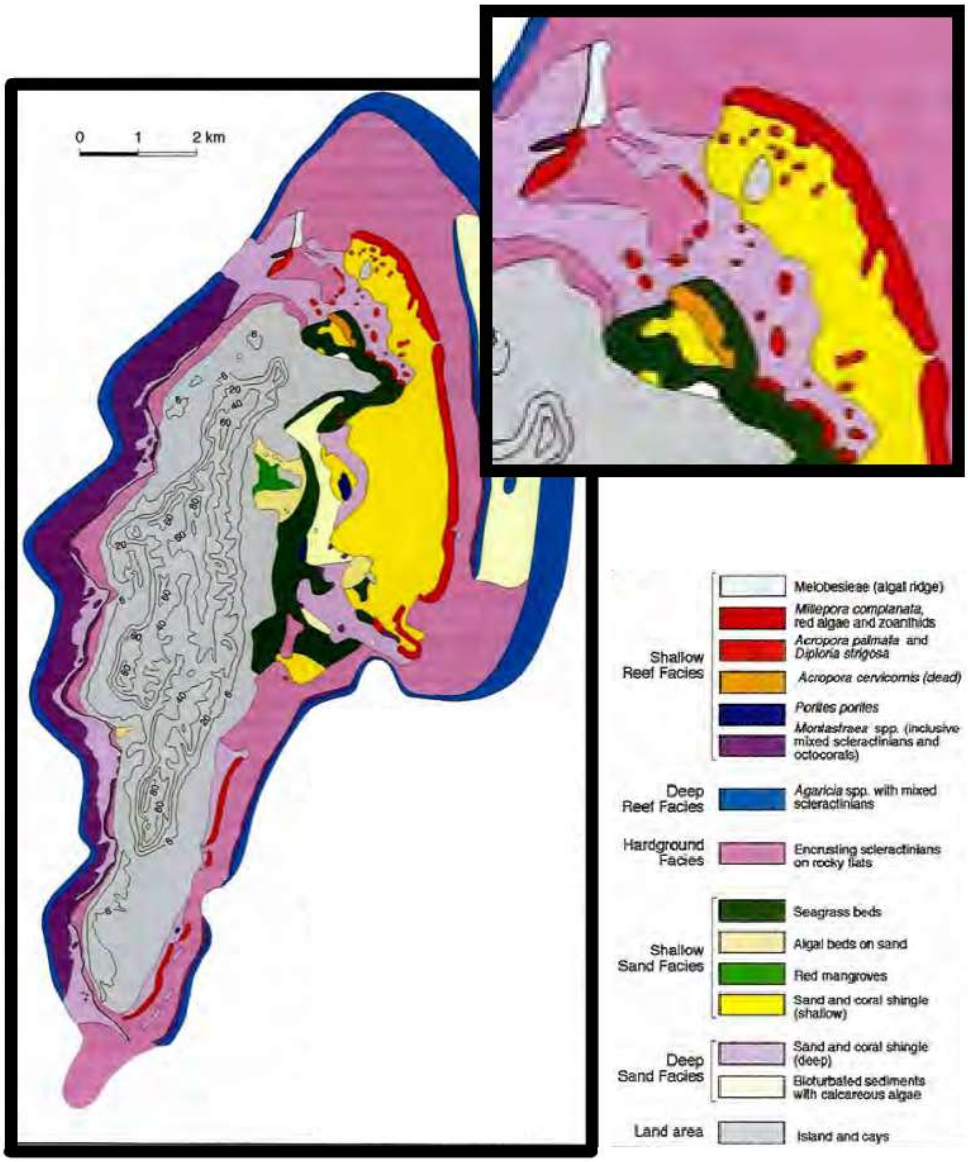

Figure 2.30: Distribution of seabed bottom characteristics on the insular shelf and island of San Andrés. The upper left figure is the zoomed area on Spratt Bight. The different colors represent different components on the bed. In this figure the shallow reef, hard grounds, sandy beds, seagrasses, and mangroves are represented. This figure was modified from Geister & Dias (2007).

Figure 2.30 shows the location of different coastal flora elements near Spratt Bight. It can be noticed that around the study area of this research numerous different ecological features can be observed, including various species of coral and seagrass.

San Andrés is located on the Sea flower Biosphere Reserve (shown in Figure 2.31), which is the largest Marine Protected Area (MPA) of the Caribbean and seventh largest of the world. It was declared a reserve by UNESCO in 2000 and in 2005 it was the first official MPA to be acknowledged by the Colombian government. Currently the area is being managed by CORALINA, which is the autonomous intergovernmental agency that manages and regulates all natural resources on the island (Castaño-Isaza, Newball, Roach, & Lau, 2015).

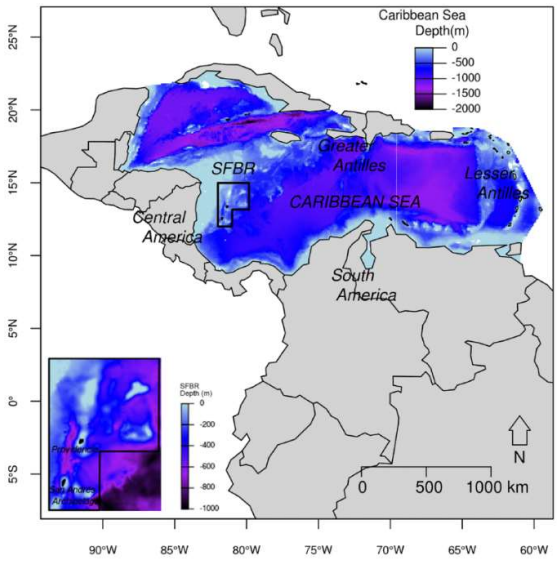

Figure 2.31: Area of the Sea Flower Biosphere Reserve (SFBR) in the Caribbean Sea. The different colors indicate the water depths in the area, showing that the reserve is located at deeper waters, on the edge of the Nicaraguan Continental Shelf (Barragán-Barrera, et al., 2019)

2.3.1 Coral reef

The reef formations are very complex in the Sea Flower Biosphere Reserve (SFBR), and a various coral species can be observed in this area. As the reef is located in open ocean, the coral structures had to adapt to heavy wave action. Between the barrier reef and the island of San Andrés a lagoon has been enclosed, which is rich in sea grass beds and other marine life (Baine, Howard, Kerr, Graham, & Toral, 2007).

The coral reef provides essential ecosystem services to the island of San Andrés. It enhances the local fishery (as fishes are attracted to it) and it functions as a wave breaker against offshore waves, protecting the coastline and the behind laying island. Furthermore, is the main source of sediment to the island beaches. When coral is damaged, eroded or dies out, it becomes a source of sand to the beaches of the island (Coca-Domínguez, et al., 2019; Rodrigues Romero, et al., 2020).

Coral reefs are fragile organisms that are very sensitive to any environmental or biological change. They are extremely sensitive to changes in light (turbidity and depth), temperature, increased and damaging fishing practices, pollution, and excess sediment due to erosion/accretion (The MarineBio Conservation Society, 2021).

Damaged coral reef is one of the factors contributing to coastal erosion in San Andrés. During a study on coral reefs, it has been found that a coral variety of the Caribbean Sea (Acropora Palmata), which is also found in San Andrés, had

suffered a disease (Klooster, 2020). Therefore, at some locations the crest of the barrier reef of San Andrés, which serves as natural protection against waves, died out and eroded, exposing the inner lagoon to more energetic waves. This extra exposure to which the beaches are being subjected, causes them to be more prone to erosion.

Over the last 30 years the coral reefs of San Andres have been slowly degrading. This is accompanied by an increase in the population of macroalgae. This effect in combination with a very slow regeneration and recovery rate of coral species may represent a danger to the health and existence of the coral reef. The figure below shows how the macroalgae population is slowly increasing while the coral population is decreasing. The abundance and richness values of coral species show a phase shift from corals to algae as the dominant organisms (INVEMAR, 2019).

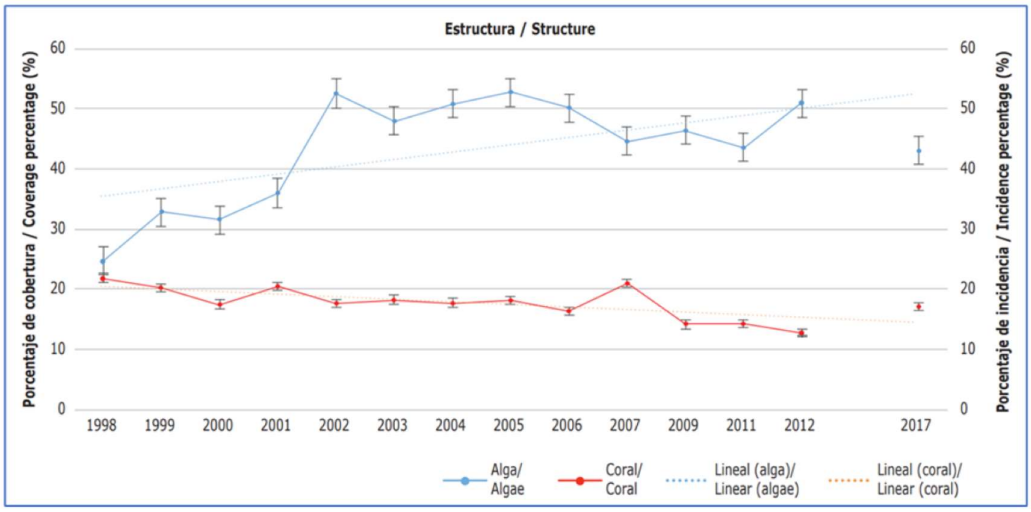

Figure 2.32: The graphs show variations in coral and algal cover and urchin abundance over the 1998-2017 monitoring period (Invemar, 2019). monitoring period 1998-2017 (INVEMAR, 2019).

2.3.2 Sea grass

Seagrass meadows are ecosystems dominated by angiosperm plants submerged under seawater. Seagrasses grow by attaching themselves to different types of substrates such as mud, sand, clay and sometimes on rocks. The seagrass ecosystem is very important in San Andrés (and Colombia) because of the important ecosystem services it provides.

Seagrasses are the habitat of numerous species important for fisheries, they absorb nutrients and organic matter serving as a 'filter' for the water. They are also an important source of oxygen and an effective carbon sink (Invemar, 2009). Besides, as mentioned before, seagrasses might even represent up to 50% of the sediment sources in San Andrés (Universidad del Norte - IDEHA, 2009).

Beside the biochemical value of seagrasses, these ecosystems are also able to prevent coastal erosion. The size of the patch and the density of shoots are important factors contributing to sediment trapping. The larger and denser the meadow, the better it is able to stabilize and retain sediment. Seagrasses has the effect to reduce bed shear stress levels, preventing the resuspension of sediment. In other words, they contribute to retaining sediments that that are within the reef flat system.

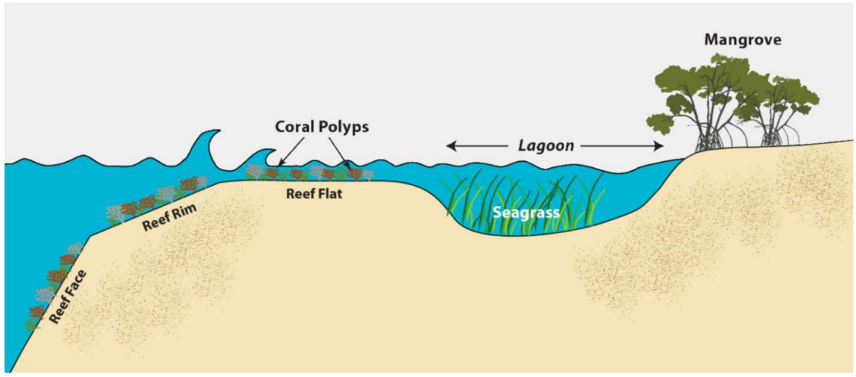

Figure 2.33: Typical schematic of the seascape of San Andrés (Adapted from Gunnel, 2016)

Furthermore, seagrasses are also able to reduce wave heights within the coral lagoon. These ecosystems are often found within fringing reef ecosystems (most often growing on the shoreward side as shown in Figure 2.33). For this reason, it is important to note that the waves that propagate over the seagrass meadows are often already dampened by the submerged structure of the reef crest. However, due to the seagrasses, the water column experiences drag forces as it travels over the seagrass canopy, hereby potentially reducing wave height. Model studies indicate that seagrass can reduce wave height by 40% under non-storm conditions (Guannel, Arkema, Ruggiero, & Verutes, 2016).

Tourism is the most important economic activity in the SAI; therefore, the measures that have been taken to promote tourism in these landscapes are not necessarily in line with conservation objectives, as it has been promoted as a sun, sea, and beach destination. The two main human drivers of seagrass decline in the Spratt Bight are: harvesting due nuisance to tourism, and fishing (or tourist) boats damaging the seagrass cover with their . Near shore seagrass harvesting is no longer common practice in San Andres, however, a few years ago it was normal to harvest seagrass near the shore so that tourists would have clean water to swim in the Spratt Bight. At the same time the fishing boats that are left on the beach or that take tourists to Johnny Cay can also damage the seagrass beds with the propellers of their engines and the currents they produce. In addition, dragging anchors from these smaller vessels can be detrimental to the seagrasses. Unfortunately, once seagrass meadows are affected by this type of intrusion, it is very difficult for them to recover their area.

Figure 2.34: Aerial picture of Spratt Bight Beach. On the left a picture taken in 1956. On the right a Google Earth (2019) image of 2020. The dark patches in both images can be recognized as sea grass meadows. The red circle indicates where the majority of the sea grass has been degraded.

Figure 2.34 Shows aerial photos of San Andrés to compare the seagrass area between 1956 and 2020. It can be seen that in 1956 there was a significant larger seagrass area near the beach than can be seen now a days, confirming what was explained about the deterioration of seagrass meadows.

2.3.3 Mangroves

In San Andrés five locations were identified where mangroves trees grow: Hooker Bay (34.0 ha), Cocoplum (27.1 ha), Salt Creek (3.8 ha), Sound Bay (12.5 ha), and Smith Channel (17.8 ha), as can be seen in Figure 2.31 and Figure 2.35. At Spratt Bight Beach there are no known locations in which mangroves grow and can grow.

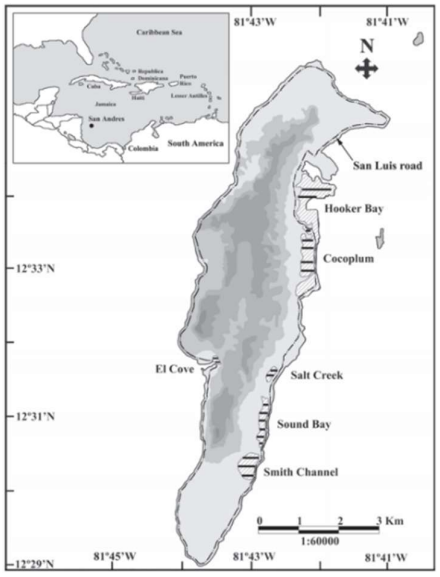

Figure 2.35: Island of San Andrés. The area containing mangrove forests are shaded in gray (Urrego et al., 2018)

Since the colonization of San Andrés in the 18th century, mangrove forests have been cut for the production of crops, majorly coconut production (González, Urrego, Martínez, Polanía, & Yokoyama, 2010). Losses of mangrove forests have been related to coastal erosion and might also be an important factor in San Andrés (Urrego, Correa-Metrio, & González-Arango, 2018).

Mangrove forests are known to provide numerous ecosystem services to human communities including coastal protection and food supply. The root system of the mangrove forests dampens the incoming waves allowing sediment to settle and therefore creating areas of accretion rather than erosion (Spalding, Mclvor, Tonneijck, Tol, & van Eijk, 2014).

2.4 Socio-economic Analysis

Spratt Bight is the most densely populated area of San Andrés. It has the largest beach of the island, and the majority of the touristic activity is concentrated in this region. For this reason, the beach is not only environmentally important, but as it is one of the pillars of the economy of the island, it also has a great economical value (Martín-Prieto, et al., 2013).

Historical Context

The island of San Andrés is located in the Colombian department of San Andrés, Providencia, and Santa Catalina. Due to its geographical localization, San Andrés has historically had a greater affinity with islands of the Caribbean Sea, especially with Jamaica. At the end of the 18th century, slaves and farmers came from Jamaica to San Andrés to populate the islands (Meisel-Roca, Aguilera-Díaz, Yabrudy-Vega, & Sánchez-Jabba, 2016). According to historian and economist Adolfo Meisel-Roca (2016), these settlers managed to maintain their culture different than that of the mainland of

Colombia until 1953. From that on the island was declared a duty-free port, which generated a wave of immigration to the island.

From 1953 on, both tourists (interested in the quotas granted by the new regulations for the purchase of duty-free goods) and Colombian traders settled on the island, leaving the local inhabitants (the Raizales), as a local minority and without control of the main economic activities. Furthermore, due to exacerbated immigration an accelerated demographic growth was generated on the island, making SAI one of the most densely populated islands in the Caribbean. This led to serious environmental deterioration as a result of the increase in waste generation, untreated waste (water) dumping into the sea, overexploitation of fisheries, and the reduction of coral cover. This situation could only be addressed with the creation of the Corporation for Sustainable Development of the Archipelago of San Andrés, Providencia, and Santa Catalina (CORALINA) in 1995 (Sánchez-Jabba, 2016).

Economic Context

Until SAI was declared a free port, the island's economy depended on agriculture, especially the cultivation of coconut and cotton for export. After the declaration of the free port, the economy focused on commercial activity and then, with the economic opening of Colombia from the 1990s onwards, with which the free port no longer had commercial competitive advantages, the hotel and restaurant sector increased its share of GDP and trade declined. By 2012, the economic activities of hotels and restaurants, commerce's, transport, and communications contributed 52.7% of departmental GDP (Meisel-Roca, Aguilera-Díaz, Yabrudy-Vega, & Sánchez-Jabba, 2016).

At present, fishing is not an important line of the island's GDP, however it is still important for food supply and security. Part of the island's economic problem is that the infrastructure that remained on the island was associated with the free port-based economy, and, to date, San Andrés has not managed to generate competitive advantages for international tourism. Additionally, and even more serious for the economy, is the economic, cultural, and social marginalization of the Raizales, who do not have the human capital and opportunities necessary to actively participate in local development (Meisel-Roca, Aguilera-Díaz, Yabrudy-Vega, & Sánchez-Jabba, 2016).

Social Context

In accordance with the above, an analysis of the human capital of SAI by María Aguilera-Diaz (2016), allows us to conclude that, despite advances in education, with literacy levels that exceed national averages, and the living conditions of the island's population (according to indicators associated with height, life expectancy and mortality rate), poverty levels are on the rise in San Andrés.

According to data compiled by the Governor's Office of the Archipelago, in 2018 the indicator of Unsatisfied Basic Needs (UBN) in San Andrés was estimated at 43%, which has facilitated the involvement of young Raizales in drug trafficking. San Andrés plays an important role in this activity due to its geographic location, close to Central America and the United States. As a result, criminal drug gangs have formed, and their disputes have led to an increase in violence (homicides) in San Andrés (Sánchez-Jabba, 2016).

Coastal squeeze

In San Andrés, erosion and accretion are natural phenomena that happen depending on seasonality. By building too close to the coastline, the hard structures do not give the beach the dynamicity it requires. What often happens is that structures are placed close to the beach during calmer periods, when the beaches are wide. Naturally, when wave conditions change, the beach profile starts displacing landwards, compromising the integrity of these structures, and therefore putting the local community in risk. With coastal squeeze, the natural variability if the beach is not accounted

for during the placement of structures, and the coastline loses its possibility to displace without affecting constructions and consequently the local population.

Figure 2.36: Shore line of Spratt Bight over the past 60 years (Martín-Prieto, et al., 2013).

Figure 2.36 shows development of the increasing number of constructions and structures near the coast over the years. It can be seen that the boulevard of Spratt Bight, hotels and other commercial establishments started locating within a few meters of the coastline. During milder seasons beaches wider beaches can be observed, however, when erosion events start displacing sediment, the waterline can get as close as the boulevard (Martín-Prieto, et al., 2013).

Role of Natural Coastal Protection Strategies

In the socio-economic context presented, it is evident that the natural resources associated with the coast and sea of San Andrés provide vital ecosystem services for the well-being of the island's population. In this context, fishing stands out as the basis for food security, while the beaches as the main tourist attraction.

Despite the advances in sustainability, the declaration of the Sea Flower Biosphere Reserve, the community organizations and their political-administrative structure, the island's current socio-economic development model is still unsustainable (Sánchez-Jabba, 2016). This translates into a spiral of environmental, social, and economic decline. In this environment, nature-based measures for the protection against coastal erosion can play a fundamental role, as they contribute in a decisive way to generate adequate conditions for the sustainable ecological and integral human development of the island of San Andrés.

Prevent coastal erosion is essential to maintain and boost the economy of the island. When done through the recovery of ecosystems such as coral reefs, sea grasses and mangroves, it can contribute to the improvement of the quality of life of the local population that depends on fishing both as an economic activity as the basis of their food security.

Furthermore, on the island of San Andrés a high percentage of the infrastructure, including fish landing sites, fish markets, roads, telephone and electricity lines, water lines, the airport, homes, and hotels, is located close to the coastal zone and at risk of coastal erosion. This generates the need to take coastal protection measures as a basis for not only local development but also safety.

Finally, it should be noted that according to PMEC (Klooster, 2017), the lack of inter-institutional coordination, and in the case of San Andrés, especially between the local and central levels of government is one of the main problems of governance of coastal erosion in San Andrés in particular and in Colombia in general.

There are many institutions that have jurisdiction and authority on the coastal area of San Andrés. CORALINA (regional autonomous corporation for the sustainable development), the Ministry of Environment (MADS), the Maritime and Port Authority (DIMAR), the National Fishing and Aquaculture Institute (INPA), the Departmental Fishing Board and the native community called Raizales. These institutions, organizations, and groups are responsible for San Andrés and its coastal area (Baine, Howard, Kerr, Graham, & Toral, 2007).

Having that many organizations involved in decision making requires a strong organizational structure. Currently there is no such structure that offers institutional support and represents the different interests when the implementation of coastal protection measures is needed. This often leads to protracted and less effective processes while coastal protection measures require immediate attention on the island (Baine, Howard, Kerr, Graham, & Toral, 2007).

In Appendix C a list of the important stakeholders on San Andrés is presented. There also a schematization can be found where the power and the interest of each of these stakeholders are plotted.

3 Modelling Study

For this research, a modelling study has been carried out in order to better understand the wave, current and sediment transport patterns on the island that drive the morphology of Spratt Bight Beach. The hydrodynamic modelling of the different environmental conditions and its resulting sediment transport patterns area are essential to be able to answer research questions 1 and 2 stated in Chapter 1.

In the next sections the model choice is explained, and the modelling methodology is further developed. Finally, the results of the modelling study are presented.

3.1 Model Choice

Different models can be used when modelling different timescales and spatial scales. Some models are more suitable for smaller time and spatial scales (e.g., XBeach), others are more suitable for larger scales (e.g., UNIBEST), as shown in Figure 3.1.

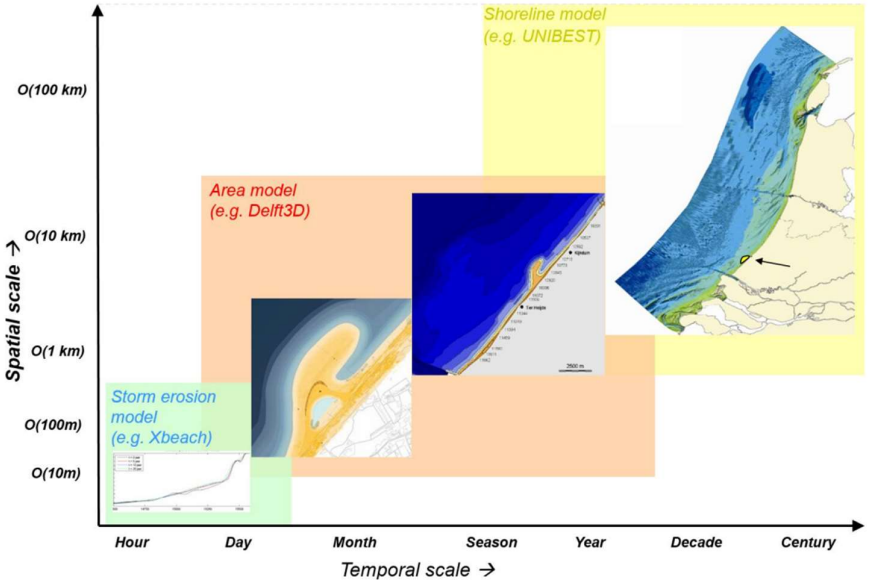

Figure 3.1: Application range of models made by A. P. Luijendijk

Every model has its advantages and short comings. Delft3D (Deltares, 2014; Deltares, 2022) for example, is not able to simulate the infra-gravity waves and their effect on the hydrodynamics of the study area. On the other hand, XBeach (Roelvink, et al., 2009) requires a finer resolution to be able to run smoothly, therefore increasing the computational demand (Buckley, Lowe, & Hansen, 2014). In order to choose the most suitable model for this study, the different limitations, time- and spatial scales of the models have to be taken into account.

As the study area is located in a system dominated by coral reefs and sandy beaches, it is expected that infra-gravity waves will play an important role in the morpho- and hydrodynamics (van Dongeren, et al., 2013). On the other hand, the short-waves effects are also expected to have significant effect on the system, as wave induced water level set-up, flow velocities and shear stresses (Gourlay, 1996).

3.1.1 XBeach

XBeach is an open-source numerical model originally developed as a phase-averaged model, resolving the short-wave variations on the wave group scale and the long waves associated with them; with a spatial scale of kilometers and temporal scale of storms (Deltares, 2017). In this way it possible to simulate hydrodynamic and morphodynamic processes and impacts on sandy beaches and dunes. Since its original development, the model has also been used to better understand the role of coral reefs hydrodynamics and its impact on the behind located sandy coasts, and other applications (van Dongeren, et al., 2013; van Rooijen, et al., 2016; Roelvink, McCall, Mehvar, Nederhoff, & Dastgheib, 2018).

The model includes the short-wave hydrodynamic processes (refraction, shoaling and breaking), infragravity wave related processes (generation, propagation, and dissipation), wave induced set-up and unsteady currents. The morphodynamic related processes of the model include bed load, suspended sediment transport and bathymetry update. The model has been extensively validated with numerous laboratory and field tests (Deltares, 2017).

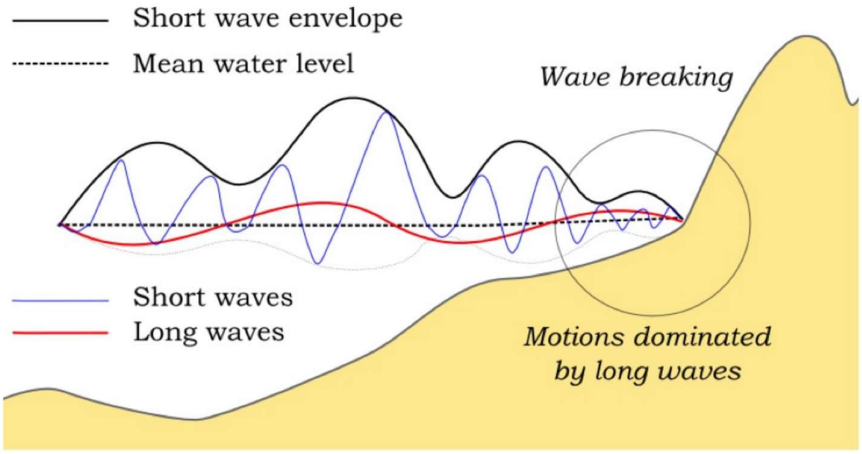

Figure 3.2: Sketch of relevant wave processes in XBeach (Deltares, 2017).

Since its original development by Roelvink et al. (2009), additional model options have been implemented:

- Surfbeat mode (XB-SB): short-wave variations on the wave group scale (short-wave envelope) and the long waves associated with them are resolved.
- Non-hydrostatic mode (XB-NH): non-linear shallow water equations and pressure correction terms are applied, allowing to model individual waves as well as infragravity waves.

Intermezzo 3.1: Infragravity waves

Infragravity waves are low frequency waves induced by short wave height variations. Their typical period is between 25 s and 250 s and while their offshore height can be of a few centimeters, near the coast they can reach up to a few meters, principally during storm conditions (Holthuijsen, 2007).

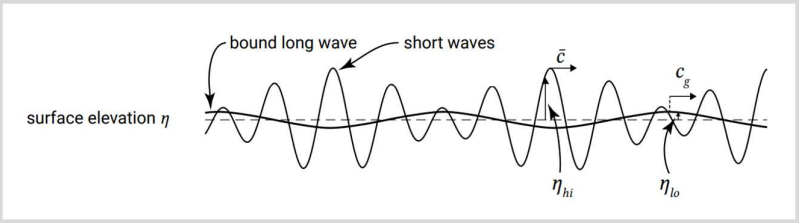

Figure 3.3: Process of bound long wave generation due to short wave height variation. In the figure c is the celerity (phase velocity), c_g is the group velocity, n_{hi} is the high frequency wave (long wave) water elevation and n_{lo} is the low frequency wave (short wave) water elevation. Modified from Bosboom & Stive (2021)

In a wave group, short waves with slightly different wave lengths and frequencies are superposed creating a pattern with varying wave heights within the group (as shown in Figure 3.3). Due to these variation in wave heights, the radiation stresses vary as well, being lowest on the lower waves and highest under the higher waves. A gradient in radiation stresses has to be compensated with a difference in water level, creating a set-up where they are lowest (under the lower waves) and a set down where the radiation stresses are largest (under the higher waves). The result is a wave with the length and frequency of the group as shown in Figure 3.3 (Bosboom & Stive, 2021).

The infragravity waves can play an important role in the cross-shore sediment transport patterns in the coastal zone. As shown by Roelvink and Stive (1989), the contribution of the infragravity waves to the sediment transport is offshore directed before the entering the (short wave) surf zone, and shoreward directed in the inner part of the surf zone.

Using XB-SB saves considerable computational time, but with the trade-off of not simulating the phase of the short-waves. XB-NH is a more detailed and complete model, which solves all short- and infragravity waves, however it is computationally more expansive.

3.1.1.1 Surfbeat (XB-SB)

The main processes included in XB-SB are:

- Short-wave driven currents (longshore current, rip currents and undertow)
- Wind-driven currents for local wind set-up
- IG waves
- Runup and rundown of long waves (swash)

In the Surfbeat module of XBeach (XB-SB), the short-wave motions are solved using the variation of the wave envelope (short-wave height) on the scale of wave groups. It has a dissipation model and a roller model to represent momentum stored at the surface after breaking. The variations exert a force on the water column through radiation stress gradients, driving longer period waves (IG waves) and unsteady currents, which are solved through the nonlinear shallow water equations in XB-SB (Deltares, 2017).

The model can be applied in a 2DH area, which means that the results are simulated in a 2D domain with a depth averaged sense. The model is solved on a curvilinear staggered grid, in which the incoming short-wave energy will vary along the seaward boundary and in time (depending on the wave boundary conditions) (Deltares, 2017).

XB-SB is usually necessary when the focus on dissipative beaches, or coral environments, in which the short-waves are mostly dissipated by depth-induced wave breaking.

3.1.1.2 Non-Hydrostatic (XB-NH)

The main advantages of using XB-NH are (Deltares, 2017):

- Short-wave runup and overwashing are included
    - Might be important in case of steep slopes such as gravel beaches and coral reefs
- IG waves
- Wave asymmetry and skewness are explicitly solved
- Diffraction is included
    - This process roughly approximated in the short-wave averaged models as XB-SB (and Delft3D-WAVE)

XB-NH was developed by the TU Delft and Deltares (as a version of the SWASH model (Zijlema, Stelling, & Smit, 2011)). For its calculations depth-averaged flow due to waves and currents are computed using the non-linear shallow water equations, including a non-hydrostatic pressure correction (Deltares, 2017).

With XB-NH the short-wave action balance is no longer needed, as short and long waves is resolved together in the Non-Linear Shallow Water (NLSW) equations. However, in the short wave-resolving mode a much higher spatial and temporal resolution is needed. This makes XB-NH very computationally expensive. Wave breaking is implemented by disabling the non-hydrostatic pressure term when waves exceed a certain steepness, after which the bore breaking equations takes over (Deltares, 2017).

Results show that the model does not perform very well when waves remain in relatively deep water ($kh > 1$). This is expected as the numerical dispersion relation for a depth averaged model only approximates the linear dispersion relation for relatively shallow water (low kh values). This requirement may result in enforcing the boundary in a region near (or in) the surf zone, where $kh \leq 1$, where nonlinear contributions can have a large influence (Ridder, et al., 2021).

3.1.2 Delft3D

The main advantages of using Delft3D (Deltares, 2014; Deltares, 2022) are:

- Simulation of detailed sediment transport patterns and morphology
- Ability to simulate the longshore and cross-shore transport, and flow patterns
- Presenting sediment transport processes in sufficient detail while remaining computationally efficient
- Being designed for experts and non-experts (user friendly and robust)

Delft3D is a process-based model and makes an effort to approach reality by explicitly representing all the essential physical processes acting on sediment in the coastal environment. The model is developed by Deltares and has different modules that can be used for different purposes. In this research the applicability of the model will focus on 2 main modules: Delft3D-WAVE (D3D-W) and Delft3D-FLOW (D3D-F).

With the combined effort of the D3D-F and the D3D-W modules, the software is capable of modelling waves, tides, currents, and (under their influence) solve the sediment transport. The model gives insight into water levels, depth-averaged velocities, and bed-shear stress (Deltares, 2022). Both modules are run simultaneously and coupled as shown in the schematization below.

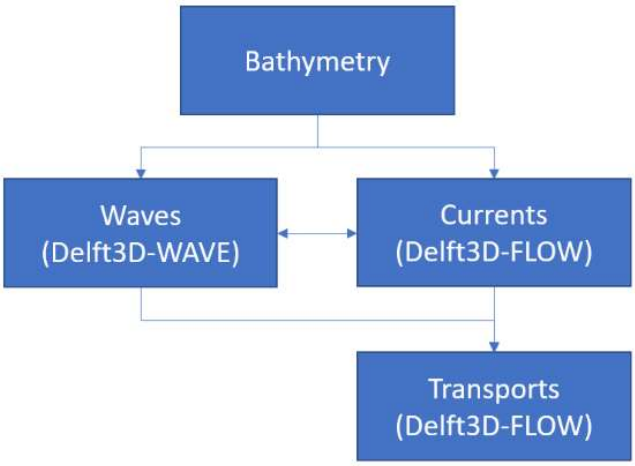

Figure 3.4: Schematization of the coupling of Delft3D-WAVE with Delft3D-FLOW

Delft3D-WAVE is a 2DH wave propagation model that runs the SWAN model (Simulating WAves Nearshore) developed by the TU Delft. In this model waves are described by the 2D wave action density spectrum. It requires user defined input wave and wind data at the boundaries, after which it simulates the wave propagation, generation by wind, nonlinear wave-wave interactions, and wave dissipation for a given bathymetry (Deltares, 2014).

Delft3D-FLOW is a multi-dimensional hydrodynamic and morphological simulation program which calculates non-steady flow and transport phenomena resulted from tidal and meteorological (wind and waves) forcing. The flow model can be used to predict the flow in shallow seas, coastal areas, estuaries, lagoons, rivers, and lakes. D3D-F solves the unsteady shallow water equations in two (depth-averaged) or in three dimensions. The system of equations consists of the horizontal equations of motion, the continuity equation, and the transport equations for conservative constituents. Besides, the model solves the Navier Stokes equations for an incompressible fluid, under the shallow water and the Boussinesq assumptions (Deltares, 2022).

The main area of application of Delft3D are:

- Tide and wind-driven currents
- Online sediment transport and morphology
- Wave-driven currents
- Non-hydrostatic flows

A more in-depth model description including model formulations can be found in Appendix D.

3.1.3 Summary & Model Choice

Although XBeach might be more complete and incorporate more in detail processes, these comes with a cost: computational power and time. These highly time demanding modelling activities would not fit within the time frame of this research. To reduce the computational time, it would be necessary to reduce the amount of boundary conditions and interest area. For this reason, it has been chosen to **go forward with Delft3D** to simulate the environmental conditions on Spratt Bight Beach. Below a summary of the specifications, advantages and disadvantages of the considered models are shown.

XB Surfbeat	XB Non-Hydrostatic	Delft3D
Specifications		
Describes short wave variations on the wave group scale and the long waves associated with them are resolved Models wave energy	Non-linear shallow water equations are used Waves are simulated individually Methods used are similar to the one-layer version of the SWASH model Models surface elevation	Waves described with two-dimensional wave action density spectrum Models wave energy Suitable for long term modelling conditions (months to years)
Main Advantages		
Accounts for **infragravity waves** More **complete** model (less than XB-NH)	Wave **asymmetry and skewness** are resolved Accounts for diffraction Accounts for **infragravity waves** More **complete** model	Computationally **efficient** **Robustness** Suitable for experts and non-experts (user-friendliness)
Main Disadvantages		
Expansive computational time (less than XB-NH) $\Delta x \approx 1/10\ L_{wave}$ - high **resolution** required to run smoothly	**Expansive computational time** **Wave number** kh $<\approx 1$ at boundary to run smoothly $\Delta x \approx 1/30\ L_{wave}$ - high **resolution** required to run smoothly	Does not account for **infragravity waves**

Table 3.1: Overview of specifications, main advantages, and disadvantages of the different models: XB-SB, XB-NH and Delft3D. In the table, the wave number $k = \frac{2\pi}{L_{wave}}$ and L_{wave} = wavelength.

It is known that electing for Delft3D comes with certain limitation. The main limitation is that the effects of infragravity waves are not taken into account. This limitation will be described in the Discussion (Chapter 6).

3.2 Morphological Modelling: Delft3D

3.2.1 Model Set-Up

3.2.1.1 Computational Grid

Three computational grids were prepared for the model of the island of San Andrés and Spratt Bight: two for D3D-W and one for D3D-F. The two D3D-W grids were nested in each other such that the incoming waves of the smaller domain

are generated by the larger domain. When the waves that were imposed at the boundaries of the larger domain, travels through this grid and reaches the smaller domain, they are automatically converted into wave boundary conditions for the second domain. The D3D-F computational grid is the same as the smaller domain for D3D-W. Figure 3.5 shows the computational grid that covers the entire area around the island of San Andrés and the surrounding ocean waters, and the smaller grid that covers Spratt Bight Beach and the coral reef area.

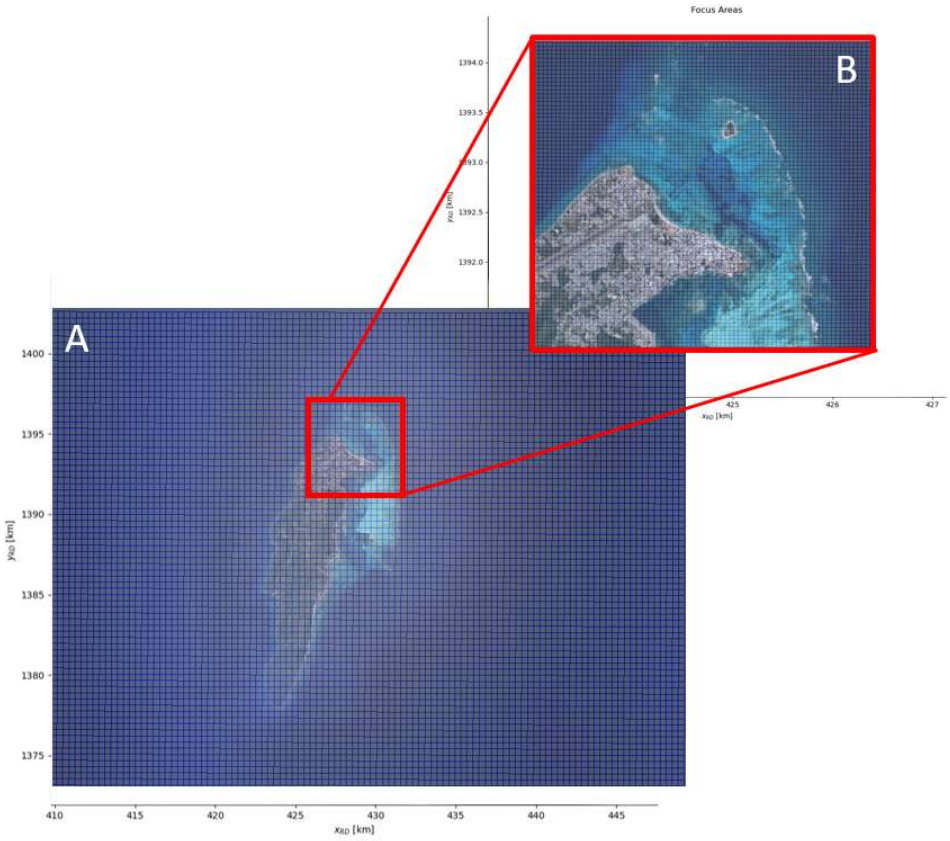

Figure 3.5: Computational grid and area. The larger area (A) corresponds to overall the island of San Andrés and was only used for D3D-W; the smaller area (B) was nested inside the larger area and corresponds to Spratt Bight Beach

The larger grid is where the wave boundary conditions are applied (D3D-W). This domain extends 30 km in the Northern direction and 40 km in the Western direction, it has 105 by 90 cells and an approximate resolution of 350 m. To decrease computational time, it is decided to apply a coarse resolution to this grid as the water depths are very high outside the interest area and will not influence the wave heights entering the area of interest. It was decided to use such a large domain as the imposed waves at the boundary need enough space to develop fully before entering the focus area.

The smaller domain (area B in Figure 3.5) extends 3.25 km in the Northern direction and 3.5 km in the Western direction, has 360 x 360 cells and a resolution of approximately 13 m. This computational grid is applied on D3D-W and D3D-F. In the case of D3D-W, the grid is nested into the larger grid as previously explained. This domain is the area in which D3D-W and D3D-F will work simultaneously to calculate the sediment transports in this area (as shown in Figure 3.4). The smaller grid is chosen to be larger than the interest area in order to avoid boundary effects to influence the processes within the interest area.

3.2.1.2 Bathymetry

The bathymetry used for the smaller grid is the same as described in Section 2.2.3, but with a few adjustments:

- In order to make sure the waves enter the interest domain smoothly; it was made sure that all boundaries had the same depth and that there were no depth gradients in the first few cells.
- All depth greater than 50 m were set to 50 m. As this depth is large enough for the highest simulated waves to not feel the bottom and start dissipating, this was done to save computational time.

The figure below shows an impression of the bathymetry of the computational domain.

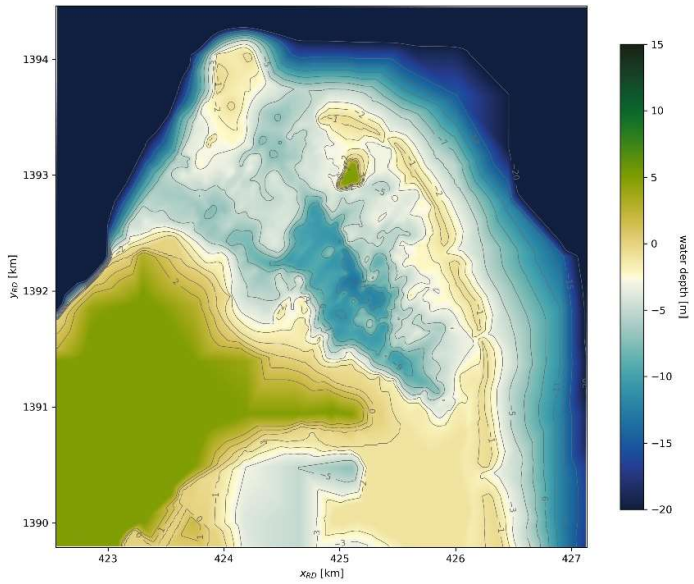

Figure 3.6: Computational domain and bathymetry used as input for the numerical models.

For the larger domain the bathymetry retrieved from GEBCO (2020), which has a resolution of 1° (as explained in Section 2.2.2 and Appendix A). In order to have a smooth bathymetry which is compatible with the 350 m resolution and would fit within the grid, the depth data was triangularly interpolated using QUIQCKIN from Delft3D.

3.2.1.3 Boundary Conditions

The boundaries of the Delft3D model are divided into D3D-W and D3D-F boundary conditions. Wave, wind, and tide can be imposed on the boundary conditions of D3D-W model. The D3D-F model requires a set of initial and boundary conditions for water levels and horizontal velocities in order to get a mathematically stable model running.

Waves

An important boundary condition for the wave model is the offshore wave climate. The data used to derive the wave boundary conditions was taken from WWIII as described in Section 2.2.3 and Appendix B. The dataset presents time series of wave heights, lengths, periods, and directions. These boundary conditions are imposed on all 4 sides of the larger grid (in Figure 3.5A). The waves than travel through the grid until the reach the smaller grid (in Figure 3.5B). Figure 3.7 shows a schematization of how the nested D3D-W model uses the simulated waves in the larger domain as boundary conditions for the smaller domain.

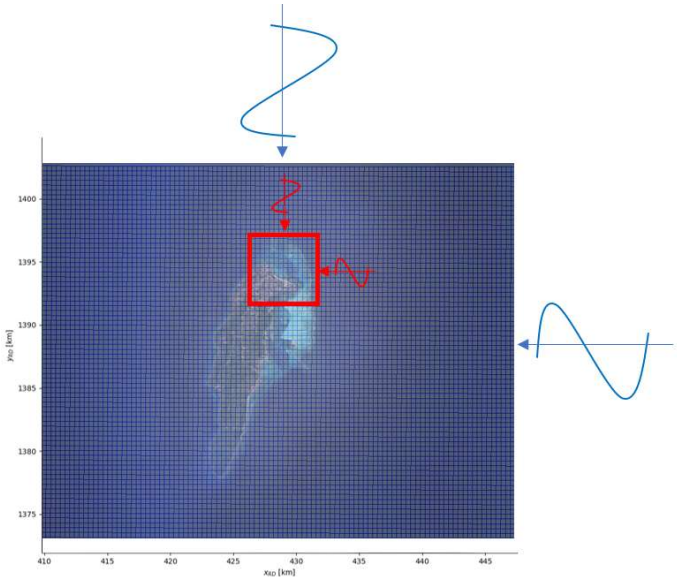

Figure 3.7: Schematization of how the imposed boundary conditions at the offshore boundary of the larger grid travels through its area until reaching the focus area at Spratt Bight.

In the model wave set-up is activated, together with diffraction and non-linear triad interactions. Originally D3D-W did not have the option to model diffraction, however in the latest versions a refraction-diffraction approximation is included. This relation is expressed in terms of the directional turning rate of the individual wave components in the wave spectrum. It consists of a parametric approximation of diffraction (Deltares, 2014).

The exact wave climate that is being imposed on the boundary conditions are further described in Section 3.2.2.

Tide

As mentioned in Section 2.1, tide data is poorly available. However, it is known that the difference between HAT (Highest Astronomical Tide) and LAT (Lowest Astronomical Tide) is approximately 0.35 m. In Section 2.2.3.3 it was already described that San Andrés is governed by a micro-tidal regime. With such low tidal levels, the tidal influence has been considered negligible and was not used as input for the model. Further discussion about this topic will be done in Chapter 6

Flow

D3D-FLOW boundaries can be "land-water" lines, which are called "closed boundaries", or they can be "water-water" boundaries, called "open boundaries". Closed boundaries in which velocities normal to these boundaries are set to zero. Open boundaries are imposed to restrict the computational area and so the computational effort. The wave and flow reflection on open boundaries should always be minimal (Deltares, 2022).

As will be explained in Section 3.2.2, the modelling study of this research will focus on 2 main wave directions: 0°N and 80°N. In D3D-F one set of boundary condition was selected per wave direction modelled:

- 0°N: Northern and Southern boundaries are open boundaries in which the water level is set to be equal to the mean water level (0 m) and flow can pass freely. The Easter and Western boundaries are closed boundaries, in which the flow velocities are set to zero and water level can move freely (Figure 3.8 left).

- 80°N: Northern and Southern boundaries are open boundaries in which the water level is set to be equal to the mean water level (0 m) and flow can pass freely. The Easter and Western boundaries are closed boundaries, in which the flow velocities are set to zero and water level can move freely (Figure 3.8 right).

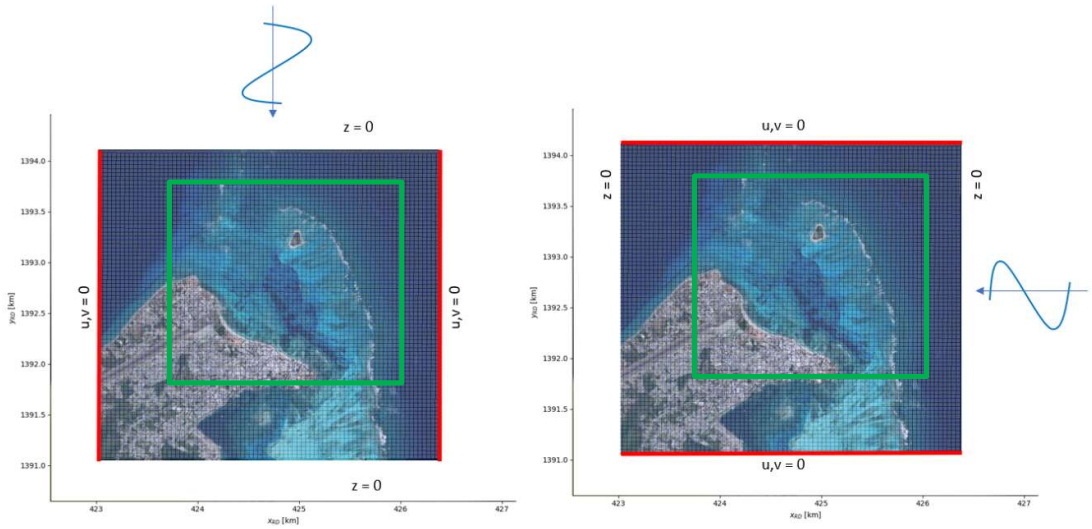

Figure 3.8: Boundary conditions for D3D-F. On the left the boundaries for waves coming from the North (0°N). On the right the boundaries for waves coming from the East (80°N). The red lines indicate the boundaries in which velocities are zero. The green boxes indicate the interest area from which the results will be shown in Chapter 4.

These layouts for boundary conditions were selected as it is assumed that outside the lagoon (at the offshore areas) water levels are approximately equal to the mean water level, as it is assumed that wave induced water level set-up does not happen in this area.

The boundaries were selected far enough of the interest area (the green boxes in Figure 3.8), so that the boundary effects could not influence this area. Besides, reflection parameters were implemented (α = 200 s^2) in order to avoid reflection problems at the open boundaries.

The results that will be presented in Chapter 4 exclude the computational boundaries of the model and focusses only on its interest area. This is done because boundary effects are detected at the boundaries, which do not comply with reality. As the boundaries are chosen far enough of the interest area, they do not have any influence on the results presented in Chapter 4. In Appendix E results are shown for the entire domain, showing there is no influence of the boundaries in the interest area.

3.2.2 Method

The model must represent the existing situation as accurately as possible. However, simulating all wave conditions in a 1-on-1 time scale is too time consuming. For this reason, the wave data is schematized. This means that the timeseries has to be converted into a number of characteristic conditions which is a representation of the most relevant conditions of the timeseries.

Wave angle

A sensitivity study has been conducted to better understand what wave conditions have the greatest impact on Spratt Bight Beach with respect to flow velocities and sediment transport. To get insights about the most relevant wave angle, different simulations were run applying boundary conditions of equal wave heights and period, but with different angels

of incidence: 0°N, 20°N, 40°N, 60°N and 80°N. The significant wave height and peak period (respectively 2 m and 8 seconds) were used for these simulations. The figure below shows some result of the wave fields and flow velocities.

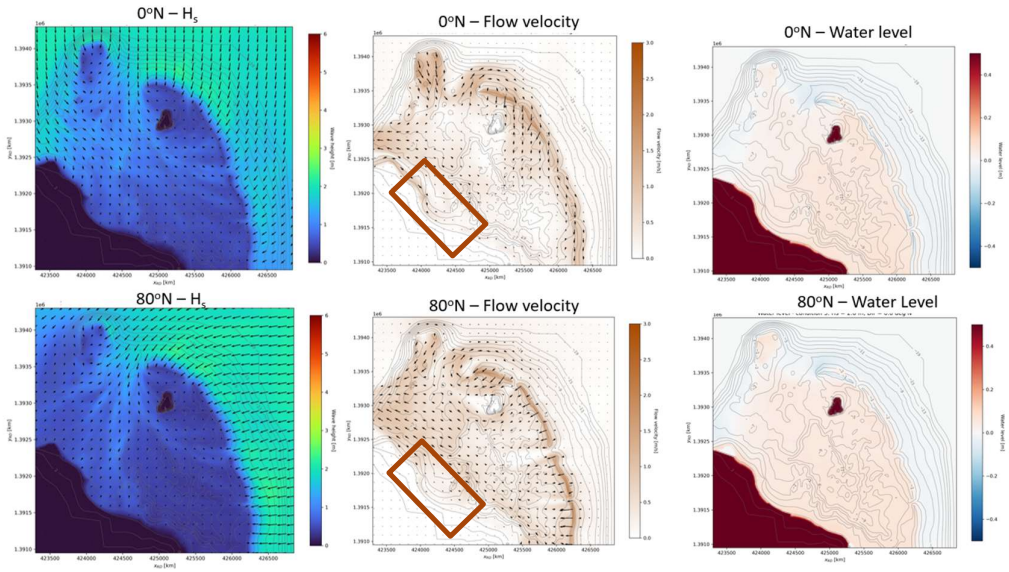

Figure 3.9: Comparison between simulations of waves coming from 0°N and 80°N. Both simulations were done with 2 m waves with 8 s period.

Waves coming from the North stood out presenting a flow velocity pattern that is significantly different from the mean wave direction. In Figure 3.9 it can be noticed that the 0°N condition shows a Southeastward long-shore current, which is not observed in the 80°N condition. This effect seems consistent with the erosion patterns observed in Section 2.2.4, where in Figure 2.27 erosion is observed on the west and accretion on the east (near the breakwater). This will be further explained in the Chapter 4.

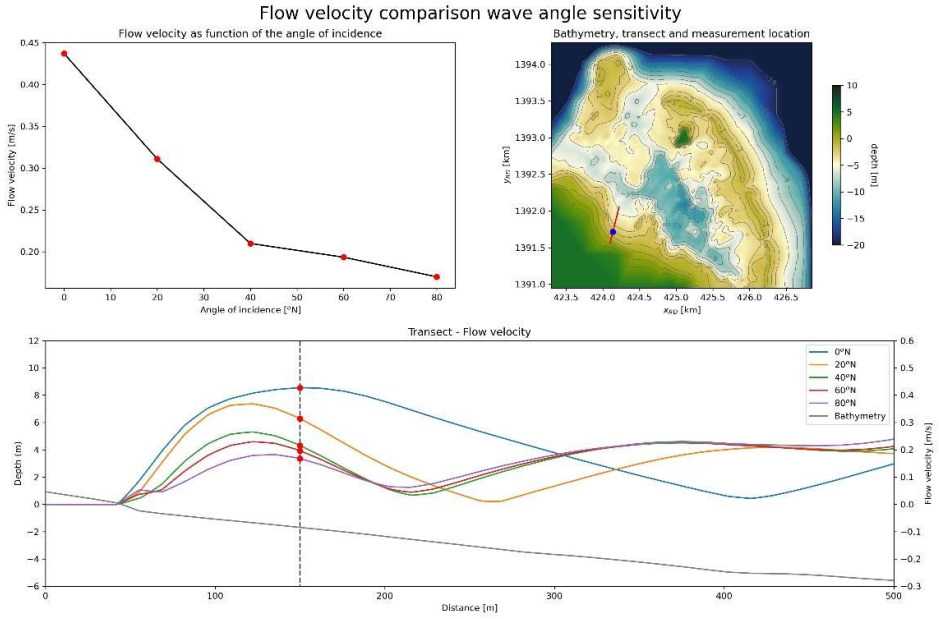

Figure 3.10: Sensitivity of flow velocity (near the coast, across a transect) to the wave angle. Waves coming from 0°N, 20°N, 40°N, 60°N and 80°N were tested using wave heights of 2 m and periods of 8 s. The upper right figure shows the bathymetry of the study area. The red line indicates the

transect taken and the blue dot the location at which point data is taken for the sensitivity test. On the upper left the flow velocities extracted at the location of the (previously described) blue dot are plotted against the wave angle of incidence. Finally, the lower plot shows the cross-shore profile of the bathymetry (gray line), and of the flow velocities (colored lines) at the transect depicted in the upper right figure.

As can be seen in the Figure 3.10, the lower the angel of incidence the higher the flow velocities along the coast. For this reason, is has been chosen to simulate 2 wave angles representing 1) the mean wave heights coming from the East and 2) the waves coming from the North. For this representation waves coming from 0°N are selected to represent the Northern incoming waves and 80°N the Eastern waves.

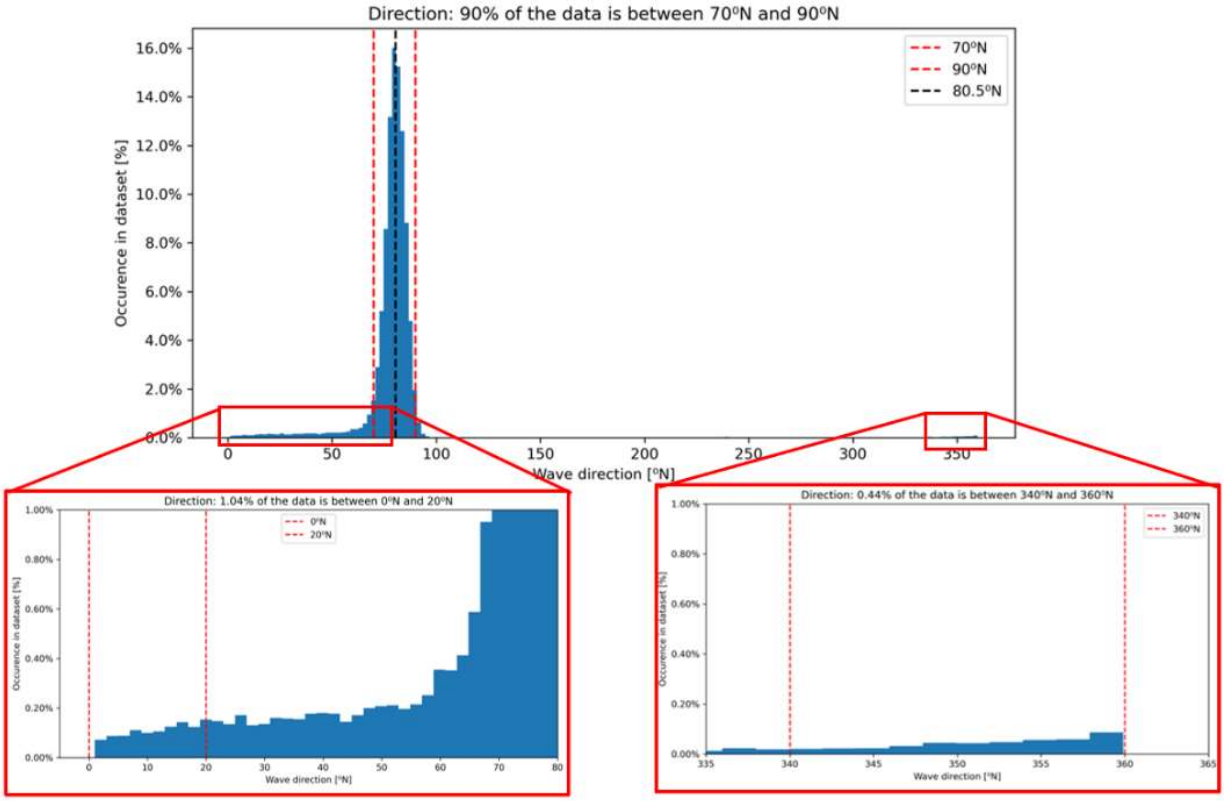

Figure 3.11: Histogram indicating the occurrence of waves with directions between 70 °N and 90°N, 0°N and 20°N, and 340 °N and 360°N. The two lower figures show a zoomed version of the upper figure.

As shown in Figure 3.11, 90% of the incident waves have a wave direction between 90°N and 70°N. The mean wave direction is 80°N, and approximately 1.5% of the waves are coming from the North (between -20 °N and 20 °N)

Wave height and period

Ten different wave height classes were defined in the range between 1.0 m until 5.5 m with steps of 0.5 m. With a wave height of 5.5 m being a representation of the most extreme wave condition. The corresponding wave periods were determined using the mean wave steepness (s), in which the period is dependent of the wave height according to the relation below.

$$T_p = \sqrt{\frac{H_s \cdot 2\pi}{s \cdot g}}$$

Figure 3.12 shows how these periods were selected within the wave steepness. It was chosen to neglect the swell waves (characterized by long periods and lower heights) and only consider sea waves (higher waves with lower periods). This is done to be able to compare the Northern wave climate with the Eastern wave climate. As the Northern wave climate does not contain swell waves (as shown in Section 2.2.3.2), it was chosen to not take them into account for this study. Further implications regarding this choice are addressed in Chapter 6.

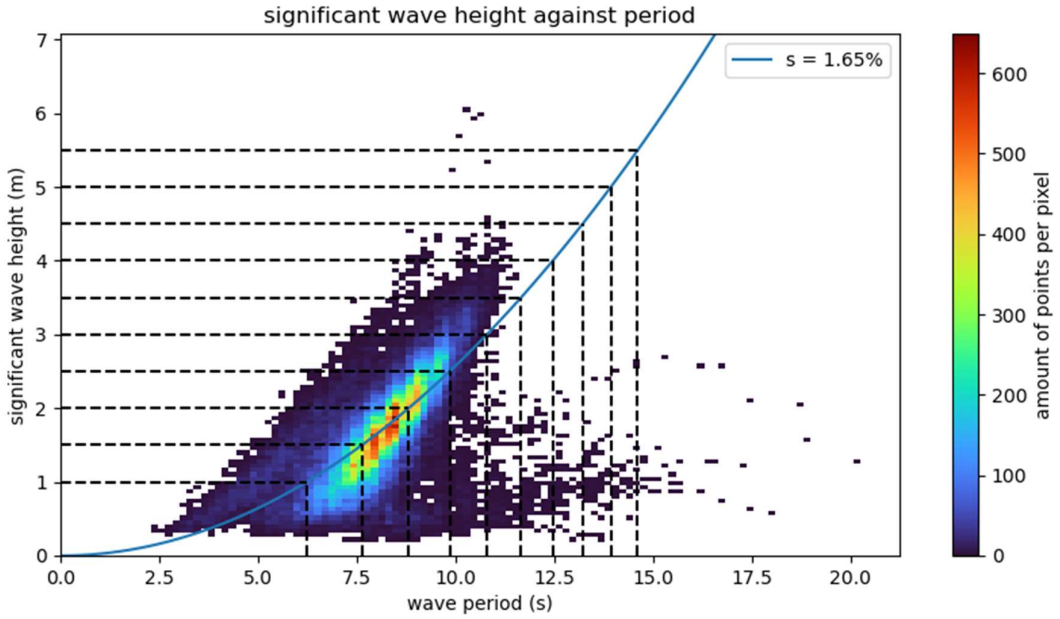

Figure 3.12: Wave heights and periods within the WWIII data set and its occurrence. The blue line corresponds to the mean wave steepness, which is used to determine the wave periods serving as input for the D3D model. The black dashed lines indicate the value of the wave period that corresponds to the wave heights.

Wind

Wind fields were implemented in the D3D-W model in order to realistically model the environmental conditions on and around San Andrés. As there is no more forcing after the waves leave the offshore boundary, wind can influence wave growth behind the coral reef after they break over it. Besides, imposing a wind field creates more wave diffusion behind the reef, which also contributes for a more realistic wave field.

However, as mentioned in Section 2.1, wind data is poorly available and real data could not be used as input. For this reason, it has been chosen to empirically and iteratively choose a wind field that is compatible with the wave field selected. This is done by choosing wind velocities that are high enough to be representative for the wave field applied, but not too high that it would influence the wave conditions offshore. The wind directions are the same as the corresponding wave directions. The graph below shows the relation between wave height and wind speed used as input in the model.

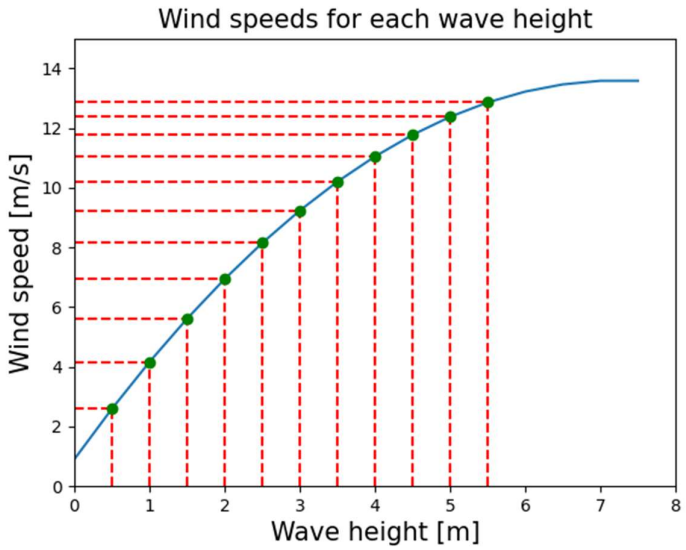

Figure 3.13: Empirical relation between wind speed and wave height used as input for D3D-W model. The red dashed lines and green dots indicate the value of the wind speed that corresponds to the wave heights.

For practical reasons it was chosen to use the same wind direction as the wave direction as input for the model.

Simulation Period

Each condition is run for a certain period of time (the simulation period). This time span has to be large enough to be able to neglect spin-up time and initial instabilities. Besides, it has to be made sure that the hydrodynamic processes are fully developed. At the same time the simulation time cannot be too large in order to save computational time and due to the time frame of this research. For this reason, an optimal simulation time was found. This has been done iteratively and set to 720 min (12 hours). This means that each condition is simulated for 12 hours.

Output is generated every 30 minutes, which means that there are 24 result outputs for every simulated condition. Finally, the results used for analysis are taken from the last timestep, in which the hydrodynamic conditions are fully developed. This is done as it is not necessary to exactly quantify each and every process, but to get an indication of the overall trends of the system reacting on the wave forcing.

Other Assumptions and Simplifications

Firstly, the morphological feature of D3D-F is turned off, which means that bathymetry is not updated during the simulations. In a simulation where the bathymetry is updated, D3D-F calculates a new bed level based on the sediment transports, which serves as input for the model's next time step. This choice is made because of the fact that it is not possible to validate the model's results using real data. In this way a new (possibly inaccurate) bathymetry could influence wave and flow patterns, which is not desirable.

Secondly, it has been assumed that the bed in the entire domain is composed by sand. The implication of this choice is that there is an infinite supply of sediment available to be transported. This means that the model results will actually display sediment transport capacities instead of actual sediment transport. More about this assumption is explained in Chapter 6.

Summary of Simulated Conditions

In total 20 wave conditions were simulated (shown in Table 3.2). The waves coming from the West (Between 70°N and 90°N, representing 90% of the waves) are represented by the 80°N conditions and the waves coming from the North (1.5% of the time) are represented by the 0°N conditions. This data will serve as input for the D3D-W model, which will than produce hydrodynamic input for D3D-F.

Data WW3					
Condition	**H_S [m]**	**T_P [s]**	**Wave Direction [°N]**	**Wind Speed [m/s]**	**Wind Direction [°N]**
1	1.0	6.23	0	4.50	0
2	1.5	7.63	0	6.00	0
3	2.0	8.81	0	7.50	0
4	2.5	9.85	0	8.50	0
5	3.0	10.79	0	9.50	0
6	3.5	11.66	0	10.25	0
7	4.0	12.46	0	11.00	0
8	4.5	13.22	0	11.75	0
9	5.0	13.93	0	12.25	0
10	5.5	14.61	0	12.50	0
11	1.0	6.23	80	4.50	80
12	1.5	7.63	80	6.00	80
13	2.0	8.81	80	7.50	80
14	2.5	9.85	80	8.50	80
15	3.0	10.79	80	9.50	80
16	3.5	11.66	80	10.25	80
17	4.0	12.46	80	11.00	80
18	4.5	13.22	80	11.75	80
19	5.0	13.93	80	12.25	80
20	5.5	14.61	80	12.50	80

Table 3.2: Data variables retrieved from WW3 model and used as input for the Delft3D model.

4 Results

This chapter presents the results of the Delft3D model simulating the existing situation at the coastal system of Spratt Bight. These results will be analyzed and serve as a tool to answer the sub- research questions presented in Section 1.3. The dominant hydro- and morphodynamic processes as wave incidence, wave induced water level set-up, flow velocities, sediment transport and shear stresses are shown and analyzed. The results are divided into hydrodynamic processes (Section 4.1) and sediment transport processes (Section 4.2).

As twenty different environmental conditions were simulated and not every condition has the same level of relevance, a selection of the most important findings is shown. It is chosen to present the conditions with average wave height (2 m) and extreme wave height (5.5 m) in combination with the situations with waves coming from average direction (80°N) and an episodic event direction (0°N) as stated in the previous section. For the complete overview of the results see Appendix E.

It has to be considered that there is a large uncertainty in the sediment transport formulations (therefore also the results), especially in a data poor environment as Spratt Bight. Modelling sediment transport requires proper calibration and validation using data from the study area for representative hydro- and morphodynamic conditions (Bosboom & Stive, 2021). Unfortunately, this is not the case of this research. For this reason, it has to be kept in mind that the results shown in the next sections are indicative and overall trends in sediment transport behavior.

Finally, the results that will be presented in this chapter exclude the computational boundaries of the model and focusses only on its interest area. This is done because boundary effects are detected at the boundaries, which do not comply with reality. As the boundaries are chosen far enough of the interest area, they do not have any influence on the results presented in this chapter. In Appendix E results are shown for the entire domain, showing there is no influence of the boundaries in the interest area.

4.1 Hydrodynamics

Wave field: Eastern waves

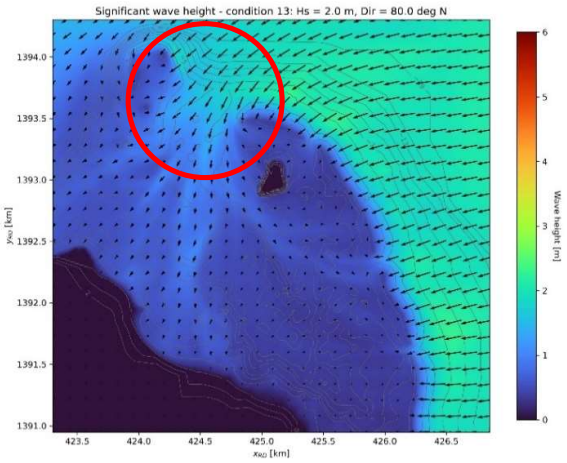

Figure 4.1: Model results showing the wave field for 2 m high waves coming from the East. The red circle indicates the openings through which most of the waves are penetrate the lagoon.

The Figure 4.1 shows the results of the wave modelling for the 2 m Eastern wave condition. It can be seen that waves break propagate towards the coral reef and break upon its steep depth gradients. This creates a surf zone just before and on top of the barrier reef, after which the waves propagate further inside the lagoon with a much lower height. Besides this mechanism, these Eastern waves also can reach the lagoon through a gap on the Northern side of the reef (indicated with the red circle in Figure 4.1). As these waves do not break on the coral reef, they can penetrate the lagoon with much more height and energy, being slowly damped by the mild slope at this area.

Wave field: Northern waves

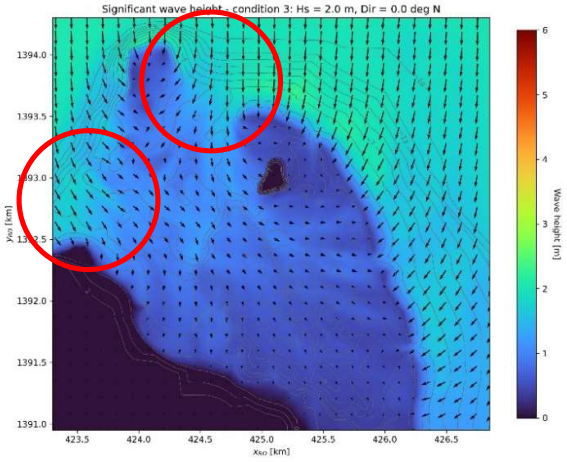

Figure 4.2: Model results showing the wave field for 2m wave coming from the North. The red circles indicate the openings through which waves can penetrate the lagoon.

Figure 4.2 shows the results of the wave modelling, but now for the Northern 2 m. It can be seen that, as well as the Eastern waves, the Northern wave are also breaking upon the coral reef, through the same processes as explained before. The main difference is through which opening the more energetic waves are entering the lagoon. As waves coming from the East predominantly reach the lagoon through Northern gap, the Northern waves penetrate the lagoon through both the openings: on the Northern and the Western side (indicated with the red circles in Figure 4.2). When reaching the latter, these waves start being influenced by the bathymetry, refracting towards the headland, and propagating further inside the lagoon.

Water Level

At coastal zones influenced by coral reefs, wave induced water level set-up can be observed upon the coral reef. This effect can also be observed in Spratt Bight, as can be seen in in the model results shown in Figure 4.5. Here, the cross-shore profile of the wave height for different transects are shown. The steeply decreasing wave height at the lower two plots indicates the presence of a surf zone at that area. In the upper transect shown in Figure 4.5, a less abrupt wave height decrease can be observed. At this area waves can enter the lagoon through the Western opening.

Intermezzo 4.1: Wave induced set-up and radiation stresses

Waves approaching the coral reef can generate a water level set-up inside the lagoon at the reef top. If the boundaries of the coral lagoon are closed or semi-closed, and outflow is restricted, waves breaking on the reef top will "pump" water over it and cause ponding inside the lagoon. This process is shown in Figure 4.3.

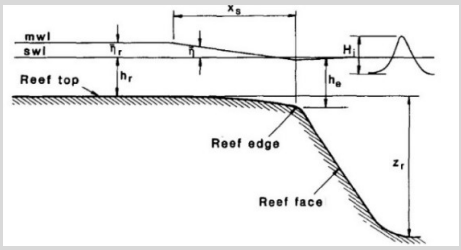

Figure 4.3: Schematization of increase in water level at reef top (or coral lagoon) after breaking on the reef edge. Adapted from Gourlay (1996).

This effect can be explained by means of the radiation stress theory, in which the wave force (F_x: dependent on the radiation stresses) balances the pressure force (P_x: dependent on the water level (η)) (Bosboom & Stive, 2021; Gourlay, 1996). Assuming an alongshore normal coastline and normally incident waves, the force balance can be expressed as follows:

$$F_x + P_x = 0 \qquad \text{Equation 4.1}$$

In which:

$$F_x = \frac{dS_{xx}}{dx} \quad \text{and} \quad P_x = \rho g(h_0 + \bar{\eta})\frac{d\bar{\eta}}{dx}$$

As can be seen in Equation 5.1, there is a balance between the wave force and the pressure force. The pressure force is dependent on the water level and its gradient ($d\eta/dx$), while the wave force depends on a gradient in radiation stresses (dS_{xx}/dx). The magnitude of the radiation stress in the wave propagation direction depends on wave height (H_{rms}), the water depth (h), and the wavelength (λ) according to the following formulation (Bosboom & Stive, 2021):

$$S_{xx} = (2n - 0.5)E$$ Equation 4.2

In which:
n is the ratio between the wave group velocity and the phase velocity
E is the wave energy formulated as: $E = \frac{1}{8}\rho g H_{rms}^2$

In an idealized alongshore uniform coastal area, waves are breaking at the surf zone, which means that their height is decreasing compared to before entering the surf zone (Bosboom & Stive, 2021). According to Equation 5.2, S_{xx} is dependent on the wave energy (E), which leads to a decreasing wave height and therefore decreasing radiation stresses. A decreasing S_{xx} in the landward direction means that there is a negative cross-shore gradient of the radiation stresses ($dS_{xx}/dx < 0$). According to Equation 5.2, in order to be in equilibrium, the water level gradient needs to be positive ($d\eta/dx > 0$). This equilibrium balance leads to a difference in water level at both sides of the water column (higher towards the coast). This phenomenon is called wave set-up. The opposite effect can be observed at the shoaling zone in which waves grow, generating a positive gradient in radiation stresses, and therefore a wave induced set-down (Bosboom & Stive, 2021). Figure 4.5 shows a schematization of the set-up effect.

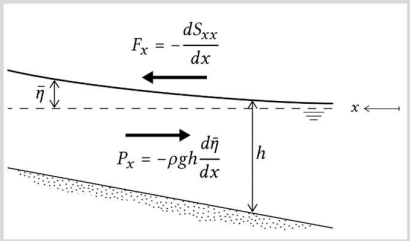

Figure 4.4: Schematization of the force balance between wave force (Fx) and pressure force (Px) adapted from Bosboom & Stive (2021)

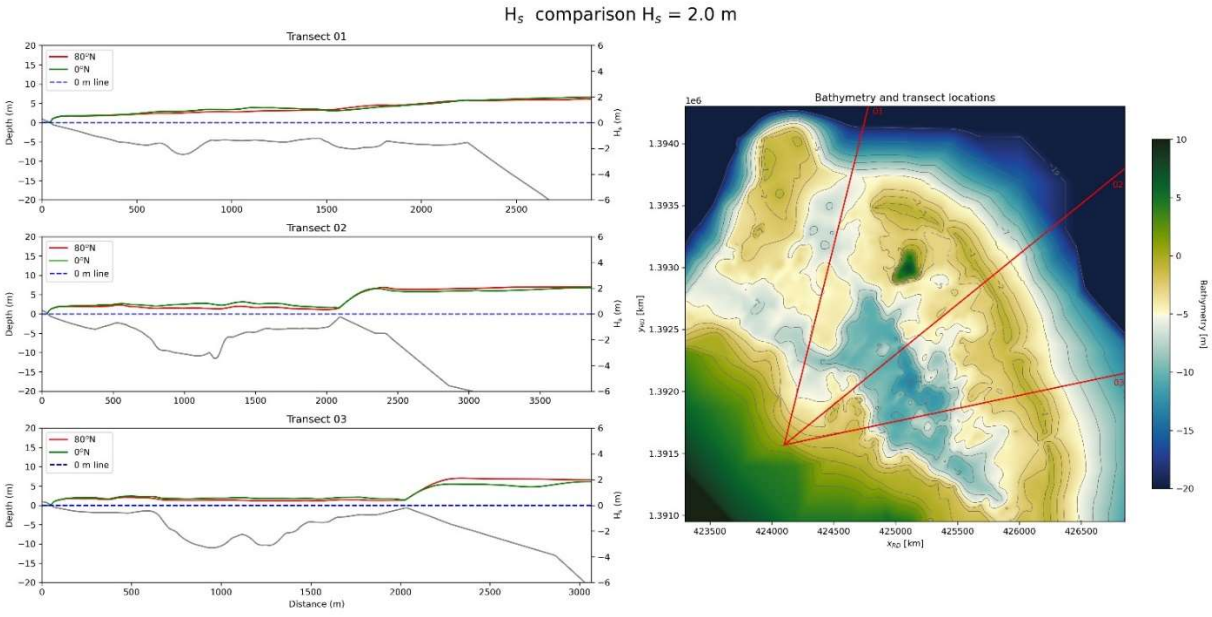

Figure 4.5: Model results showing the cross-section of the significant wave height of the 2 m offshore waves. On the right side of the figure the bathymetry is plotted, in which the three lines indicate the transects of the cross-sections shown on the left. On the left, cross-shore profiles of the wave height are plotted for each of these transects. The red line indicates waves coming from the East, the green line waves coming from the North.

The result of waves breaking on the coral reef is that there arises a water level difference between the lagoon and the area at the surf zone. This induces a pressure difference driven flow in which water flows from higher to the lower pressure. In other words, water starts flowing inside the lagoon. As water accumulates inside the lagoon, water levels

start to increase behind the coral reef. This effect can be observed in the model results shown Figure 4.6. In this figure the same transects of Figure 4.5 are shown, however now the water level is plotted in the cross-sectional profiles.

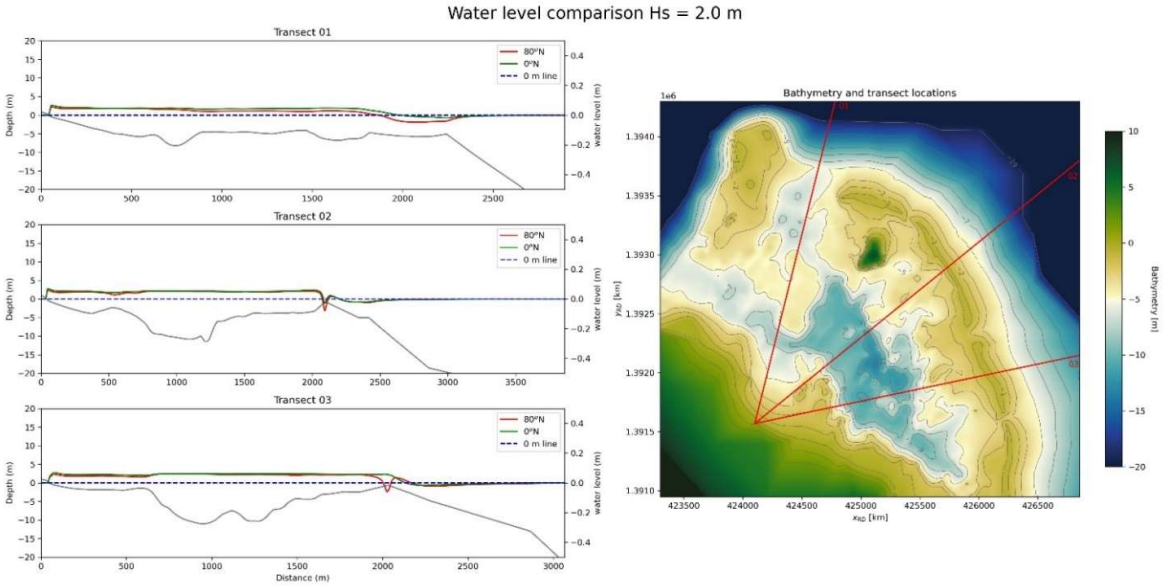

Figure 4.6: Model results showing the cross-section of the water level for different transects for the 2 m offshore wave. On the right the bathymetry is plotted, in which the three lines indicate the transects of the cross-sections shown on the left. On the left, cross-shore profiles of the wave height are plotted for each of these transects. The red line indicates waves coming from the East, the green line waves coming from the North.

In the figure above it can be seen that for an offshore significant wave height of 2 m, the model results show a water level set-up inside the coral lagoon of almost 0.1 m. Water level set-up in the lagoon increases even more with increasing incoming wave height. Figure 4.7 shows how offshore significant wave heights of 5.5 m can increase the water level up to up to 0.4 m above the MSL.

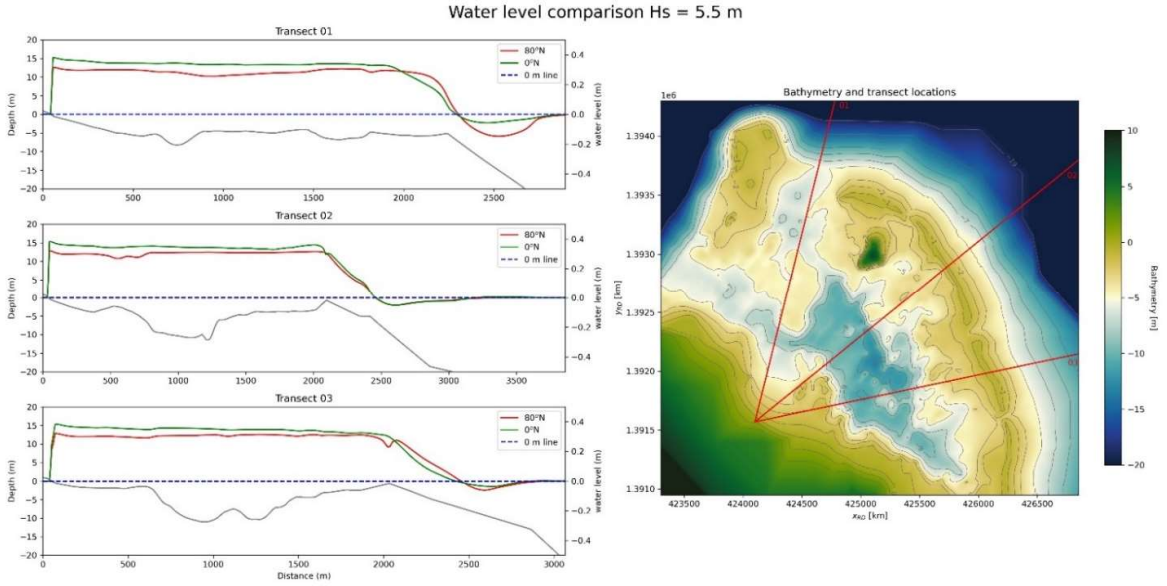

Figure 4.7: Model results showing the cross-section of the water level for different transects for the 5.5 m offshore wave. On the right the bathymetry is plotted, in which the three lines indicate the transects of the cross-sections shown on the left. On the left, cross-shore profiles of the wave height are plotted for each of these transects. The red line indicates waves coming from the East, the green line waves coming from the North.

Flow Velocities

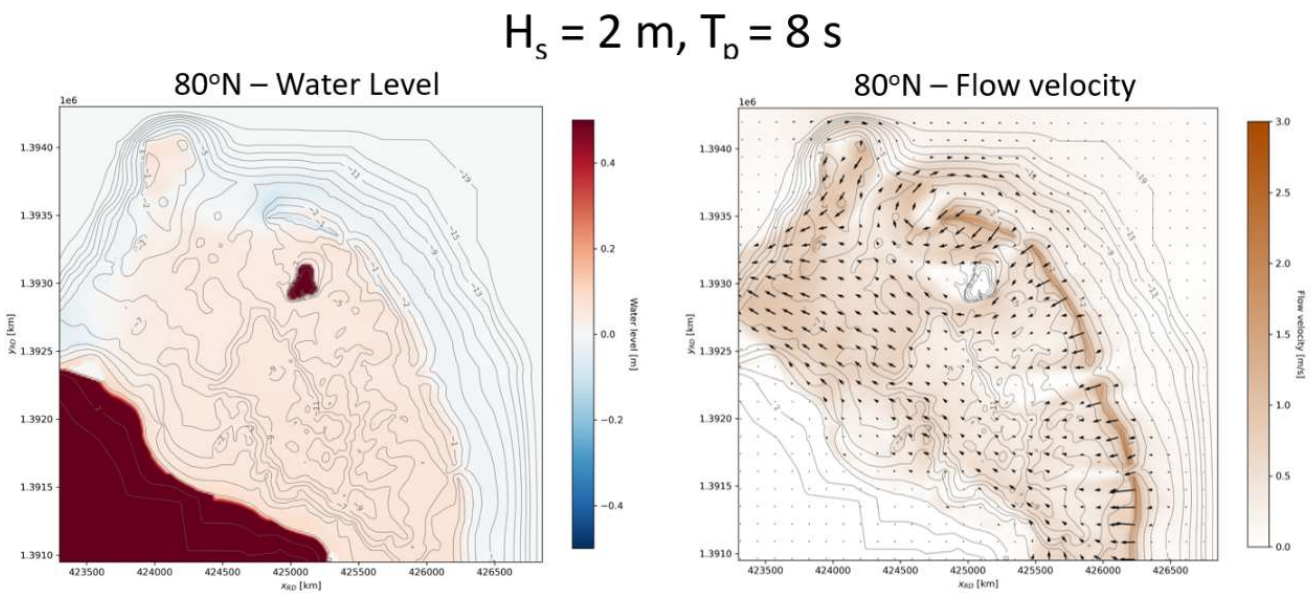

Figure 4.8: On the left: model results for the water level set-up. The red shades indicate higher water levels and the blue shades lower water levels. On the right: model results of the flow velocity field. The black arrows indicate the direction of the current, while the orange shades indicate the magnitude of the velocity. Both simulations were made with Eastern waves of 2 m.

Water cannot be 'pumped' indefinitely inside the lagoon without creating a pressure difference between the lagoon and the external (offshore) environment. At certain moment, the water level difference between the lagoon and the area outside the lagoon starts inducing a flow velocity. This flow velocity is directed towards the location of lowest water level and resistance. In the case of the Spratt Bight coastal are, it is the western opening in the coral reef. This effect can also be observed in the model results shown in the Figure 4.8.

Figure 4.8 shows the magnitudes and the directions of the flow velocity in the model (on the right) and the water levels associated with it (on the left). It can be seen that water level increases inside the lagoon, inducing a current towards the West, where there is an opening without coral barriers. At this location the absence of coral structures and water level set-up makes it the 'easiest way out'.

For waves coming from the North, the same processes can be observed (as can be seen in Figure 4.9). In this figure water is again accumulated behind the coral reef and has the tendency to leave the lagoon at the Western opening.

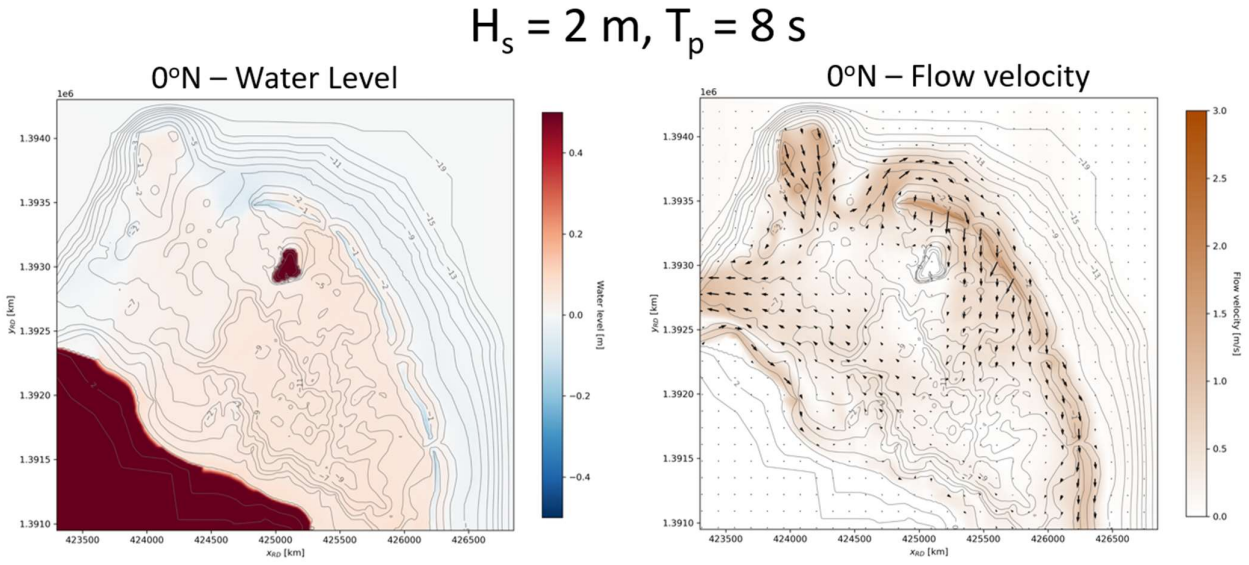

Figure 4.9: On the right: model results of the flow velocity for 2 m waves coming from the North. On the left: model results of the water level set-up for the same condition. The red rectangle shows an area of increased water level set-up, due to waves breaking at this area.

However, during this condition a stronger secondary current towards the Southeast is observed, along the coast of Spratt Bight. This current is explained by means of the Northern waves that reach the lagoon from the West due to refraction, as shown in Figure 4.2. In this situation, the radiation stresses also have an important contribution to the process flow generation. However, in this case not only the pressure related term, but also the advection part of the radiation stresses plays a role. The latter is responsible for the transport of momentum by the particle velocity, which is in wave propagation direction (see Intermezzo 4.2). With this being said, flow velocities generated by Northern incoming waves in Spratt Bight can be explained by both the advection and the pressure related components of the radiation stresses. Figure 4.11 shows how both waves coming from the North and from the East enter the protected area in the lagoon through the Western gap and reach the headland (indicated with the red circle).

Intermezzo 4.2: Wave induced longshore current

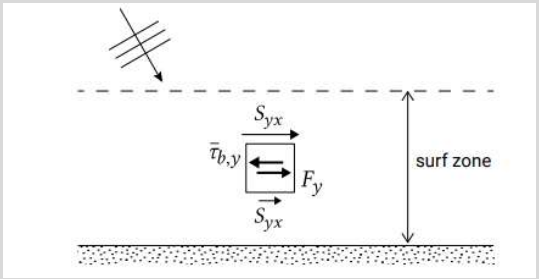

Figure 4.10: Forces acting on the water column in a longshore uniform coastline. The longshore current driven by obliquely incident waves is from left to right. (Bosboom & Stive, 2021).

At an alongshore uniform coast, waves approaching the shoreline with a certain angle drive a force in the y-direction (along the coast), which induces a longshore current in the surf zone. Figure 4.10 shows the direction of the advection related component of the radiation stresses and its balance with the bed shear stresses (τ_b). For an (ideal) alongshore uniform and uninterrupted coastline, the pressure gradient cannot develop in the longshore direction the same way (as explained through

uninterrupted coastline, the pressure gradient cannot develop in the longshore direction the same way (as explained through Equation 5.1) it does for the cross-shore direction. The gradient in radiation stresses induces a force ($F_y = -\frac{dS_{yx}}{dx}$), which is responsible for a wave force in alongshore direction, which is counteracted by the shear stresses (τ_b). As a consequence, the transfer of momentum from the wave motion to the mean flow results in a longshore current in the direction of the wave propagation (Bosboom & Stive, 2021).

$$S_{yx} = n \cdot cos(\theta) \cdot sin(\theta) \cdot E$$

As can be seen, S_{yx} is a function of the wave angle (θ), wave energy (E) and the ratio between the wave group velocity and the phase velocity (n). In order to respect the conservation of energy theory, the alongshore driving force has to be dependent of the dissipation of the wave energy (wave breaking), as there can only be a gradient in radiation stresses if the wave energy somehow decreases (or increases). As the alongshore forcing can only develop when waves are breaking, the longshore current is restricted to the surf zone (Bosboom & Stive, 2021).

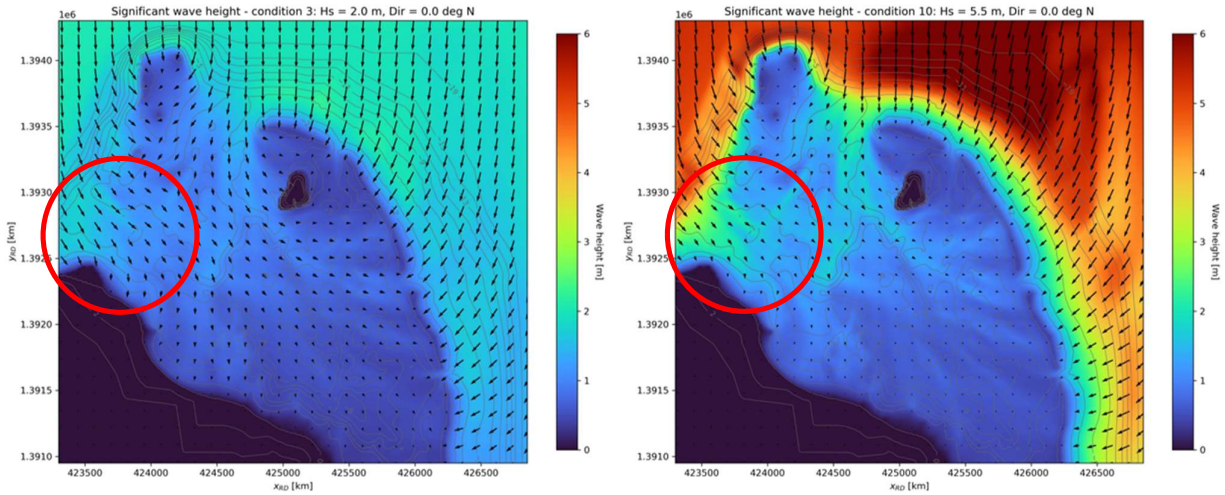

Figure 4.11: Model results showing the wave field of for 2 m and 5.5 m waves coming from the North and. The red circles indicate the Western opening through which waves can penetrate the lagoon.

Thus, what happens during the Northern wave conditions is that, firstly, waves coming from the North refract due to the depth contours and enter the lagoon through the Western opening (as shown in Figure 4.11). There they start breaking when reaching the coast, initiating the formation of a surf zone nearshore. This surf zone is responsible for A) a an alongshore current in wave propagating direction (dS_{yx}/dx) and B) a local water level set-up at the headland at the entrance of the lagoon, inducing a pressure gradient driven flow (dS_{xx}/dx).

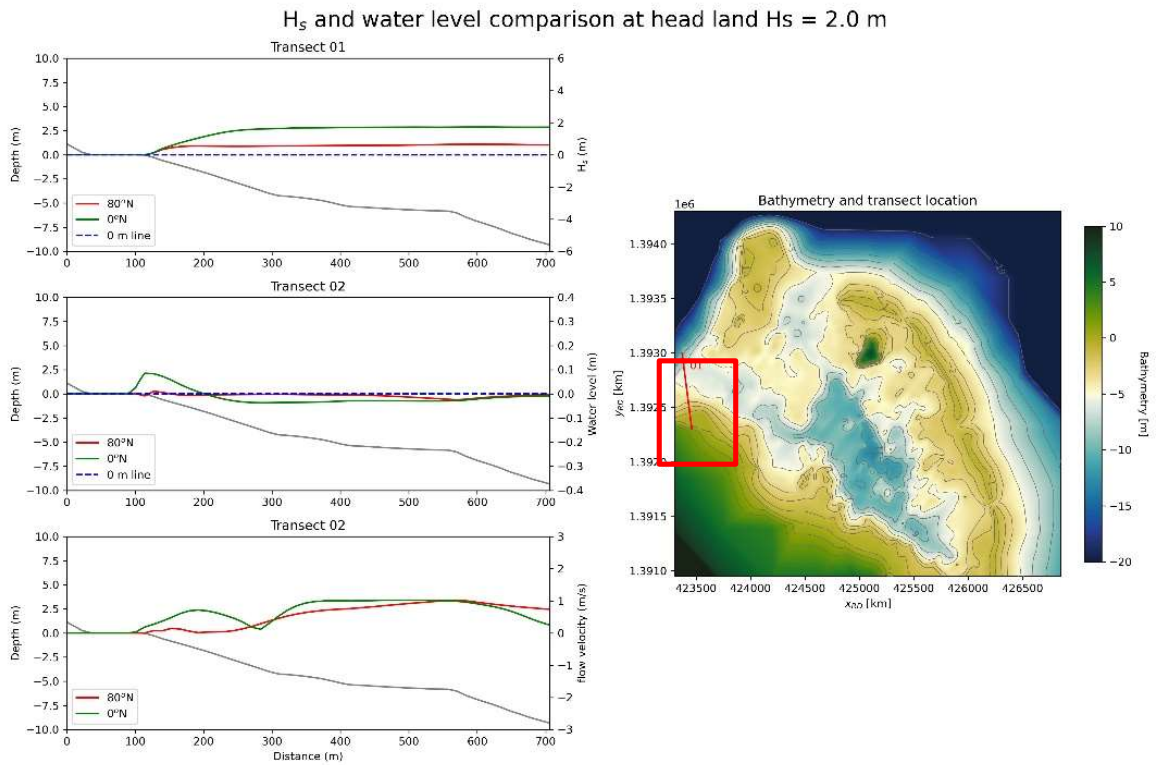

Figure 4.12: Cross-section of model results at Western opening towards the lagoon. The cross-sections are taken from the transects shown with the red line on the left figure. The upper profile indicates the wave height, the second shows the water level set-up and the lower cross-section shows the flow velocities. The green line indicates the 0°N conditions and the green line the 80°N conditions. Both are simulated with 2 m wave heights.

Figure 4.12 shows the wave heights, water levels and flow velocities at the Western entrance of the lagoon. A transect is taken in order to show the difference between the processes induced by the Northern waves and the Eastern waves. It can be seen that the Northern waves almost don't lose any energy before reaching the shore, while the Eastern waves are much lower at this area. This generates a water level set-up that is almost 10 times higher for the Northern waves than for the Eastern waves. The velocity fields generated by this set-up are shown in the figures below.

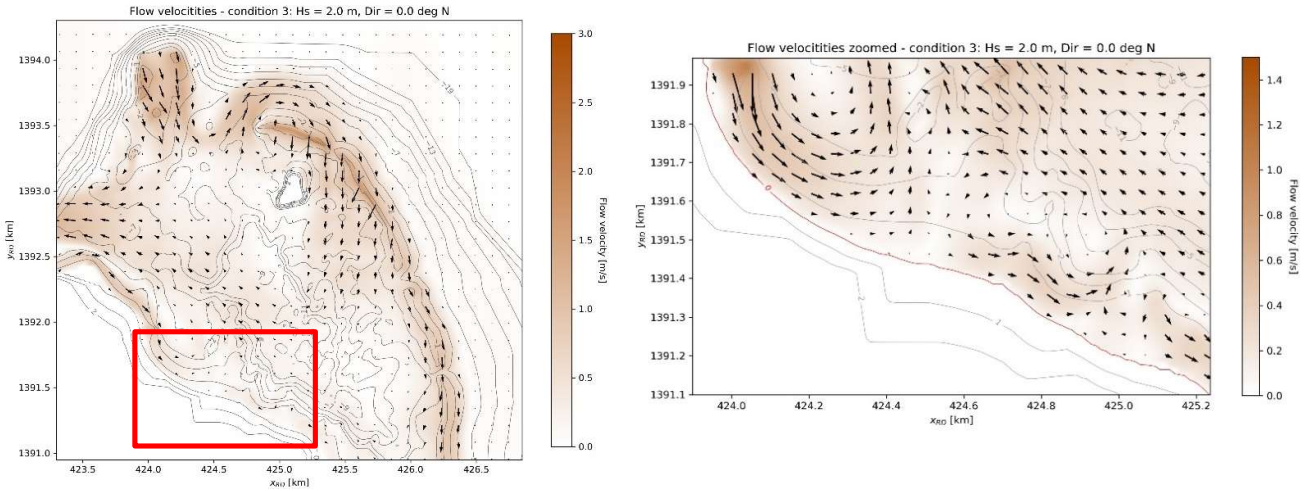

Figure 4.13: Model results of the flow velocity field for the 2 m Northern waves. On the right a zoomed image is shown focusing on the interest area.

The consequence of both the increased waves and water level is a flow velocity profile which is higher for the Northern waves than for the Easter waves. This current extends itself along Spratt Bight Beach coastline and is directed southwards. This effect is shown in Figure 4.13. Figure 4.14 shows how this is very weakly observed for waves coming from the East.

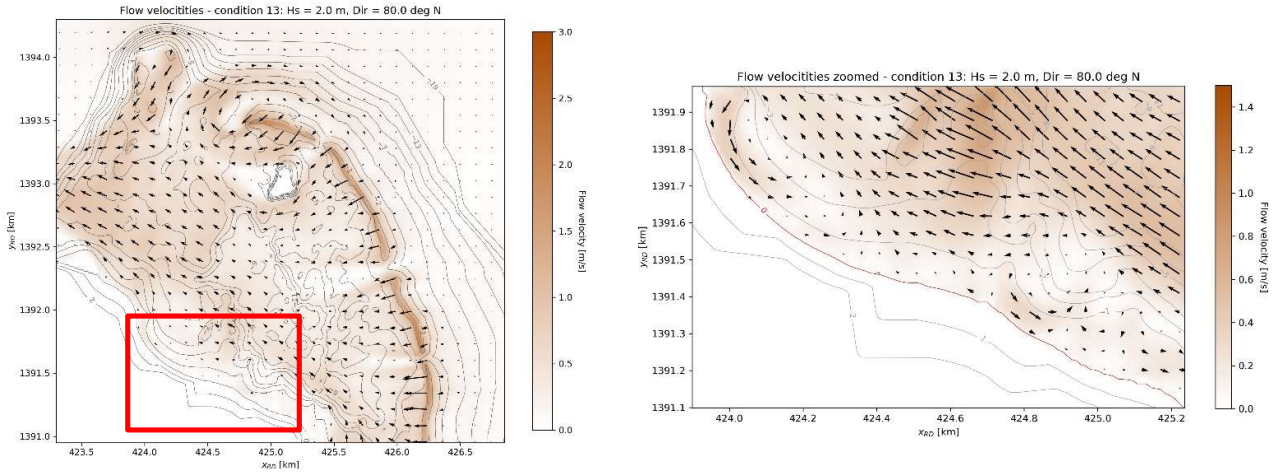

Figure 4.14: Model results of the flow velocity field for the 2 m Eastern waves. On the right a zoomed image is shown focusing on the interest area.

Storm Conditions

The previously explained effects and processes are even more enhanced during storm conditions. The figure below shows the flow velocity pattern for both the 0°N wave condition (left) as the 80°N wave condition (right).

In Figure 4.15 and Figure 4.16 it can be seen that the velocity patterns are much stronger than the ones shown in Figure 4.13 and Figure 4.14. This indicated the intensification of these patterns during storm conditions.

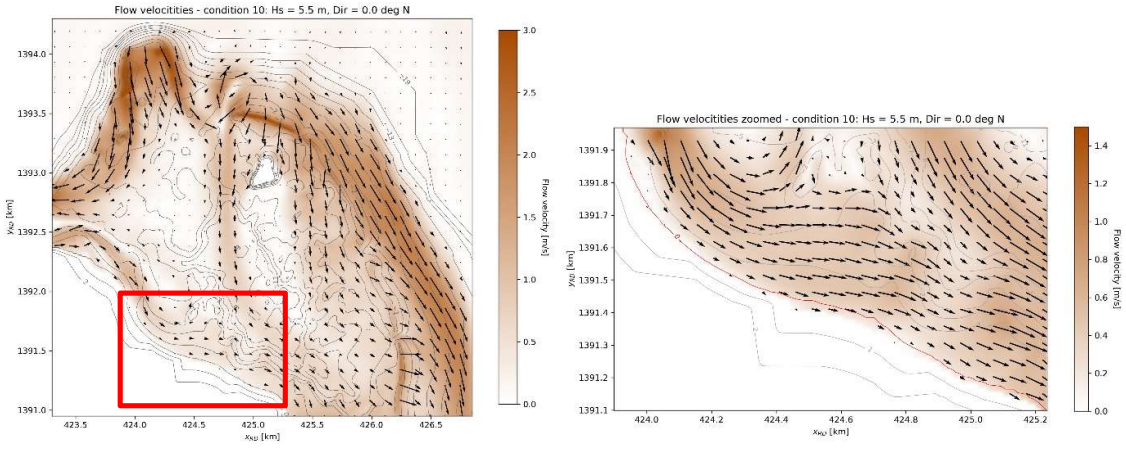

Figure 4.15: On the left the model results of the flow velocity field for 5.5 m waves coming from the North are shown. On the right the figure is a zoomed in area (taken from the red rectangle).

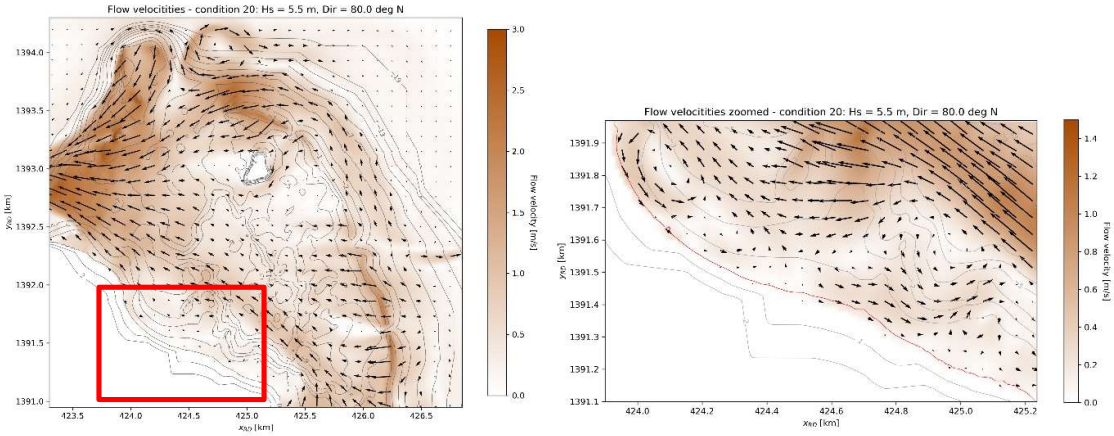

Figure 4.16: On the left the model results of the flow velocity field for 5.5 m waves coming from the East are shown. On the right the figure is a zoomed in area (taken from the red rectangle).

An overview of the effect of the wave height on the flow velocity near the coast is shown in Figure 4.17 and Figure 4.18 (respectively for Eastern and Northern waves). Here it is shown how the flow velocities increase when the offshore wave height is increased. This means that the higher the wave height the stronger are the currents induced by them.

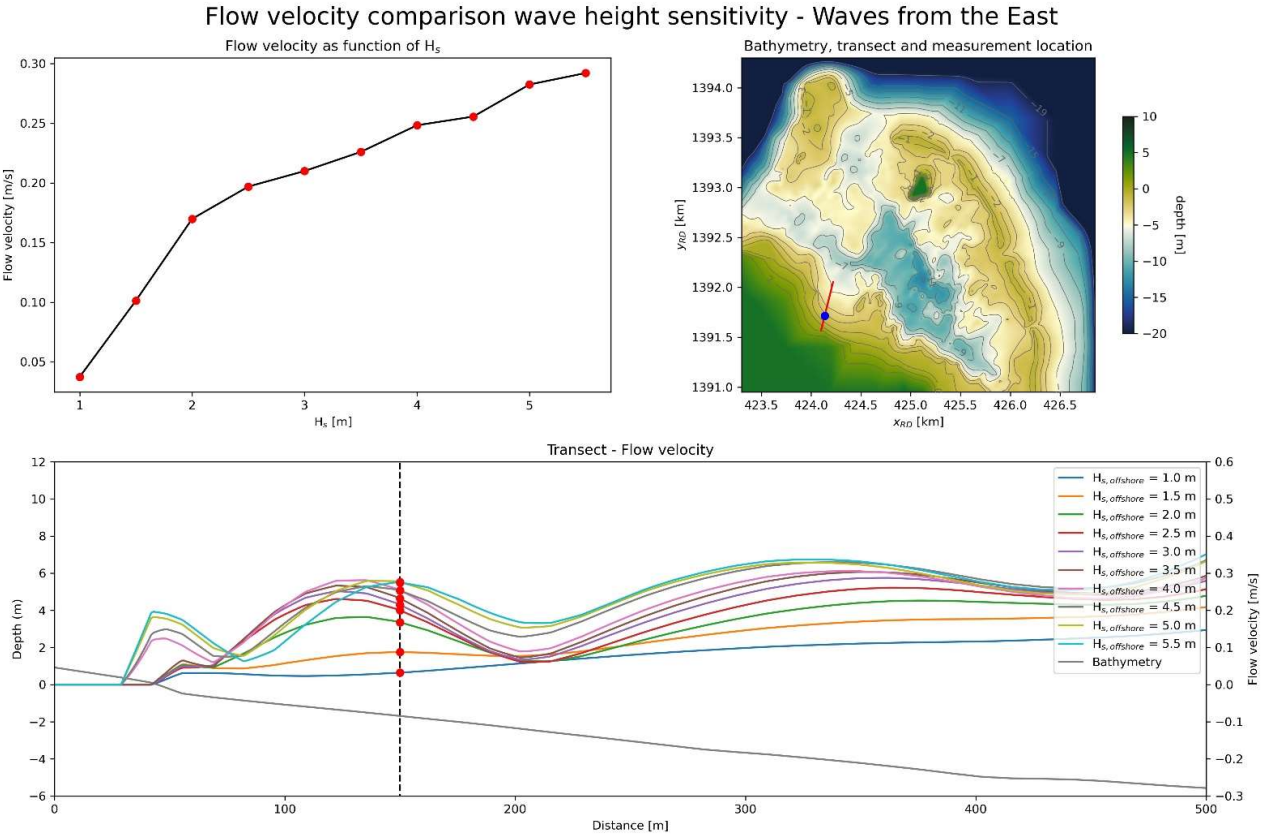

Figure 4.17: Influence of the Eastern waves on the flow velocity (near the coast, across a transect). Flow velocities induced by offshore waves of 1 m, 1.5 m, 2 m, 2.5 m, 3 m, 3.5 m, 4 m, 4.5 m, 5 m, 5.5 m are shown. The upper right figure shows the bathymetry of the study area. The red line

indicates the transect taken and the blue dot the location at which point data is taken. On the upper left the flow velocities extracted at the location of the (previously described) blue dot are plotted against the significant wave height. Finally, the lower plot shows the cross-shore profile of the bathymetry (gray line), and of the flow velocities (colored lines) at the transect depicted in the upper right figure.

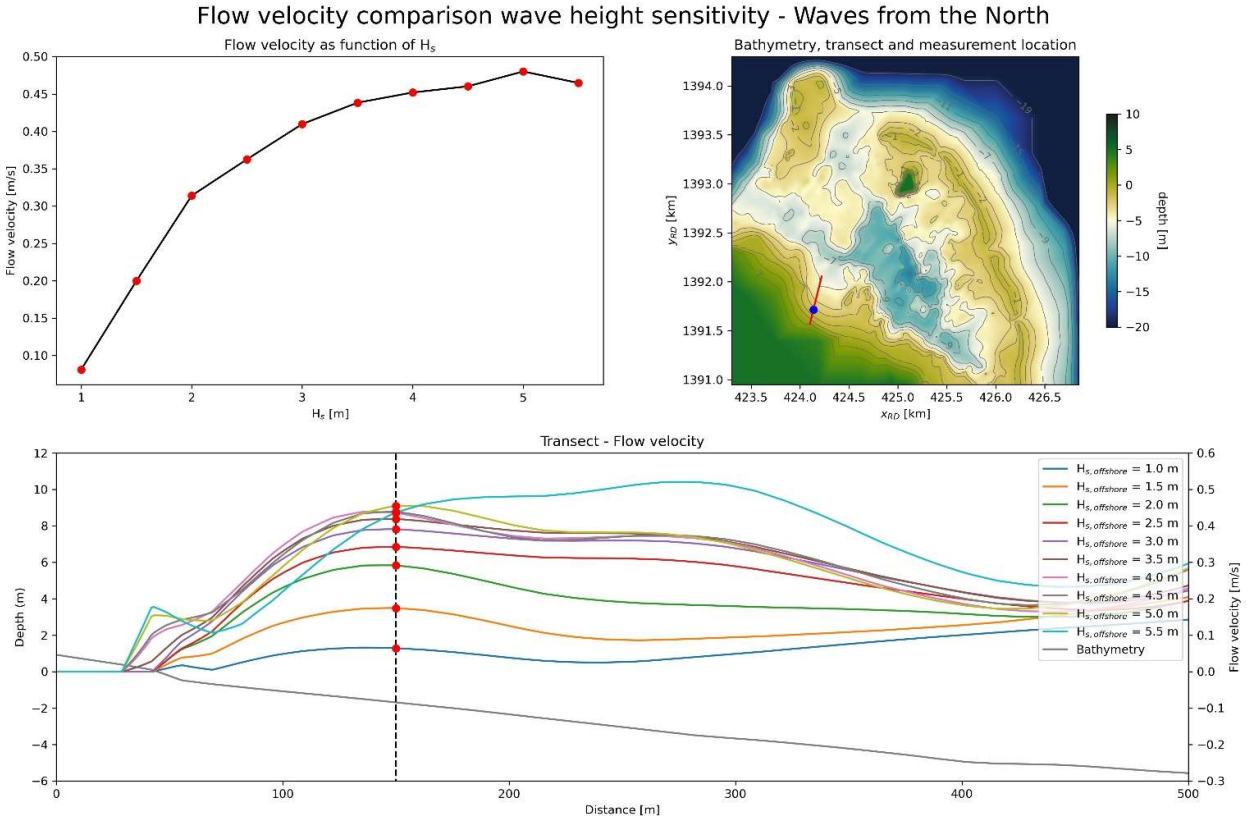

Figure 4.18: Influence of the Northern waves on the flow velocity (near the coast, across a transect). Flow velocities induced by offshore waves of 1 m, 1.5 m, 2 m, 2.5 m, 3 m, 3.5 m, 4 m, 4.5 m, 5 m, 5.5 m are shown. The upper right figure shows the bathymetry of the study area. The red line indicates the transect taken and the blue dot the location at which point data is taken. On the upper left the flow velocities extracted at the location of the (previously described) blue dot are plotted against the significant wave height. Finally, the lower plot shows the cross-shore profile of the bathymetry (gray line), and of the flow velocities (colored lines) at the transect depicted in the upper right figure.

4.2 Sediment Transport

On both ends of Spratt Bight Beach there is no sediment supply available from adjacent beaches. On the Western side there is a breakwater, after which there are no sandy beaches in westward direction (as shown in Figure 4.19). The available sediment for Spratt Bight is coming from inside the lagoon. This source of sediment can possibly reach the beach through cross-shore transport phenomena, which is mostly driven by the oscillatory motion of the waves (Bosboom & Stive, 2021).

Figure 4.19: Google Earth (2019) image showing boundaries of Spratt Bight Beach where there is absence of a sediment source.

The morphodynamic results shown in this section are mostly sediment transport capacity patterns rather than actual sediment transports. As mentioned in Section 3.2.2, it has been assumed that sediment is widely available, meaning an infinite supply of sediment has been considered.

The considerations above are important to notice because, regardless of the strength of the transport velocities, sediment transport will only occur if there is sediment available in the area. Either in the bed or in the form of sediment concentration, through supply from adjacent coasts. If there is no sediment available to be transported, the actual transport might be smaller than the transport capacity (which are shown in the model results).

The objective of the modelling study is to look into what environmental conditions are causing coastal erosion at Spratt Bight Beach. The erosion pattern as shown in Figure 4.20 is an example of a beach profile Spratt Bight can assume during certain conditions. In this figure it can be seen that, according to the report of FINDETER (2020), sediment is intensively transported Southwestwards during episodic events.

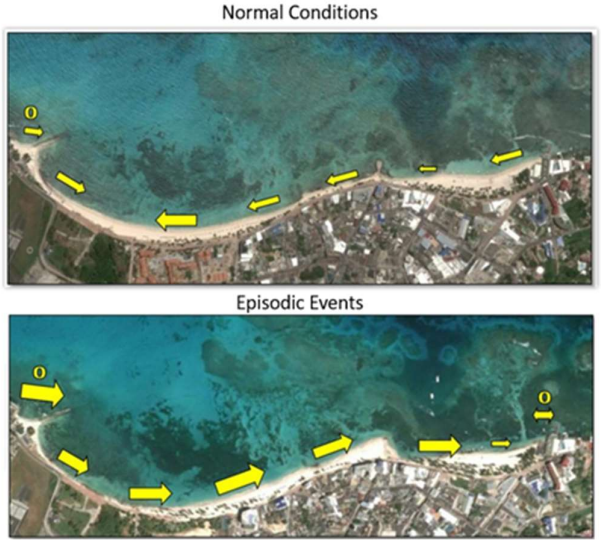

Figure 4.20 Sediment transport conditions during normal conditions with waves coming from the East (upper figure), and during episodic conditions driving the sediment towards the southwest of the beach. The yellow arrows indicate the direction of the flow (FINEDETER, 2020).

As previously explained, during events with Northern wave conditions, the flow velocities along the beach are increased and southeastward directed. This pattern is shown in Figure 4.16. Since the transport is usually in the direction of the instantaneous flow velocity, it can be derived that the sediment transport S(t) is proportional to $u|u|^{n-1}$. This proportionality can be interpreted as the product of a transporting velocity u and the sediment load stirred by waves and currents proportional to $|u|^{n-1}$ (Bosboom & Stive, 2021).

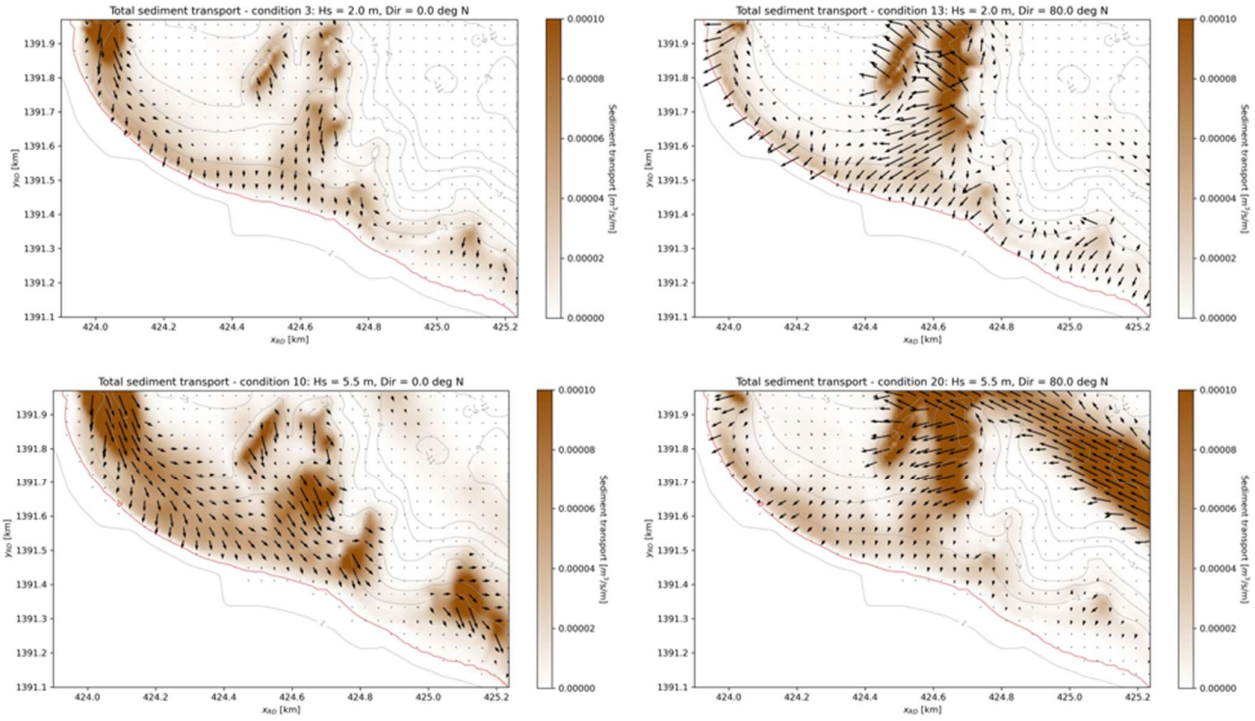

Figure 4.21: Sediment transport patterns along the coast of Spratt Bight. In this case the plot is focused on the interest area nearshore. The two left images represent the waves coming from the North, while the right image show the transports as result of the waves coming from the East. The upper images are both for wave conditions of 2 m and the two lower images represent waves of 5.5 m height.

Figure 4.21 shows the computed sediment transport patterns for waves coming from the North and from the East. It can be seen that specially for the Northern wave conditions (on the left), the overall direction of the sediment transport matches the flow velocities found in Figure 4.16. It can also be seen that the sediment transports for the waves coming from the East (on the right) are mostly shoreward directed. This pattern can be attributed to the relatively low longshore flow velocities in this area during these conditions (as shown in Figure 4.8 and Figure 4.16) and the oscillatory motion of the waves in cross-shore direction. As the flow velocities are relatively higher and dominate during the occurrence of Northern waves, flow dominates the sediment transport pattern during these conditions, generating a sediment transport pattern towards the Southwest. This confirms the pattern shown in Figure 4.20.

Intermezzo 4.3: Cross-shore sediment transport

The wave orbital motion is very important for the sediment transport in cross-shore direction, but it has almost no influence on the transports in longshore direction. It can even be said that the wave orbital motion is approximately cross-shore directed in the nearshore (Bosboom & Stive, 2021). Sediment transport is dependent on a current related term and a wave related term. The total sediment transport can be expressed with the following equations:

$$S_t = S_b + S_s$$

$$\underbrace{\langle S_s \rangle}_{\text{time-averaged sediment transport rate}} = \underbrace{\int_a^h UC\,dz}_{\text{current-related part}} + \underbrace{\int_a^h \overline{\tilde{u}\tilde{c}}\,dz}_{\text{wave-related part}}$$

$$S_b = BD_{50} \underbrace{\frac{U}{C_h}\sqrt{g}}_{\substack{\text{current only} \\ \text{transports} \\ \text{the sediment}}} \exp \underbrace{\left[\frac{-0.27(s-1)D_{50}\rho g}{\mu\langle|\tau_{cw}|\rangle}\right]}_{\substack{\text{wave-current shear stress} \\ \text{stirs up the sediment}}}$$

In the equations above, S_s denotes suspended load transport and S_b bed load, of which the sum results in the total sediment transport (S_t). The suspended load is dependent of a velocity term (time-averaged (U) and oscillatory ($\tilde{u}$) flow) and a concentration term (time-averaged (C) and oscillatory ($\tilde{c}$) concentration). The bed load depends on the Bijker coefficient (B), particle diameter (D_{50}), a mean flow current (U), Chézy coefficient (C_h), relative density (s), a ripple coefficient (μ) and, the time-averaged shear stress magnitude for the combined wave-current motion (τ_{cw}).

In a situation in which there is a weak mean flow signal, the sediment transport is mostly induced by the cross shore directed oscillatory motion of waves nearshore. When the waves enter shallow water, they start feeling the bottom, shoaling and begin to assume a skewed profile. In this situation the orbital velocities under the crest and in the wave propagating direction (towards the coast) become higher, while the orbital velocities at the trough and opposite to the wave direction (offshore directed) become smaller.

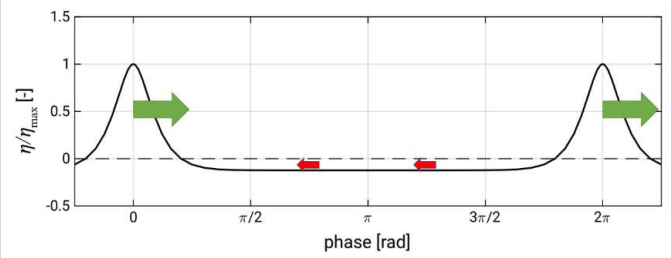

Figure 4.22: Representation of a skewed wave, in which the propagation direction is to the right. Modified from Bosboom & Stive (2021).

This situation is mostly valid for the bed load, however in the case of the suspended load the wave-related suspended sediment transport mechanism is very complex to model, and little is known about the intra-wave concentrations, making such computations very uncertain (Bosboom & Stive, 2021). More detailed information about how sediment transport is modelled is presented in Appendix D.

4.3 Cause of Erosion at Spratt Bight Beach

From the model results presented above, it became clear what hydro- and morphodynamic processes drive the coastal system of Spratt Bight. During average conditions (90% of the time) waves come from the East, break on the barrier reef, and induce a water level set-up inside the lagoon. This set-up creates a water level difference between the lagoon and the offshore environment, inducing a current pattern directed outside the lagoon, where the resistance is the smallest: the western opening. Figure 4.23 shows a schematization for these processes at Spratt Bight.

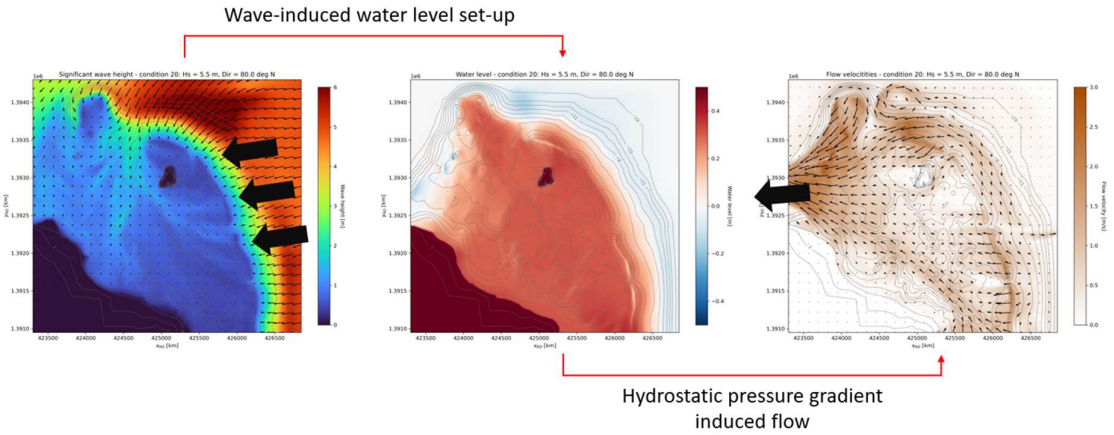

Figure 4.23: Schematization of the hydrodynamic processes within the coastal system of San Andrés for 5.5 m waves coming from the East. The left figure represents the model results of the wave heights, the middle figure represents the water level set-up and finally, the right figure represent the flow velocities.

During episodic events, in which waves are coming from the North, the situation is slightly different. The same water level set-up is generated within the lagoon, however, now also a wave induced longshore current is generated along the beach of Spratt Bight. The figure below shows the important processes in the case of the Northern incident waves. In the figure it can be seen how the approaching waves not only break over the reef, but also refract into the lagoon through the western opening and reach the headland.

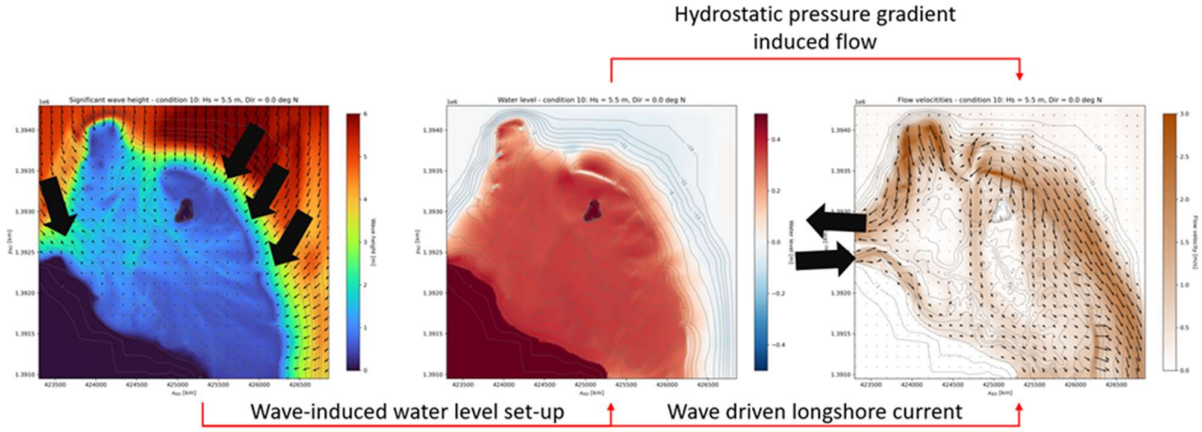

Figure 4.24: Schematization of the hydrodynamic processes within the coastal system of San Andrés for 5.5 m waves coming from the North. The left figure represents the model results of the wave heights, the middle figure represents the water level set-up and finally, the right figure represent the flow velocities.

This longshore current mainly drive a sediment transport pattern along the coast which mostly matches the directions of the flow velocity for the same wave condition. The figure below shows the flow velocity pattern for the Northern waves (on the left) and the sediment transport patterns (on the right).

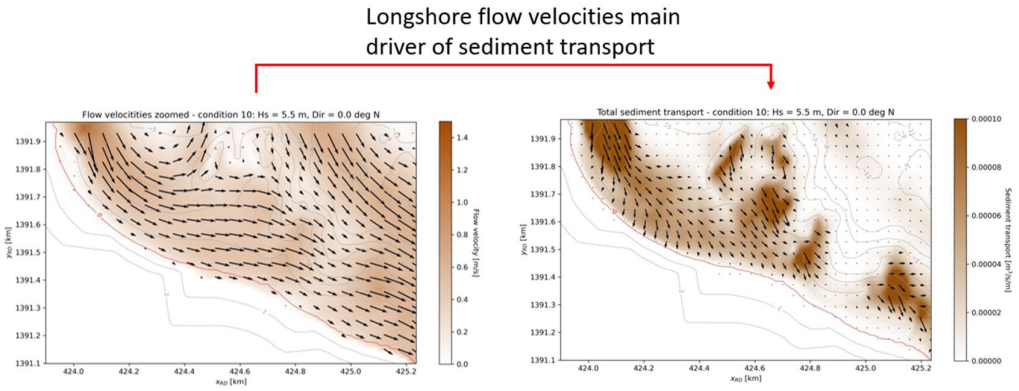

Figure 4.25: Model results showing flow velocity field (left) inducing sediment transport pattern (right)

The fundament behind change of coastal profiles is that it occurs where there are sediment transport gradients and/or sediment sinks or sources of sediment. If the same the amount of sediment transported inside the system and outside the system, there is no erosion nor accretion. In the case of a positive gradient (acceleration) of the sediment transport, erosion is observed. When there is a negative gradient in the transport velocities (deceleration), accretion is observed (Bosboom & Stive, 2021).

As there is a breakwater at the western end of the beach, it can be assumed that there is no sediment input at that area. The absence of longshore input of sediment to the system and high sediment transport rates mean that erosion is happening at the lea side of the breakwater. This is confirmed by Figure 4.20 of FINDETER (2020).

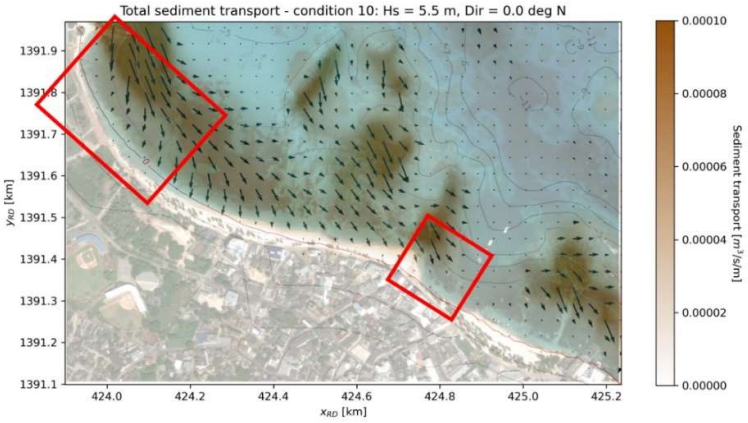

Figure 4.26: Model results of sediment transport rates for 5.5 m waves coming from the North. The results are overlayed on a satellite image from FINDETER (2020) in which erosion patterns are shown due to episodic events.

Figure 4.26 shows an overlay of Figure 4.20 and the total sediment transport for 5.5 m high waves coming from the North. The left rectangle indicates the location of erosion on the beach, which matches the model results with high sediment transport velocities and the assumption that there is a low sediment input due to the breakwater.

The second rectangle (on the right) in Figure 4.26 shows a local acceleration of the sediment transport field, indicating erosion should be observed. This also matches the erosion profile observed in the overlayed satellite picture. Besides, due to the breakwater (Espolón Tiuna), the availability of sediment is limited, and erosion happens as a consequence.

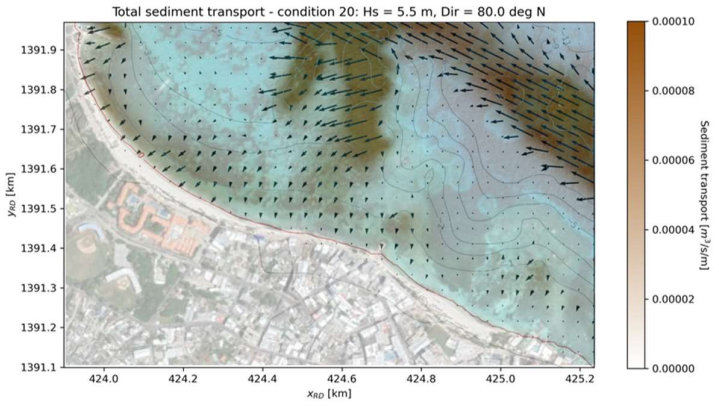

Figure 4.27: Model results of sediment transport rates for 5.5 m waves coming from the East. The results are overlayed on a satellite image from FINDETER (2020) in which the beach profile is shown for normal conditions.

Figure 4.27 shows the overlay of satellite image of San Andrés retrieved from FINDETER (2020) and the total sediment transport for 5.5 m high waves coming from the east. Here it can be seen that the sediment transports are directed towards the coast and the west, restoring the beach (dynamic) equilibrium profile. Besides, it can also be noticed that the sediment transport rates during these conditions are much lower than during the Northern wave conditions. This shows how the wave conditions with average direction of incidence have a lower capacity of restoring the beach profile, making it take longer to restore equilibrium than to disturb it by a Northern wave event.

Finally, as described in Section 2.2.4, the highest morphological variability can be observed during the storm season. This matches the periods in which the Northern waves are mostly observed, as shown in Figure 4.28.

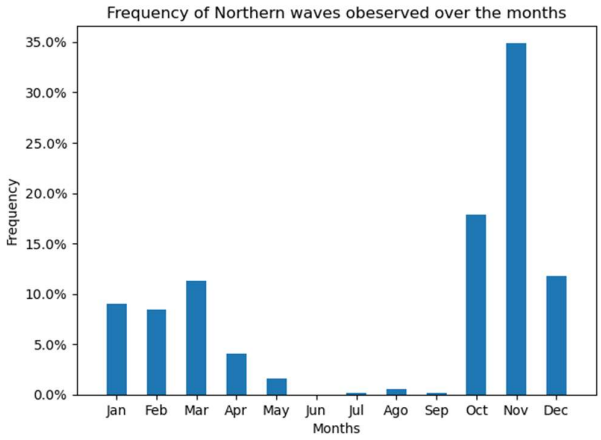

Figure 4.28: Histogram showing the frequency of waves coming from the North in San Andrés.

With this, there is strong evidence that the Northern waves are responsible for the erosion events described in Figure 4.20 by FINDETER (2020).

5 Mitigation Measures

In order to mitigate and prevent the erosion problem in San Andrés as described in this report, three solutions are being proposed. These measures were developed using the Building with Nature (BwN) philosophy, in which multi-functional, sustainable, and socially accepted solutions are being discussed. A qualitative evaluation of the solutions is made.

The developed solutions should: 1) Reduce the **wave heights** reaching Spratt Bight Beach. 2) Reduce the **longshore flow velocities** along the coast of Spratt Bight. 3) Prevent **sediment of leaving** the coastal system. 4) Increase the **sediment budget** of the coastal system. 5) Add **ecological and social value** to the area. With these goals in mind three solutions were proposed: seagrass restoration, beneficial reuse of dredged material and implementation of artificial coral reefs.

Despite the advances in the development of sustainability in San Andrés, the declaration of the Sea Flower Biosphere Reserve in 2000, the community organizations, and their political-administrative structure, the island's current socio-economic development model is still unsustainable. This translates into a spiral of environmental, social, and economic decline (Sánchez-Jabba, 2016). In this environment, nature-based measures for the protection against coastal erosion can play a fundamental role, as they contribute in a decisive way to generate adequate conditions for sustainable, ecological, and integral human development of the island of San Andrés. In this chapter the proposed measures for Spratt Bight Beach are further explained and analyzed.

5.1 Building with Nature Philosophy

The application of the Building with Nature (BwN) philosophy to design solutions for water-related infrastructure is a relatively new approach in the sustainable development, however becoming a growing trend in the present hydraulic engineering field. Societal (urbanization, growing energy demand, etc.) and environmental (climate change, sea level rise, etc.) trends are requiring high demands on hydraulic engineering projects and the associated water system management. Solutions that are not multifunctional and without due consideration of the surrounding system are no longer accepted. Stakeholder involvement, multi-functionality and sustainability are required (de Vriend, van Koningsveld, Aarninkhof, de Vries, & Baptist, 2015).

The main objective is to create better solutions for environmental and societal challenges of this century. This is addressed in the global agenda by means of the Sustainable Development Goals (SDG's) (United Nations, 2015). The strength of measures designed using the BwN philosophy is that they are in line with the SDG's, which is an important motivation to choose this approach over traditional engineering methods.

The Building with Nature approach by EcoShape (2020) is used, since there are many examples of successful application of these solutions in the Netherlands and around the world. The BwN design philosophy aims to create solutions that are:

- In harmony with the behavior of the natural system
- Let nature do part of the work
- In close collaboration with stakeholders and local communities
- Of added value for nature, (local) economy and society

5.2 Possible Alternatives

5.2.1 Sea Grass Restauration

The health and condition of the seagrass ecosystems benefits other adjacent ecosystems and their associated species. People depend directly on the sea for their livelihoods, and it has tangible and far-reaching benefits for many parts of society. Besides as mentioned in Section 2.3, seagrasses can represent up to 50% of the sediment sources in San Andrés (Universidad del Norte - IDEHA, 2009).

As a starting point and according to the Coastal Erosion Master Plan for Colombia (2017), the clearing of mangroves and other vegetation, extreme fishing and tourism around coral reefs is affecting ecosystems in and around the coastal zone. This indirectly affects the system's ability to retain sediment or to reduce wave energy before reaching the beach (Guzman, Posada, Gusman, & Morales, 2009).

In Section 2.3 it is explained that seagrasses can exert a drag force on the water column as it travels over the seagrass canopy, hereby reducing wave height by up to 40% under non-storm conditions (Guannel, Arkema, Ruggiero, & Verutes, 2016). In addition, they reduce bed shear stress levels, preventing the resuspension of sand, therefore contributing to retaining sediments that are within the reef flat system.

As indicated in the previous chapters, the fringing reef surrounding Spratt Bight Beach results in a less energetic coastal environment. Maintaining a healthy ecosystem of corals and seagrasses that can expand and grow is essential to keep the wave energy low inside the lagoon behind the coral reef, therefore avoiding exacerbated coastal erosion problems. Despite the widely benefits of seagrasses, there is a steady decline in their healthy cover in San Andrés (INVEMAR, 2019), and action is needed to prevent further degradation or, in the worst case, a total collapse of the system.

5.2.1.1 Specifications

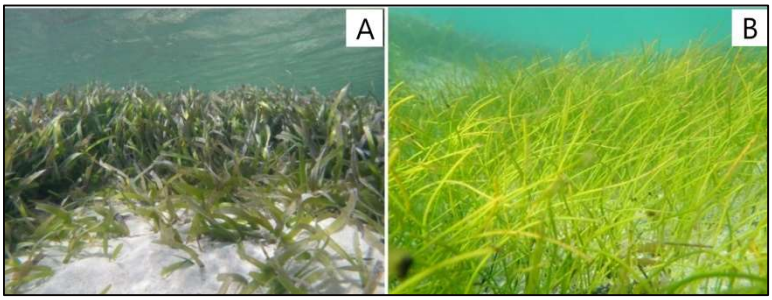

Figure 5.1: Different seagrass species that can be found on San Andrés. A) turtle grass (Thalassia testudinum) and B) manatee grass (Syringodium filiforme) (CORALINA-INVEMAR, 2012)

Initial conservation and restoration efforts should focus on identifying the pressures affecting seagrass health. Anthropogenic stressors should be removed or diminished so that coral reef and seagrass ecosystems can recover and become more resilient and cope with large-scale natural disasters/hazards, such as cyclone events and rising ocean temperatures. Sources that alter environmental conditions for nutrients and turbidity need to be identified, restricted, and monitored. Ensuring that abiotic conditions for coral and seagrass growth are optimal is the first step towards restoration and conservation.

Restoration and recovery of seagrass beds ensure ecological benefits, including acting as nursery, refuge and feeding grounds for many species of juvenile fish, invertebrates, and a wide variety of species such as sea turtles. In addition, seaweed restoration and recovery play an important role in reducing wave height, producing oxygen and cleaning

seawater by absorbing polluting nutrients that travel from land to sea. Restoration or recovery actions can be carried out with species present such as A) turtle grass (Thalassia testudinum) and B) manatee grass (Syringodium filiforme), by direct seeding through propagules or seeds or by transplanting whole seedlings, as shown in Figure 5.1 (INVEMAR, 2019).

Seagrass productivity can be limited by light availability, which is a key requirement for seagrass expansion. Turbid conditions are therefore detrimental to their survival, as they hinder the penetration of light into the water column (Ralph, Durako, Enriquez, Collier, & Doblin, 2007). Seagrass growth may also be limited by nutrients. In tropical, non-deltaic waters (such as San Andrés), insufficient nutrients in pore water can limit growth. However, eutrophic conditions are also not ideal, as fast-growing algal species are able to compete with seagrasses for light. Finally, temperature conditions should not be too warm for marine plants to grow, as warming of shallow waters can significantly affect marine plant populations.

Clonal growth is the main factor in the lateral expansion of seagrass beds. Expansion by germination is much slower, as environmental requirements for successful seed germination are much more stringent. Habitat restoration efforts should focus on creating suitable environmental conditions for both types of expansion, as the former increases the rate of restoration, and the latter contributes to a more diverse gene pool. If environmental requirements are met at the restoration site, large-scale manual transplantation of seagrass is often successful (Matheson, Reed, Dos Santos, Mackay, & Cummings, 2016).

This involves taking seagrass shoots from donor populations and transplanting them into areas where seagrass growth is suitable. Seed-based restoration is also successful but is less common because it requires more work. Seeds can be mixed with local sediments and injected into the substrate. The main advantage of using seeds is that the donor grassland is less damaged (Matheson, Reed, Dos Santos, Mackay, & Cummings, 2016).

5.2.1.2 Social and environmental impacts

As described above, coral reef and seagrass recovery and restoration can help increase wave attenuation by increasing friction, stabilizing the seabed, and preventing coastal erosion. A comprehensive environmental and social impact assessment is needed to identify sites previously populated by seagrass, as these sites could be used for reclamation and restoration. The assessment would also allow further identification of potential bottlenecks and strengths of the solution.

In addition, sources of degradation (effluent run-off, trawling of nets on the seabed, over-tourism, etc.) could be better identified and managed. According to experts, fishermen indicated that they use several coral reef channels as access routes to Spratt Bight Beach, so remediation and restoration initiatives should be tailored to fishermen's use to ensure that newly planted or restored seagrass is not damaged.

Water quality and fisheries management are examples of non-structural measures that can be taken to prevent conflicts while rehabilitating and restoring seagrass. However, restoring seagrass by these means has its own complications. Identifying sources of eutrophication and addressing them requires a long and painstaking process on the part of stakeholders. If deterioration is indeed a problem, local government agencies and other stakeholders (such as beachfront hotel owners) need to be involved in identifying possible solutions.

Water resources need to be managed to prevent untreated water from reaching the coast. Projections of annual tourism and population growth are needed to see how water use may change. In addition, in-depth stakeholder engagement is needed to identify possibilities for action. Both fishermen and the tourism sector depend on intact ecosystems (e.g., fishing, diving, viewing, etc.) and need to be involved in developing solutions. The formulation and implementation of participatory management plans for marine vegetation, can provide an interesting tool for the environmental authority

(Coralina) to address the sources of damage to natural ecosystems, as well as the technical and stakeholder involvement activities necessary for their restoration.

Figure 5.2: Example of how seagrass is collected for restoration

An improved ecosystem could represent advantages for the artisanal fisheries sector due to the multiplication of breeding and nursery habitats for commercially targeted species. Together with regulations, fisheries policies and strategies for gear and size regulation can increase stocks and thus boost local livelihoods. In addition, the beneficiaries of seagrass restoration can include the local community through improved water quality or reduced shoreline erosion.

5.2.1.3 Costs

A more detailed feasibility study is needed to calculate the exact financial budget required to restore seagrass. In general, seagrass and coral reef restoration are among the most expensive marine ecosystems to restore, while mangroves tend to be cheaper and on a larger scale. Some initial price indications can be given based on previous research, where coral reef restoration costs are estimated to range from $1,717 USD to $2,879,773 USD per hectare (Foo & Asner, 2019). Similar costs are also known for seagrasses, ranging from $9,000 USD to over $1 million per hectare (Downs, 2014). The success rate of restoration depends largely on-site selection and the choice of suitable plants. Experts advise monitoring coral reefs and marine plant restoration to increase the success rate. There are different monitoring options, which affect costs; the cheapest options are community-based monitoring or remote sensing, while expert fieldwork is more expensive.

1. Marine vegetation restoration

Specifications	Pros	Cons	Costs
➢ Natural recovery (presence or past history of seagrass meadows) ➢ Planting rhizomes (rhizome planting when small areas require restoration) ➢ Seeding seagrass (seeding for large scale restoration)	+ Protective: wave attenuation, current reduction, seabed stabilization, prevention of coastal erosion + Environmental: carbon sequestration, biodiversity habitat. Also, fish, crab nurseries, shelter and food for marine species + Economic: Potential increase in of commercially targeted species	– Tourism sensibility and disconformity	• **Initial investment** Costs have a very wide range — Average costs 10.50 USD/m^2 • **Monitoring and maintenance costs** Monitoring of water quality and vegetation growth — 25.000 USD These costs are highly dependent on the type of labor to be used

5.2.2 Beneficial Reuse of Dredged Material and Artificial Coral Reefs

To give a purpose to the maintenance dredged sand from the access channel, a possible solution against erosion could be applying a sand nourishment with sediment taken from maintenance works. This measure ensures there is enough width for recreational activities and coastal safety along its length.

By adding sand to the system in Spratt Bight the beach width and the total sediment volume increases. This allows the beach to still keep its dynamicity and periodical change in sediment transport direction, and at the same time ensuring a minimal width between the waterline and the structures near the coast (boulevard, hotels, and restaurants). Although the sediment is moved to the east and west, there will always be enough beach width for recreation, touristic activity, and safety.

This sediment source was investigated by INVEMAR in a field campaign (2021). During this field research information about grainsize, pollutants, organic material and density was collected and analyzed in laboratory. This information and data are important as the extracted material should be compatible with the sediment at Spratt Bight Beach. Besides the fact that it ensures the sediment is not contaminated and cannot damage the ecosystem, it also avoids big differences in coastal dynamic effects with respect to the original situation. The result of this study shows that the sediment from the access channel of the Port of San Andrés is compatible with the sand on Spratt Bight Beach and that pollutants will not present an issue when using it as nourishment material.

It must be considered that Spratt Bight (and San Andrés as a whole) is an ecologically sensitive area in which fine sediments can cause negative impacts. Dredging and nourishing should therefore be done using environmentally friendly techniques and an environmental impact assessment (EIA) should be carried out before the operations start.

5.2.2.1 Historical Context of the reuse of dredged material

According to several studies and expert knowledge (Appendix F and Universidad del Norte - IDEHA, 2009), beaches of San Andrés have already been nourished and land has been reclaimed using dredged material from the access channel. The figure below shows a map in which the reclaimed land for the port of San Andrés can be identified.

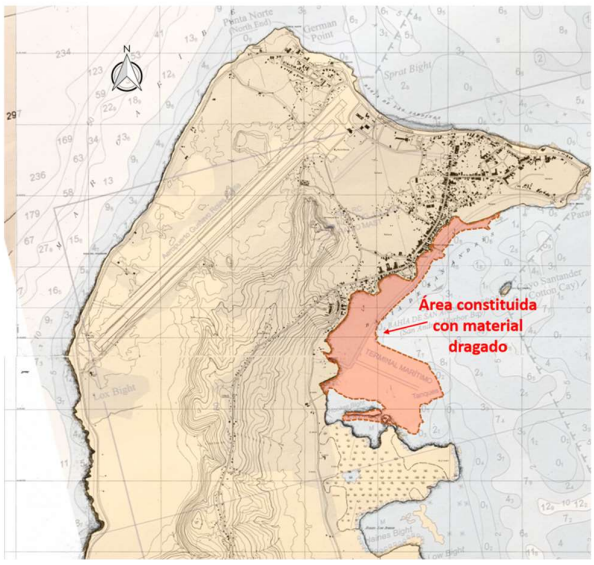

Figure 5.3: Map of the Northern part of San Andrés. The orange area is where land was reclaimed between 1963 and 1988. Adapted from CIOH (2008) and Ministerio de Obras Publicas (1963)

In 1964 and 1987 the Van Suramericana company dredged the port's access channel to construct the quay wall of Texaco. This resulted in a great land reclamation project that added approximately 500,000 m2 (50 ha) of dry area to SAI. Part of this area is nowadays what is called the maritime terminal (at the Southern part), and to the North the area was reclaimed to construct part of the road that goes around the island (Universidad del Norte - IDEHA, 2009).

During the deepening of the navigable channel in 1993, the dredged material was reused on several beaches, including Spratt Bight. The government of San Andrés decided that among the beaches contemplated with nourishment activities would Spratt Bight with 20,000 m^3 distributed over a length of 1,000 m (Universidad del Norte - IDEHA, 2009).

The exact technique used for the dredging and nourishing activities and the impact it caused on the environment during that period are unknown. However, previous studies and reports do not show severe impacts and changes of the environment during this period (Geister & Dias, 2007).

5.2.2.2 Specifications: reuse of dredged material

The amount of sediment necessary to nourish Spratt Bight Beach depends on the beach width that is wanted to be achieved. An average profile of Spratt Bight is shown in the figures below. It can be seen that the average profile is shallow and has a very mild slope. This means that not a lot of nourished material is needed to increase its beach width.

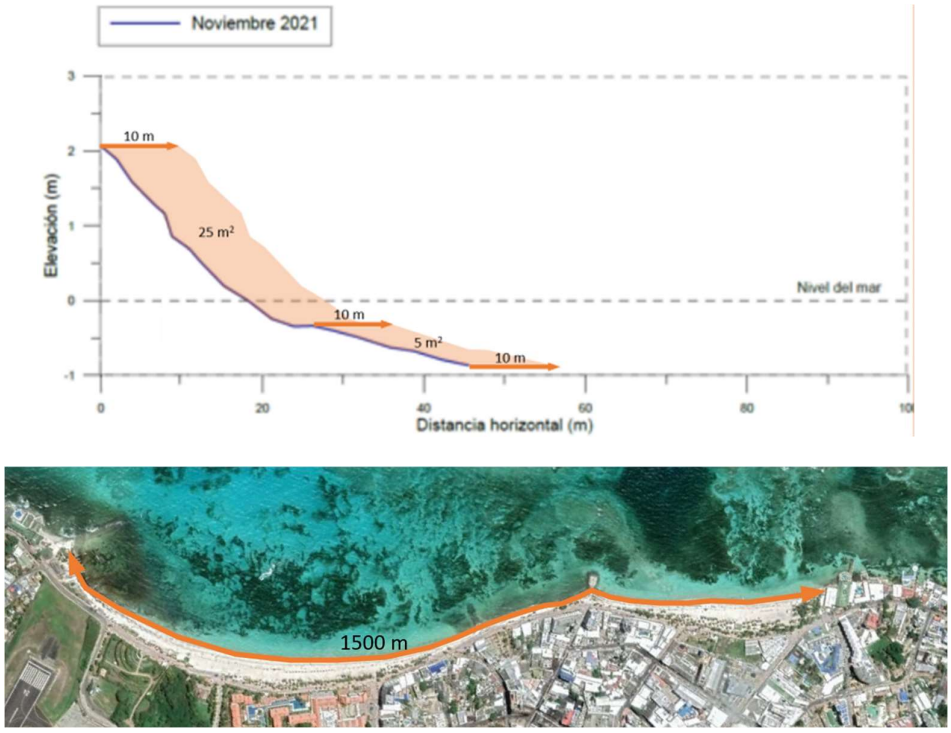

Figure 5.4: Above an average beach profile from Spratt Bight taken during the field campaign of INVEMAR (2021). In the graph the profile was moved 10 m seawards and the area between the two profiles is shown (approximately 30 m2). Below the length of Spratt Bight Beach is shown. Adapted from INVEMAR (2021)

If the beach is nourished until an additional width of 10 m (as shown in the figure above), the cross-sectional area of the beach would increase approximately 30 m^2. With a total beach length of 1500 m, 45.000 m^3 of sediment would be needed. An additional 30% needs to be taken to account for initial sediment loss due to unsettled fine sediment particles. Finally, a total of 60.000 m3 would be needed to increase the beach width of Spratt Bight by 10 m.

Necessary volume to nourish Spratt Bight Beach						
Volume (m^3)	6.000	30.000	60.000	90.000	120.000	150.000
Beach width (m)	1	5	10	15	20	25

Table 5.1: Nourishment volumes necessary to achieve each corresponding beach width

Table 5.1 shows the sediment volumes needed (in m^3) to increase the beach width by 1 m until 25 m. As indicated in the findings of the field campaign of INVEMAR (2021), there is 200.000 m^3 of usable sediment available in the access channel, which is enough to nourish Spratt Bight.

During the dredging activities, a dredging vessel would collect the material on the selected location and transport it to Spratt Bight Beach to increase its width. This transportation of sediment can be done by various ways:

- The dredged material can be collected by vessels, transported to the beach by trucks and spread by bulldozers. This is possible as only a small amount of sediment is necessary to nourish the beach.
- The dragged material can be stored on a hopper vessel, which would sail to Spratt Bight and dump the sediment through tubes/pipelines on the beach. Bulldozers would then have to relocate and spread the sediment over the beach.
- While dredging, the vessel could be connected to a long tube/pipeline (of a few km) and the sediment is then transported instantly to the beach. This method also requires bulldozers to relocate the sediment and the pipeline onshore.

In order to prevent ecological damage, the first option would be preferred, as it is the method that releases the smallest amount of fine sediment during nourishment activities.

After nourishing it is necessary to make sure that the newly placed sand will not be eroded and that the old beach equilibrium profile would be installed again. As explained in Chapter 4, sediment is mildly transported from East to West and during episodic conditions it is more strongly transported from West to East. Applying nourishment measures will not change this transport behavior. In order to prevent the sediment to be lost, bypassing the breakwaters and headlands on the beach, other appropriate measures have to be taken into account.

An option would be to review the location and the dimensions of the current breakwaters (shown in Figure 5.5) in order to improve them and optimize their impact on the coast. The breakwaters could be restructured applying artificial coral reefs as done by ReefSystems (www.reefsystems.org) and Reefy (www.reefy.nl). In this way adding ecological value to the system.

Figure 5.5: Position of the different breakwaters in Spratt Bight.

5.2.2.3 Specifications: artificial coral reefs

Near the beach

By extending and improving the breakwater on the Western end (Espolón Pescadores, shown on the West of Figure 5.5) waves that penetrate the lagoon through the western opening in the coral reef are attenuated. This attenuation of the higher waves close to the beach is likely to result in not only lower long-shore fluctuations, but also the reduction of the cross-shore fluctuations of the beach profile.

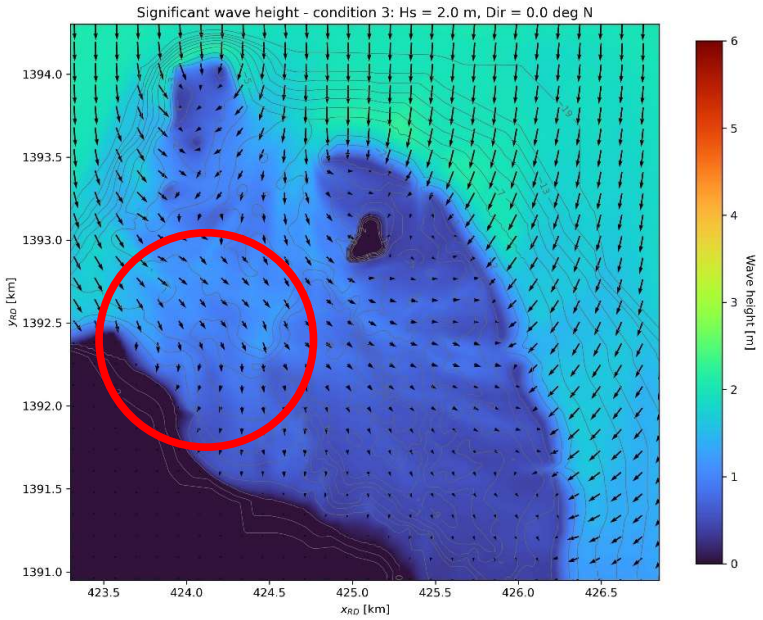

Figure 5.6: Model results of the wave field for 2 m waves coming from the North. The red circle shows the decrease in wave height as the wave penetrate the lagoon.

As shown in the red circle of Figure 5.6, there is a strong decrease of wave height while penetrating the lagoon and propagating towards the coastline. For this reason, it is advised use the Espolón Pescadores as a basis to construct the new artificial reef breakwater. A schematization of the location of the breakwater is shown below.

Figure 5.7: Impression of location for breakwaters in order to avoid sediment losses due to longshore transport after nourishment. On the left examples of artificial coral reefs.

Besides the restoration and improvement of Espolón Pescadores with artificial coral reefs, an extra artificial reef breakwater should be constructed on the east end of the beach. This should be done in order to prevent the sediment, driven to the east during Northern wave conditions, to be lost over the headland. In the report of Universidad del Norte (2009), a design of a possible breakwater on the SE side is made with more specifications.

Finally, it is advised to remove Espolón Tiúna and Espolón Jeno's Pizza. Both breakwaters not only don't have any functionality as they are displayed in the current situation, but they might also even increase erosion in the middle section of the beach due to their shadow zone.

At the Western opening

During events in which offshore waves come from the North reaching the lagoon through the Western opening, a longshore transport is induced (as explained in Chapter 4). By blocking the waves before reaching the shore, they are prevented of generating a current along the coastline.

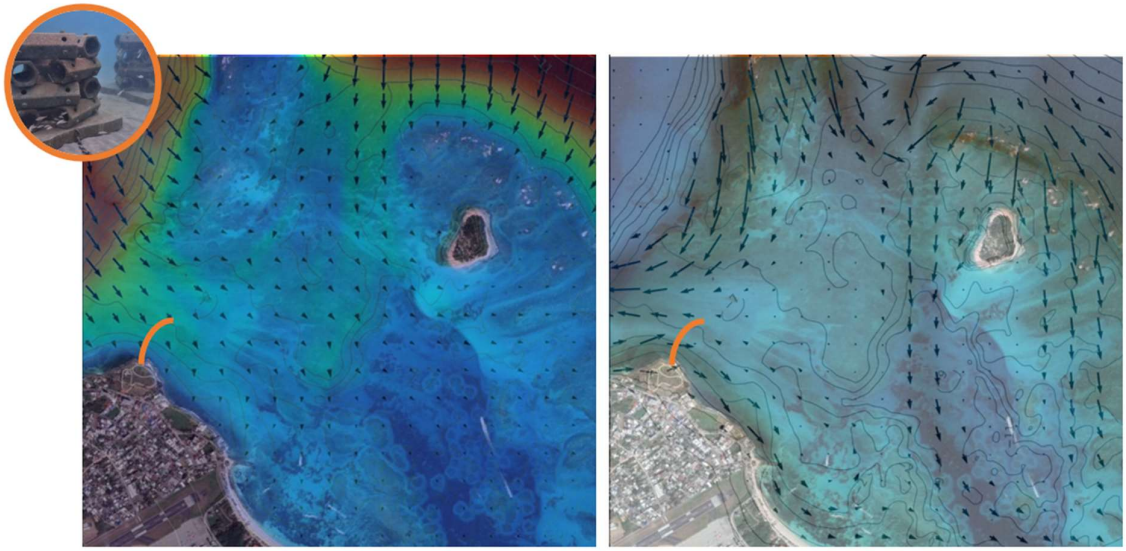

Figure 5.8: Impression of location of breakwater on the headland in the Western opening in the coral reef. On the left the wave field is shown for 5 m waves coming from the North. On the right the flow velocities for the same offshore wave conditions are shown.

Figure 5.8 shows how the breakwater could potentially prevent waves of reaching the headland and at the same time block the southeastward directed longshore current.

Although the breakwater would contribute to the general water level set-up inside the lagoon (as done by the coral reef explained in Chapter 4), by preventing the longshore current, sediment would less frequently be transported to the south and erosion events would be prevented. Besides, the general water level set-up effect caused by the artificial coral reef structure would have a minor additional effect on the total water level increase due to the existing coral reef.

Ecological aspects of artificial coral reefs

During their polyp phase, corals need a hard substrate to settle on in order to grow into a reef structure. Space is often a limiting factor in tropical waters and can be provided by building artificial structures underwater, which can speed up the restoration process (Higgins, Metaxas, & Scheibling, 2022). Structures as of ReefSystems and Reefy have already proven the efficiency of artificial reef in stimulating coral growth.

It is crucial that these structures remain stable even during storms, otherwise any newly obtained coral growth may be damaged or die if the artificial structure moves. Production, rearing and transplantation of corals can greatly accelerate the reef-building process. Direct transplantation of donor fragments is a simple, inexpensive, and often successful method. Naturally broken pieces of coral or small fragments cut from live corals are "nursed" to a suitable size before being planted. A more laborious method, but one that results in a more diverse gene pool, is the rearing and culture of coral larvae. How this is done depends on the rearing strategy of the coral species (spawning and broadcast rearing), but in essence, this method aims to increase the chances of successful fertilization of the gametes. The fertilized eggs are then either grown to a suitable size before being transplanted (Higgins, Metaxas, & Scheibling, 2022).

To facilitate the re-establishment of coral growth and the ecological functions of natural reefs, the structure must also have a certain level of roughness, i.e., structural complexity. One of the aspects of coral reef ecosystems that drives species diversity is their geometric complexity. This provides a wide range of niches that can be occupied by many organisms. This mimics the topography of coral reefs and increases the likelihood of ecosystem functioning similar to that of a natural coral reef (Higgins, Metaxas, & Scheibling, 2022). This complexity in surface and structure is provided by both ReefSystems and Reefy (as shown in Figure 5.9).

Figure 5.9: Different types of Artificial reef designs. On the left Reefy's design (www.reefy.nl). On the right Reefsystem's design (retrieved from retrieved from www.reefsystems.org).

The design chosen will need to be reviewed in detail during the next phases of the project (e.g., pre-feasibility, which is not part of the current scope). It is recommended that the results of the One Million Corals project (Infobae, 2021) are reviewed. In this initiative, Colombia has set an ambitious target of restoring 200 hectares of coral reefs in several regions. These regions include the Sea Flower Biosphere Reserve (SFBR). It is a collaboration of the Ministry of Environment, Parques Nacionales Naturales (PNN), Conservation International Colombia, Corales de Paz and other environmental and social organizations. In addition, companies such as Reefy and ReefSystems are pioneering new designs to address coastal erosion and structural complexity of artificial reefs. According to these companies, their artificial reef designs were already successfully tested in pilots around the world and in wave flumes to test their stability.

Once a breakwater is built, it has an immediate impact on wave height, contributing to the prevention of erosion. Coral restoration, on the other hand, is a long and arduous process, which can take years, even decades, before it can have an impact on coastal erosion. Other ecosystem services, such as increased fisheries yields and carbon sequestration, will also take time to take effect. However, if reef conditions remain healthy, coral ecosystems can keep pace with sea level rise, while grey infrastructure cannot (Higgins, Metaxas, & Scheibling, 2022).

The marine flora population surrounding Spratt Bight beach will also benefit from the breakwater. The reduced wave climate conditions are likely to be more suitable for the growth and expansion of marine flora. As the flora cover increases, bio-geomorphological processes will favor sedimentation and prevent resuspension (as explained in Section 5.2.1).

Besides, the tourism sector will also benefit from the new coral reef. As described in Section 2.4, a large proportion of visitors of San Andres are interested in ecotourism related to its coral reef system. Increasing the coral reef areas, more opportunities are created to attract these tourists. In addition, artificial reefs are still a rare environment, which could attract more tourists (divers) to the area. The artificial reef system could become a postcard for the island.

Finally, the development of the artificial coral reef should be closely monitored to ensure that the newly placed coral grows properly and integrates into the natural system. Macroalgae and coral growth tend to have a competitive relationship, and without the presence of grazing species (e.g., parrotfish and sea urchins), the artificial reef is likely to be invaded by these macroalgae, decreasing survival rates of coral larvae after settlement (INVEMAR-CORALINA, 2012).

5.2.2.4 Environmental Impact of Nourishments

Dredging and nourishments cause disturbances of the seafloor, which have effects on the ecology of the area. These effects can be direct (e.g., eliminating the fauna living in the sediment) or indirect (e.g., affecting the habitat quality through release of mud and other fine sediments). They can be local and restricted to the dredged or nourished area, or far-field due to the influence on environmental processes. Seagrass meadows and coral reefs around Spratt Bight are likely to be sensitive to the release of fine sediment associated with dredging and nourishments. It can be expected that in the clear Caribbean waters of San Andrés, where suspended sediments are not normally observed, the sensitivity to these effects can be high. To take stock of the possible negative impacts nourishments and dredging activities can have on the ecosystem in Spratt Bight (and San Andrés as a whole) it is advised to carry out a thorough environmental impact assessment (EIA).

Besides, there are a few environmentally friendly nourishment and dredging techniques that could be considered when carrying out these activities. For a more in-depth analysis of the environmental impact of dredging and nourishing see Appendix G by Peter Herman from Deltares.

5.2.2.5 Costs for reuse of dredged material

In conversations with local contractors in Colombia, it has been found that deepening the access channel of San Andrés and nourishing the beach of Spratt Bight would cost approximately 12 US dollars per cubic meter. According to the calculations made in Table 5.1, if the beach would be extended by 10 m, 40.000 m^3 would be needed, which means a total cost of approximately 720.000 US dollars. This price includes mobilization and demobilization of the vessel to SAI. Possible periodic maintenance costs would have the same unit price as capital dredging: 12 USD/m^3.

One or two bulldozers would also be needed to re-locate the sediment placed on the beach. According to the local contractor, the price of this machinery would approximately be between 15.000 and 20.000 US dollar, including man hours. This price is calculated based on 2 to 3 weeks of operations.

2. Reuse of dredged material

Specifications	Pros	Cons	Costs
➢ 60.000 m^3 to nourish 10 m beach width ➢ More than 100,000 m^3 available in approach channel ➢ Sediment in the approach channel seems to be compatible with Spratt Bight sand ➢ Beneficial use of dredging material has been applied before in SAI (1964, 1988, 1993)	+ **Dredging will be done anyway**, so costs are saved (do work with work) + **Soft and flexible solution**: no permanent impact on the coast + Widening of the beach will provide more room for (formal and informal) **commercial activitie**s on Spratt Bight beach	- **Sediment plume** might disrupt the ecosystem - **Not a stand alone solution**: needs to be implemented in combination with another solution due to possible stability issues - Sand extraction is believed to **cause more erosion** in the surrounding of the approach channel	• **Initial investment** • Dredging and nourishment costs (including vessel transportation costs) — 12 USD/m^3, 720.000 USD for 10 m width • Equipment costs (2x bulldozers) — 40.000 USD • **Periodic maintenance** • Dredging and nourishment costs — 12 USD/m^3 • **Monitoring costs** • Carry out ESIA (Environmental and Social Impact Assessment) before dredging and nourishing — 100.000 USD • Monitoring of beach profiles (review necessity of maintenance), sediment plumes and its impact on ecosystem — 25.000 USD/campaign

5.2.2.6 Costs for artificial coral reefs

Although grey infrastructures, as conventional breakwaters, are considered to have low maintenance and operating costs (OPEX), by their nature they are less flexible in coping with changes in the environment. In addition, CAPEX and OPEX costs vary according to the type and size of monitoring solution chosen. Monitoring costs can also be reduced for nature-based solutions if communities are involved on a voluntary basis. Ideally, local materials should be used for construction and maintenance, otherwise costs can increase substantially in isolated locations such as San Andres. In addition, training would be needed to determine whether the necessary skills exist on the island to maintain such structures.

Maintenance and monitoring of these structures is more complex compared to standard grey infrastructure, although ReefSystems experts indicated that maintenance can be minimal, as corals and plants will populate the structures on their own.

Furthermore, biological surveys should be conducted on a regular basis to monitor reef health and water quality parameters. The frequency of these monitoring campaigns will therefore determine the order of magnitude of the costs. The costs given in the following summary are based on expert opinion and meetings with ReefSystems. Although the costs of coral reef restoration are considerable in this proposal, there are funding institutions for coral reef restoration that can support.

3. Artificial Coral Reef

Specifications	Pros	Cons	Costs
➢ Artificial coral is used to restore and reconstruct existing breakwaters ➢ Coral reefs decrease wave heights due to friction and wave breaking ➢ There are different types of artificial coral that can be used to close the gap ➢ Artificial coral reefs have successfully been applied in different parts of the world	+ Wave height behind the coral reef will decrease together with the variation in wave direction induced by storm events. This means a smaller fluctuation in sediment transport direction + Enhancement of biodiversity + Enhancement of eco-tourism + If reef conditions remain healthy, the coral ecosystems can keep up with sea level rise + The reduced wave climate conditions are likely more suitable for seagrass growth and expansion	- If unstable, the artificial coral structure could damage the natural coral reef and cause ecological problems - The structure will change the sediment dynamics on the beach, possibly having (small) unpredictable effects - Coral grow very slowly, meaning that the time is needed before the structure is in equilibrium with the ecological system	• **Initial investment** • Coral reef restoration: very high: 120 USD/m² x width = 5 m = 120 USD/m • **Monitoring costs** • Carry out ESIA (Environmental and Social Impact Assessment) before dredging and nourishing: 100.000 USD • Monitoring water quality and coral growth: 25.000 USD/campaign

6 Discussion

Although this research made a great contribution to the better understanding of the different systems in Spratt Bight and San Andrés as a whole, there are a few limitations which have to be taken into account while reading this report. This Chapter contains the discussion on the methods, model and results as presented in this research and the associated implications for the main conclusions.

6.1 Model Choice

In Section 3.1 XBeach and Delft3D are presented. It is discussed which model is elected to be used for further modelling study of this research. This choice might have certain implications on the conclusions taken as there are a few differences in the processes taken into account for each model.

The main difference between XBeach and D3D is that XBeach is able to resolve the long waves associated with the short-wave variations on the wave group scale, while D3D is not. This means that choosing D3D implies neglecting the effect of these long waves (also called infragravity waves) in the system.

Infragravity waves can play an important role in the cross-shore sediment transport patterns in the coastal zone, as shown by Roelvink and Stive (1989). This process is being neglected while using D3D. In order to have an idea of the influence of long waves on the system, a few simulations have been carried out using XBeach. As done by van Dongeren et al. (2013), the impact of the infragravity waves on the governing reef processes is evaluated through the relative importance of these waves on bed shear stresses on the lee side of the reef crest. Waves of 2 m height and coming from the East are simulated (condition 13 in Table 3.2). The results of this simulation are presented and discussed more in detail in Appendix I.

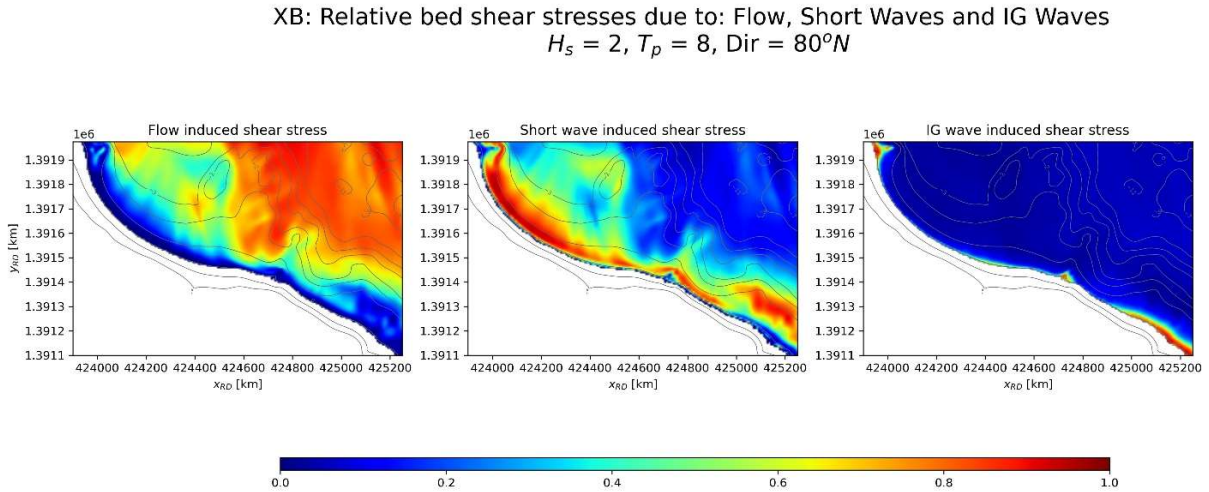

Figure 6.1: The fraction (denoted by the colorbar) of total bed shear stress driven by the mean currents, short waves, and IG waves, respectively. Appendix I gives an overview of the non-normalized shear stresses calculated in XBeach.

The short wave, long wave and flow velocity action generate a shear stress on the bed. The effect of the bed shear stresses is to stir up of sediment which is consequently transported by the mean current. In Figure 6.1 the relative importance of the short waves, mean flow and infragravity waves on the shear stresses is presented. These are calculated in accordance with the formulations as presented by van Dongeren (2013) (as explained in Appendix I). Here every component of the shear stress (flow, short wave and infragravity wave) is summed up and divided by the total amount of shear stress. The result is a ratio for which every component is responsible for inducing shear stresses in the bed (as presented in Figure 6.1). As can be seen, the infragravity waves present a minimal portion of the total shear stresses for this wave condition. This might imply that their relevance is minimal for the system and therefore also the sediment transports. It has to be kept in mind that the model is not validated and calibrated, which means that there might be substantial deviances from the reality.

Although the XBeach results show that the influence of the infragravity waves is negligible, in the research of van Dongeren et al. (2013) it has been found that the contribution of the infragravity waves to the total shear stresses can have a dominant contribution in the near shore zone (possibly accounting for up to 50% of the shear stress in the lagoon). In his research, van Dongeren shows that the dynamics of infragravity waves can have great importance across fringing reefs and their lagoons, possibly having a significant impact on numerous reef processes, including sediment transport. For this reason, it is expected that infragravity waves might have a significant influence on the system and more research is needed to be able to better understand and explain its influence on Spratt Bight Beach.

XBeach model

Besides the infragravity waves, there are other differences within both models. Not only within the formulations and processes described in the model, but also in the research specific set-up, grid, parameters, and boundaries used. This might possibly create a mismatch between the D3D results shown in Chapter 4 and the XBeach results. The exact factors and reasons causing this mismatch fall outside the scope of this research. Further recommendations about this topic are made in the Chapter 8. Furthermore, a more detailed description of the set-up for the XBeach model is presented in Appendix H.

A schematization of the XBeach model set up used for this research is shown in Figure 6.2. Here the default boundaries are used: back and front boundaries are the non-reflecting, while the lateral boundaries are both Neumann boundaries. These were selected as it has been shown to work quite well and given reasonable results in previous similar studies and research (Deltares, 2017).

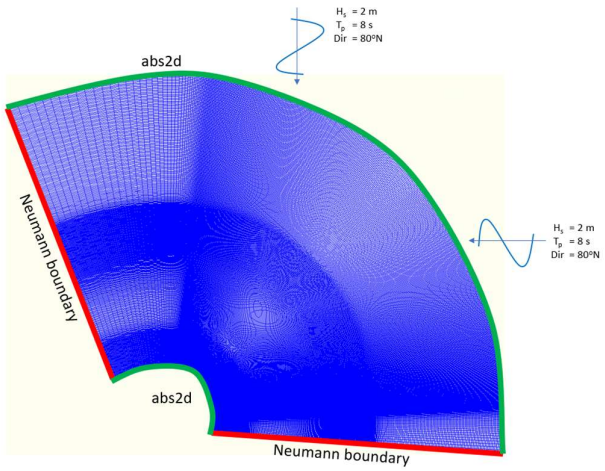

Figure 6.2: Schematization of the model set-up done for XBeach. The set-up of this model is further explained in Appendix H.

However, in the case of this research this boundary condition resulted in a continued outflow of water towards outside the domain, especially for the Northern wave condition. This resulted in a drop in water level over time as can be seen in Figure 6.3.

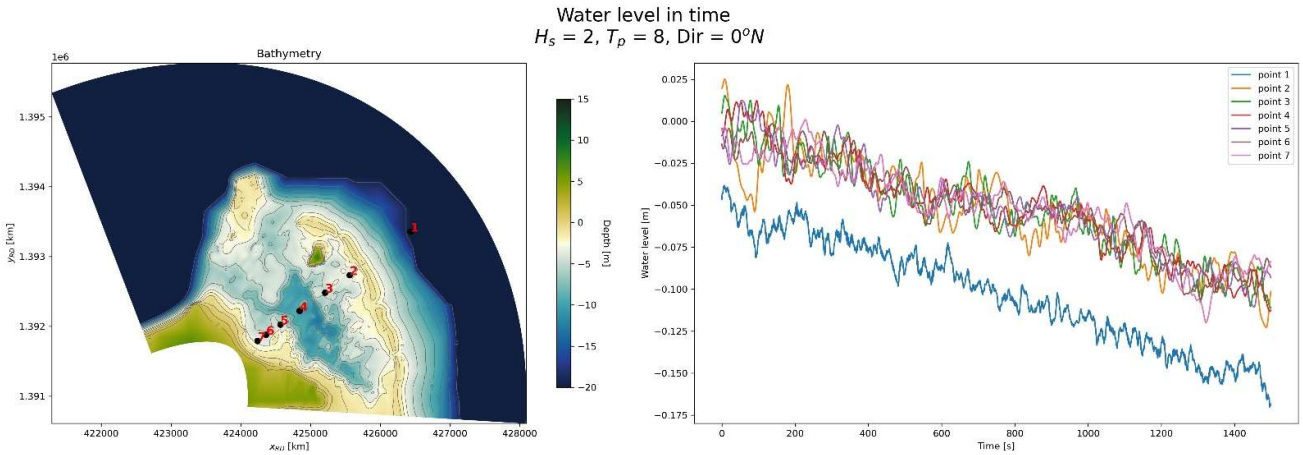

Figure 6.3: On the left the bathymetry of domain for the XBeach model. The black dots represent the locations from which the water levels were extracted. These water levels are plotted in time in the left figure. The water levels were extracted every 0.5 seconds over a simulations time of 25 minutes. The different lines (on the left) represent each extraction (point shown on the right).

Figure 6.3 shows the model results for the water level over time of the XBeach model. Here 2 m Northern waves are being simulated. Seven locations are selected along a transact in which the water level is plotted for each of the points on every 0.5 s. It can be seen that there is a downwards trend of the water level, indicating an outflow of water. Figure 6.4 shows the flow velocity field for the same condition. The red rectangle indicates where in the velocity field the discharge is being directed outside the domain.

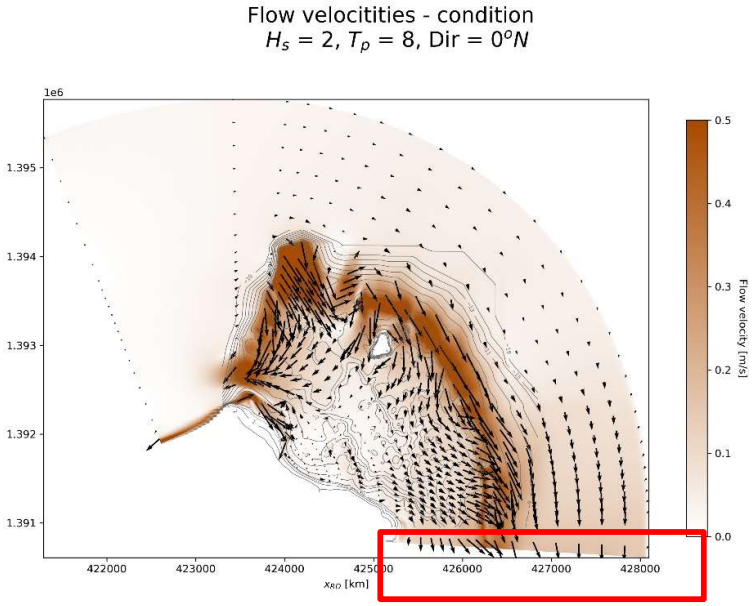

Figure 6.4: XBeach results of the flow velocity field for 2 m Northern waves. The red rectangle indicates the location where the flow velocities are directed outside the domain.

The longshore flow velocities are generated by wave breaking on the reef and radiates towards the boundary. As there is no incoming flow velocity on the other side of the domain serving as input for this out going discharge, the model starts losing water. As the Neumann boundary prescribes a water level gradient ($d\eta/dx$) flow can pass freely over the boundary with the same velocity it is flowing towards it. This problem could be corrected by applying another lateral boundary condition. However, other boundary conditions might result in other challenges that has to be solved. Finding the perfect setup for this model to be able to make a representative simulation of the coastal processes in San Andrés fall outside the scope of this research. Further recommendations are addressed in Chapter 8.

6.2 Research Limitations

As explained in Chapter 1 and 2, the study area of this research is located in a data poor environment. The main implications are that, in order to deal with the missing data, many assumptions have to be made. Besides, it is not possible to do a proper validations and calibration of the model through historical data, making it necessary to reach out to expert judgement for that purpose.

Utilizing expert judgment is not necessarily an inadequate an inaccurate method to verify results, as their expertise and experience are often good enough to approach reality. However, using this resource means that there is a wide uncertainty in the results as their accuracy is questionable. It is not possible to know for certain if a certain process, flow velocity, sediment transport, erosion and accretion is entirely correct through expert judgement. Having the model calibrated and validated with real data gives more certainty to its results.

Furthermore, the lack of data also has implications in uncertainties related to the assumptions and simplifications that had to be made. Below the most important information and data gaps (which could have a significant impact on the model results) are presented.

6.2.1 Bathymetry

As mentioned in Chapter 2, the retrieved bathymetric dataset did not account for some of the areas that are essential for the modelling study. Figure 6.5 shows a visualization of the bathymetry data that was received from INVEMAR for this research.

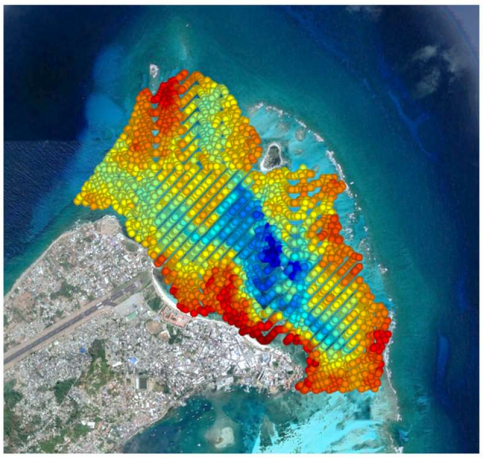

Figure 6.5: Visualization of the bathymetry data set received from INVEMAR. The red colors represent shallow water, and the bluer the colors are the deeper the water

From the figure above it can be seen that water depths inside the lagoon are taken into account, however near the beaches, the coral reef and the areas outside the protected area are not part of the measured area.

For this reason, it was necessary to use various data sources (Navionics (2021) and nautical charts (CIOH, 2008)) to come to a bathymetry that included the entire research area. As a consequence, the bathymetry used in the model is not an exact representation of the reality, and therefore not entirely accurate. This may cause uncertainties in the validity of the model results.

Coral reef

The depth of the reef top is of essential knowledge when modelling wave penetration inside the coral lagoon. Not knowing this information might have major consequences for the model results, as it is decisive for the wave breaking rate at the reef top. Besides the slope of the barrier reef is also essential for understand at which point waves are breaking and therefore influencing the water level inside the lagoon (as described in Chapter 4).

Beach profile

Besides information about the coral bathymetry, the beach profile is also very important for the modelling study, as it defines the width of the surf zone and how the waves break. This might have a consequence for the results on the sediment transport rates near the beach, adding extra uncertainty to the results presented in Chapter 4.

Breakwaters

In the data set retrieved from INVEMAR and in the other data sources used to create the bathymetry of Spratt Bight, breakwaters are not accurately represented. Their exact underwater depth, dry height and width are not known in detail and were not taken into account in the model. The breakwaters in San Andrés might increase or decrease erosion patterns at the beach as they block the sediment flux along the beach, affecting the results presented in Chapter 4.

6.2.2 Water level data

Water level data was not available. This includes tides, storm surges and sea level rise (SLR). Although data of the latter is presented in Section 2.2.2 (Figure 2.22), it was chosen to not account for SLR. This is mainly because it represents a small variation.

Tide

Tide is not included into the model's boundary conditions. Although the tidal levels are low, it might still influence the system. Wave set-up on a coral reef is the largest at low tide (small submergence) and lowest at high tide levels (large submergence). Wave-generated water levels might even exceed normal high tide levels during low tide. On the other side, the wave-generated flow is small at low tidal water levels and increases to a maximum at high tide, before reducing to zero when the submergence is large (Gourlay, 1996). However, due to the lack of a dataset and the small tidal range in San Andrés (0.35 m), the influence of the horizontal and vertical tide is assumed to be negligible and has not been taken into account in the model boundary conditions.

The influence of this choice on the model is that the variability of the water level due to the tide can influence the wave induced water level set-up inside the lagoon. At high tide less waves break on the coral reef, resulting in a lower water level set-up (lower gradient in radiation stresses dS_x/dx). At low tide, the water level at the reef top is lower, inducing more wave breaking, and therefore a higher wave induced water level set-up (higher gradient in radiation stresses dS_x/dx). This can influence the intensity of the flow velocities, and therefore the sediment transport.

Storm surge

Besides tidal the information, there is no record on the water levels and storm surges on the island. This might mean an extra underestimation of wave energy passing over the coral reef during storm conditions, leading to an underestimation of the wave climate nearshore. Besides, the location of the surf zone also becomes inaccurate, resulting in a possible deviation of the sediment transport results.

6.2.3 Wave data

Firstly, there is no offshore wave data measurements available from San Andrés, therefore the wave data is taken from the global wave model WaveWatchIII (WW3) (2019). The fact that the data is generated by a model and not actual measurements near San Andrés might result in a deviation from the real situation.

Secondly, during the simulations in D3D-W swell waves were not included. Due to the time constrain of this research it was chosen to reduce the wave climate into 20 conditions, all sea waves. Although swell waves do not seem to have another direction than the mean sea wave direction, swell waves might influence the system differently as they have a much longer period, reaching over 20 s as can be seen in Figure 6.6.

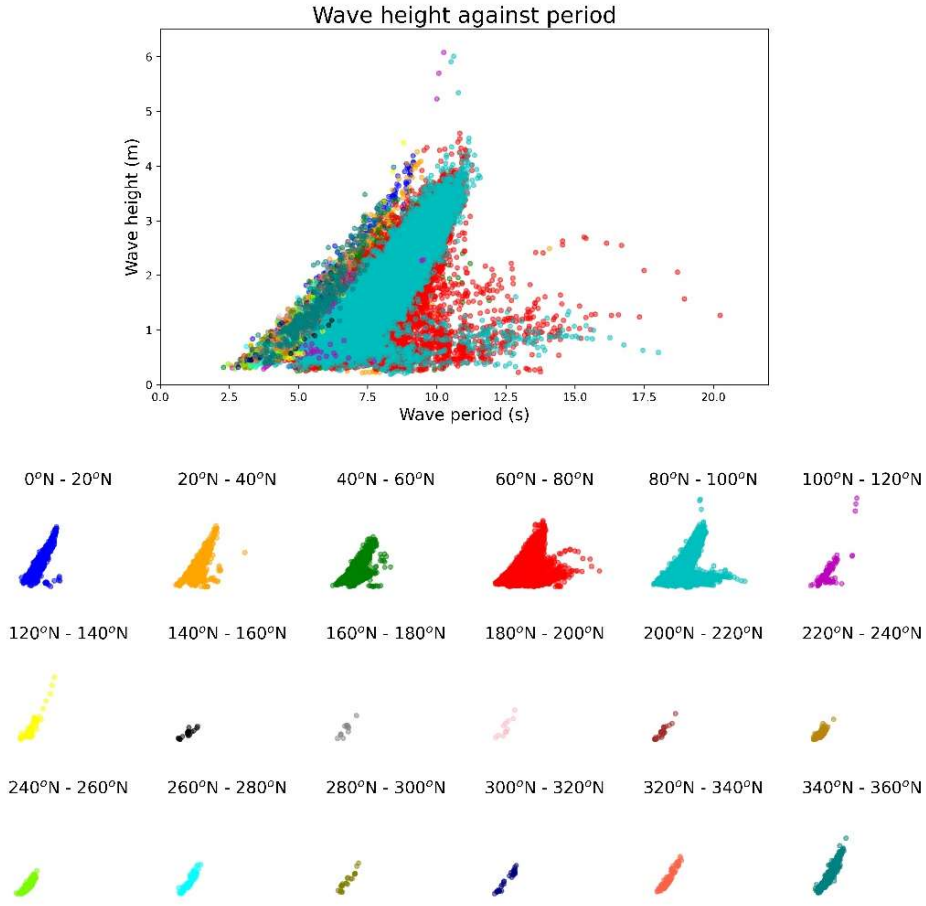

Figure 6.6: Significant wave height plotted against the wave period of the offshore waves retrieved from WW3. The different colors represent different wave direction bins. Swell waves can be recognized by the longer periods and lower heights, mostly situated in the lower right quadrant of the figure.

6.2.4 Wind data

In Section 2.2.1 and 2.2.4 it was described how extreme weather conditions could produce wind speeds strong enough to transport sediment from Spratt Bight Beach towards the behind laying boulevard and streets. This illustrates the importance wind speeds could have on the system. However, these wind speeds were not taken into account due to the lack of data available about the wind speeds.

Although the WW3 model, of which the wave data was extracted, included wind speeds and directions within its outputs, these data were considered to be inaccurate. According to experts of Arcadis, during the validation of the WW3 model, errors were encountered. For this reason, another approach was selected to include the wind within the boundary conditions in the model (described in Chapter 3). However, this approach did not include winds that occur during heavy storms as for example of cyclonic winds. These winds can create an extra wind driven water level set-up, possibly causing an underestimation of the cross-shore transports due to undertow or other types of return currents.

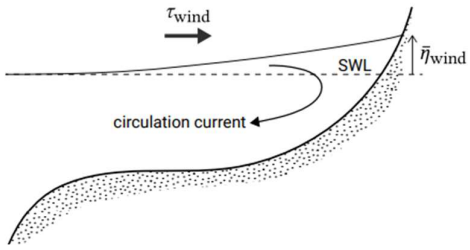

Figure 6.7: Wind drive water level set-up balancing wind shear stress, producing a circulation current due to the pressure difference. This current is which is offshore directed (Bosboom & Stive, 2021).

6.2.5 Seabed cover

As mentioned in Chapter 3, it has been assumed that the bed in the entire domain is composed by sand. This assumption is made due to the low amount of data about the exact locations where there is a sandy bed, coral, or seagrasses in the lagoon. Furthermore, within the timeframe of this research there was not enough time to account for this aspect.

The implication of this choice is that there is considered to be an infinite supply of sediment available to be transported within the system. This means that the model results will display sediment transport capacities instead of actual sediment transports, without taking sand buffers and limiters into account.

Besides the influence on the sediment transport, the seabed composition also has an influence on the bed roughness, which influences flow velocities and wave heights. Not taking them into account can have consequences for the model results shown in Chapter 4.

6.2.6 Morphology and sediment transport

It is chosen to not use the morphological feature of D3D-F, meaning that the bathymetry is not being updated during the simulations. In a simulation where the bathymetry is updated, D3D-F calculates a new bed level based on the sediment transports, which serves as input for the model's next time step. This is shown in Figure 6.8.

This choice is made due to the fact that it is not possible to validate the model's results using real data, as previously explained. In this way a new (possibly inaccurate) bathymetry could influence wave and flow patterns. This is not desirable, and therefore it has been chosen to derive the erosion and accretion pattern using sediment transport rates.

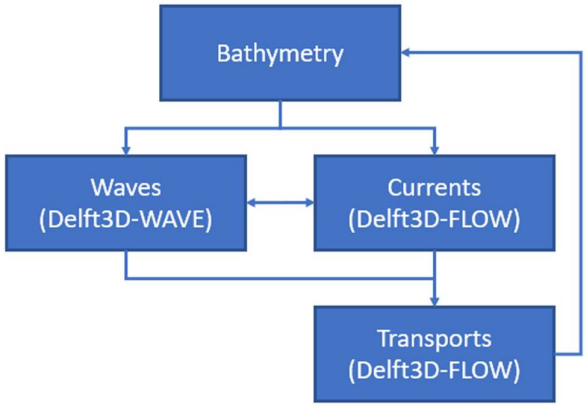

Figure 6.8: Schematization of the coupling of Delft3D-WAVE with Delft3D-FLOW, including the update of bathymetry.

The implication for this choice is that no actual accretion and erosion are being calculated, but the sediment transport patterns are being used as sedimentation and erosion indicators.

Furthermore, the large difference between the different sediment transport formulations (principally the bed load formulations), creates an increased uncertainty in sediment transport computations. It is highly advised to only relay on the sediment transport results from numerical models when there is enough confidence in the computations. This means that the model should be properly calibrated, preferably with real data form the considered study area (Bosboom & Stive, 2021). As this is not possible within this research, the sediment transport results presented in Chapter 4 should be interpreted carefully and serve as indication for the reality, and not as absolute truth. The exact numbers presented in this Chapter might severely deviate from reality.

Validation through beach profiles

There is very little information concerning the erosion pattern in San Andrés. Figure 2.26 shows the different beach profiles of Spratt Bight Beach for different years between 2004 and 2016 on arbitrary months. Comparing between different years says little about what the seasonal erosion/sedimentation pattern is, but more about its overall behavior. Besides, the exact date of the measurement is also not specified, making it difficult to link a certain condition to it.

Finally, the data retrieved from WW3 as described in Section 2.2.3 and Appendix B goes from 1979 until 2009, while 5 of the 10 profiles presented in Figure 2.26 are measured after that period. Having that little data points complicates the process of linking storm condition from the WW3 dataset to a beach profile and making a conclusion about the nature of the erosion.

The consequence is that the model results cannot be validated using these profiles. Ideally, it should be possible to link each beach profile shown in Figure 2.26 to a wave climate. This wave condition would than would be simulated in the morphological model so that similar erosion and accretion patterns could be identified. Not being possible to make that link between Figure 2.26 and the WW3 dataset makes this validation process impossible.

6.3 Summary

Summary of Limitations	
Model choice	Choosing D3D over XBeach results in neglecting processes that might be important for the coastal system of Spratt Bight. On the other side, XBeach is a more complex model for which more time is needed to set-up and running.
Bathymetry	Multiple sources of bathymetry data were used to create the input used in the numerical model. This might have led to inaccuracies in the simulation results.
Water level data	There was no water level data available (storm surges, set-up due to wave action or astronomic tides, etc.). In order to have a more complete modelling study and the possibility to somewhat validate the model, these datasets would have been necessary.
Wave data	Due to time constrains only a selected amount of wave conditions were simulated in the numerical model. This might influence the results as a complete overview of the effect of the different wave conditions is missing. Although the wave conditions were carefully selected to best represent the overall conditions on the island, it would still be recommended to increase the amount and variety of conditions simulated in the model.
Wind data	Wind data was not available for the modelling exercise. As wind in San Andrés can be very strong due to cyclonic activities, it would be recommended to add it to the model input in order to have a more compete overview of the effects of the environmental conditions on the island.
Seabed cover	The seabed cover was not implemented in the model. It was assumed that the entire bad is consistent of sand. This might affect the model result as it has influence on the availability of sediment, and wave and flow behavior.
Morphology and sediment transport	Due to the fact that validation through available bathymetric and beach profile data is not possible, it was chosen to not let the model influence the bathymetry during the simulations. This means that no erosion/accretion patterns could be identified. The consequence is that the analysis on erosion and accretion is made in a qualitative sense based on the results of the sediment transport and flow patterns.

7 Conclusion

The goal of this research is to identify the causes of erosion on Spratt Bight Beach and to propose solutions to mitigate it using the Building with Nature approach. In this Chapter the answer to the research sub-questions elaborated in Chapter 1 will be given. The answer to the main research question is found by answering these sub-questions. By answering these sub-questions, the objective of the research is obtained. The main research question to be answered is:

"What are the main causes of coastal erosion at the Spratt Bight Beach and, using the Building with Nature approach, what possible mitigation measures could be applied?"

7.1 Sub-questions

1. What are the loads acting on the coastal system?

Waves dominate the coastal system in San Andrés and are the main driver of the processes in the coastal system. The hydrodynamic conditions in San Andrés are characterized as a wave dominated environment. The wave climate at the island is mainly composed by wind and swell waves. Maximum wave height can reach up over 6 m with a corresponding wave period of over 10 s.

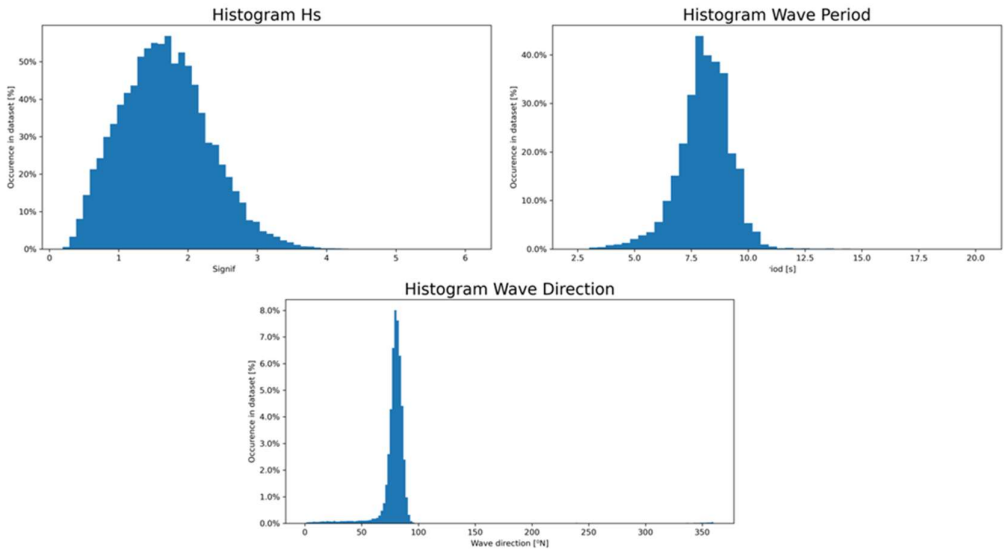

Figure 7.1: Histograms of the wave climate in San Andrés. On the left the significant wave height, in which the mean significant wave height is indicated by the black line and is equal to 1.67 m. In the middle the wave period, where the black line indicated the mean period of 8.08 s. On the right histogram of the offshore wave angle of incidence, in which the black line indicated the mean wave angle of 80.5°N.

As shown in Figure 7.1, the wave directions in San Andrés are very concentrated from the East, such that 90% of the waves are coming between 70°N and 90°N. The consequence of that is that beaches (including Spratt Bight), and mostly the barrier reef on the east side of the island are under constant wave attack.

There are also less frequently observed wave angles of incidence **coming from the North**, in which 1.5% of the incident waves come between -20°N and 20°N. These waves might have a great impact on the morphology of Spratt Bight. The figure below shows the frequency per month the Northern waves are observed. It can be seen that most of these waves are observed between October and March, which approximately coincides with the storm seasons of San Andrés.

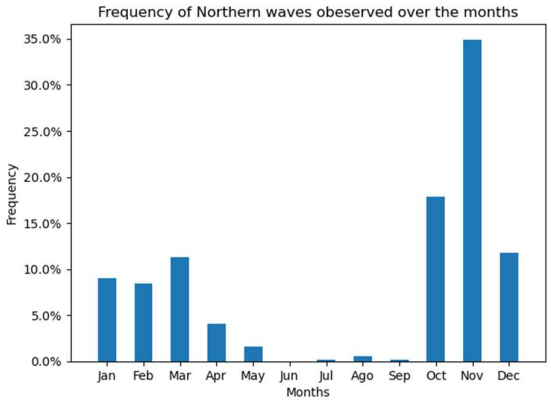

Figure 7.2: Histogram showing the months in which Northern waves are reaching San Andrés.

Both Eastern and Northern waves enter the coral lagoon overtopping the crest of the coral reef and due to refraction and diffraction thought the main openings in the reef system: on the North and the West. This is shown in the summarizing figure below (Figure 7.4).

The **tidal range** on San Andrés are minimal and are not assumed to drive important coastal processes on the island. The tidal environment is characterized by being a micro-tidal, with a maximum range not higher than 0.35 m. Therefore, the influence of the tide on the system assumed to be limited. However, although the horizontal tide is assumed to be small, the vertical tidal component can have influence on the water depth at the crest of the coral reef, determining the amount of waves breaking over it.

Extreme weather conditions as hurricanes and tropical storms are a periodical reality in San Andrés. On average the island of San Andrés is heavily affected by hurricanes at least once every 10 years. Between the months of September and November, these events are more likely to be observed. When reaching the coast of San Andrés, these storms can generate offshore wave heights of up to 6 m, heavy rains, and wind velocities of over 120 km/h. As winds can be very strong, they can generate wind induced sediment transports, driving the sand from the beach towards the urban areas of Spratt Bight. Resulting in a sediment output from the system.

Sea Level Rise is below the world's average and therefore doesn't have great influence on the system. However, it is still a topic of future concern as San Andrés is a low laying island with small altitudes and erosion due to relative SLR can have an effect on the island's beach width.

Due to the increasing **urban pressure** in San Andrés, buildings were constructed closely to the coastline. These hard structures do not give the beach the space it requires. This phenomenon is called coastal squeeze and happens when the

natural variability if the beach is not accounted for during the placement of structures, and as a consequence, the coastline loses its possibility to displace without affecting constructions and consequently the local population.

Figure 7.3: Shore line of Spratt Bight over the past 60 years (Martín-Prieto, et al., 2013).

Figure 7.3 shows development of the increasing number of constructions and structures near the coast over the years. It can be seen that the boulevard of Spratt Bight, hotels and other commercial establishments started locating within a few meters of the coastline.

Finally, the figure below shows a summary of the main loads action on the coastal system of San Andrés.

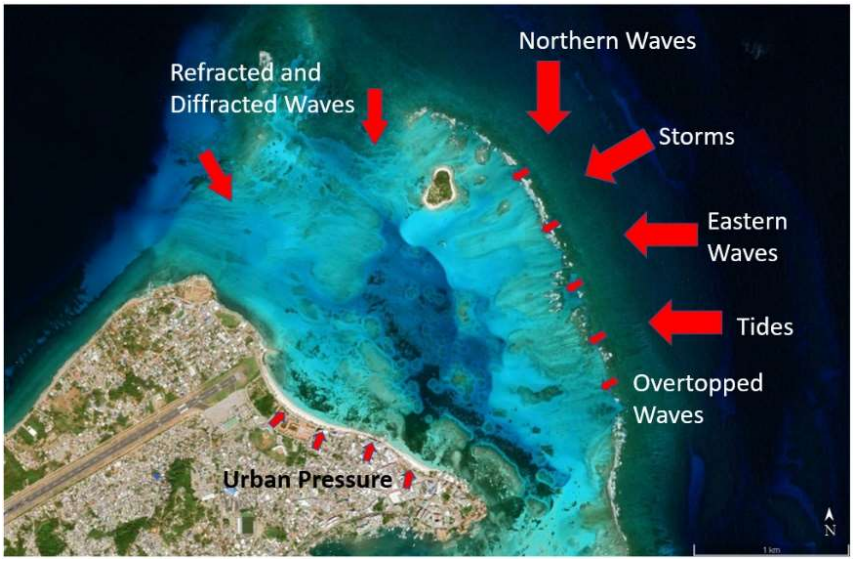

Figure 7.4: Schematization of the main loads acting on the coastal system of San Andrés

2. *How are the hydrodynamic processes causing erosion on Spratt Bight?*

Waves approaching San Andrés predominantly break over the coral reef. This creates a surf zone right before and on the reef, after which the waves further propagate inside the lagoon with less energy.

The result of the waves breaking on the reef is that it generates a water level difference between the lagoon and the area at the surf zone. This induces a water level difference driven flow. Consequently, water starts flowing from the surf zone (outside the lagoon) into the lagoon, where the water levels are lower. After entering the lagoon, the water can only leave the system through the Western opening in the coral reef. The figure below shows a schematization of this process.

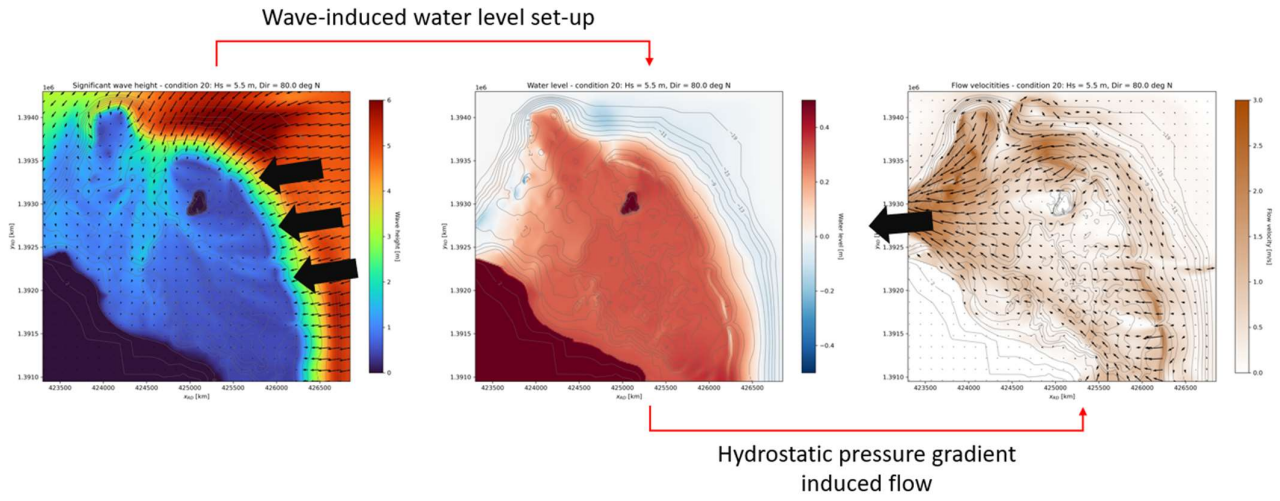

Figure 7.5: Schematization of the hydrodynamic processes within the coastal system of San Andrés for 5.5 m waves coming from the East. The left figure represents the model results of the wave heights, the middle figure represents the water level set-up and finally, the right figure represent the flow velocities.

These flow velocities induce a sediment transport near the coast that is mostly directed to the coast and the west, as shown in the figure below.

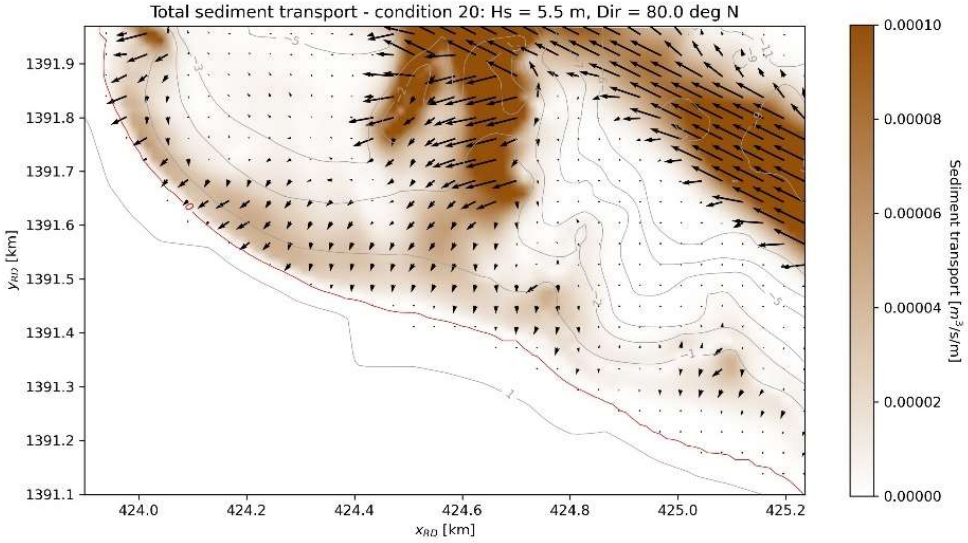

Figure 7.6: Model results for the sediment transport field of Spratt Bight. The simulated conditions are of 5.5 m waves coming from the East

When waves are coming from the North the same processes happen, however, now also a wave induced longshore current is generated along the beach of Spratt Bight.

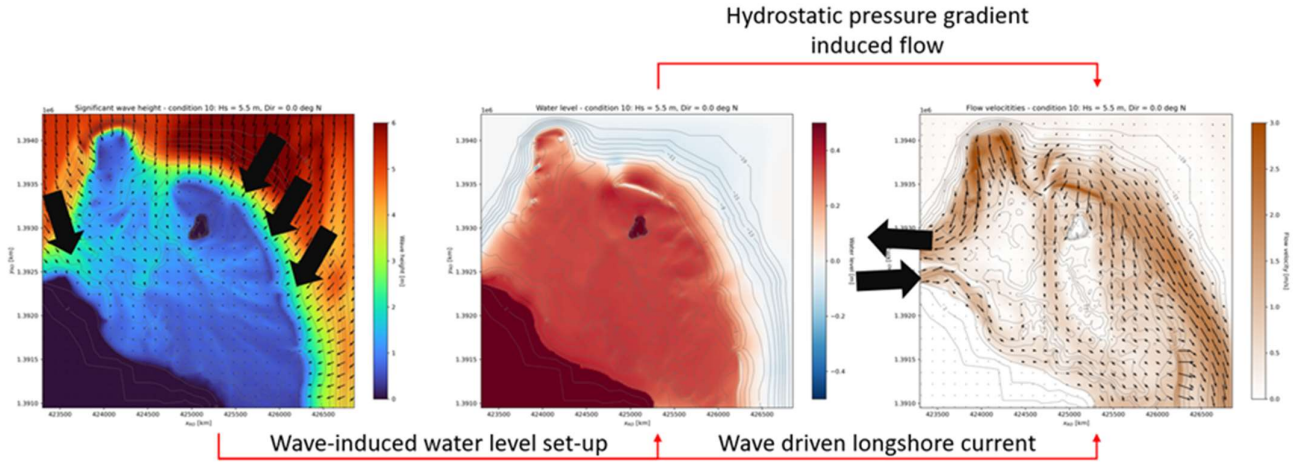

Figure 7.7: Schematization of the hydrodynamic processes within the coastal system of San Andrés for 5.5 m waves coming from the North. The left figure represents the model results of the wave heights, the middle figure represents the water level set-up and finally, the right figure represent the flow velocities.

Waves coming from the North penetrate the inner lagoon through the opening on the Western side, indicated with the black arrow in Figure 7.7. When reaching this opening, these waves start being influenced by the bathymetry, refracting towards the headland, and propagating further inside the lagoon. Waves breaking on the western side of Spratt Bight induce a eastward directed longshore current. This longshore flow velocity induces a sediment transport that is directed to the East as shown in the figure below.

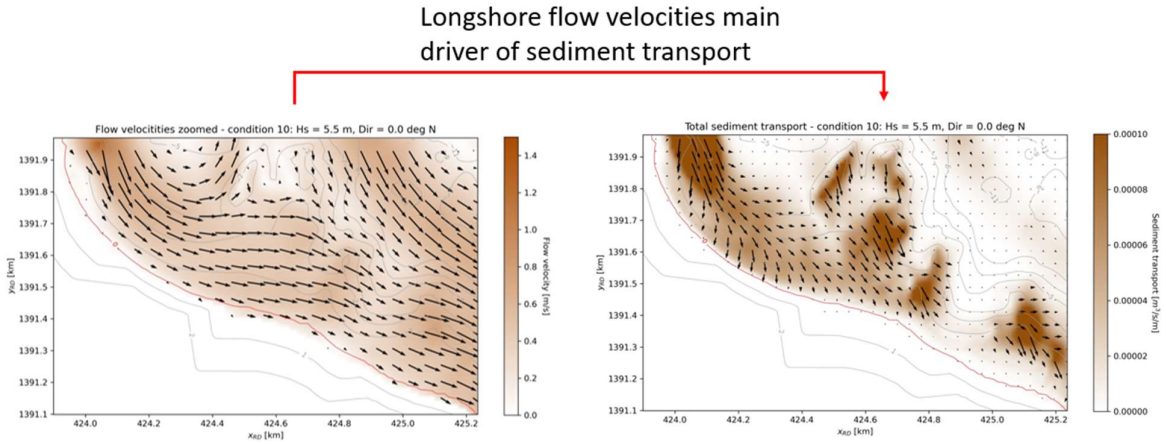

Figure 7.8: Model results showing the effect of 5.5 m waves are coming from the North (0^0N) on flow velocity field (left) and sediment transport pattern (shown on the right).

The consequence of this sediment transport pattern is that erosion is observed where there is acceleration of the sediment transport patterns and accretion where the sediment transport pattern decelerates. The figure below shows an overlay of the satellite image right after an erosion event took place and the sediment transport patterns modelling results.

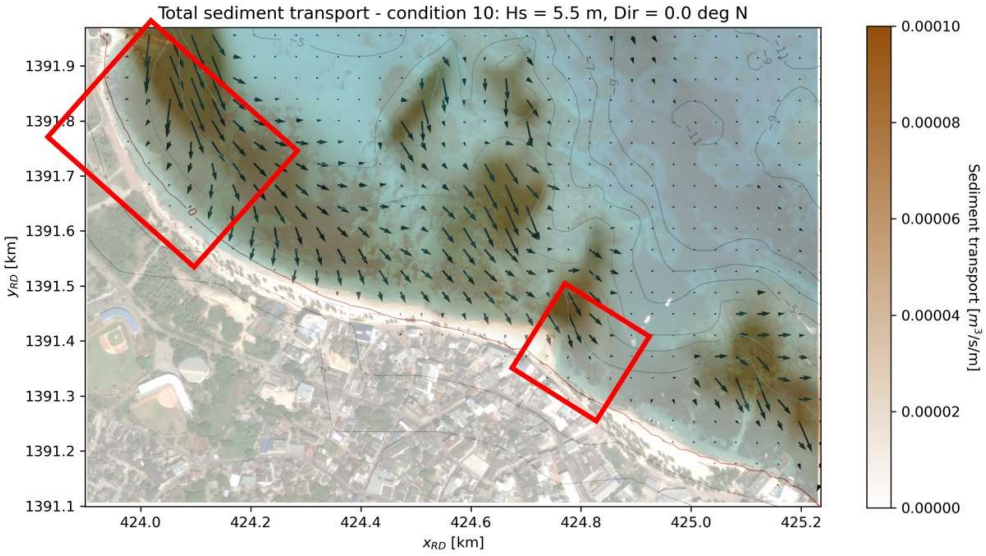

Figure 7.9: Model results of sediment transport rates for 5.5 m waves coming from the North. The results are overlayed on a satellite image from FINDETER (2020) in which erosion patterns are shown due to episodic events.

After such an erosion event, it takes a relatively large amount of time to restore the previous (dynamic) equilibrium. This is due to the less strong flow and sediment transport velocities induced by the average waves coming from the East (shown in Figure 7.6).

3. What mitigation measures can at the same time protect Spratt Bight, enhance the ecosystem, and benefit society?

To protect Spratt Bight Beach against coastal erosion three solutions were developed through the Building with Nature approach. The goal of these solutions is to:

1) Reduce the **wave heights** reaching Spratt Bight Beach.
2) Reduce the **longshore flow velocities** along the coast of Spratt Bight.
3) Prevent **sediment of leaving** the coastal system.
4) Increase the **sediment budget** of the coastal system.
5) Add **ecological and social value** to the area.

With these goals in mind, the proposed solutions are: seagrass restoration, beneficial reuse of dredged material and implementation of artificial coral reefs.

1. Sea grass meadows

Seagrasses are able to stabilize the sediment, avoiding it to be displaced by waves and currents. It does so by increasing the critical shear stress of the seabed, increasing the necessary threshold velocity of sediment to move. Besides, seagrasses also increase the friction between water and seabed, reducing flow velocities and wave heights, which are important drivers of sediment transport on the island.

Ecologically speaking, seagrass meadows are important ecosystems on the islands. Over the past 80 years these seagrasses have been removed and damaged on Spratt Bight. Restoring these ecosystems would give back its before existing

ecological value. Besides, it is an important source of oxygen and an effective CO_2 sink. Finally, it also attracts different marine species, increasing biodiversity at the area.

As said before seagrasses can attract different species, which includes commercially important fishes and other marine species. This would improve the fisherman activities on the island. Besides, ecotourism is an important source of revenue to the island, meaning that an improved biodiversity would also improve this sector.

2. Beneficial reuse of dredged material

By reusing dredged material as nourishment for Spratt Bight Beach improves its width and prevents that erosion rates are damaging tourism and coastal structures. Besides safety it also is a circular and more sustainable way of widening the beach. First, dredged material is used as a resource instead of a waste, as was done before. This saves several vessel trips and therefore the CO_2 footprint of these activities. Due to the same reason, costs are saved, making these kinds of projects much cheaper.

3. Artificial coral reefs

In order to prevent the waves of reaching Spratt Bight Beach, a longshore sediment transport to be generated along the beach and, to maintain the nourished sediment in place, hard structures are needed. Making these structures out of artificial coral reefs can have several benefits, besides wave, current, and sediment transport attenuation effects. Artificial coral reefs enhance ecology attracting a large amount of fauna and flora. Other ecosystem services are increased fisheries yields and carbon sequestration. Besides, coral ecosystems can keep pace with sea level rise, while grey infrastructure cannot.

Moreover, the tourism sector will also greatly benefit from the new coral reef. A large part of the visitors going to San Andres are interested in ecotourism specifically related to its coral reef system. Increasing the coral reef areas, creates more opportunities to enhance this sector. Additionally, as artificial reefs are still a rare environment, it could attract more tourists to the area, potentially becoming a postcard for the island.

A schematization summarizing the different mitigation measures and where they can be applied is shown in the figure below.

Figure 7.10 schematization of the locations where the proposed mitigation measures could be applied in Spratt Bight. 1) Seagrass restoration, 2) Beneficial reuse of dredged material and 3) Artificial coral reefs.

8 Recommendations

In this Chapter the recommendations are made based on the discussion and conclusions of this research (Chapters 6 and 7). The recommendations are divided into two parts: 1) 'Further Research', in which it will be explained and describe what other research should be done in order to improve the findings and what could be done next; And 2) 'Institutional Recommendations', in which the Institutions of San Andrés will be addressed proposing next steps for the erosion problem on the island.

8.1 Further Research

Firstly, during the wave simulations in D3D-W limited number of environmental conditions were considered. In next research it is recommended to consider a broader range of wave climate conditions. It is known that simulating all conditions is not possible due to a limited computational power, however a broader range of wave directions, and periods would be recommended to assess the impact of other conditions on the sediment transport pattern on Spratt Bight Beach. Besides tides were considered too be negligible for the modelling study due to its limited height. However, it would be interesting to assess its importance and whether this assumption is correct in further research.

Eolian sediment transport is not considered in this research. As strong winds can transport sediment from the beach towards the inner area of Spratt Bight, it would be recommended to used eolian sediment transport models as Aeolis (Hoonhout & de Vries, 2016) in order to assess these transports and its impact on the sediment budget.

As described in Chapter 6, the seabed cover was all considered to be sand (leading to infinite sediment supply), and exact dimensions of the breakwaters in Spratt Bight were not taken into account. Although their impact is considered to be limited on the system as a whole, it is recommended to include them in the next project phases as they might be important definitive and execution designs of mitigation measures. Different seabed covers (sand, rock, coral, and seagrass) have different influences on the shear stresses and friction coefficients. Besides it also influences the available supply of sediment being transported.

In Chapter 6 the different results obtained with XBeach, and its set-up are discussed. More research is recommended in order to further optimize the set-up of this model. In this way the influence of the long bound waves (infragravity waves) could be further investigated, as they are believed to be of great importance to the system (van Dongeren, et al., 2013).

Moreover, it is recommended to run the Delft3D model including the morphological changes in the bathymetry as shown in Figure 6.8. In that way it becomes possible to assess the sedimentation/erosion patterns at the study area, instead of using the sediment transport velocities as an indicator.

Finally, due to the time constrain of this research, the mitigation measures could not be evaluated quantitatively and were only assessed qualitatively. It is recommended to conduct a thorough modelling study to quantify the actual efficiency of the different solutions. The solutions could be implemented applying the same model as used to describe the system, and therefore be able to make a quantitative comparison of the a 'before and after' situation. This would strengthen the argumentation regarding the implementation of the solutions on Spratt Bight.

8.2 Institutional Recommendations

Data Poor Environment

As repeatedly mentioned in this study, the lack of data on the San Andrés presents various limitations for understanding the system and being able to develop efficient mitigation measures against coastal erosion on the island. In order to solve this problem some recommendations are made.

First periodic data measurement campaigns should be organized, and wave measurement buoys should be deployed on strategic spots on offshore (outside the coral lagoon) and inside the coral lagoon of the island. This would improve modelling capacity as hydro- and morphodynamic model results could then be calibrated and validated. Moreover, yearly coastline measurements or measurements after great storm events are recommended in order to better validate the hypothesis raised in this research.

Besides future data collection, another challenge that should be addressed is the unavailability of existing datasets. It is known that there is a lot of data that was gathered over the years by different institutions and organizations over the years in San Andrés. However, this data is not publicly available due to (among other arguments) private investments that have been made in order to collect it.

In order to increase the public availability of environmental data on San Andrés, it is recommended to create a form of cooperation between these different research institutes and organizations, possibly creating a new governmental body, so that knowledge, data gathering, monitoring and maintenance efforts are centralized on a higher level.

Mitigation Measures

Regarding the mitigation measures, the first recommendation is to avoid the use of hard structures as a solution against coastal erosion. On its own it might not be the most suitable approach in a highly dynamic coastal area such as San Andrés. These types of measures should be applied in combination with softer and more sustainable measures as sand nourishments. Besides, the placement of any permanent structure should always be done involving stakeholders, local community as well as ecological considerations (as is prescribed within the Building with Nature design approach (Van Eekelen & Bouw, 2020)).

This research will help identify the erosion problem on Spratt Bight, serving as a basis for the development of specific measures to be implemented within a socio-economic and ecological context. As it is not providing hands-on measures that are right away implementable, it is recommended to further follow the Building with Nature design approach as described in the Figure 8.1. In Chapter 1 this design approach is introduced, and it is stated that this research would only focus on the first two steps: 1) understand the system and 2) identify alternatives.

For this reason, it is recommended to, in a next phase of this project, further develop the prosed alternatives with respect to steps 3, 4 and 5, as shown in the figure below. The first next step is to evaluate each alternative to select an integral solution. Here is would be necessary to apply a Multicriteria Analysis (MCA) in which different aspects of the proposed solutions would be evaluated according to (amongst other) physical, ecological, and socio-economic context.

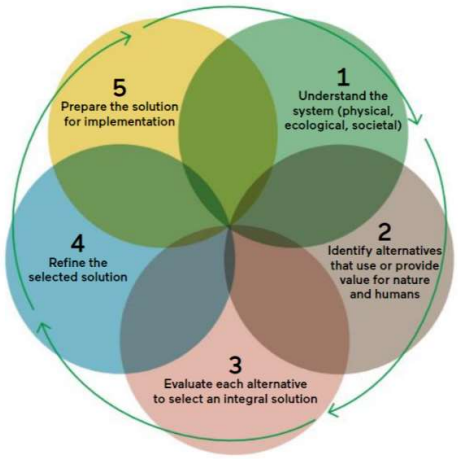

Figure 8.1: Building with Nature design approach from van Eekelen and Bouw (2020)

Possible criteria for the MCA could be:

- Functionality
  - e.g., total won beach width, certainty of success and feasibility of implementation.
- Ecological value
  - e.g., negative impact of implementation, potential to attract fauna and flora, potential to increase biodiversity
- Recreational value
  - e.g., disturbance on recreational activities, accessibility, safety.
- Socio-economic value
  - e.g., potential impact on tourism, potential impact on fisheries.
- Costs
  - e.g., construction costs, maintenance costs.

After the evaluation an integral and multipurpose solution should be selected and refined. The latter should be done through a thorough modelling study (as described in Section 8.1) to quantify the actual efficiency of the selected solution. Besides Environmental and Social Impact Assessment (ESIA) should be carried out in order the determine the impact the selected measure could have on the coral reef, seagrasses, biodiversity, water quality and other ecological aspects, as well as on the local economics. The selected solution should be subjected to a broad participation of related social and institutional actors in order to create synergy between the local community and the to be implemented solution.

Finally, after the selected solution is further detailed, it can be publicly offered in a tender to different contractors, which would make an executable design to be implemented. The implementation should be carefully monitored in order to ensure no negative environmental impact is being made (especially when applying dredging and nourishment techniques). When monitoring the ecological impact, it is recommended to not only monitor the aspects as turbidity levels, water quality, etc., but also measure the degree of environmental impact through sensitive receptors at the implementation. These receptors can be useful to indicate whether turbidity levels are too high for the flora and fauna to handle.

Not only during, but also after implementation the solutions should closely be monitored in order to make sure the selected and implemented solution is returning results not only in the context of coastal erosion but also in ecological and socio-economic sense. It is recommended to periodically monitor the sediment erosion/accretion behavior on Spratt Bight and also whether the ecological as social aspects of the solution are working (how much biodiversity is being

created, whether fauna and flora are being attracted to the implemented solutions, number of tourists being attracted to the area, etc.). In this way, the success of the selected solution can be assessed, and undesired surprises prevented.

After the successful implementation of the selected mitigation measure at Spratt Bight Beach, the focus can be shifted to other sites with structural coastal erosion, taking advantage of the proposed solutions for Spratt Bight. As shown in Chapter 1, erosion is a problem that is not only happening in Spratt Bight, but also at other locations at the Eastern side of the island. The findings made and solutions proposed for Spratt Bight could also (in a modified form) be applied to these other locations. It is recommended to do further research on these locations and apply the same design cycle as shown in Figure 8.1, in order to come up with sustainable multipurpose Building with Nature solutions.

Finally, the structuring of a coastal erosion project for San Andrés, based on the results of this project, can also be an opportunity for bilateral project cooperation between The Netherlands and Colombia. In general, international cooperation can be considered as an important source of funding and knowledge exchange. The collaboration between Colombia and The Netherlands is already well known and developed for years. This could be used to further develop the island sustainable approach against coastal erosion.

Bibliography

Aguilera-Díaz, M. M. (2016). *Geografía económica del archipiélago de San Andrés, Providencia y Santa Catalina.* Bogotá: Banco de la Republica.

Baine, M., Howard, M., Kerr, S., Graham, E., & Toral, V. (2007). Coastal and marine resource management in the Galapagos Islands and the Archipelago of San Andres: Issues, problems and opportunities. *Ocean and Coastal Management, 50*(3-4), 148-173.

Barragán-Barrera, D., do Amaral, K., Chávez-Carreño, P., Farías-Curtidor, N., Lancheros-Neva, R., Botero-Acosta, N., . . . Palacios, D. (2019, 2). Ecological niche modeling of three species of stenella dolphins in the Caribbean basin, with application to the seaflower biosphere reserve. *Frontiers in Marine Science, 6*(FEB).

Bosboom, J., & Stive, M. (2021, 2). *Coastal Dynamics.* Delft, The Netherlands: TU Delf Open.

Buckley, M., Lowe, R., & Hansen, J. (2014). *Evaluation of nearshore wave models in steep reef environments.* Crawley: Ocean Dynamics.

Cado van der Lely, A., van Eekelen, E., Honingh, D., Leenders, J., McEvoy, S., Penning, E., . . . van Zelst, V. (2021). *Building with Nature: a future proof strategy for coping with a changing and uncertain world.* Retrieved from http://www.ecoshape.org/

Castaño-Isaza, J., Newball, R., Roach, B., & Lau, W. (2015, 2). Valuing beaches to develop payment for ecosystem services schemes in Colombia's Seaflower marine protected area. *Ecosystem Services, 11*, 22-31.

CIOH. (2008). *Isla San Andrés - Compilación efectuada por en Centro de Investigaciones Oceanográficas e Hidrograficas - 201.* CIOH. Santa Marta: CIOH.

Coca-Domínguez, O., Ricaurte Villota, C., D.F. Morales-Giraldo, D., & Luna, K. (2019, 12). *State of the beaches of San Andrés, Providencia and Santa Catalina (2015-2019).* Santa Marta: INVEMAR. Retrieved from https://n2t.net/ark:/81239/m9937t

CORALINA-INVEMAR. (2012). *Atlas de la Reserva de Biósfera Seaflower. Archipiélago de San Andrés, Providencia y Santa Catalina.* Santa Marta: CORALINA-INVEMAR.

D. I. López, C. Segura-Quintero, P. C. Sierra-Correa, & J. Garay-Tinoco. (2012). *Atlas de la Reserva de Biósfera Seaflower. Archipiélago de San Andrés, Providencia y Santa Catalina.* Santa Marta.

de Vriend, H. J., van Koningsveld, M., Aarninkhof, S., de Vries, M., & Baptist, M. (2015, 6). Sustainable hydraulic engineering through building with nature. *Journal of Hydro-Environment Research, 9*(2), 159-171.

Deltares. (2014). *Delft3D-WAVE - Simulation of short-crested waves with SWAN: User Manua.* Delft: Deltares.

Deltares. (2017). *XBeach Manual: Release pre-1.22.4344.* Delft: Deltares.

Deltares. (2022). *Delft3D-FLOW - Simulation of multi-dimensional hydrodynamic flows and transport phenomena, including sediments: User Manual.* Delft: Deltares.

Downs, M. (2014, March 11). *Investing in Seagrass Can Yield Big Returns, But It Requires Patience.* Retrieved from Cool Green Science: https://blog.nature.org/science/2014/03/11/investing-in-seagrass/

FINEDETER. (2020, 3). *Proyecto para la Recuperacion del las playas de North End (Spratt Bight), Isla de San Andres (Departamento Archipielago de San Andrés, Providencia y Santa Catalina, Colombia).* Bogotá: FINEDTER.

Foo, S. A., & Asner, G. P. (2019). Scaling Up Coral Reef Restoration Uding Remote Sensing Techniques. *Frontiers in Marine Science.*

GEBCO. (2020). GEBCO 2020 Grid. *GEBCO Compilation Group.* doi:10.5285/a29c5465-b138-234de053-6c86abc040b9

Geister, J., & Dias, J. (2007). *Ambientes Arrecifales y Geologia de un Archipielago Oceanico: San Andres, Providencia y Santa Catalina (Mar Caribe, Colombia) con Guía Campo.* Bogotá, Colombia. Retrieved from www.ingeominas.gov.co

González, C., Urrego, L., Martínez, J., Polanía, J., & Yokoyama, Y. (2010). Mangrove dynamics in the southwestern Caribbean since the 'Little Ice Age': A history of human and natural disturbances. *Holocene, 20*(6), 849-861.

Google Earth Pro 7.3.4.8248. (2019, March). SAI, San Andrés, Providencia y Santa Catalina, Colombia: Maxar Technologies. Retrieved July 1, 2021, from http://www.google.com/earth/index.html

Gourlay, M. (1996). Wave set-up on coral reefs. 1. Set-up and wave-generated flow on an idealised two dimensional horizontal reef. *Coastal Engineering*, 161-193.

Guannel, G., Arkema, K., Ruggiero, P., & Verutes, G. (2016). The Power of Three: Coral Reefs, Seagrasses and Mangroves Protect Coastal Regions and Increase Their Resilience. *PLoS ONE.*

Guzman, W., Posada, B. O., Gusman, G., & Morales, D. (2009). *Programa Nacional de Investigacion Para la Prevencion, Mitigacion y Control de la Erosion Costera en Colombia.* INVEMAR.

Harborne, A., Mumby, P., Micheli, F., Perry, C., Dahlgren, C., Holmes, K., & Brumbaugh, D. (2006). The Functional Value of Caribbean Coral Reef, Seagrass and Mangrove Habitats to Ecosystem Processes. *Advances in Marine Biology, 50*, 57-189.

Higgins, E., Metaxas, A., & Scheibling, R. E. (2022). A systematic review of artificial reefs as platforms for coral reef research and conservation. *PLOS ONE 17.*

Holthuijsen, L. H. (2007). *Waves in Oceanic and Coastal Waters.* Cambridge, USA: Cambridge University Press.

Hoonhout, B. M., & de Vries, S. (2016). A process-based model for aeolian sediment transportand spatiotemporal varying sediment availability. *Journal of Geophysical Research: Earth Surface*, 1555-1575.

Infobae. (2021, September 14). Convenio por casi 9.000 millones de pesos busca acelerar la siembra de corales en San Andrés. *Infobae.* Retrieved from https://www.infobae.com/america/colombia/2021/09/14/convenio-por-casi-9000-millones-de-pesos-busca-acelerar-la-siembra-de-corales-en-san-andres/

INVEMAR. (2009). Colombia 50% Ocean. Retrieved from http://www.invemar.org.co/publicaciones

INVEMAR. (2015, 2). *Erosion Costera en la Isla de San Andrés - Informe Final.* Santa Marta, Colombia. Retrieved from http://www.invemar.org.co

INVEMAR. (2019). *Estado de los Pastos Marinos en las Islas San Andrés y Providencia en 2016 y 2018.* Santa Marta: Invemar y Coralina.

INVEMAR. (2021). *Adapatacion Basada en la Naturaleza Para Mitigar la Erosion Costera en San Andrés, Caribe Colombiano.* Santa Marta, Colombia: INVEMAR.

Klooster, J. (2017, 11). *Plan Maestro Erosion Costera de Colombia - Informe Principal.* Amersfoort, The Netherlands.

Klooster, J. (2020, 7). *Plan Maestro Erosion Costera de Colombia - Follow up: Second mission and final report.* Amersfoort, The Netherlands.

Lenstra, K. J. (2020). *Cyclic channel-shoal dynamics of ebb-tidal deltas.* Utrecht: Faculty of Geosciences, Universiteit Utrecht.

Martín-Prieto, J., Roig-Munar, F., Pons, G., Rodríguez-Perea, A., Alvarado, M., & Mir-Gual, M. (2013, 1). Description of erosion processes in Spratt Bight (San Andrés Island, Colombia) using Sequential End Point Rates (EPR). *Journal of Coastal Research, 65*, 997-1002.

Matheson, F. E., Reed, J., Dos Santos, V. M., Mackay, G., & Cummings, V. J. (2016). Seagrass rehabilitation: successful transplants and evaluation of methods at different spatial scales. *New Zealand Journal of Marine and Freshwater Research*, 96-109.

Meisel-Roca, A., Aguilera-Díaz, M. M., Yabrudy-Vega, J., & Sánchez-Jabba, A. M. (2016). *Economía y medio ambiente del archipiélago de San Andrés, Providencia y Santa Catalina.* Bogotá: Banco de la República.

Ministerio de Obras Publicas. (1963). *Restitucion Aerofogrametrica de San Andres (Isla).*

Navionics. (2021). *Navionics.* Retrieved from https://www.navionics.com

Posada, B., Henao Pineda, W., & Morales-Giraldo, D. (2011). *Diagnóstico de la erosión costera del territorio insular colombiano.* Santa Marta, Colombia.

Ralph, P. J., Durako, M. J., Enriquez, S., Collier, C. J., & Doblin, M. A. (2007). Impact of light limitation on seagrasses. *Journal of Experimental Marine Biology and Ecology*, 176-193.

Rangel-Buitrago, N., Anfuso, G., & Williams, A. (2015, 9). Coastal erosion along the Caribbean coast of Colombia: Magnitudes, causes and management. *Ocean and Coastal Management, 114*, 129-144.

Ridder, M. P., Smit, P. B., Dongeren, A. R., McCall, R. T., Nederhoff, K., & Reniers, A. J. (2021). Efficient two-layer non-hydrostatic wave model with accurate dispersive behaviour. *Coastal Engineering.*

Rodrigues Romero, P., Riano Suarez, D., Ramirez Riano, L., Lopez Porras, G., Escobar Oviedo, C., Espanol Nino, W., . . . Ayure Alba, L. (2020, 11). *Estudio Ambiental Estrategico sobre el Estado del Arte del fenomeno de erosion costera en el Archipelago de San Andrés, Providencia y Santa Catalina y recomendaciones en el marco del Control y la Vigilancia Fiscal.* Bogota.

Roelvink, D., McCall, R., Mehvar, S., Nederhoff, K., & Dastgheib, A. (2018). Improving predictions of swash dynamics in XBeach: The role of groupiness and incident-band runup. *Coastal Engineerin*, 103-123.

Roelvink, D., Reniers, A., Dongeren, A. v., Vries, J. v., McCall, R., & Lescinski, J. (2009). Modelling storm impacts on beaches, dunes and barrier islands. *Coastal Engineering*, 1133-1152.

Roelvink, J. A., & Stive, M. J. (1989). Bar-generating cross-shore fow mechanisms on a beach. *Journal of Geophysical Research*, 4785–4800.

Royero, J., Moreno, J., & Lizano, O. (2015, 5). Evaluation of Extreme Waves Associated with Cyclonic Activity on San Andrés Island in the Caribbean Sea since 1900. *Journal of Coastal Research, 31*(3), 557-568.

Sánchez-Jabba, A. M. (2016). *Manejo ambiental en Seaflower : reserva de biósfera en el Archipiélago de San Andrés, Providencia y Santa Catalina.* Bogotá: Banco de la Republica.

Smithsonian Tropical Reaserch Institute. (2015). Introduciton to the Greater Caribbean. Retrieved from https://biogeodb.stri.si.edu/caribbean/en/pages/generalinfo

Spalding, M., Mclvor, A., Tonneijck, F., Tol, S., & van Eijk, P. (2014). *Mangroves for coastal defence Guidelines for coastal managers & policy makers Suggested Citation.* Retrieved from www.nature.org.

The MarineBio Conservation Society. (2021). Coral Reefs. *The MarineBio Conservation Society.* Retrieved from https://www.marinebio.org/creatures/coral-reefs/

The World Bank. (2019). World Development Indicators. Retrieved from https://datacommons.org/place/country/COL?utm_medium=explore&mprop=count&popt=Person&hl=en

Thomas, Y.-F., Nicole-Lerma, A., & Posada, B. O. (2012). *Atlas climatológico del mar C aribe colombiano.* Invemar, Santa Marta.

United Nations. (2015). *THE 17 GOALS.* Retrieved from https://sdgs.un.org/goals

Universidad del Norte - IDEHA. (2009). *Isla de San Andrés. Estudios y diseños relacionados con la sostenibilidad de la playa Spratt Bight.* San Andrés: FONADE – Gobernación de San Andrés.

Urrego, L., Correa-Metrio, A., & González-Arango, C. (2018). Colombian Caribbean mangrove dynamics: Anthropogenic and environmental drivers. *Boletin de la Sociedad Geologica Mexicana, 70*(1), 133-145.

van Dongeren, A., Lowe, R., Pomeroy, A., Trang, D. M., Roelvink, D., Symonds, G., & Ranasinghe, R. (2013). Numerical modeling of low-frequency wave dynamics over a fringing coral reef. *Coastal Engineering*, 178-190.

Van Eekelen, E., & Bouw, M. (2020). *Building with Nature. Creating, implementing and upscaling Nature-based Solutions.* Rotterdam: EcoShape.

van Rooijen, A., McCall, R., van Thiel de Vries, J., van Dongeren, A., Reniers, A., & Roelvink, D. (2016). Modeling the effect of wave-vegetation interaction on wave setup. *Journal Of Geophysical Research: Oceans*, 4341-4359.

WW3DG. (2019). *User manual and system documentation of WAVEWATCH III version 6.07.* Technical Note, NOAA/NWS/NCEP/MMAB, Wave Watch III Development Group, College Park, MD, USA.

Zijlema, M., Stelling, G., & Smit, P. (2011). SWASH: An operational public domain code for simulating wave fields and rapidly varied flows in coastal waters. *Coastal Engineering*, 992–1012.

List of Tables

List of Figures

Appendices

Picture of Spratt Bight Beach taken on November 2021 during the workshops organized to inform and receive feedback from the stakeholders on the project "Cooperación técnica Prevención de la erosión costera en San Andrés, Colombia" (credits to Sander Carpay)

Appendix A - Bathymetry Data

The bathymetry data that will be used in the different modelling studies is composed by different sources:

- Data received from a field study performed by INVEMAR in 2018.
- NAVIONICS nautical chart (2021)
- CIOH (Center of Ocean and Hydrological Investigation of Colombia) Nautical chart (2008)
- Information from a study made by FINDETER (Territorial Development Financer in Colombia) (2020)
- GEBCO (2020)

The bathymetric data received from INVEMAR was used as the main and most reliable data source, and therefore the basis for the dataset. However, as there were a few missing gaps in the retrieved data, complementary information needed to be consulted. The figure below shows the process of producing the bathymetry.

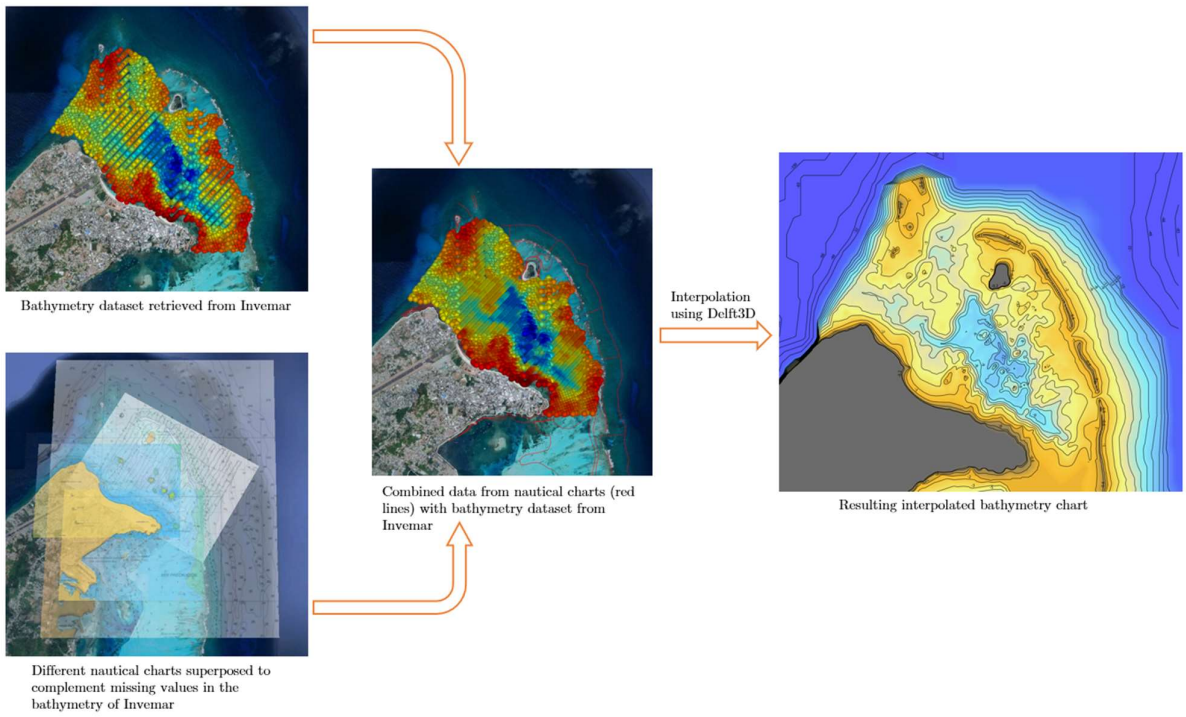

Figure 0.1: Method used to obtain an integral and complete bathymetry dataset based on the retrieved data from INVEMAR and other sources.

Vectors were then drawn over certain depth lines of the bathymetry charts where data was missing. These vectors were exported as polygons to Delft3D-QUICKIN and converted into depth samples with an x, y and z value ('.xyz' format). The combination of dataset and chart data was then interpolated over a grid with mesh width of 13 m, generating the bathymetry shown in Figure 2.8. Furthermore, information (besides coordinates and water depths) about the dataset retrieved from INVEMAR is also not available, therefore it was assumed that the reference water level is equal to MSL (mean sea level).

Finally, the bathymetry for the large-scale modelling was retrieved from GEBCO (2020), which returns a datapoint every 1 km latitude and longitude. This is enough for a large-scale model, but too coarse to model effects nearshore. Figure 0.2 shows an impression of the GEBCO bathymetry.

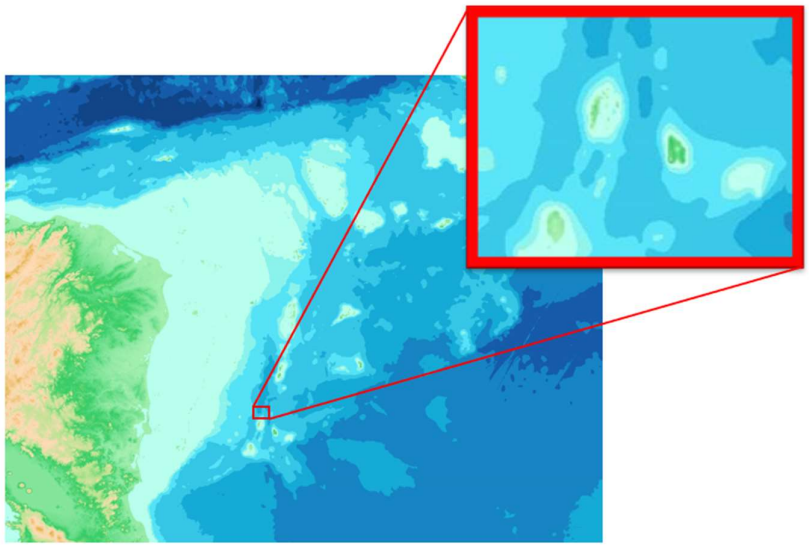

Figure 0.2: Representation of Bathymetry retrieved from GEBCO (2020). The darker the blue colors, the greater the water depth. Green and yellow colors indicate depths above 0 m (above MSL)

Appendix B - Wave Data

Wave data were retrieved from a dataset of 30 years (between 1979 and 2009) at measuring station 42058 located at 14.394° N 74.816° W, approximately 775 km E from San Andrés. To be converted into usable data for the location of San Andrés, a wave transformation was made with WaveWatchIII (WW3) (2019), which is a third-generation wave model developed at NOAA/NCEP and has an already validated global wave model, where data can be extracted at specific geographical locations.

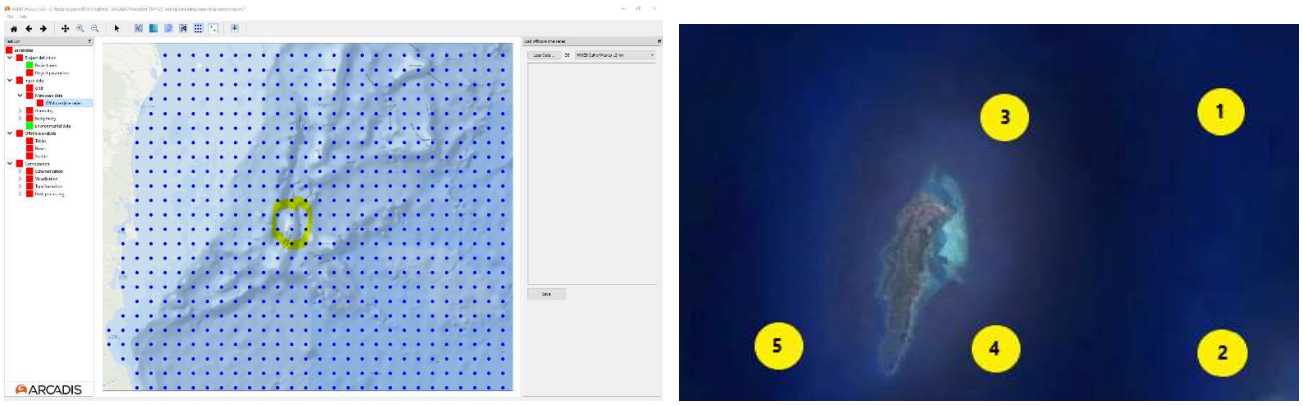

Figure 0.3: Location of virtual buoys used to extract the wave data for San Andrés

Data extraction points are generated every 0.1° latitude and longitude as shown in the figure above. For this study, data from 5 locations were extracted:

1. 25 km NE of San Andrés (12.6° N, 81.5° W)
2. 25 km SE of San Andrés (12.5° N, 81.5° W)
3. 10 km N of San Andrés (12.6° N, 81.6° W)
4. 5 km SE of San Andrés (12.5° N, 81.6° W)
5. 10 km SW of San Andrés (12.5° N, 81.8° W)

To avoid interference from shallow area on the wave data, points 2, 3 and 4 were discarded as they were too close to the coast and the influence of shallow areas could affect the data. Location 5 was discarded because it is situated at the West side of the island. As the predominant wave direction is form the East, this location was being sheltered by the island and its data was not representative for this study. Finally, data from location 1 was considered to be the most representative for the island's wave climate, as the majority of the waves approach San Andrés from the NE (as shown in the wave rose of Figure 2.11). The variables of the WW3 data are described in the table below.

Data WW3		
Variable	**Description**	**Unit**
y	Year	-
m	Month	-
d	Day	-
h	Hour	-
lat	Latitude	decimal degrees North
lon	Longitude	decimal degrees North
Dir_sea	Wave direction	degrees
Hs_sea	Significant wave height	m
T_sea	Mean wave period	seconds

Table 0.1: data variables retrieved from WW3 model

The figure below shows the time series which was retrieved from the WW3 model.

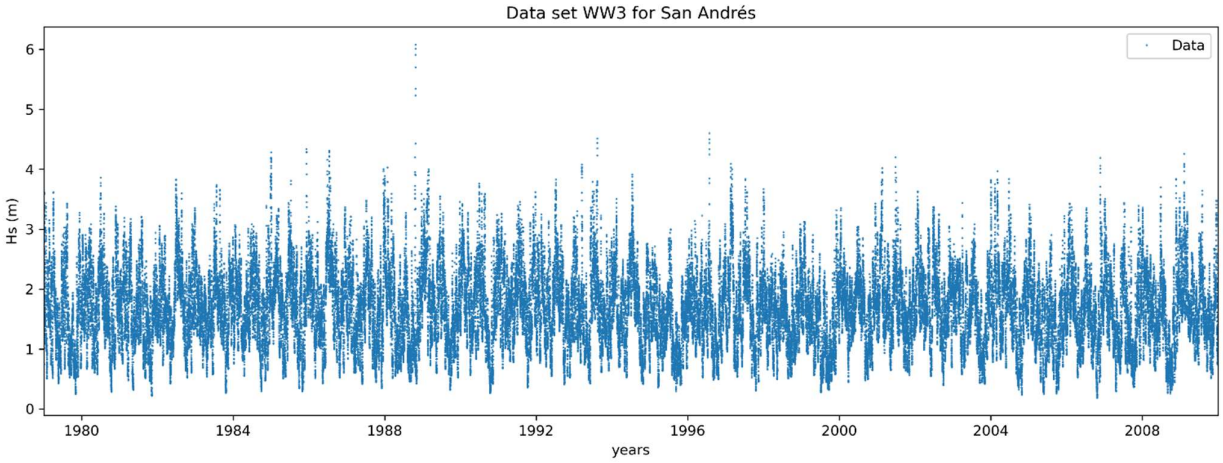

Figure 0.4: Wave data series between 1979 and 2010 extracted form location 1.

The figure below shows the wave period plotted against the wave height, demonstrating the wave steepness of the retrieved wave data. On the right the wave rose is shown.

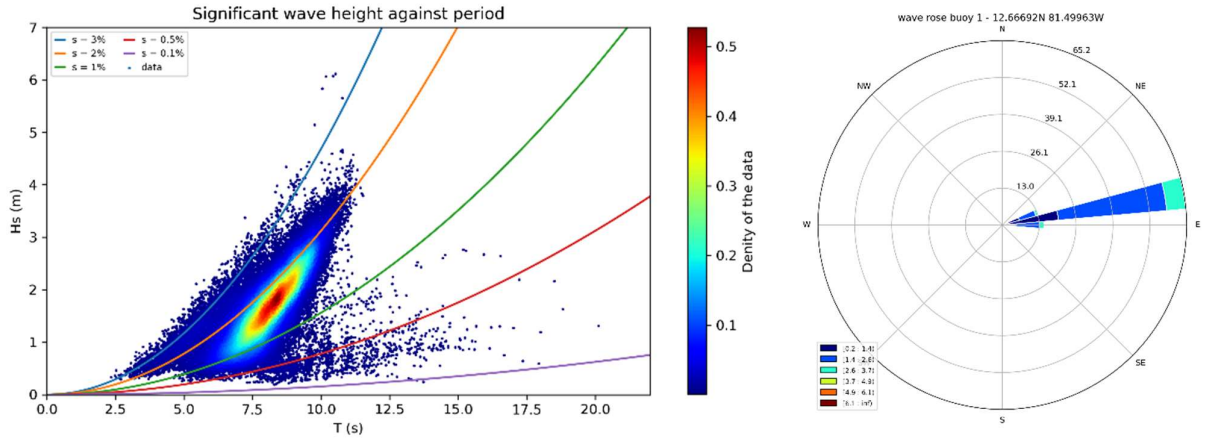

Figure 0.5: (On the right) Distribution of significant wave height versus mean wave period for offshore waves approach San Andrés. The colored lines represent different wave steepness. (On the left) Wave rose for offshore waves

Appendix C - List of important stakeholders

According to Romero Rodrigues (2020), the principal stakeholders involved in the coastal, urban and water related matters are the ones listed below:

- UNGRD: Unidad Nacional para la Gestión del Riesgo de Desastres (National Unit for Disaster Risk Management)
- MADS: Ministerio del Ambiente y Desarrollo Sostenible (Ministry of Environment and Sustainable Development)
- CORALINA: Corporación Autónoma para Desarrollo Sostenible del Archipiélago de San Andrés, Providencia y Santa Catalina (autonomous intergovernmental agency that manages and regulates all natural resources on the island)
- INVEMAR: Instituto de Investigaciones Marinas y Costeras (marine research institute of Colombia)
- ANLA: Autoridad Nacional de Licencias Ambientales (Nacional Authority for Environmental Matters)
- PNN: Parques Naturales Nacionales de Colombia (Nacional Natural Parks of Colombia)
- IDEAM: Instituto de Hidrología, Meteorología y Estudios Ambientales (Environmental, Meteorological and Hydrological research institute)
- MHCP: Ministerio de Hacienda y Crédito Público (Ministry of the Economy)
- SGC: Servicio Geológico Colombiano (Colombian Geografical Research Institute)
- FONTUR: Fondo Nacional de Turismo (National Tourism Fund)
- DIMAR: Dirección General Marítima (General Maritime Directorate)
- CIOH: Centro de Investigaciones Oceánicas y Hidrográficas (Center of Ocean and Hydrological Investigation)
- ENC: Ejército Nacional de Colombia (military)
- MinTransporte: Ministry of Transport
- INVIAS: Instituto Nacional de Vías (National road, rail, and waterways institute)
- MME: Ministerio de Minas y Energía (Ministry of Mining and Energy)
- MinInterior: Ministry of internal affairs
- MCIT: Ministerio de Comercio, Industria y Turismo (Ministry of Commerce, Industry and Tourism)
- Entidades Teritoriales: Raizales (San Andrés local community)
- Gobernacion de San Andrés (Departmental government of San Andrés)
- Municipios de San Andrés (Municipality of San Andrés)

The figure below shows a chart in which the importance and influence of the different stakeholders is represented. It can be seen that the most important stakeholders are UNGRD, the departmental Government, CORALINA, DIMAR, the Municipality, ministry of Environment, The National Parks and INVEMAR. It can also be seen that the local community (Raizales) has high influence, however almost no importance.

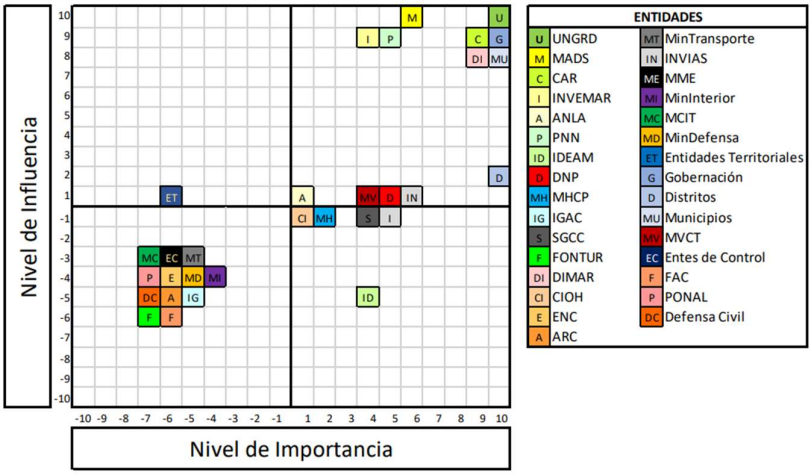

Appendix D - Detailed model description Delft3D

Here the Delft3D-WAVE and Delft3D-FLOW models will be described in more detail. The fragments used in this Appendix are extracted from the PhD work of Lenstra (2020, pp. 119-123).

Hydrodynamics: Currents

The numerical model Delft3D is used in 2DH mode, where the model is run in depth-average sense. The flow velocities in the x- and y-direction, u, and v, and the water level with respect to still water, η, are calculated by solving the depth-averaged shallow water equations and the continuity equation as shown in the equations below.

$$\frac{\partial u}{\partial t} + u\frac{\partial u}{\partial x} + v\frac{\partial u}{\partial y} - fv = -g\frac{\partial \eta}{\partial x} - \frac{\tau_x}{\rho h} + \frac{F_{w,x}}{\rho h} + \\ + \frac{1}{h}\left[\frac{\partial}{\partial x}\left(\mathcal{A}\frac{\partial u}{\partial x}\right) + \frac{\partial}{\partial y}\left(\mathcal{A}\frac{\partial u}{\partial y}\right)\right],$$

$$\frac{\partial v}{\partial t} + u\frac{\partial v}{\partial x} + v\frac{\partial v}{\partial y} + fu = -g\frac{\partial \eta}{\partial y} - \frac{\tau_y}{\rho h} + \frac{F_{w,y}}{\rho h} + \\ + \frac{1}{h}\left[\frac{\partial}{\partial x}\left(\mathcal{A}\frac{\partial v}{\partial x}\right) + \frac{\partial}{\partial y}\left(\mathcal{A}\frac{\partial v}{\partial y}\right)\right],$$

$$\frac{\partial h}{\partial t} + \frac{\partial (hu)}{\partial x} + \frac{\partial (hv)}{\partial y} = 0,$$

Where:

- t is time
- f the Coriolis parameter
- g the gravitational acceleration
- h the local water depth
- ρ the density of water
- A the spatially uniform horizontal eddy viscosity
- τ_x and τ_y are x and y components of the bed shear stress for the waves and currents

The bottom roughness is determined by using the Chézy formulation with a uniform Chézy coefficient of 65 $m^{1/2}$ s^{-1}. Moreover, the components of the wave-induced force per surface area, F_x and F_y, are computed by D3D-W and are discussed below.

In the equations above, the first three terms represent the temporal acceleration and the advective acceleration in the x- and y-direction. The last term corrects for the Coriolis effect. The right-hand side consists of the pressure gradient term, the bed friction, the wave-force, and a term that incorporates the effect of turbulent and sub-grid fluid motions. Moreover, the third equation accounts for the incompressibility of water.

Hydrodynamics: Waves

Delft3D-WAVE uses the numerical model SWAN (Simulating WAves Nearshore) to do its wave simulations. SWAN is a phase-averaging spectral wave model, which computes the wave spectral action density, N, using the wave action balance equation in its stationary as shown below.

$$\frac{\partial (c_{g,x} N)}{\partial x} + \frac{\partial (c_{g,y} N)}{\partial y} + \frac{\partial (c_{g,\theta} N)}{\partial \theta} + \frac{\partial (c_{g,\sigma} N)}{\partial \sigma} = \frac{S}{\sigma}$$

In which:

- θ is the spectral direction
- σ is the relative frequency
- $c_{g,x}$ and $c_{g,y}$ are the wave group velocity components
- S represents the generation, dissipation, and redistribution of wave energy

The first two terms on the left-hand side of the equation describe the propagation of wave energy in x- and y-direction, the third term represents refraction due to spatial gradients in currents or water depth, and the fourth term accounts for any change in relative wave frequency spectrum.

On the righthand side is the Energy sources and sinks term, which is limited to wave breaking, white-capping and bottom friction.

Subsequently, Delft3D-WAVE communicates the resulting wave-induced force to Delft3D-FLOW, which is determined by:

$$F_{w,x} = -\frac{\partial T_{xx}}{\partial x} - \frac{\partial T_{xy}}{\partial y}$$

$$F_{w,y} = -\frac{\partial T_{yx}}{\partial x} - \frac{\partial T_{yy}}{\partial y}$$

In which the elements of the radiations stress tensor are:

$$T_{xx} = \int_0^{2\pi}\int_0^{\infty} E\left(n\cos^2\theta + n - \frac{1}{2}\right)\, d\sigma\, d\theta,$$

$$T_{yy} = \int_0^{2\pi}\int_0^{\infty} E\left(n\sin^2\theta + n - \frac{1}{2}\right)\, d\sigma\, d\theta,$$

$$T_{xy} = S_{yx} = \int_0^{2\pi}\int_0^{\infty} E\, n\, \sin\theta\, \cos\theta\, d\sigma\, d\theta,$$

$$n = \frac{|\vec{c_g}|}{c_w} = \left(\frac{1}{2} + \frac{\kappa h}{\sinh 2\kappa h}\right),$$

Sediment transport

In Delft3D, sediment transport below a threshold height is treated as bed load and above this threshold it is treated as suspended load. Both sediment transport mechanisms are split into transport due to waves and currents.

Bed load

The current-related bed load transport in the x- and y- direction, $q_{b,c,x}$ and $q_{b,c,y}$, is calculated from the depth-averaged velocity as shown below.

$$q_{b,c,x} = 0.5\frac{u}{|\vec{u}|}\frac{\tau_s^2}{\rho}\frac{d_{50}}{d_*^{0.3}}\frac{\tau_s - \tau_{cr}}{\tau_{cr}}\mathcal{H}(\tau_s - \tau_{cr}),$$
$$q_{b,c,y} = 0.5\frac{v}{|\vec{u}|}\frac{\tau_s^2}{\rho}\frac{d_{50}}{d_*^{0.3}}\frac{\tau_s - \tau_{cr}}{\tau_{cr}}\mathcal{H}(\tau_s - \tau_{cr}),$$

In which:

- τ_s is the shear stress experienced by the sediment due to both current and wave motion
- τ_{cr} the critical shear stress below which no bed load transport occurs
- H the Heaviside step function
- d_{50} and d_* are the median and dimensionless sediment diameter, respectively

The bed load transport components are modified to include gravitational bed-slope effects in longitudinal and in transverse directions using the formulations below:

$$q^*_{b,c,x} = \alpha_s q_{b,c,x} - \alpha_n q_{b,y},$$
$$q^*_{b,c,y} = \alpha_s q_{b,c,y} + \alpha_n q_{b,x}.$$

Where:

$$\alpha_s = 1 + \alpha_{bs}\left[\frac{\tan\psi}{cos\beta_s\left(\tan\psi - \tan\beta_s\right)} - 1\right],$$
$$\alpha_n = \alpha_{bn}\sqrt{\frac{\tau_{cr}}{|\tau|}}\tan\beta_n,$$

- α_{bs} and α_{bn} are tuning parameters
- β_s and β_n are the bed slope angles in the streamwise and transverse direction (positive down), respectively
- ψ is the internal angle of friction of bed material (assumed to be 30° for sand)

In the presence of waves, to incorporate the wave orbital velocities, the magnitude of the current-related bed load transport is divided by the factor

$$\sqrt{1 + r^2 + 2|r|\,cos\,\varphi}$$

Where:

φ equals the angle between currents and wave propagation direction and

$$r = \left(\frac{|u_{on}| - u_{Cr}}{|\vec{u}| - u_{Cr}}\right)^3$$

In which:

- u_{on} is the maximum of the (asymmetric) intra-wave near-bed horizontal velocity in the direction of the waves based on the significant wave height
- u_{cr} is the critical depth-averaged velocity for initiation of motion based on τ_{cr}.

The components of the wave-related bed load transport $q_{b,w,x}$ and $q_{b,w,y}$ are given by:

$$q_{b,w,x} = r|\vec{q}_{b,c}| \cos\varphi,$$
$$q_{b,w,y} = r|\vec{q}_{b,c}| \sin\varphi,$$

Where φ is the local angle between the direction of wave propagation and the positive x-axis. Finally, the current- and wave-related bed load transport are combined to obtain the total bed load transport as presented below.

$$q_{b,x} = q_{b,c,x} + BedW \cdot q_{b,w,x},$$
$$q_{b,y} = q_{b,c,y} + BedW \cdot q_{b,w,y}.$$

Suspended load

For the suspended load transport due to currents, the wave- and depth-averaged sediment concentration, c, follows from the depth-averaged advection-diffusion equation as stated below.

$$\frac{\partial(hc)}{\partial t} + \frac{\partial(huc)}{\partial x} + \frac{\partial(hvc)}{\partial y} - D_H\left[\frac{\partial}{\partial x}\left(h\frac{\partial c}{\partial x}\right) + \frac{\partial}{\partial y}\left(h\frac{\partial c}{\partial y}\right)\right] = w_s(c_{eq} - c).$$

In which:

D_H is the spatially uniform horizontal eddy diffusivity

w_s the hindered sediment settling velocity.

c_{eq} the equilibrium concentration, which depends on the skin friction due to the currents and waves

The terms on the left-hand side describe (from left to right) the temporal gradient in depth-integrated sediment concentration, the spatial gradient in sediment advection in both directions, and the diffusive processes due to gradients in sediment concentration in both directions.

Based on the computed sediment concentrations, the current-related suspended transport rates in x- and y-directions are computed as:

$$q_{s,c,x} = huc - D_H\frac{\partial c}{\partial x},$$
$$q_{s,c,y} = hvc - D_H\frac{\partial c}{\partial y}.$$

Appendix E - Overview of Results

In this appendix all results of the modelling study with Delft3D will be shown. As 20 different environmental conditions were simulated and not all of them have the same relevance, it has been chosen to show them in the appendix, to which can be referred.

Waves

0°N Conditions

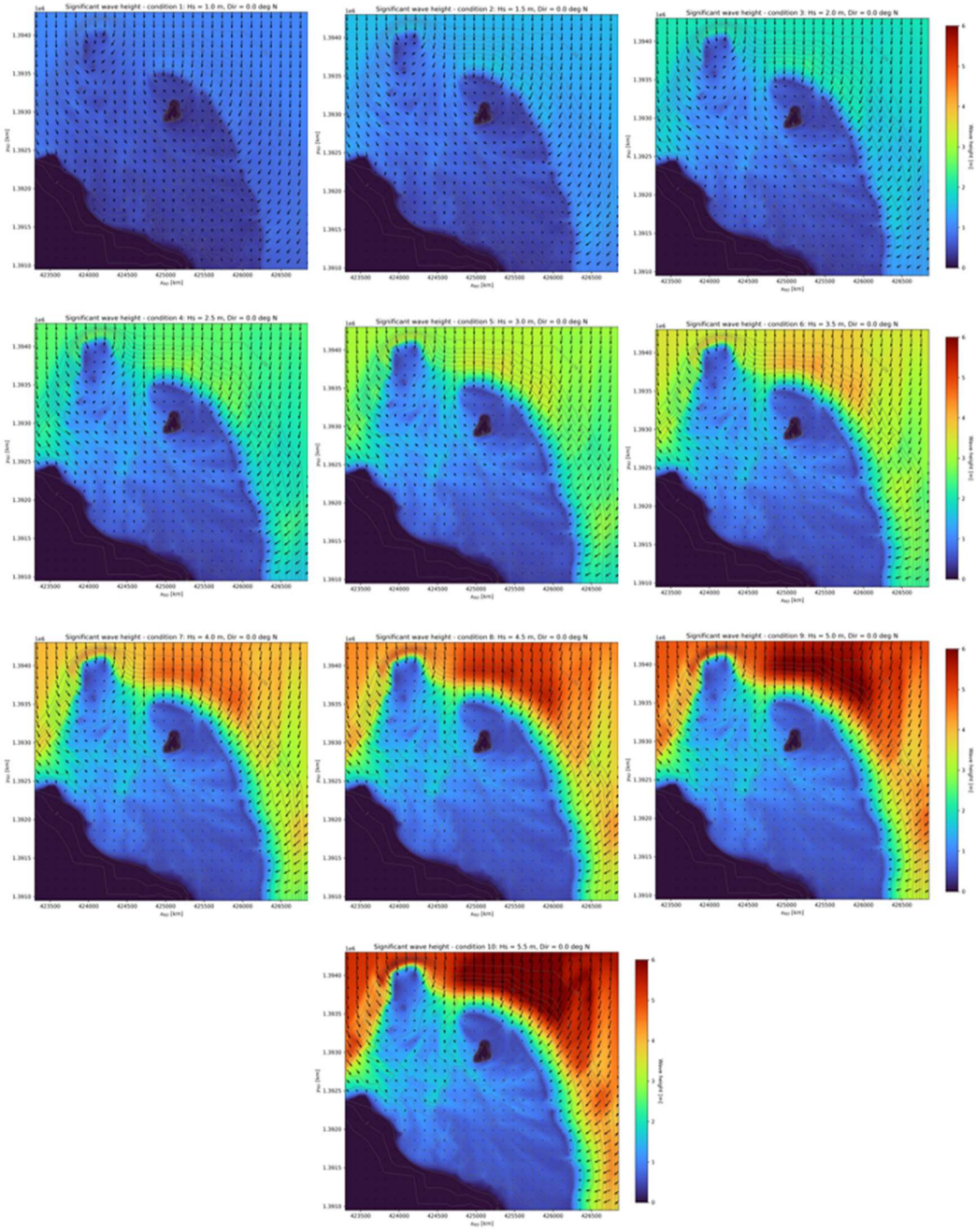

80°N Conditions

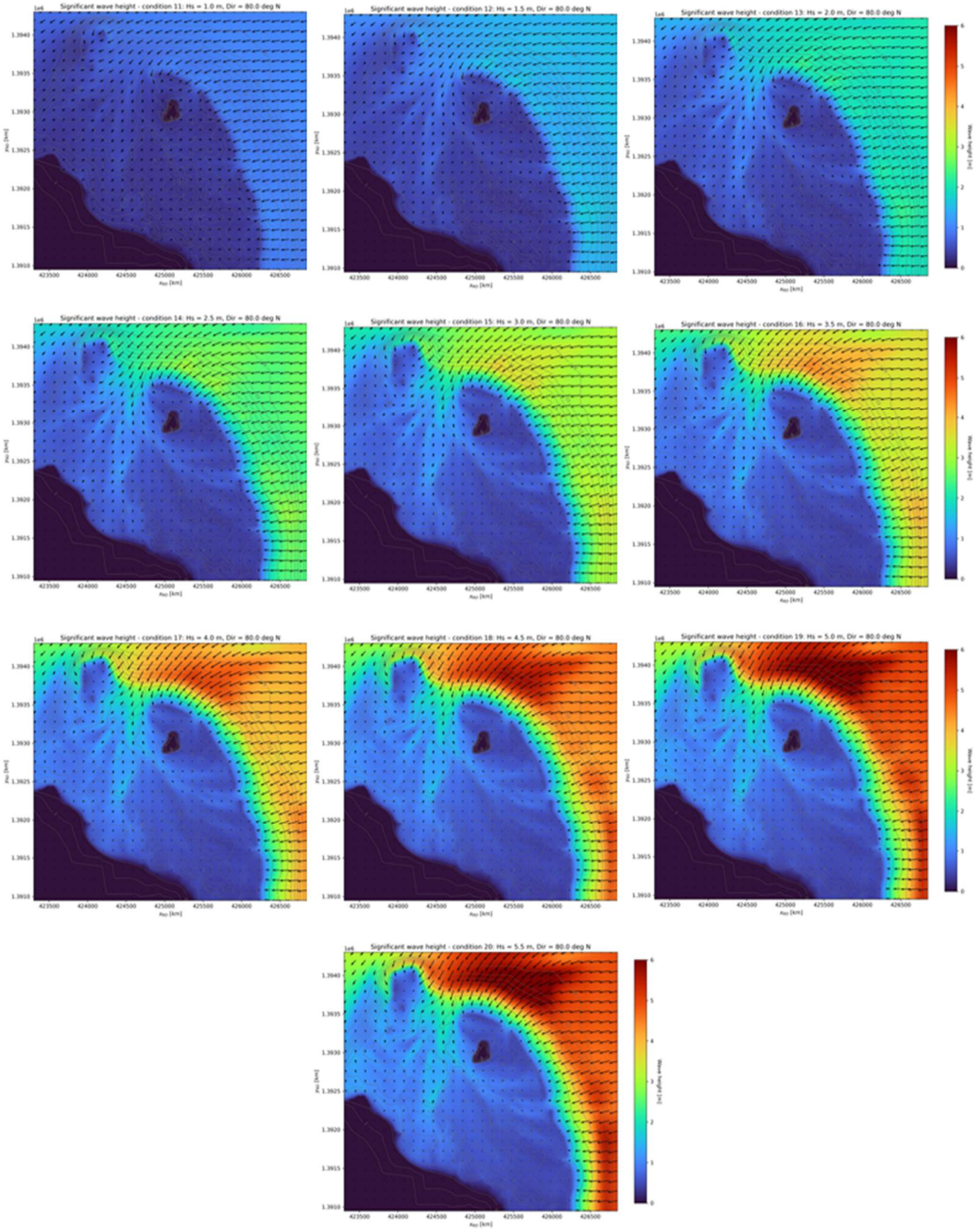

Water levels

0°N Conditions

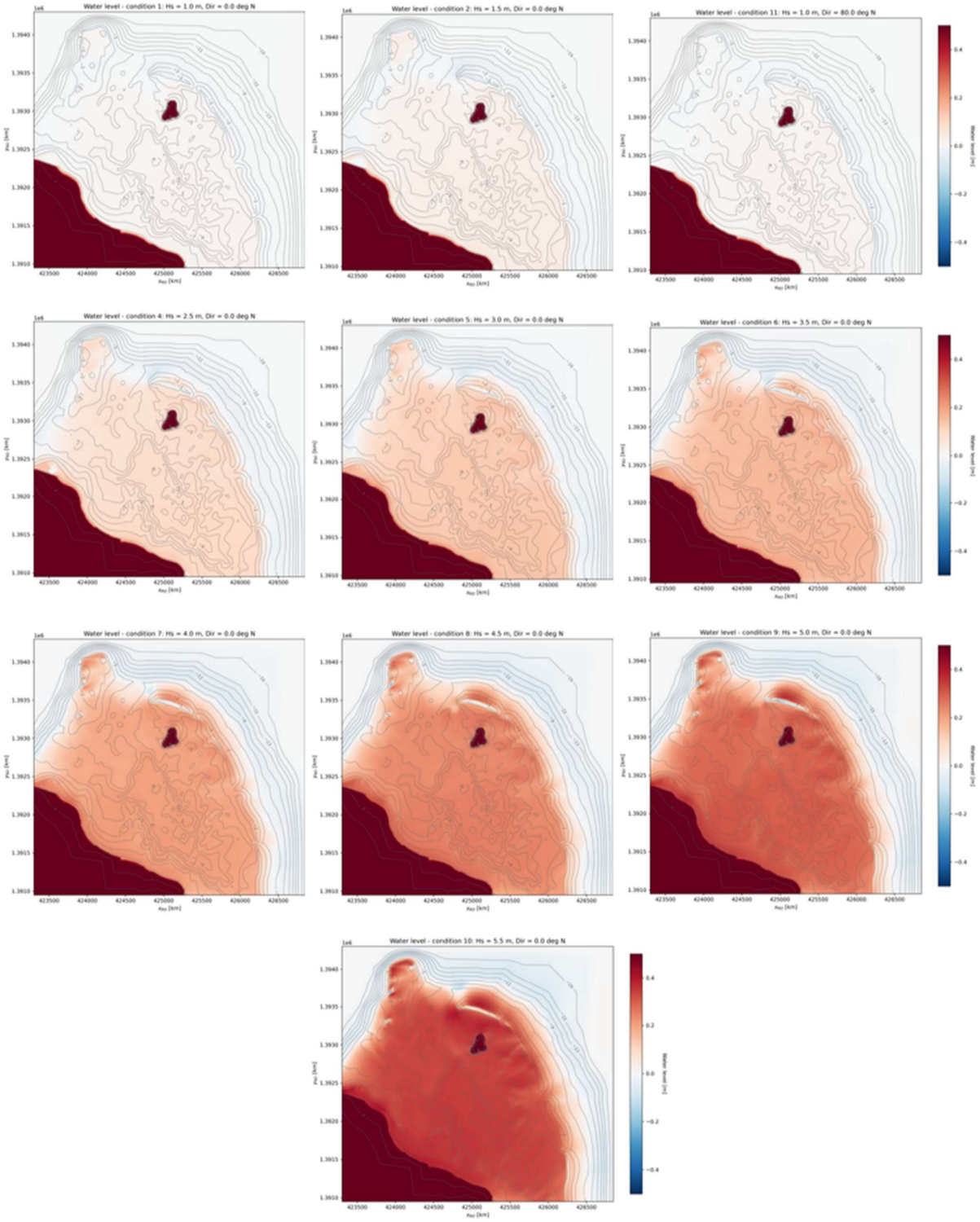

80°N Conditions

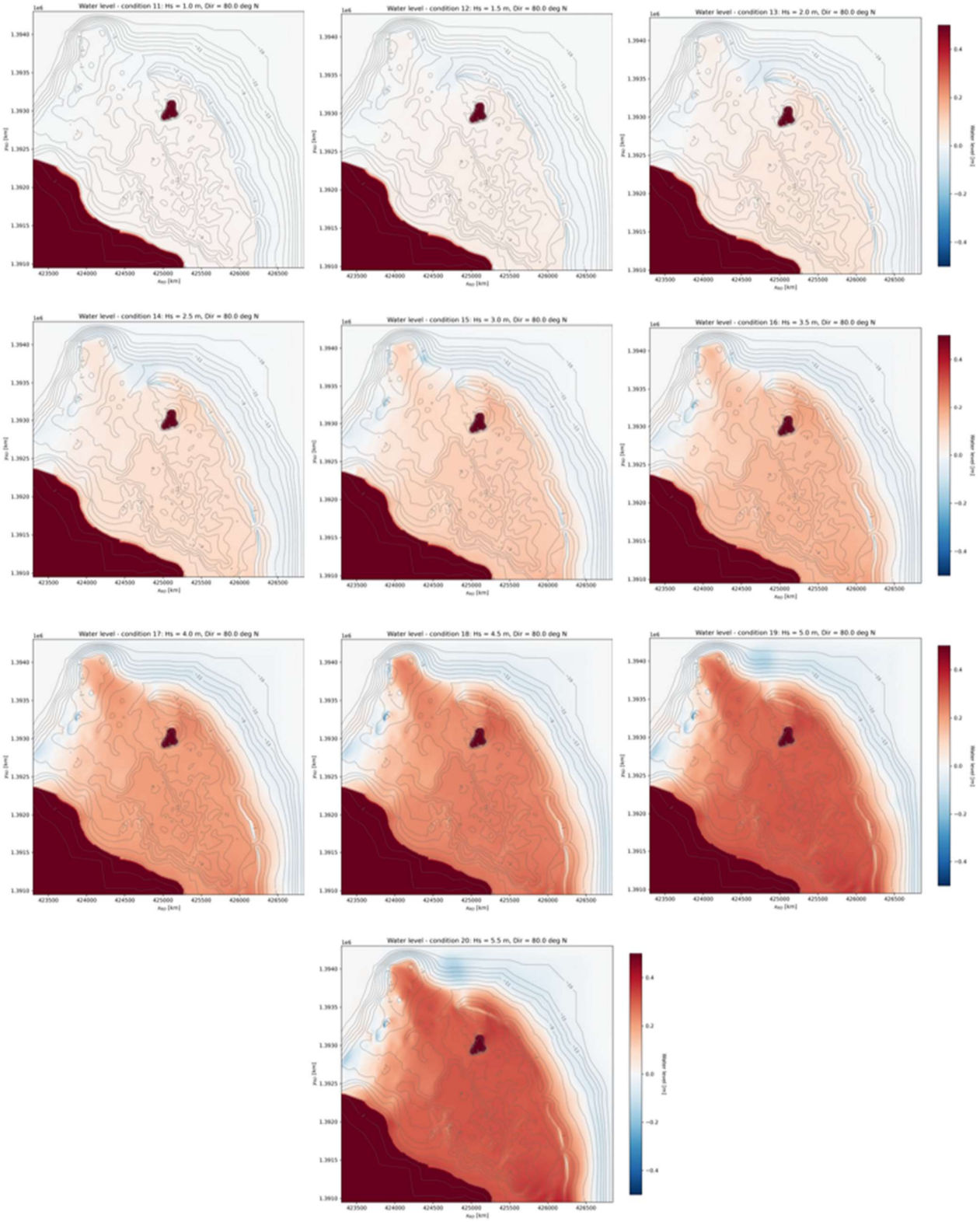

Flow Velocities

0°N Conditions

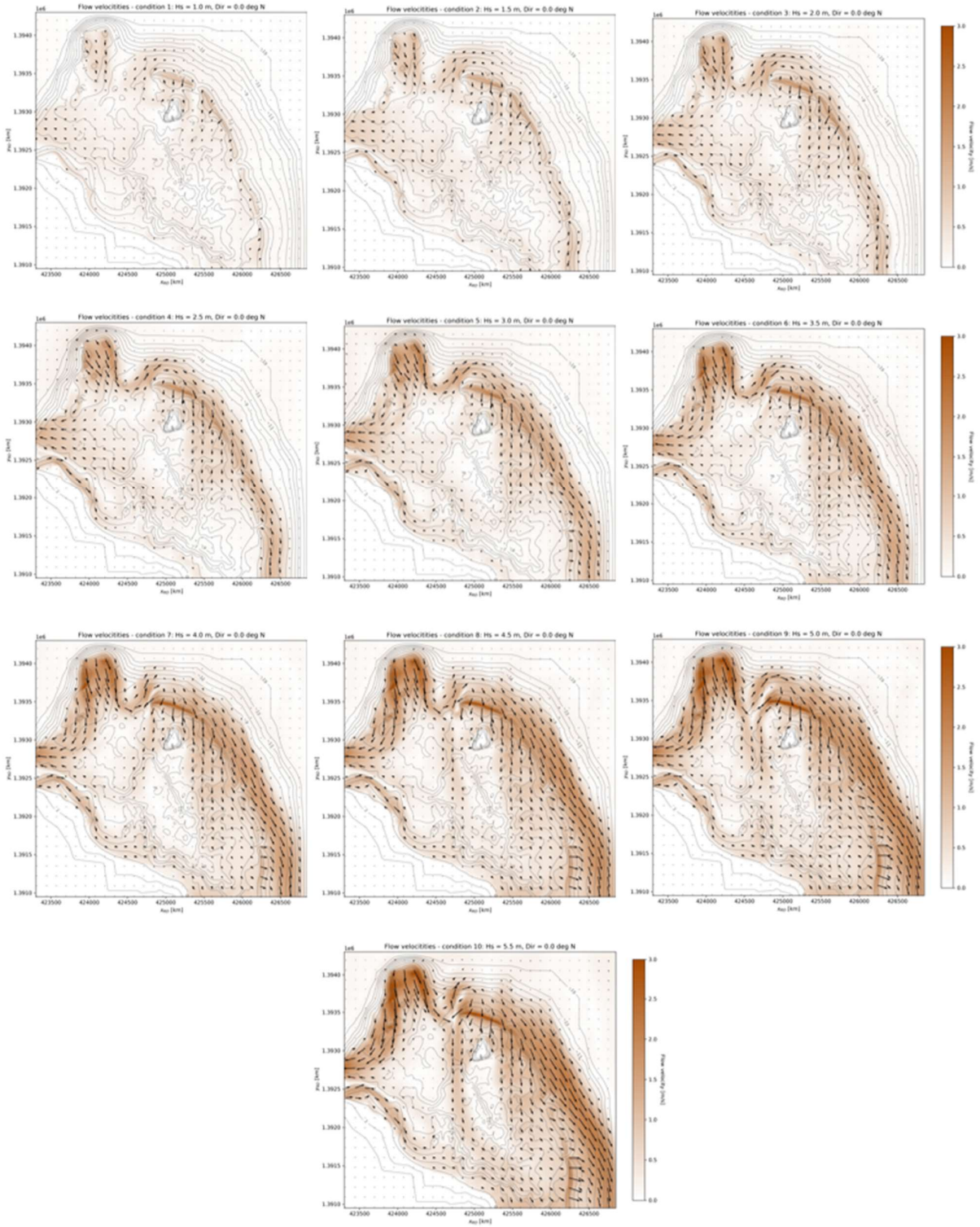

80°N Conditions

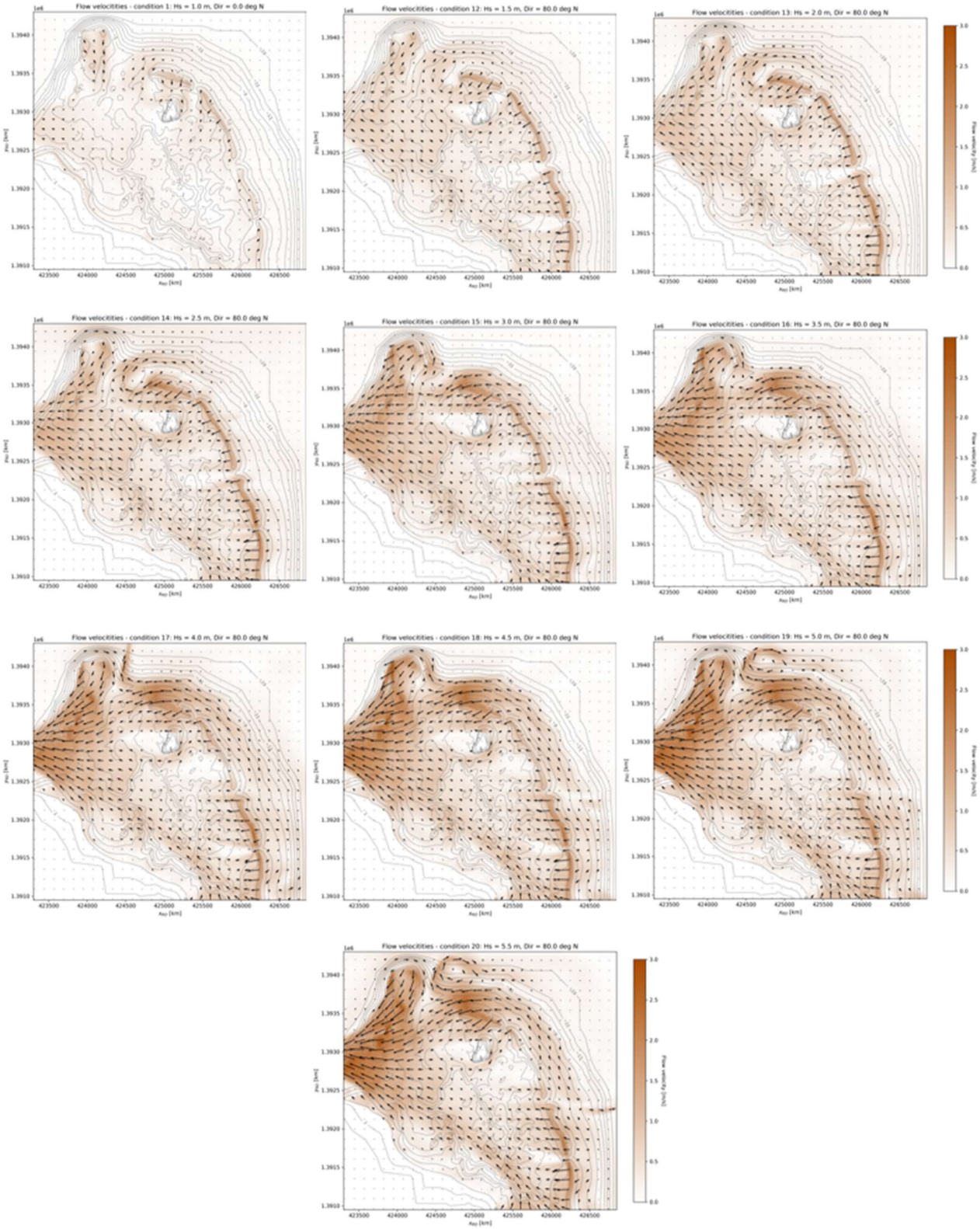

Flow Velocities Zoomed in

0°N Conditions

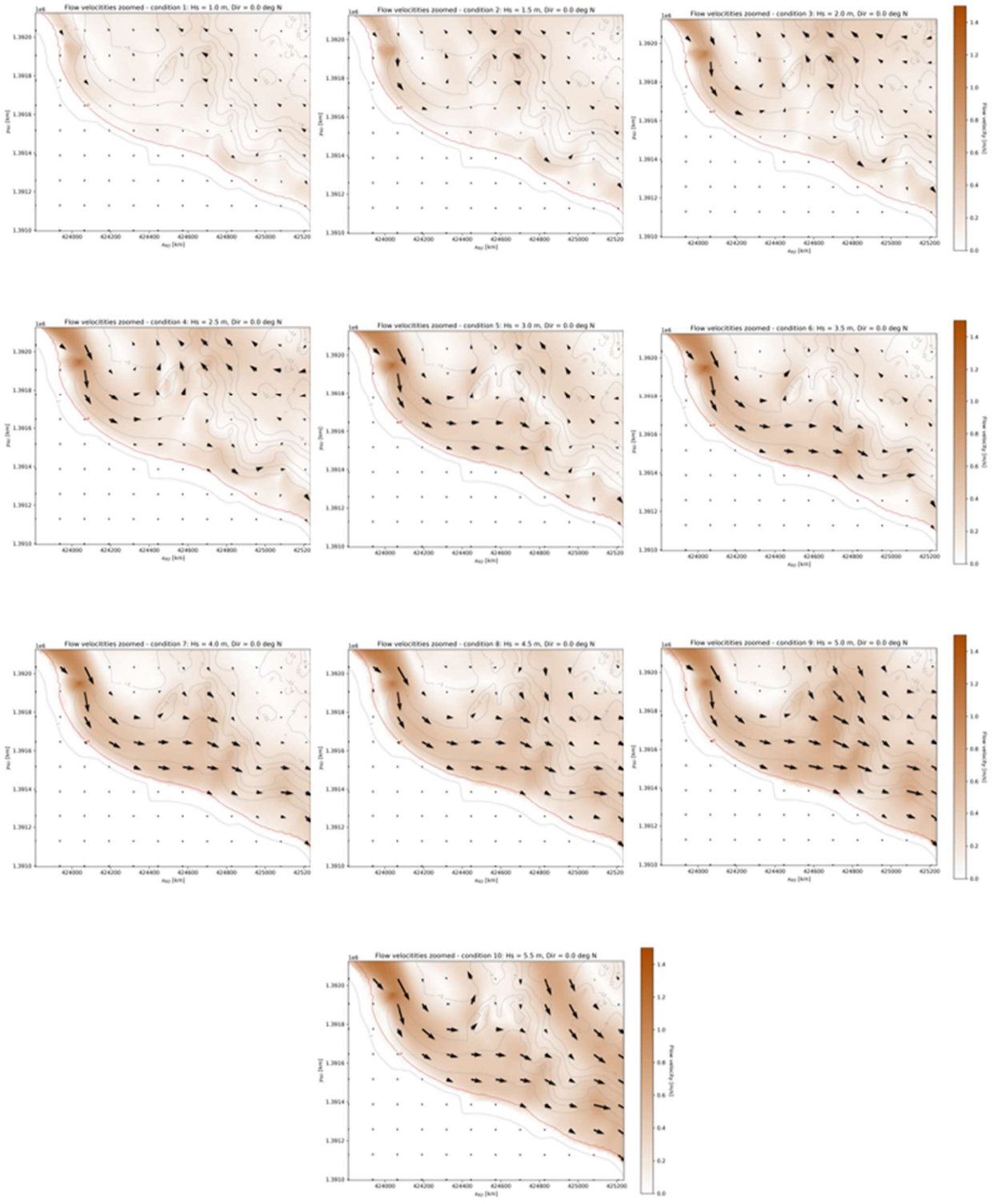

80°N Conditions

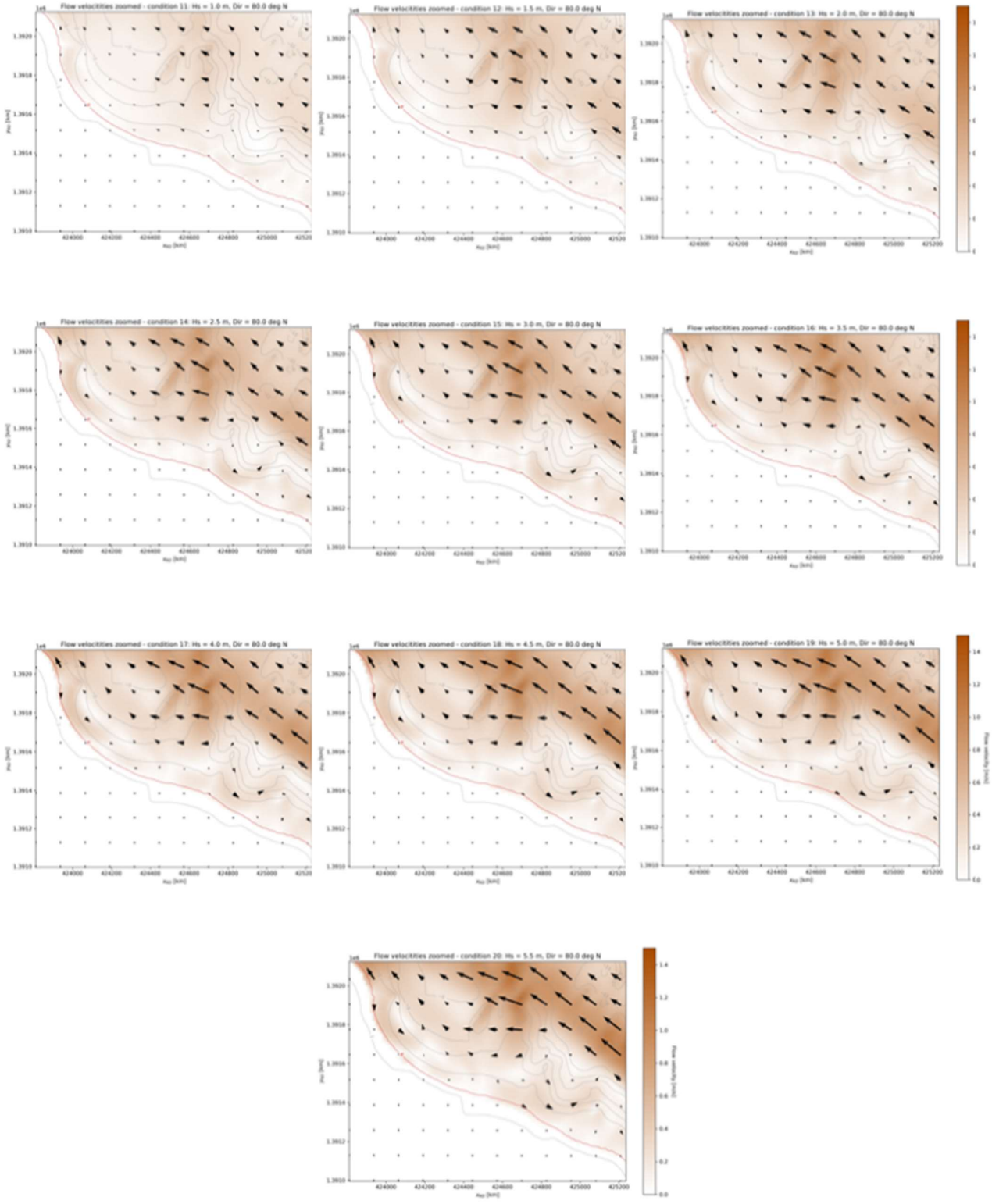

Sediment Transport near shore

0°N Conditions

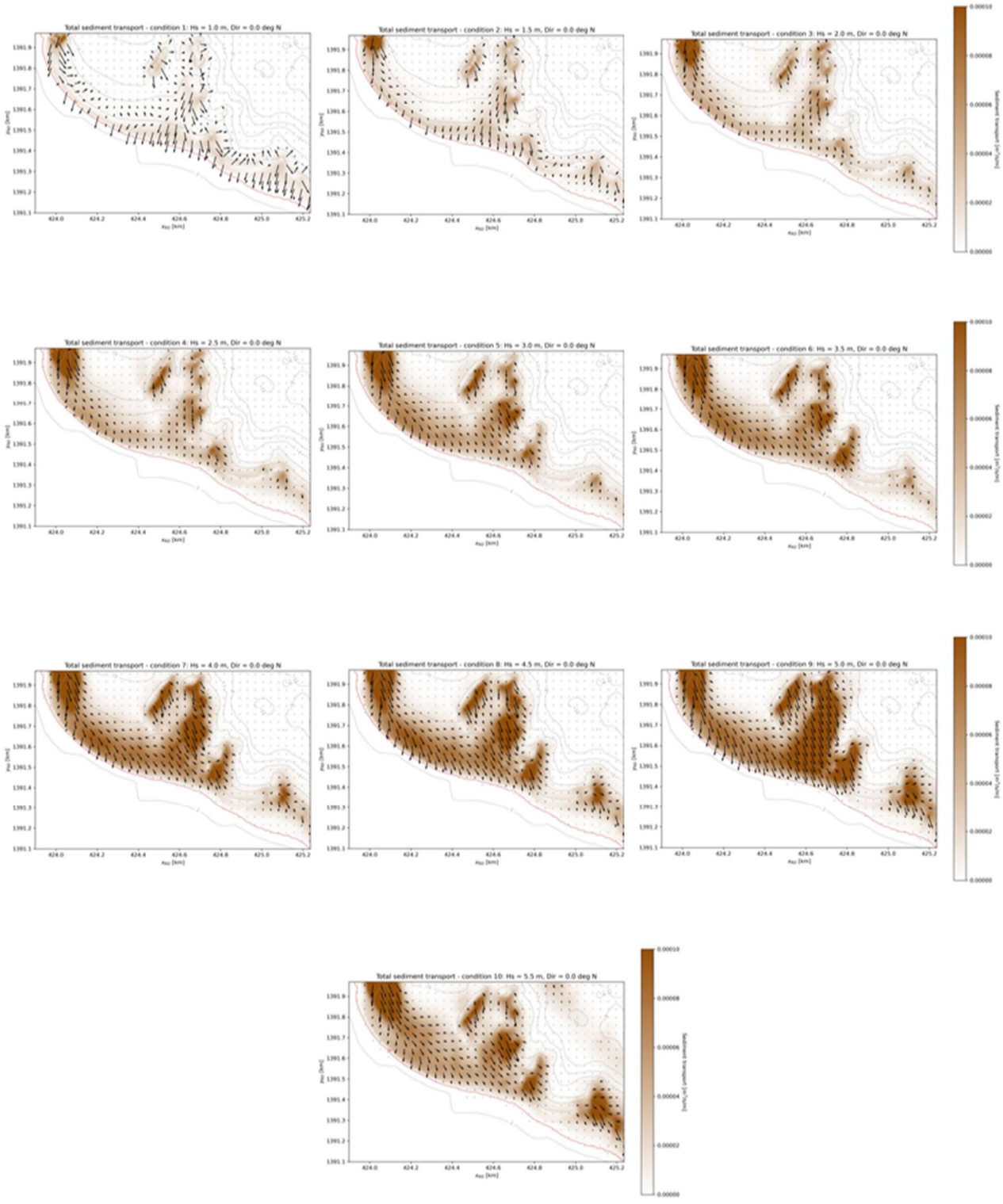

80°N Conditions

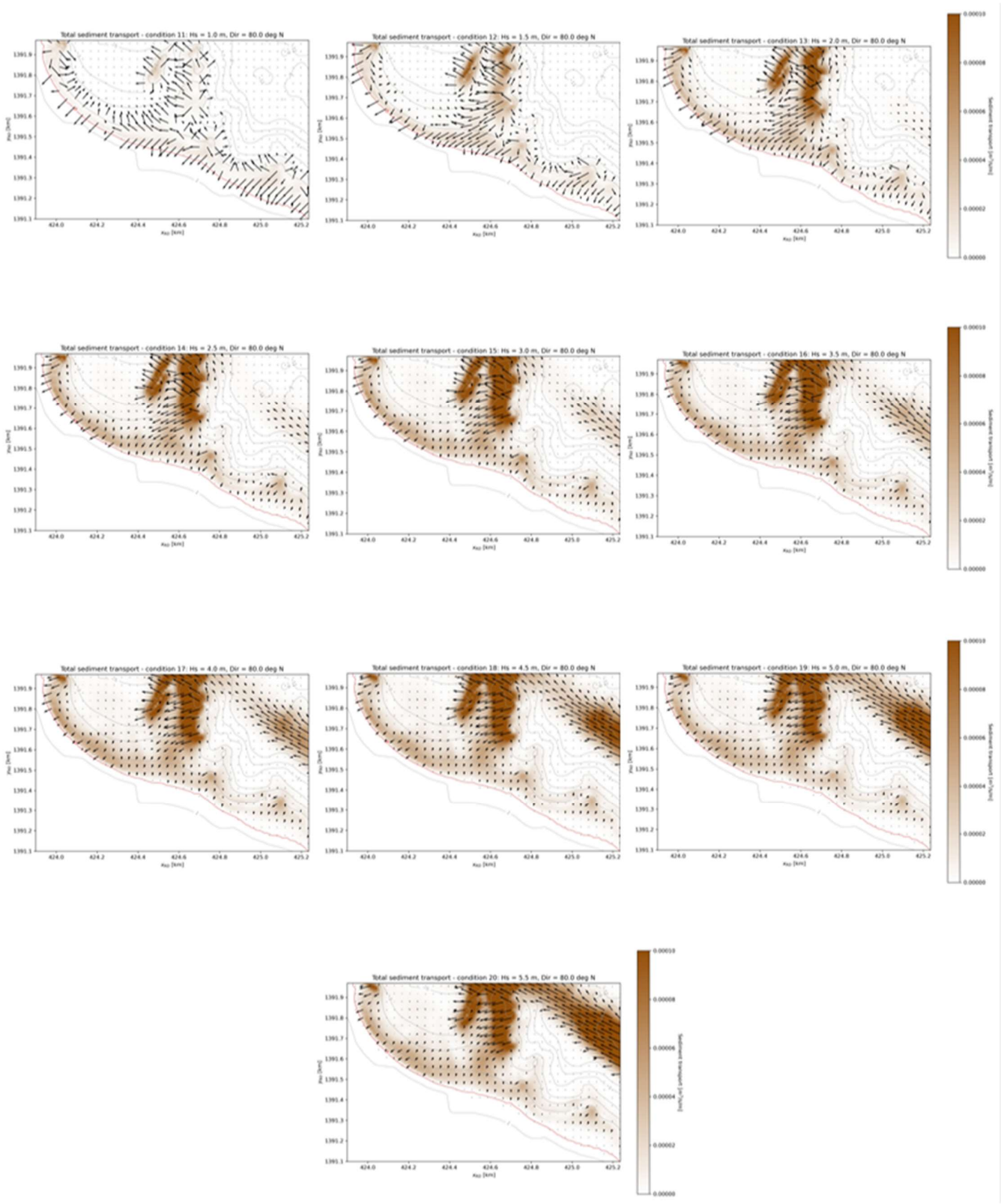

Shear Stresses near shore

0°N Conditions

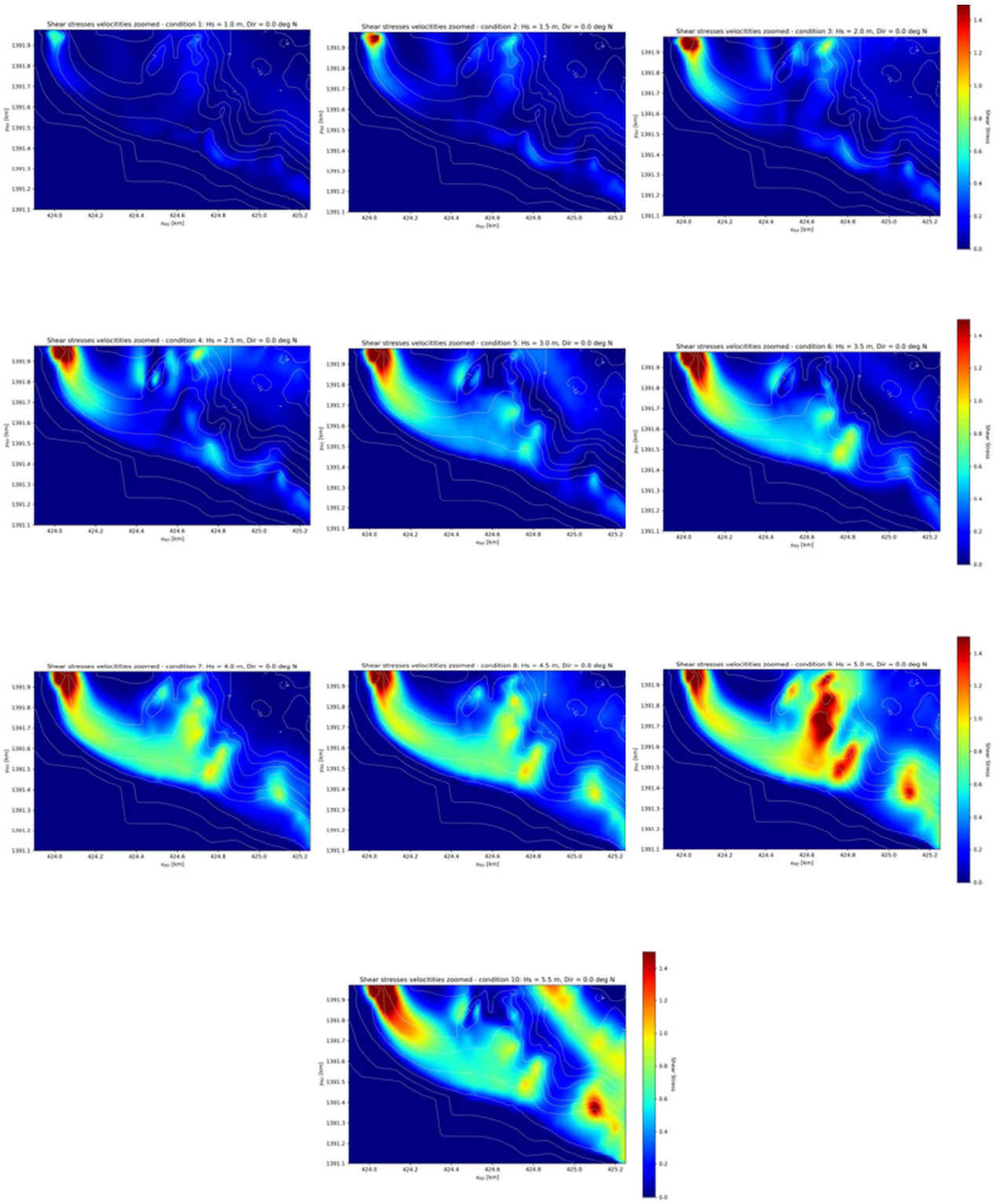

80°N Conditions

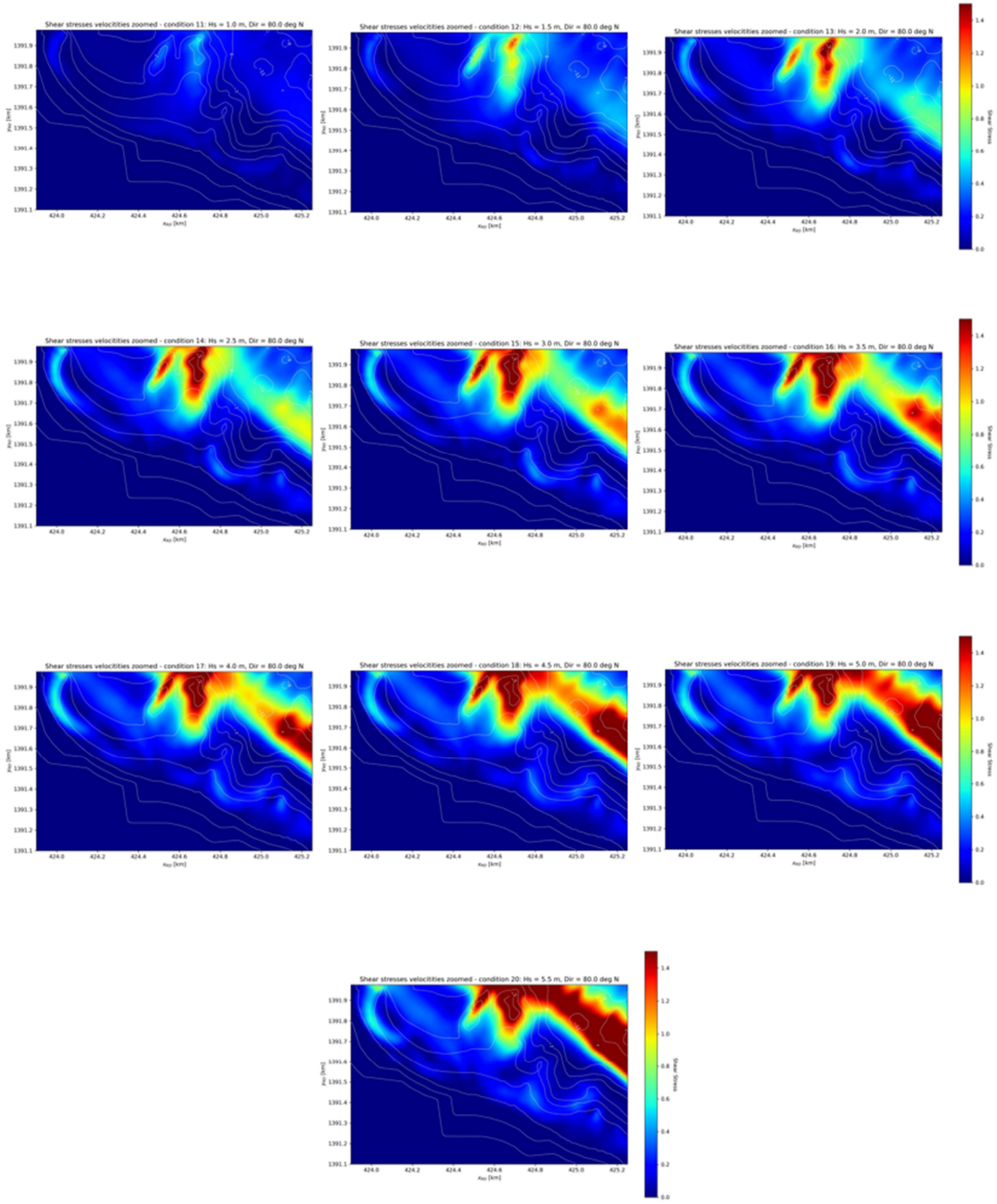

Overview of results within the entire domain: 5.5 m wave

Northern waves

Eastern waves

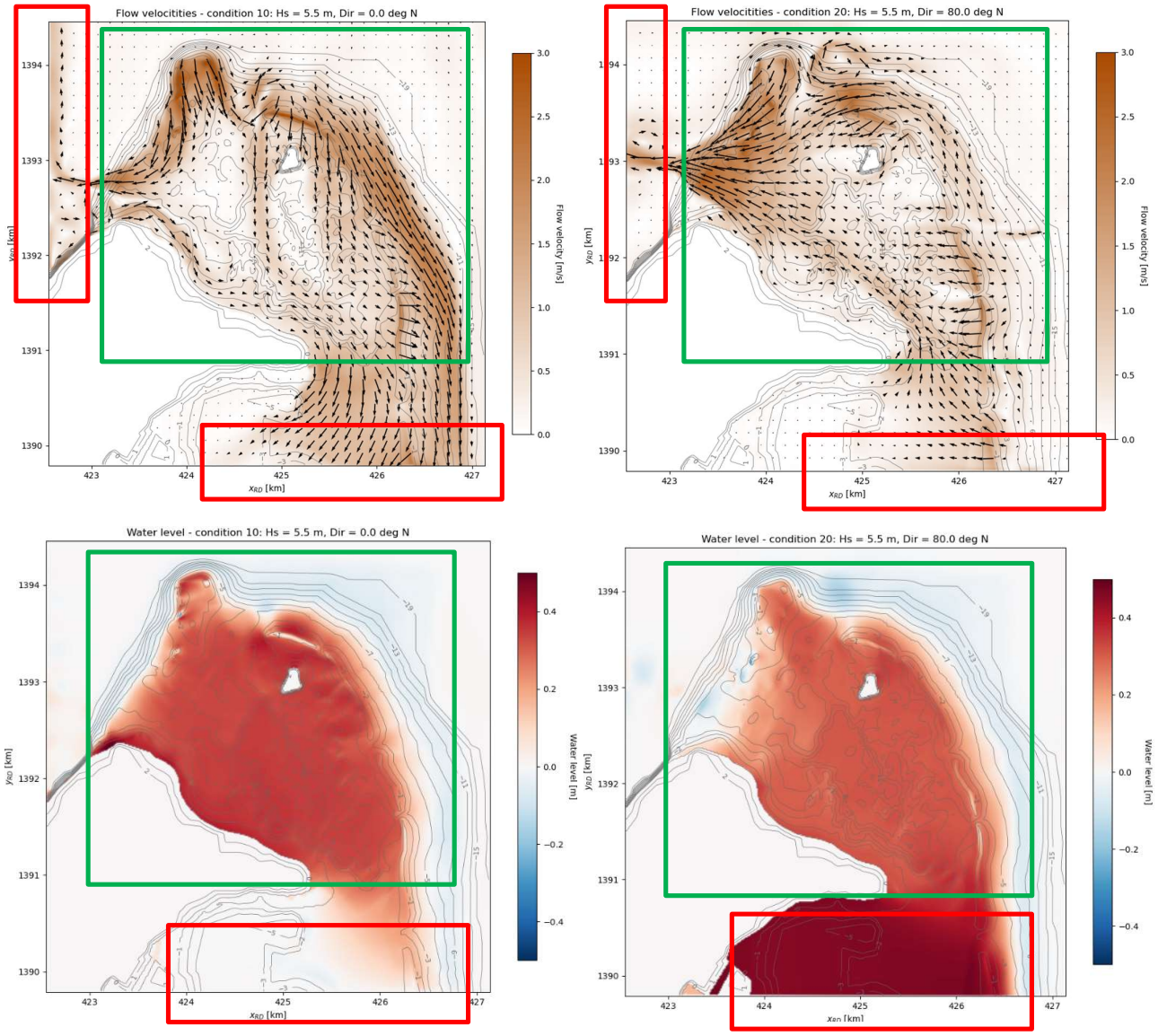

It can be seen that the flow velocities and water levels experience a few boundary anomalies (red boxes) which do not comply with reality. It can also be seen that these anomalies have minor influences in the interest area within the green boxes in the figures.

The same is true for the 2 m wave conditions shown in the figures below.

Overview of results within the entire domain: 2.0 m wave

Northern waves

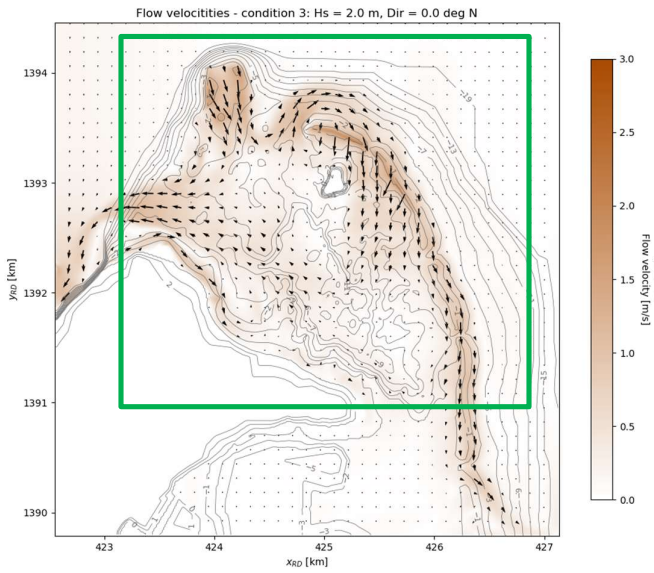

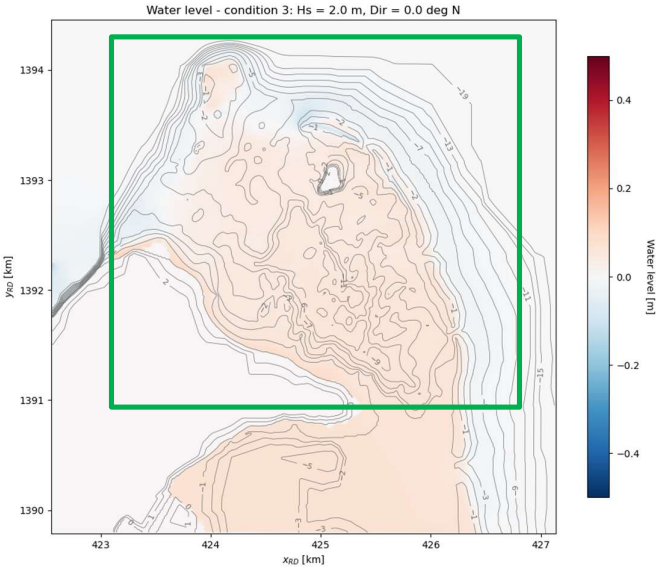

Eastern waves

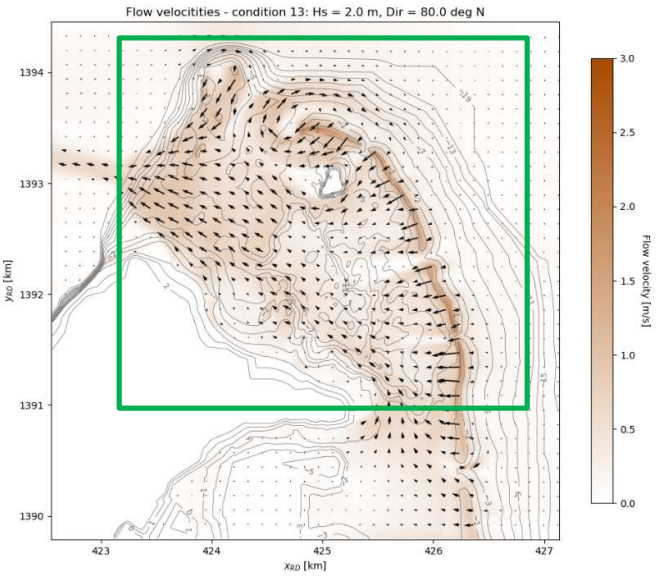

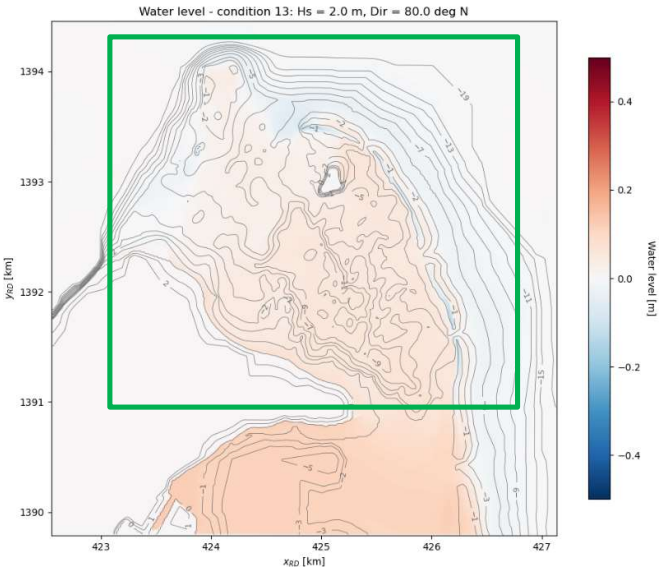

Appendix F - Pictures of San Andrés 1988

In this appendix pictures can be seen of the port of San Andrés in 1988, in which land is being reclaimed to construct part of the port of San Andrés.

DRAGADO PUERTO DE SAN ANDRES
(S#1302) Agosto 1988

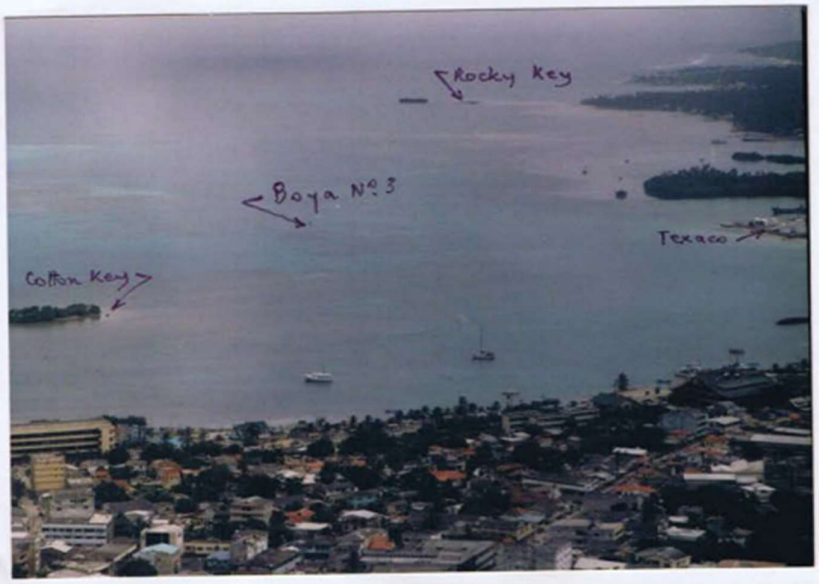

FOTO 26. Panorámica del puerto.

FOTO 27. Panorámica del puerto y canal de acceso.

DRAGADO PUERTO DE SAN ANDRES
(S#1302) Agosto 1988

FOTO 28. Panorámica del puerto y canal de acceso. Nótense las barras de arena.

FOTO 29. Vista hacia el muelle Intendencial y la Bahía Hooker.

CANAL DE ACCESO AL MUELLE DE SAN ANDRES
Septiembre/88 (S#1331)

FOTO # 0. Muelle de Texaco desde el mismo sitio.

FOTO 1. Draga de "Drexco" que dragó el muelle de Texaco.

CANAL DE ACCESO AL MUELLE DE SAN ANDRES
Septiembre/88 (S#1331)

FOTO 2. Entrada a Bahía Hooker desde el muelle de Texaco.

FOTO 3. Muelle de Texaco.

SAN ANDRES. CANAL DE ACCESO
C-329, Febrero/89 (S#1336)

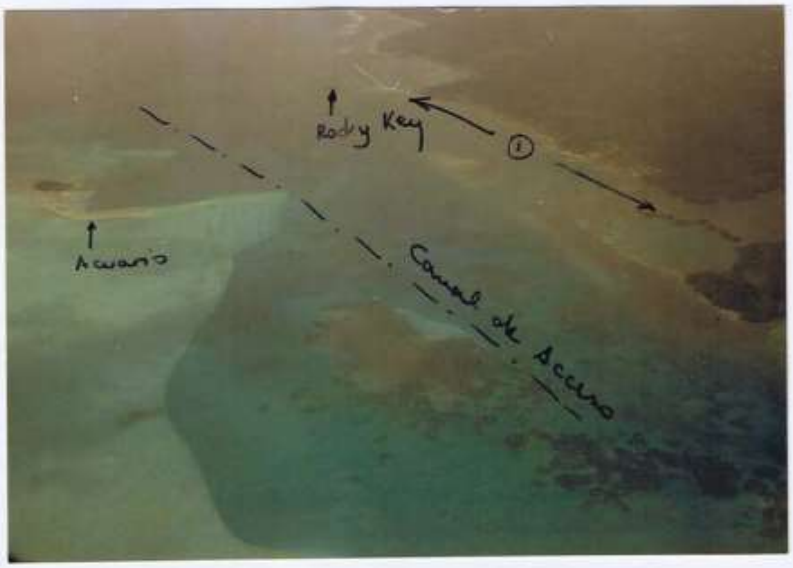

FOTO # 1. Vista general del canal de acceso y zona de vertimientos No.1.

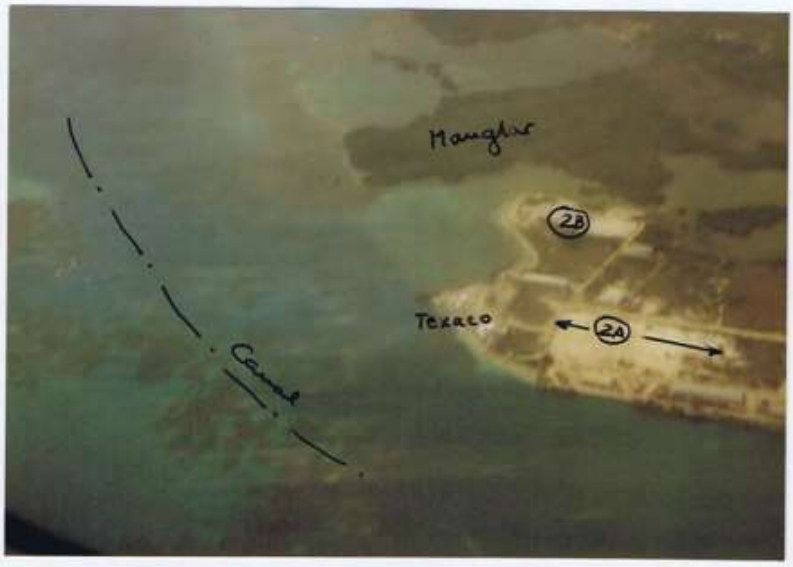

FOTO # 2. Llegada al muelle. Zonas de depósito 2A y 2B.

Appendix G - Ecological Aspects of Dredging and Sand Nourishment by Peter Herman (Deltares)

This is a fragment of the contribution given by Prof. dr. ir. Peter Herman from Deltares for the project Arcadis is carrying out for RVO in San Andrés (2022). Deltares is part of the consortium that is working on this project. In this fragment Peter Herman explains the ecological dangers, damages and nuisance dredging and nourishment activities can cause.

1. Direct local effect

1.1 Entrainment

Dredging operations have direct lethal effects on the benthic fauna inhabiting sediments. Benthic fauna is restricted to the upper decimeters of the sediment and is thus 100% removed due to dredging operations. The extent of this removal is proportional to the area dredged. Per unit of volume of sand dredged, the impact decreases with increasing depth of the borrowing pit. The entrained benthic fauna does not survive the strong mechanical forces during dredging operations, so that the sediment is stripped of its fauna at the moment when it is dumped onto the nourishment area (Newell et al., 1998). Consequently, the dumped sediment will also need to be recolonized by benthic fauna.

Entrainment of fish and pelagic fauna is generally considered to be minor, but it can be a problem for eggs and larvae in spawning areas. Temporal restriction of dredging operations outside of spawning seasons is a necessary precaution to avoid this effect (Todd et al., 2014).

1.2 Burial

Recolonization of dumped sediment could, in principle, be done by the animals originally living in the dumping area. However, survival of the burial may be limiting for these animals. The effect of burial depends on the type of sediment used, temperature, speed of burial, and species affected (Baptist et al., 2008). The tolerance of species to fast burial (dumping) is limited to the range of centimeters to a few decimeters. When sediment accretion is gradual as in many natural geomorphological processes, animals can usually adapt much more easily and tolerate much larger burial depths, although some species can be extremely sensitive (an example is *Mya arenaria*, a big clam that loses its ability to move vertically in the sediment as it grows older – it is fatally affected by both burial and erosion above the range of appr. 5 cm).

The volume and thickness of dumped sediment layers in coastal nourishment usually exceed the tolerance limit of the local fauna. Consequently, the fauna will, just as in the borrow areas, be dependent on recolonization processes for restoration.

Seagrass meadows are very sensitive to burial (Erftemeijer and Robin Lewis, 2006). Burial by as little as a few cm can be lethal for some species, especially for the long-living larger species with the highest biodiversity value. Loss of seagrass at or nearby beach nourishments will decrease the stability of the nourished beach, as seagrass has a strong stabilizing influence on beaches (James et al., 2019; James et al., 2021). Considering the sensitivity of nearby seagrass to burial, any excess nourishment (i.e., nourishment beyond the limits of what constitutes a morphologically stable beach) should be avoided. It would serve as a local source of sand that will deposit onto the seagrass beds and destabilize them, with adverse effects on beach stability as a consequence.

1.3 Release of toxicants

Dredging may play an important role in the remobilization of toxicants accumulated in marine sediments. Many toxicants are associated to the fine fractions of sediments. Both natural (e.g., tides and waves, bioturbation) and anthropogenic (e.g., dredging) factors can remobilize these fine fractions and the associated toxic load, which leads to spatial redistribution of pollution but also to exposure of biological communities to the toxic load. The processes have been reviewed by (Roberts, 2012), who reports cases of increased loading of organisms with toxicants around dredging operations, however with few or no cases of acute responses and usually limited scales of distribution of the effects. Disposal of toxic dredge spoils is strictly regulated in most countries and is therefore not a major source of pollution. It is a condition that needs to be checked prior to the execution of any dredging operation.

1.4 Noise

Dredging operations produce noise, that may scare away marine mammals. There are few indications of direct injury to the animals' ears caused by the noise of dredging, but changes in behavior and space occupation by mammals after dredging operation intensified have been observed. The causal link to the noise is, however, difficult to establish. Todd et al. (2014) extensively review the literature on this and other aspects of dredging in relation to marine mammals.

2. Far-field effects

2.1 Turbidity effects

Dredging operations can locally increase suspended sediment concentrations. Fines that are dredges, are washed overboard and create a density current around the ship that can quickly sink to the bottom. From there the fine sediment can settle or be distributed to a wider area. Increased suspended sediment concentrations have a negative ecological impact because they decrease light availability for primary production by algae and macrophytes, and because they hinder the feeding process of all organisms relying on filtration of the water. Both benthic species (e.g. mussels) and pelagic species rely on that feeding mechanism. It is observed that their feeding and growth depend on the ratio between food (e.g., algae) and inorganic material in suspension. Increased turbidity can both decrease the food content and increase the inorganic content.

Increased turbidity also leads to increased deposition of fine material in the area surrounding the dredging location. The extent of that area depends strongly on the local bathymetry and hydrodynamic conditions. The fines deposited in the area can smother organisms, which can be lethal for sensitive species (Wilber and Clarke, 2001). The effects are particularly important for seagrass and corals, two sensitive groups of species with a very important ecological role. We refer to reviews of the literature on these groups in the sections below.

2.2 Turbidity and seagrass habitat degradation

Apart from direct mechanical removal by dredging, seagrass beds suffer mostly from increased turbidity, leading to lower light levels and smothering that have often proven fatal for these very important structuring elements in the ecosystem (Erftemeijer and Robin Lewis, 2006). Past dredging activities have had devastating effects on seagrass beds, as seagrass is very sensitive to both decreases in light intensity and smothering of the leaves. It is, however, possible to model the effect of dredging and dumping and to keep the conditions around the dredging areas within the tolerance limits of seagrass. These careful considerations have reduced the negative influence of dredging on seagrass in recent years (Erftemeijer and Robin Lewis, 2006).

2.3 Coral habitat degradation

The vulnerability of corals to increased turbidity and smothering strongly depends on the type of corals present in the area (Erftemeijer et al., 2012). Usually, the resident community is adapted to the local conditions and has a tolerance range that reflects the natural variability in conditions present at the site. It therefore requires careful consideration of the local conditions to determine tolerance limits for dredging operations, in order to avoid overloading corals with fine

sediments. In any case, even within tolerance limits the response of corals to the additional stress of increased suspended sediment is costly in terms of energy for the species. It may therefore affect the species' ability to withstand other forms of stress (Erftemeijer et al., 2012).

2.4 Effects through bio-geomorphological effects

The loss of populations of so-called 'ecosystem engineers' (Jones et al., 1996), species that physically modify their habitat and affect the possibilities of other species to live there, may have large-scale ecological consequences for areas well beyond the area touched by dredging or nourishment. Seagrass and corals are examples of such ecosystem engineering species, as are oyster beds, Ross worm colonies etc. Negative effects on coral reefs leading to mortality of the reef, may lead to drastic changes in the protection of coastal bays from ocean waves (Keyzer et al., 2020). Likewise, seagrass beds have been described to protect beaches and bays from erosion, a bio-geomorphologic effect that may be lost if the seagrass are affected by dredging operations (James et al., 2019; James et al., 2021).

2.5 Effects through morphology

Dredging and dumping change the coastal morphology and thereby the exposure to physical processes (e.g., bottom shear stress from waves and currents), transport pathways of sediment and organic matter, depth below the surface and light conditions, etc. This will affect the habitat quality and may cause a change of the community in the dredged or nourished area, but also in surrounding areas that are affected by the transport of matter and energy. Steepening the coastal profile, as an example, will change the places where most wave energy dissipates, and will increases the risk for sediment redistribution from the beach to the deeper foreshore. It will also affect the habitat suitability of the profile for organisms.

In a coastal profile, there is an equilibrium between the shape (e.g., steepness) of the coastal profile and the grain size of the sediment. Changing the profile may lead to the loss of some sediment fractions (e.g., loss of fine sediment upon steepening), with knock-on effects on the biological community living in the coastal sands. A reverse chain of effects can occur when nourishing with too coarse sediment. McLachlan (1996) has documented the changes to benthic fauna in a beach nourished with too coarse sediment. He demonstrates that the clear correlation between fauna and median grain size was caused by the morphological adaptation of the coastal profile to the coarser sediment, which in turn led to the spatial concentration of wave energy that limited the occurrence of certain species.

2.6 Recolonization

The rate of recolonization depends on the habitat characteristics of the nourished area (e.g., the degree of exposure to waves and currents, grain size distribution, depth etc.) and on the characteristics of the pristine fauna in the area. In regularly disturbed areas, e.g., the shallow foreshore of a beach, or estuarine conditions with highly variable salinity, the local fauna will consist mostly of opportunistic species that can rapidly colonize new habitats. Recolonization in those conditions may be completed in less than one year, especially if the nourished area is also subject to the same forms of stress (Newell et al., 1998). However, recolonization by species of undisturbed mature communities generally takes more time, up to 5-6 years. The time to recolonization may even be longer if the sediment needs time to consolidate and reach biogeochemical equilibrium (Newell et al., 1998).

2.7 Habitat change

In general, recolonization will not lead to the same community as was present before the nourishment. The nourishment changes the characteristics of the habitat and will therefore be recolonized by a community that is adapted to the new habitat characteristics. The most frequent change in habitat characteristics is in the grain size of the sediment. Often nourishments use different grain size, e.g., finer sand in places with gravel substrate. Grain size of the sediment is one of the most dominant habitat characteristics determining the community composition of benthic animals, and consequently

a change in grain size will also lead to a different community recolonizing the dredged habitat. Changes in grain size have been observed at nourishment locations (Speybroeck et al., 2006) but also at sand mining locations due to the practice of in-situ screening. It leads to habitat changes that cause prolonged and consistent changes in the faunal community (Barrio Froján et al., 2011).

2.8 Landscaping mining pits

Landscaping the habitat of sand mining pits has been used as a way to promote the biodiversity of the recovering benthic fauna in the sand mining operations of Maasvlakte II (De Jong et al., 2016). It has been shown that, depending on the depth of the mining pit, the bottom shear stress in the pit can be modified and the fauna adapts to the bottom shear stress. Richer fauna in terms of productivity and abundance was found at lower values of bottom shear stress. However, these areas also accumulated more fine sediment and more organic matter, thus increasing the risk of hypoxia close to the bed. A modeling approach is proposed to optimize the ecological footprint of sand extraction. By minimizing the surface area affected, the effect is lessened. However, this increases the depth of excavation and with it also the risk of poorly flushed sediments. An optimum can be found in between the extremes of very shallow and very deep excavation. The optimum will depend on the local conditions of currents and sediment composition and has to be re-estimated for every site.

3. Application to the San Andrés situation

Nourishments are one option for the preservation of Spratt Bight Beach along the Northern coast of San Andrés. Three possible sand sources have been identified (Arcadis, 2022): one to the North of the island, one in the harbor access channel and one along the Southwestern point of the island.

Several ecological points of attention are important when considering these potential borrow areas.

4. Presence of seagrass and corals in the borrow area

As has been pointed out above, seagrass meadows and coral reefs are sensitive to the release of fine sediment associated with dredging. It can be expected that in the clear Caribbean waters, where high suspended sediment concentrations are not normally observed, this sensitivity will be high. The grain size distribution of the potential borrow areas shows especially elevated fractions of the finest sediment class in the deeper stations of the harbor access channel. This fine fraction is associated with elevated organic content. It is likely that it is composed at least partly of clay minerals, but mineral composition has only been determined on the sand fraction (which is almost totally biogenic and calcareous). In any case, resuspension of this fine fraction during dredging is expected to give rise to light attenuation and smothering problems. The access channel is, moreover, situated close to seagrass meadows and mangrove areas at the coastward side, and coral reefs at the seaward side. It is, therefore, an extremely sensitive area where dredging should only be performed after thorough study of the effects on turbidity and the habitat quality for seagrass and coral. This study includes modelling of the spatial extent of potential fine sediment plumes and effects on light and sedimentation of fines. Precautionary measures can be taken if adverse effects are expected, but these will increase the price of the dredging operations. Careful selection of sands with a very small fine fraction is the better option. This should be the subject of an EIA, including tight measures for field monitoring during dredging operations.

5. Burial of seagrass in the nourishment area

From Google Earth images it appears that seagrass meadows are present close to the shore in the nourishment area. These seagrass beds can be an important factor in stabilizing the beach and preventing erosion. Nourishment of the

beach will require extreme care in order not to damage the nearby seagrass meadows by burial or excess sedimentation. This implies that the nourishment volume must be carefully selected so as not to lead to any excess unstable sand along the beach, as unstable sand will eventually move offshore and sediment in the seagrass meadow. Once the stabilizing influence of the seagrass meadows would be lost, more beach erosion could ensue, and a vicious circle may start.

6. Effects through morphology

The harbor access channel is situated across a sediment transport pathway that connects coral reefs at the seaward side to shallow bays with beaches, seagrass, and mangroves at the coastward side. Deepening this passage will create a sediment sink that interrupts the natural flow of sediment towards the coast. It might therefore have long-term effects on the stability of the coastline and the preservation of the important natural coastal areas to the West of the access channel. This effect should be thoroughly studied in order not to create coastal instability in this area, while attempting to stabilize the coast in another area.

Morphological change can also be anticipated in the Southwestern potential borrow areas. These sandy areas are situated at limited depth with great importance for the stability of the sandy coastline. Sand mining in this borrow area will significantly steepen the coastal profile and may destabilize the coastline in this part of the island. It will also decrease wave damping offshore and contribute to more focus of wave energy on the coast. Ecological consequences, as well as societal problems, may be caused by mining this sand resource so close to the coastline.

7. Effects through grainsize

From the survey by INVEMAR, it appears that suitable sand with a grain size composition similar the grain size composition of the Spratt Bight Beach, is available. It is very important that the correct grain size is used, as the morphology of the beach will adapt to the grain size of the nourishment, and this may lead to destabilization of the current beach.

8. Pollutants

Data on pollutant concentrations in the potential borrowing areas were not yet available at the time of writing of this note. Of all borrowing areas, especially the harbor access channels deserve attention in this respect. Not only is the harbor a potential source of pollution, but the sediment also has a high fine fraction to which most toxicants will adsorb.

9. Effects on fish, birds, reptiles, and mammals

Disturbances due to the dredging and nourishment operations may disturb local populations of fish, birds, reptiles and mammals. No long-term consequences of this activity should be expected, though. What could be much worse is a change of habitat (e.g., destruction of seagrass or coral reefs) that would affect the habitat of the emblematic species and would decrease the value of the area from a natural and touristic point of view.

References

Baptist, M.J., Tamis, J.E., Borsje, B.W., and van der Werf, J.J. (2008). *Review of the geomorphological, benthic ecological and biogeomorphological effects of nourishments on the shoreface and surf zone of the Dutch coast.* Texel: IMARES / Deltares.

Barrio Froján, C.R.S., Cooper, K.M., Bremner, J., Defew, E.C., Wan Hussin, W.M.R., and Paterson, D.M. (2011). Assessing the recovery of functional diversity after sustained sediment screening at an aggregate dredging site in the North Sea. *Estuarine, Coastal and Shelf Science* 92(3), 358-366. doi: https://doi.org/10.1016/j.ecss.2011.01.006.

De Jong, M.F., Borsje, B.W., Baptist, M.J., van der Wal, J.T., Lindeboom, H.J., and Hoekstra, P. (2016). Ecosystem-based design rules for marine sand extraction sites. *Ecological engineering* 87, 271-280.

Erftemeijer, P.L.A., Riegl, B., Hoeksema, B.W., and Todd, P.A. (2012). Environmental impacts of dredging and other sediment disturbances on corals: A review. *Marine Pollution Bulletin* 64(9), 1737-1765. doi: https://doi.org/10.1016/j.marpolbul.2012.05.008.

Erftemeijer, P.L.A., and Robin Lewis, R.R. (2006). Environmental impacts of dredging on seagrasses: A review. *Marine Pollution Bulletin* 52(12), 1553-1572. doi: https://doi.org/10.1016/j.marpolbul.2006.09.006.

James, R.K., Lynch, A., Herman, P.M.J., van Katwijk, M.M., van Tussenbroek, B.I., Dijkstra, H.A., et al. (2021). Tropical Biogeomorphic Seagrass Landscapes for Coastal Protection: Persistence and Wave Attenuation During Major Storms Events. *Ecosystems* 24(2), 301-318. doi: 10.1007/s10021-020-00519-2.

James, R.K., Silva, R., van Tussenbroek, B.I., Escudero-Castillo, M., Mariño-Tapia, I., Dijkstra, H.A., et al. (2019). Maintaining Tropical Beaches with Seagrass and Algae: A Promising Alternative to Engineering Solutions. *BioScience* 69(2), 136-142. doi: 10.1093/biosci/biy154.

Jones, C.G., Lawton, J.H., and Shachak, M. (1996). "Organisms as Ecosystem Engineers," in *Ecosystem Management: Selected Readings,* eds. F.B. Samson & F.L. Knopf. (New York, NY: Springer New York), 130-147.

Keyzer, L.M., Herman, P.M.J., Smits, B.P., Pietrzak, J.D., James, R.K., Candy, A.S., et al. (2020). The potential of coastal ecosystems to mitigate the impact of sea-level rise in shallow tropical bays. *Estuarine, Coastal and Shelf Science* 246, 107050. doi: https://doi.org/10.1016/j.ecss.2020.107050.

McLachlan, A. (1996). Physical factors in benthic ecology: effects of changing sand particle size on beach fauna. *Marine Ecology Progress Series* 131, 205-217.

Newell, R.C., Seiderer, L.J., and Hitchcock, D.R. (1998). The impact of dredging works in coastal waters: a review of the sensitivity to disturbance and subsequent recovery of biological resources on the sea bed. *Oceanography and Marine Biology: an annual review* 36(1), 127-178.

Roberts, D.A. (2012). Causes and ecological effects of resuspended contaminated sediments (RCS) in marine environments. *Environment International* 40, 230-243. doi: https://doi.org/10.1016/j.envint.2011.11.013.

Speybroeck, J., Bonte, D., Courtens, W., Gheskiere, T., Grootaert, P., Maelfait, J.-P., et al. (2006). Beach nourishment: an ecologically sound coastal defence alternative? A review. *Aquatic Conservation: Marine and Freshwater Ecosystems* 16(4), 419-435. doi: 10.1002/aqc.733.

Todd, V.L., Todd, I.B., Gardiner, J.C., Morrin, E.C., MacPherson, N.A., DiMarzio, N.A., et al. (2014). A review of impacts of marine dredging activities on marine mammals.

Wilber, D.H., and Clarke, D.G. (2001). Biological Effects of Suspended Sediments: A Review of Suspended Sediment Impacts on Fish and Shellfish with Relation to Dredging Activities in Estuaries. North *American Journal of Fisheries Management* 21(4), 855-875. doi: 10.1577/1548-8675(2001)021<0855:BEOSSA>2.0.CO;2.

Appendix H - XBeach Model Set-Up

XBeach (2009) is a model which is designed for simulate dune erosion during storm conditions in which different boundary conditions are defined. Since its first creation, the model has been widely applied and developed towards a vaster variety of situations and case studies. Figure 0.6 shows the layout of a general model grid set-up for XBeach. On the 'back' a non-reflective dry boundary towards which waves are propagated, a non-reflective offshore boundary (on the 'front') from which the waves propagate and two lateral boundaries ('left' and 'right') which can be a:

- Neuman boundary, in which the longshore water level gradient is prescribed (default).
- 'Wall', through which no flow can pass, so flow velocities are set to zero on this boundary.
- Non advective boundary, which is an intermediate form between a full Neumann boundary and a wall boundary.
- Velocity boundary, where the velocity of the adjacent cell in the model domain is copied.

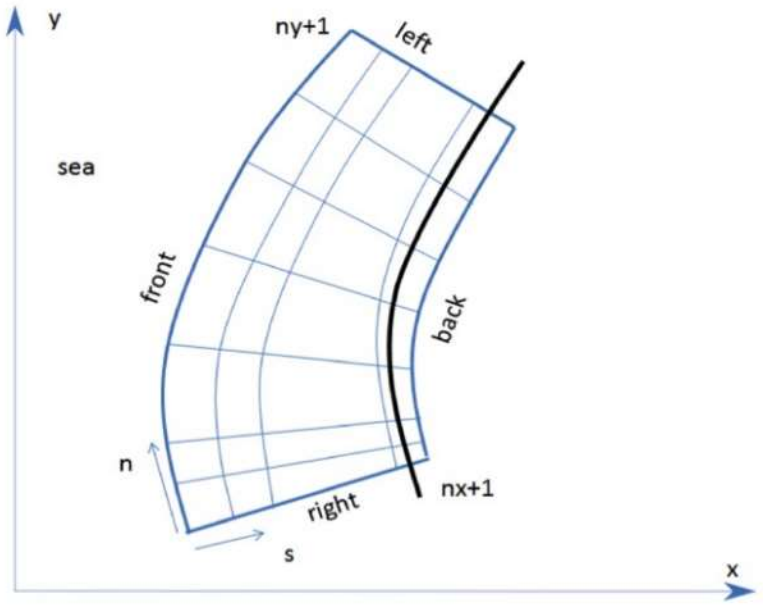

Figure 0.6: Schematization of the set-up of a curvilinear coordinate system applied on XBeach (Deltares, 2017).

The XBeach model for this research is set up using a curved-linear grid as shown below. This is done in order to prevent the effect of shadow zones in the wave field. As the simulated waves are coming majorly from the north and the west, is set-up was considered to be ideal.

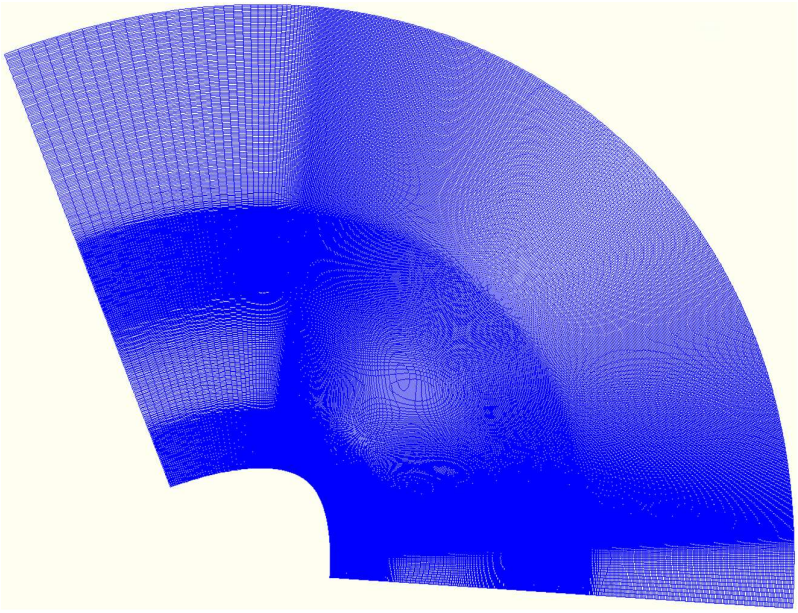

Figure 0.7: Numerical grid used for the XBeach model

The bathymetry of the domain is as shown below. In order to make sure all boundaries have the same water depth; the maximum depth is set to 50 m below MSL. This bathymetry is identical to the one used for the D3D simulations (except for the shape of the domain).

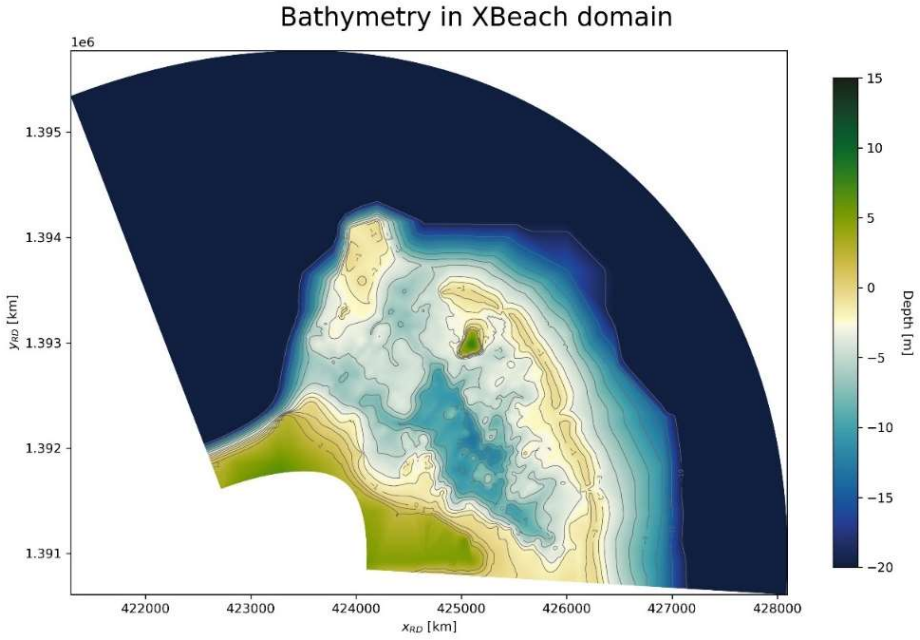

Figure 0.8: Bathymetry used for the XBeach model

The conditions simulated and the assumptions made for the environmental conditions are the same as describe in Chapter 3. The input parameter file of XBeach (params.txt) is shown in the figure below.

```
%%%%%%%%%%%%%%%%%%%%%%%%%%%%%%%%%%%%%%%%%%%%%%%%%%%%%%%%%%%%%%%%%%%%%%%%%%%%%%%
%%% XBeach parameter settings input file                                      %%%
%%%                                                                           %%%
%%% date: 01-Dec-2021 12:00                                                   %%%
%%% function: xb_write_params                                                 %%%
%%%%%%%%%%%%%%%%%%%%%%%%%%%%%%%%%%%%%%%%%%%%%%%%%%%%%%%%%%%%%%%%%%%%%%%%%%%%%%%

%%% Model Mode %%%%%%%%%%%%%%%%%%%%%%%%%%%%
wavemodel  = surfbeat
tstop      = 3600

%%% Grid parameters %%%%%%%%%%%%%%%%%%%%%%%%

gridform  = delft3d
depfile   = curv_fine_grid_newbathy.dep
posdwn    = 0
alfa      = 0
xyfile    = curv_fine_grid.grd
xori      = 0
yori      = 0
thetamin  = -90
thetamax  = 90
dtheta    = 10
thetanaut = 1

%%% Physical constants and Processes %%%%

swave        = 1
lwave        = 1
lateralwave  = wavecrest
fw           = 0.6

%%% Tide boundary conditions %%%%%%%%%%%%%

zs0                     = 0.0
tideloc       = 0
tidetype      = instant

%%% Wave boundary condition params %%%%%%

wbctype        = jonstable
bcfile         = jons.txt
```

Figure 0.9: Screenshot of the upper part of the parameters file (params.txt) used as input to run the XBeach model. This figure contains the boundary conditions and input parameters.

In the same file the output parameters are also specified. This section specifies what is wanted from the model to be returned. The figure below shows the output of the model.

```
%%% Output variables %%%%%%%%%%%%%%%%%%%%

outputformat = netcdf
tintm          = 2700
tintg          = 1800
tstart         = 900
tint           = 1.00

nglobalvar     = 1
zb0

nmeanvar       = 14
u
v
zs
H
zs1
kturb
umean
vmean
ue
ve
thetamean
taubx
tauby
urms
```

Figure 0.10: Screenshot of the second part of the parameters file (params.txt) used as input to run the XBeach model. This figure contains the output parameters and the variables the model has to return.

As can be seen in Figure 0.9, there is no lateral boundary condition specified in the input file. This means that the default for this parameter is taken. In the case of XBeach, the default lateral boundaries are Neumann Boundaries. The figure below shows the set-up of the boundaries and the simulated conditions in the domain.

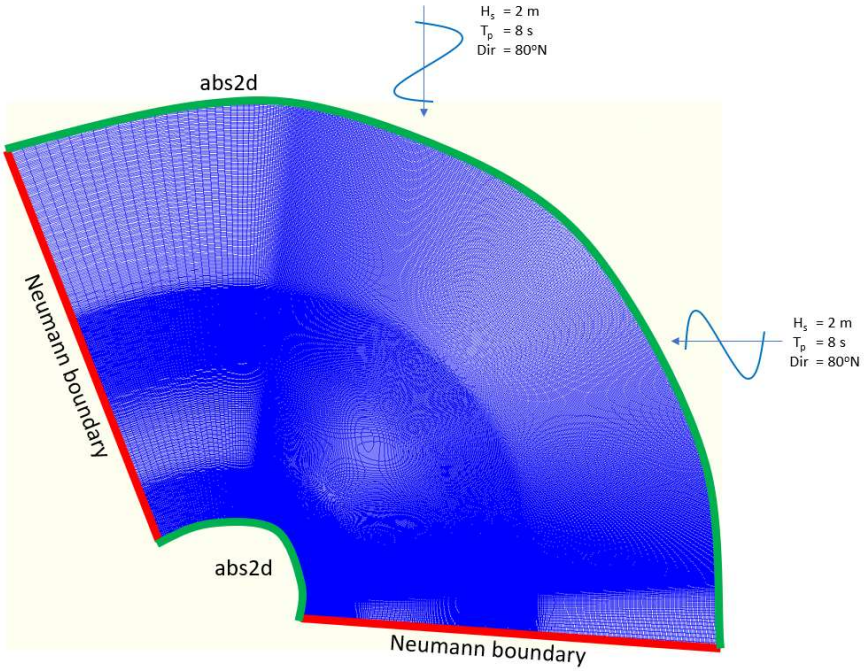

Figure 0.11: Domain used in the XBeach model with boundary conditions and simulated wave conditions.

In Chapter 6 the choice of the Neumann boundaries is discussed, and it is explained that other types of boundaries might be more suitable for these simulations.

Furthermore, the simulations are run for two simulation hours, in which the first hour is not recorded in order to remove spin-up effect, and the second hour is saved and averaged, giving results for the mean of the output parameters shown in Figure 0.10.

Appendix I - XBeach Model Results

In this appendix the results of the XB model simulations will be described. This is done in order to show the influence of the infragravity waves on the coastal system of San Andrés. As done by van Dongeren et al. (2013), the impact of the infragravity waves on the governing reef processes is evaluated through the relative importance of these waves on bed shear stresses on the lee side of the reef crest.

First, the short and long wave field is presented in Figure 0.12: Model results from XBeach presenting significant wave height of (on the left) short waves and (on the right) infragravity waves for 2 m offshore waves coming from the East. Notice that the figures are zoomed into the interest area. Besides, the scales are different between the short and the long waves. This is done because the infragravity wave height is one order of magnitude lower than the short waves.. Waves of 2 m height and coming from the East are simulated (condition 13 in Table 3.2). Here it can be seen that the short wave height is approximately one order of magnitude larger than the infragravity waves height (notice that the scales are different in the figure below).

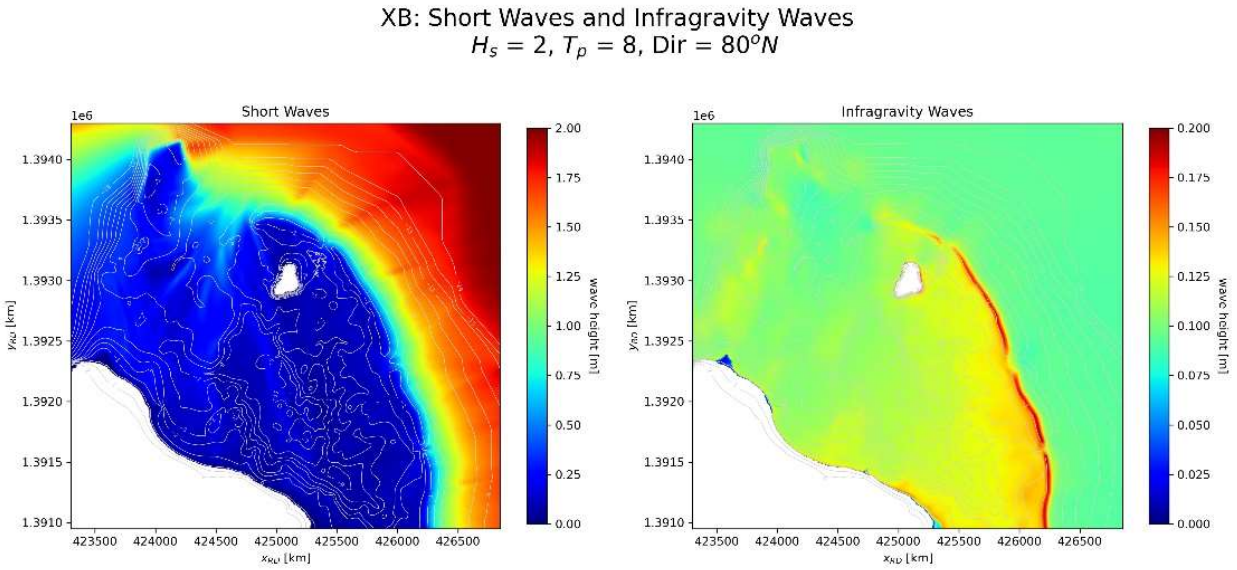

Figure 0.12: Model results from XBeach presenting significant wave height of (on the left) short waves and (on the right) infragravity waves for 2 m offshore waves coming from the East. Notice that the figures are zoomed into the interest area. Besides, the scales are different between the short and the long waves. This is done because the infragravity wave height is one order of magnitude lower than the short waves.

As in the D3D model results presented in Chapter 4, the waves coming from the East induce a water level set-up inside the lagoon. This is shown in Figure 0.13. It can be observed that the offshore water level is negative. This is due to the Neumann boundaries as described in Chapter 6. Although the results for the water level deviate from reality, the relative difference between offshore water level and water level inside the lagoon is realistic.

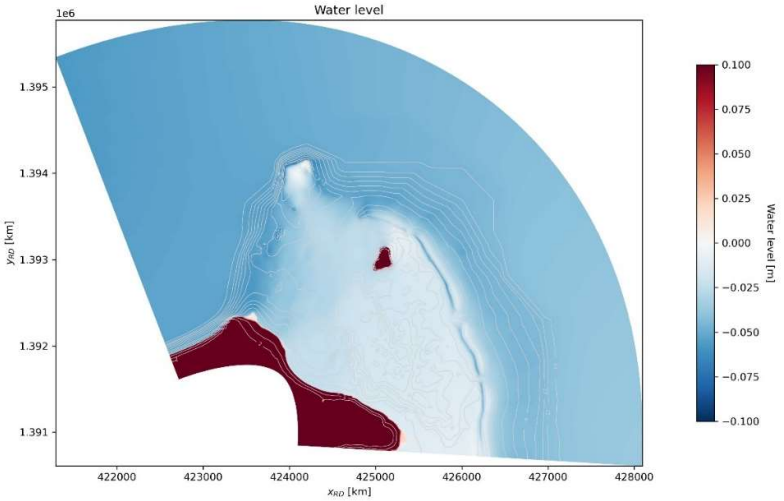

Figure 0.13: XBeach model results for the water level. Notice that the offshore water levels are below zero, which is not realistic. This effect is due to the chosen lateral boundary conditions. This is further discussed in Chapter 6.

This difference between the water level in- and outside the lagoon induces a flow velocity towards the Western opening in the coral reef (the same way as in the D3D results shown in Chapter 4). This is shown in Figure 0.14, where the flow velocities are presented for the part of the domain and a zoomed area near Spratt Bight Beach.

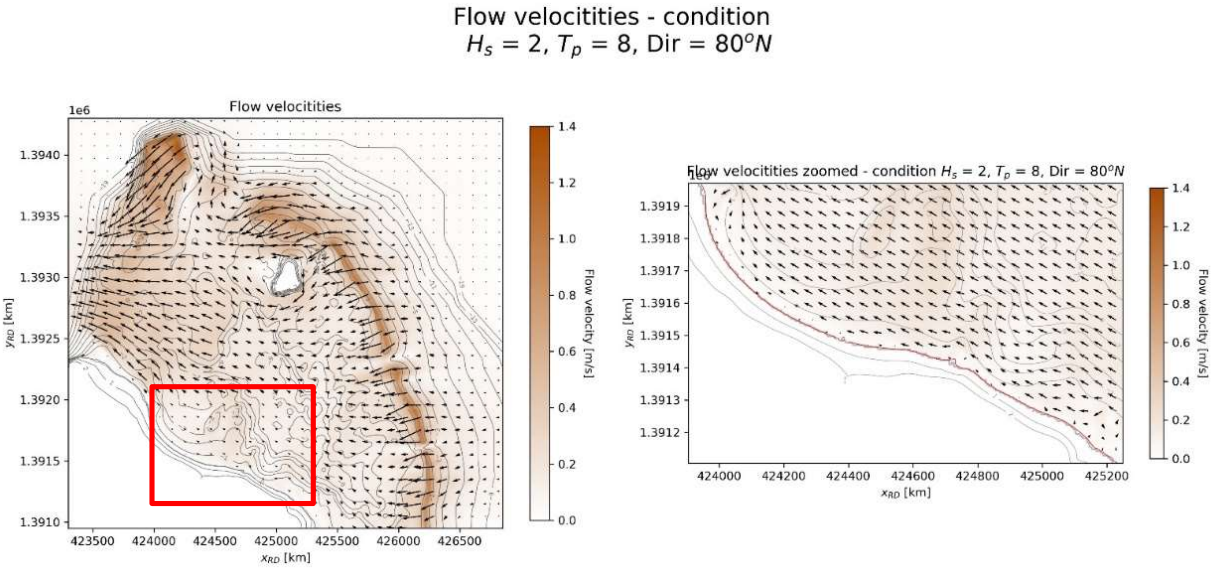

Figure 0.14: Model results from XBeach presenting flow velocities for 2 m offshore waves coming from the East.

The short wave, long wave and flow velocity action generate a shear stress on the bed. The effect of the bed shear stresses is to stir up of sediment which is consequently transported by the mean current in the form of suspended load (Bosboom & Stive, 2021). In order to understand the influence of the infragravity waves in sediment transport, the long wave induced shear stresses are quantified. This is done according to the formulations prescribed by van Dongeren et al. (2013):

$$\tau_c = \rho\ c_f\left(\bar{U}_E{}^2 + \bar{V}_E{}^2\right)$$
$$\tau_{IG} = \rho\ c_f\left(\overline{U_E^2} - \bar{U}_E{}^2 + \overline{V_E{}^2} - \bar{V}_E{}^2\right)$$
$$\tau_{sw} = \frac{1}{2}\rho\ f_w u_{rms,sw}^2$$

In which the current component of the bed shear stress (τ_c) depends on the mean velocity components ($\bar{U}, \bar{V}$) squared, the infragravity component (τ_{IG}) depends on the mean of the square of the velocity component minus the mean velocity components squared. This equals the variance of the velocity components (Var(U,V)). Finally, the short wave component of the bed shear stress (τ_{sw}) depends on the root-mean-squared (RMS) near-bottom shortwave orbital velocity ($u_{rms,sw}$) squared. In the formulations ρ is the water density, c_f is the friction coefficient associated with both the mean currents and infragravity waves, and f_w is the short-wave friction coefficient. For this modelling study c_f and f_w were chosen as being the same as done by in the research of van Dongeren et al. (2013): **c_f = 0.1 and f_w = 0.6.**

The figure below shows the shear stresses induced by the flow velocities, the short waves, the infragravity waves and the total shear stresses (respectively).

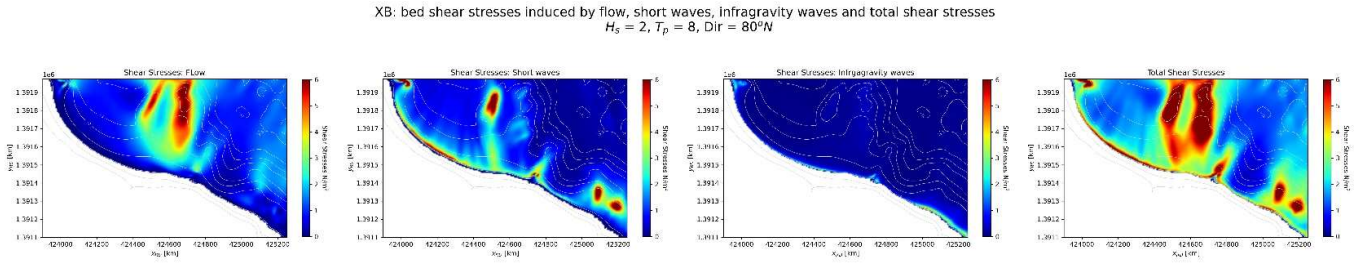

Figure 0.15: XBeach model results for the shear stresses induced by (l.t.r) flow velocities, short waves, long waves, and the total shear stresses. The simulated conditions are of 2 m waves coming from the East.

In Figure 0.15 in can be seen that the shear stresses associated with the infragravity waves are much smaller than the for the short waves and flow velocities. Consequently, the relative influence of the infragravity waves on the shear stresses will also be small. This is shown in Figure 0.16. Here, the relative influence of the flow velocity, short waves and long waves are presented. This is computed by taking every individual component influencing the shear stress (flow, short and long waves) and dividing it by the total shear stress. The result is a figure with the ratio for which every component is responsible for inducing shear stresses in the bed (as presented below).

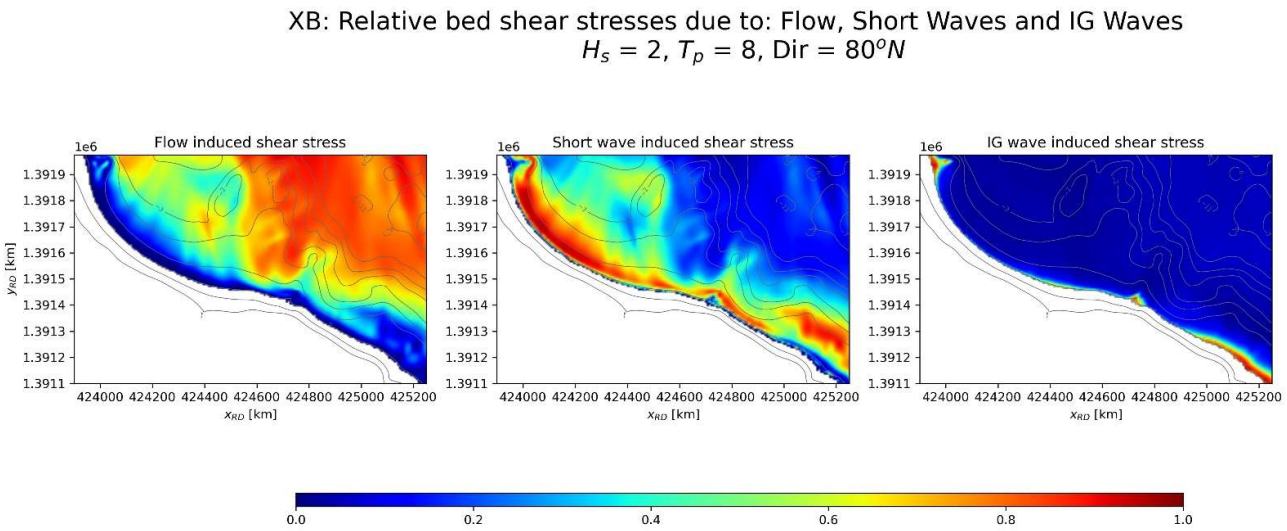

Figure 0.16: The fraction (denoted by the colorbar) of total bed shear stress driven by the mean currents, short waves, and IG waves, respectively.

As can be seen, the long waves present a minimal portion of the total shear stresses for this wave condition. This might imply that their relevance minimal for the system for the system and therefore also the sediment transports. It has to be kept in mind that the model is not validated and calibrated, which means that there might be substantial deviances from the reality.

Colophon

COASTAL EROSION AT SPRATT BIGHT BEACH, SAN ANDRÉS
A STUDY ON ITS CAUSE AND THE APPLICABILITY OF THE BUILDING WITH NATURE APPROACH

AUTHOR
Jan van Overeem

DATE
13 July 2021

NOTES